BULLETIN OF RUSSIAN STATE MEDICAL UNIVERSITY

BIOMEDICAL JOURNAL OF PIROGOV RUSSIAN NATIONAL RESEARCH MEDICAL UNIVERSITY

SUBMISSION http://vestnikrgmu.ru/login?lang=en
CORRESPONDENCE editor@vestnikrgmu.ru
COLLABORATION manager@vestnikrgmu.ru
ADDRESS ul. Ostrovityanova, d. 1, Moscow, Russia, 117997

Indexed in Scopus since 2017

Indexed in WoS since 2018

Five-year h-index is 3

Indexed in RSCI. IF 2016: 0,174

Listed in HAC 27.01.2016 (no. 1760)

Open access to archive

The mass media registration certificate no. 012769 issued on July 29, 1994
Founder and publisher is Pirogov Russian National Research Medical University (Moscow, Russia)

Approved for print 30.06.2018
Circulation: 100 copies. Printed by Print.Formula
www.print-formula.ru

ВЕСТНИК РОССИЙСКОГО ГОСУДАРСТВЕННОГО МЕДИЦИНСКОГО УНИВЕРСИТЕТА

НАУЧНЫЙ МЕДИЦИНСКИЙ ЖУРНАЛ РНИМУ ИМ. Н. И. ПИРОГОВА

ПОДАЧА РУКОПИСЕЙ http://vestnikrgmu.ru/login
ПЕРЕПИСКА С РЕДАКЦИЕЙ editor@vestnikrgmu.ru
СОТРУДНИЧЕСТВО manager@vestnikrgmu.ru
АДРЕС РЕДАКЦИИ ул. Островитянова, д. 1, г. Москва, 117997

Журнал включён в Scopus с 2017 года

Журнал включён в WoS с 2018 года

Индекс Хирша (h^5) журнала по оценке Google Scholar: 3

Журнал включён в РИНЦ. IF 2014: 0,139

Журнал включён в Перечень 27.01.2016 (№ 1760)

Здесь находится открытый архив журнала

Свидетельство о регистрации средства массовой информации № 012769 от 29 июля 1994 г.
Учредитель и издатель — Российский национальный исследовательский медицинский университет имени Н. И. Пирогова (Москва, Россия)

Подписано в печать 30.06.2018
Тираж 100 экз. Отпечатано в типографии Print.Formula
www.print-formula.ru

BULLETIN OF RSMU **2, 2018**
ВЕСТНИК РГМУ

Contents
Содержание

CRISPR-CAS SYSTEMS OF *MYCOBACTERIUM TUBERCULOSIS*: THE STRUCTURE, TRANSFORMATION IN DIFFERENT LINEAGES IN THE PROCESS OF EVOLUTION AND A POSSIBLE ROLE IN THE FORMATION OF VIRULENCE AND DRUG RESISTANCE

Zaychikova MV[1] ✉, Zakharevich NV[1], Chekalina MS[1], Danilenko VN[1,2]

[1] Laboratory of Bacterial Genetics,
Vavilov Institute of General Genetics, RAS, Moscow

[2] Department of Bioinformatics, Faculty of Biological and Medical Physics,
Moscow Institute of Physics and Technology (State University), Dolgoprudny

CRISPR-Cas systems are widespread in bacteria and archaea. They provide adaptive immunity against bacterial phages and plasmids and exert a few important functions like regulation of gene expression, DNA repair or virulence formation. We have analyzed the CRISPR-Cas systems of 7 *M. tuberculosis* lineages with fully sequenced genomes, namely Beijing, B0/W-148, EAI, Haarlem, Ural, LAM, and S. The CRISPR-Cas systems present in the analyzed genomes belong to type III-A. *M. tuberculosis* lineages differ in their CRISPR-Cas structure; in the Beijing lineage a part of the system is reduced. We have conducted a search for the functionally related partners and compensatory mechanisms of *cas*-genes using a method of phylogenetic profiling. The obtained phylogenetic profiles show that some genes have undergone similar evolutionary events. The reduction of the system's part in the Beijing lineage was accompanied by at least two evolutionary losses and one acquisition of genome regions. Exploration of alternative CRISPR-Cas functions in *M. tuberculosis* and their possible associations with other gene systems remains an exciting challenge.

Keywords: CRISPR-Cas systems, virulence, *M. tuberculosis*, Beijing lineage, phylogenetic profiling

✉ **Correspondence should be addressed:** Marina Zaychikova
Gubkina 3, Moscow, 119991; marinaz15@yandex.ru, valerid@vigg.ru

Received: 15.03.2018 **Accepted:** 20.03.2018

DOI: 10.24075/brsmu.2018.016

CRISPR-CAS СИСТЕМЫ *MYCOBACTERIUM TUBERCULOSIS*: СТРУКТУРА МОДУЛЯ, ИЗМЕНЕНИЕ В ПРОЦЕССЕ ЭВОЛЮЦИИ У РАЗЛИЧНЫХ ЛИНИЙ, ВОЗМОЖНАЯ РОЛЬ В ФОРМИРОВАНИИ ВИРУЛЕНТНОСТИ И ЛЕКАРСТВЕННОЙ УСТОЙЧИВОСТИ

М. В. Зайчикова[1] ✉, Н. В. Захаревич[1], М. С. Чекалина[1], В. Н. Даниленко[1,2]

[1] Лаборатория генетики микроорганизмов,
Институт общей генетики имени Н. И. Вавилова Российской академии наук, Москва

[2] Кафедра биоинформатики, факультет биологической и медицинской физики,
Московский физико-технический институт (государственный университет), Долгопрудный

CRISPR-Cas системы широко распространены у бактерий и архей. Они обеспечивают адаптивный иммунитет к бактериофагам и плазмидам, а также выполняют другие функции, включая регуляцию экспрессии генов, репарацию ДНК, формирование вирулентности. Нами был проведен анализ CRISPR-Cas систем полностью секвенированных геномов *M. tuberculosis* из семи линий: Beijing, B0/W-148, EAI, Haarlem, Ural, LAM, S. Проанализированные геномы содержат CRISPR-Cas систему типа III-A. Линиям в составе вида *M. tuberculosis* свойственны различия в строении CRISPR-Cas системы, в том числе редукция части системы у линии Beijing. Для *cas*-генов нами был осуществлен поиск возможных функциональных партнеров и компенсаторных механизмов с использованием метода филогенетического профайлинга. В ходе анализа филогенетических профилей (ФП) были обнаружены гены со сходным характером эволюционных событий. Установлено, что потеря части системы CRISPR-Cas у представителей линии Beijing сопровождалась по крайней мере двумя эволюционными событиями потери и одним событием приобретения участков генома. Возможность изучения альтернативных функций CRISPR-Cas систем у *M. tuberculosis* и их предполагаемая связь с другими генными системами представляет значительный интерес.

Ключевые слова: системы CRISPR-Cas, вирулентность, *M. tuberculosis*, линия Beijing, филогенетический профайлинг

✉ **Для корреспонденции:** Зайчикова Марина Викторовна
ул. Губкина, д. 3, г. Москва, 119991; marinaz15@yandex.ru, valerid@vigg.ru

Статья получена: 15.03.2018 **Статья принята к печати:** 20.03.2018

DOI: 10.24075/vrgmu.2018.016

CRISPR-CAS SYSTEMS IN BACTERIA: STRUCTURE AND CLASSIFICATION

To date, CRISPR-Cas systems have been identified in approximately 40% of bacterial and 90% of archaeal genomes [1, 2]. These systems consist of two essential components: CRISPR (Clustered Regularly Interspaced Short Palindromic Repeats) arrays and Cas (CRISPR-associated) proteins. Repetitive sequences of equal length alternating with unique regions (spacers) were described as early as 1987 in the *E. coli* genome [3], but at that time their function was unclear. In the 2000s, CRISPR-Cas systems were shown to have a role in bacterial immunity [4, 5]. By now, they have been proved to participate in a number of various cellular processes, including DNA repair, regulation of gene expression, virulence formation, etc. [6]. Interestingly, direct repeats (DR) discovered in the *M. tuberculosis* genome as early as 1990s have been used in the genotyping (spoligotyping) of mycobacteria even before the immune function of CRISPR-Cas systems was described, and their polymorphism is well-studied [7, 8].

CRISPR-Cas systems are very diverse. Each functional array contains three essential elements: repeats, spacers and a leader sequence. Adjacent to the array is a set of *cas* genes coding for proteins with various functional domains interacting with nucleic acids [9]. Although the sets of *cas* genes ensuring the performance of different components of CRISPR-Cas molecular mechanisms are different, they do have common features. For example, the majority of known active CRISPR-Cas systems contain two proteins called Cas1 and Cas2. These proteins form a complex that integrates new spacers into the array. New spacers are inserted into the array next to the leader sequence. Throughout the array's lifetime some spacers can be lost as a result of recombination between repeats [10]. Partially or fully, the array can be acquired through horizontal gene transfer (HGT) [11].

CRISPR-Cas systems are classified based on the composition of their cas-loci. According to the currently used classification, they are subdivided into 2 big classes, 5 types and multiple subtypes [12]. Class 1 (types I, III and IV) comprises CRISPR-Cas systems with multisubunit effector complexes; in class 2 systems (types II and V) all functions of the effector complex are exerted by one protein, such as Cas9 [12]. Type II CRISPR-Cas systems are of paramount importance for biotechnology and specifically for genome editing, but they are quite rare and have been detected only in bacterial genomes [12]. The majority of CRISPR-Cas systems can be unambiguously assigned to one of its 5 main types. However, there are organisms whose cas-loci do not fit into the current classification.

Cas1 and *cas2* genes, the CRISPR-Cas components involved in the integration of new spacers into the array, deserve particular attention. Although there is evidence that both of them have their role in spacer integration, all enzymatic activities necessary for this process can be found in Cas1, whereas the catalytic activity of Cas2 is not required to form a Cas1-Cas2 complex or insert a new spacer. So far, we know that Cas2 is an mRNA interferase that specifically cleaves ribosome-bound mRNA. On the face of it, such activity seems to be "inappropriate" when it comes to the integration of new spacers. However, some researchers suggest that Cas2 may have originated from ancient mobile elements, such as toxin-antitoxin (TA) systems [13, 14]. In view of this, it may be assumed that Cas2 retains its ancestral toxin-like endo-ribonuclease activity in the CRISPR-Cas system, but the latter is reversely controlled through inhibition during interaction with Cas1 and formation of the Cas1-Cas2 complex. According to this hypothesis, if the CRISPR-Cas system fails to inhibit viral growth, Cas2 is activated (possibly through Cas1 degradation) and stops translation, driving the cell to suicide or into the dormant state. Cas2 participation in spacer integration may be connected to Cas1 regulation or stabilization following the formation of Cas1-Cas2 complex, which at the same time reversely inactivates Cas2 [15]. The possible participation of Cas2 in getting the cell into a persistent state is a promising area of pathogen research (*M. tuberculosis* research, in particular).

FUNCTIONS OF CRISPR-CAS SYSTEMS IN BACTERIA

Because CRISPR-Cas systems are widely spread and very diverse, it is no wonder why more evidence of their involvement in different cellular processes appears in the literature [6]. Apart from the role in the adaptive immunity, the most well-known and well-described of CRISPR-Cas functions is regulation of gene expression. For example, the life cycle of the soil bacteria *Myxococcus xanthus* includes stages of fruit body formation and sporulation. Formation of the fruit body and further differentiation of its cells into microspores is rigorously regulated by intercellular signals and intracellular signaling cascades in which type I-C CRISPR-Cas systems of *M. xanthus* act as a component of the positive feedback loop and participate in sporulation [16].

Today, there is evidence that CRISPR-Cas systems can engage in DNA repair. It has been established that purified Cas1 (YgbT) obtained from *Escherichia coli* is capable of interaction, both at the physical and genetic levels, with key components of DNA repair systems, such as genes *recB*, *recC* and *ruvB* [17]. The researchers have demonstrated that the *ygbT* deletion strain has increased sensitivity to DNA damage.

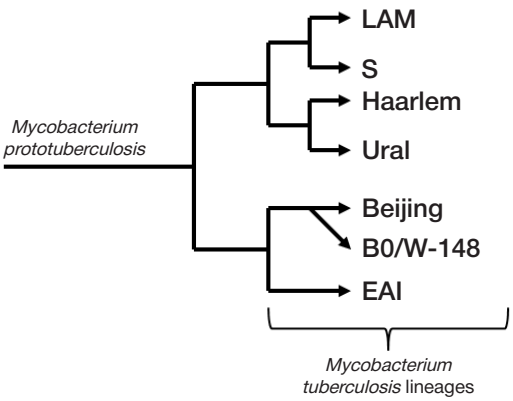

Fig. 1. The schematic representation of the phylogeny of the described *M. tuberculosis* lineages [33]

Similar phenotypes have been observed in the strains with a deleted CRISPR cluster; this indicates, at least, that some of CRISPR-Cas components are involved in DNA repair.

Another alternative function of CRISPR-Cas systems pertains to their participation in biofilm formation [18]. The study of the type 1-F CRISPR-Cas systems of the opportunistic pathogen *Pseudomonas aeruginosa* has revealed that this system inhibits biofilm formation. Such CRISPR-dependent ability relies on the interaction between a certain spacer and its prototype, the protospacer located in the bacteriophage genome. This interaction eventually leads to the induction of phage-related genes that, in turn, trigger death of surface cells. These findings suggest that CRISPR-Cas systems possess another mechanism unrelated to the adaptive immunity.

Bacteria usually regulate their gene expression post-transcriptionally by various small non-coding RNA. Although these RNA molecules control a great deal of cell physiology, only a few of them participate in the recognition of intrusive nucleic acids, ceding this role to CRISPR-Cas systems. Unlike eukaryotic systems, bacterial CRIPSR-Cas systems cleave DNA, which means that if they should engage in the regulation of endogenous genes, the bacterial chromosome will be inevitably destroyed. Surprisingly, though, in 2013 an article was published in *Nature* reporting a mechanism of post-transcriptional regulation in *Francisella novicida*, in which the virulence gene is regulated by the Cas9 protein and CRISPR-associated small RNA [19]. Hypothetically, Cas9 directs its activity against endogenous mRNA (but not DNA). So far, the association between CRIPSR-Cas systems and the ability of bacterial strains to exhibit increased virulence or even drug resistance has been shown in a number of research works [20].

Speaking of alternative functions of CRIPSR-Cas systems, some authors hypothesize that biofilm formation in *Pseudomonas aeruginosa* is a by-product of a "classical" CRISPR-Cas immune function, whereas virulence in *Francisella novicida* or development regulation in *Myxococcus xanthus* have come about independently [6]. The history of gradual discovery of different CRIPSR-Cas functions, starting with immune, resembles the exploration of RNA interference in eukaryotes. At first, RNA interference was shown to have a role in the immune defense, and it was not until later that its effects on various cellular processes were discovered, including gene regulation and heterochromatin formation [21]. Some authors draw a parallel between CRISPR-Cas systems and RNA interference [22, 23].

CRISPR-CAS SYSTEMS IN MYCOBACTERIA: GENERAL STRUCTURE AND PECULIARITIES OF CAS-OPERONE IN *M. TUBERCULOSIS* H37RV

The *Mycobacterium* genus is represented by a wide range of organisms, including human pathogens among which members of the Mycobacterium tuberculosis complex (MTBC) are the most important. This complex includes *Mycobacterium tuberculosis*, the major causative agent of tuberculosis. *M. tuberculosis* is genetically heterogenous and can be divided into several groups, or the so-called lineages. Each lineage is characterized by a certain set of mutations that have accumulated in the course of evolution [24–26]. Isolates of different lineages can be distinguished by their phenotype, specifically by the ability to develop drug resistance (DR), virulence and pathogenicity, all of which determine the severity of the disease [27, 28]. The most widespread and clinically significant lineages of *M. tuberculosis* are Beijing, Haarlem, LAM, and S. The Beijing lineage (in particular, the B0/W-148 sublineage that has emerged recently) is the most epidemiologically important one due to its high prevalence and propensity to develop DR [29, 30]. The Haarlem lineage is characterized by increased virulence [28]. Of certain interest are the lineages EAI and Ural, with their reduced virulence that makes them less prevalent [28]. EAI is an ancient lineage territorially limited to South East Asia [31]. Related to Haarlem, the Ural line is not very widespread, just like EAI, and appears to have reduced transmissibility [32] (Fig. 1).

Given its possible role in virulence formation [19, 20], CRISPR-Cas systems could become an interesting research object, especially in different *M. tuberculosis* lineages.

To date, CRISPR-Cas systems have been identified in 14 mycobacterial species [34]. All such systems are located on a chromosome. CRISPR arrays with more than 5 repeats have been identified in only 3 mycobacterial species: *M. tuberculosis* and *M. bovis*, which belong to the MTBC, and in the pathogenic *M. avium*. *M. avium* misses cas-genes that should be adjacent to the CRISPR array, and CRISPR loci in *M. tuberculosis* and

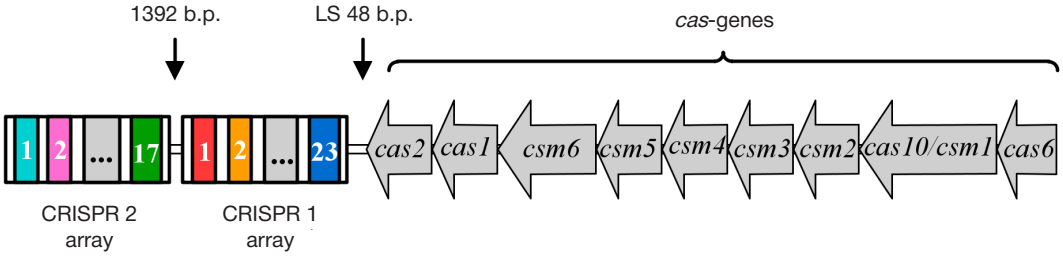

Fig. 2. Schematic of CRISPR-Cas structure in *M. tuberculosis* exemplified by the strain H37Rv. LS is leader sequence

Table 1. The comparative analysis of *cas*-genes found in 6 different lineages and one sublineage of *M. tuberculosis*

Lineage \ Gene	*cas2*	*cas1*	*csm6*	*csm5*	*csm4*	*csm3*	*csm2*	*cas10*	*cas6*
Beijing и B0/W-148	missing				100%	99%	100%	99%	100%
EAI	100%*	100%	100%	100%		100%			
Haarlem									
Ural			99%						
S				99%		99%			
LAM									

Note: * — represents percent identity computed in BLAST (https://blast.ncbi.nlm.nih.gov/Blast.cgi).

M. bovis are very similar in terms of their structure. This reflects a close evolutionary relationship between them and is consistent with their phylogeny [34, 35]. *M. tuberculosis* CRISPR-Cas systems have a structure typically found in type III-A systems [34].

We have analyzed the CRISPR-Cas systems in 41 complete genome sequences of different *M. tuberculosis* lineages available in the NCBI RefSeq database, including 13 Beijing genomes, 3 B0/W-148 genomes, 2 EAI genomes, 10 Haarlem genomes, 1 Ural genome, 2 S genomes, and 10 LAM genomes. Additionally, we have analyzed a few draft genomes, including 7 B0/W-148 genomes, 4 URAL genomes, 3 EAI genomes, and 3 S genomes, the reason being the low number of complete genomes available. Genotyping was based on marker polymorphisms [36–38]. For some genomes the genotype of the isolate was already known from the literature. The search and analysis of CRISPR-Cas systems was conducted using two algorithms: CRISPRFinder and CRISPR Recognition Tool [39, 40]. Fig. 2 shows a typical structure of *M. tuberculosis* CRISPR-Cas systems exemplified by the H37Rv strain, the standard reference genome.

The majority of the analyzed *M. tuberculosis* strains had two long CRISPR-arrays (Fig. 2) [8]. The only exception was the strain 7199-99, which belongs to the Haarlem lineage; its CRISPR2 array had been reduced starting from spacer 12 and including the region between the arrays, leading to the formation of a single array of 33 spacers. The largest number of spacers in an *M. tuberculosis* genome is 57 [8], the smallest is 10, as was the case with some of B0/W-148 strains. Adjacent to the CRISPR1 array were 9 *cas*-genes, namely *cas2*, *cas1*, *csm6*, *csm5*, *csm4*, *csm3*, *csm2*, *cas10* (*csm1*), and *cas6* (Fig.2). The *cas*-genes of *M. tuberculosis* are highly conserved. In our study no mutations were detected in *cas1*, *cas2*, *csm4*, *csm2* and *cas6*. Other analyzed genes had single random mutations (Table 1). The CRISPR2 array was separated from the CRISPR1 array by a sequence of ~ 1300 b.p. (Fig. 2) containing two annotated transposases that belong to the IS*6110* family [34]. Of note, the CRISPR-Cas systems of *M. tuberculosis* typically have a short leader sequence of 48 b.p. [34].

DISTINCTIVE CHARACTERISTICS OF CRISPR-CAS SYSTEMS IN DIFFERENT *M. TUBERCULOSIS* LINEAGES

Beijing lineage

The region containing *cas1*, *cas2*, *csm5*, *csm6* (Table 1) and the CRISPR1 array were missing in the analyzed Beijing isolates [8,

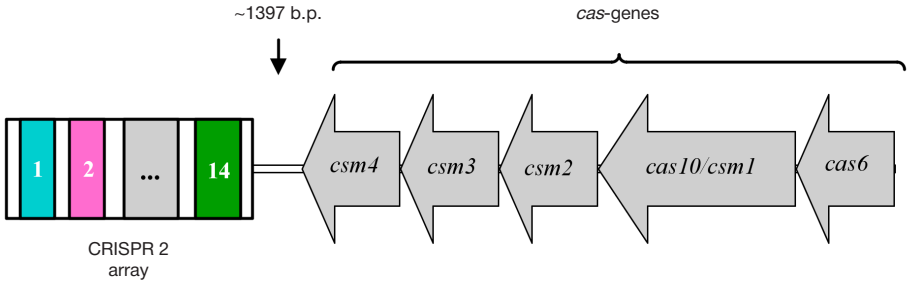

Fig. 3. The structure of the CRISPR-Cas system of the *M. tuberculosis* Beijing lineage. Ten highly conserved spacers shared by all *M. tuberculosis* lineages are located at the end of the CRISPR2 array distal to the leader sequence and are ancestral spacers mirroring the ancient state of CRISPR immunity [10]. More recent spacers are located next to the leader sequence

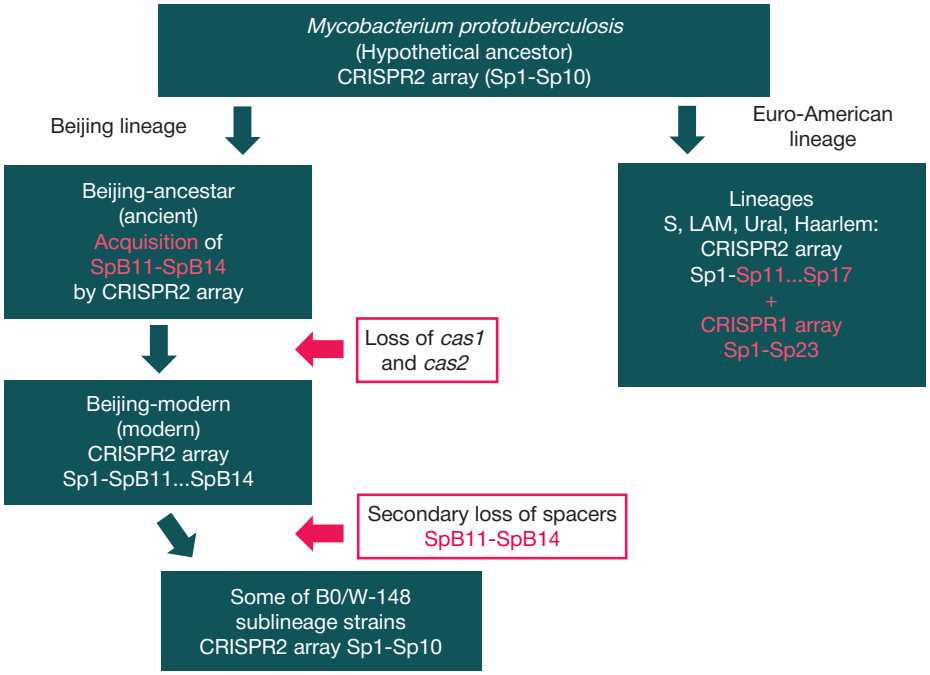

Fig. 4. Evolution of the CRISPR array in the *M. tuberculosis* Beijing lineage. After the first 10 spacers of the CRISPR2 array had been integrated (they are the most ancient ones), the Euro-American and Beijing lines separated. The spacers SpB11-SpB14 of the Beijing lineage are not identical to the spacers Sp11-Sp14 found in other *M. tuberculosis* lineages. Due to the loss of *cas1* and *cas2* genes involved in the integration of new spacers, formation of the CRISPR2 array probably stopped. The CRISPR-Cas structure of the Beijing lineage has remained intact for a long time, but its youngest sublineage B0/W-148 demonstrates a loss of 4 spacers SpB11-SpB14 that are the array's most recent acquisitions

34]. The remaining CRISPR2 array had only 14 spacers instead of 18, of which 10 (Sp1-Sp10) are shared by all *M. tuberculosis* lineages and 4 (SpB11-SpB14, B stands for Beijing) are specific to the Beijing lineage (Fig. 3). These spacers are absent in other *M. tuberculosis* lineages.

Curiously, the majority of the analyzed strains had two annotated transposases in the region between the gene *csm4* and the CRISPR2 array. In the Beijing lineage *csm4* is significantly shorter than its ortholog from other lines: the length of the protein it codes for is either 76 a.a.r. or 116 to 118 a.a.r., whereas in other *M. tuberculosis* lineages the protein length is 302 a.a.r. If the encoded protein is about 100 a.a.r. long, it cannot retain its conserved domains necessary for the interaction with *csm3* inside the *csm1–csm4–csm3* complex [41]. This implies that the interference stage may be disrupted in the Beijing lineage.

The Beijing lineage originated in North China, Korea and Japan about 7, 000 years ago [37] (Fig. 4). It appears that after this lineage separated from others, its CRISPR2 array continued to incorporate CRISPR2-specific SpB11-SpB14 spacers. This could be due to the differences in the environmental factors the pathogen had to face. Then the lineage lost a few *cas*-genes, including *cas1* and *cas2* involved in the integration of new spacers, and the array growth stopped. As a result, representatives of the Beijing line normally have only one array (CRISPR2) with 14 spacers in it. However, some isolates of the evolutionary young Beijing sublineage B0/W-148 appear to have lost a few of them. A number of these isolates lack SpB13 and SpB14, while others have lost all 4 SpB11-SpB14 spacers specific to the Beijing lineage. Interestingly, we have found these 4 spacers in the CRISPR arrays of some *M. bovis* strains.

High frequency of mutations and decreased DNA repair in the Beijing lineage described in the literature [42] may result from the reduction of the CRISPR-Cas system and can be a potential cause of variability and drug resistance observed in the lineage. A hypothesized association between reduced or missing CRISPR-Cas systems and DR is consistent with the findings of the recent study of the *Campylobacter jejuni* pathogen, which demonstrated that the strains causing the most severe gastroenteritis and post-infectious complications have shortened CRISPR-arrays or totally lack the CRISPR-Cas system [20, 43].

Ural and Haarlem lineages

A typical feature of the Ural and Haarlem lineages is spacer insertions. They occur in the CRIPSR array at the locus following the Sp3 spacer. Insertions are found in only some of the analyzed Haarlem isolates and all Ural isolates. Importantly, we observed those spacers in some *M. bovi* and two EAI isolates; therefore, past recombination events and horizontal gene transfer cannot be ruled out.

We also observed a few cases of spacer loss or acquisition by the CRISPR2 array in the Ural and Haarlem lineages. For example, 3 Ural isolates lacked the Sp4-Sp6 spacers in the CRISPR2 array, and 2 Haarlem isolates were missing the Sp6 spacer in it.

EAI lineage

Of all *M. tuberculosis* lineages, EAI has the longest CRISPR-arrays. EAI is one of the most ancient lineages, so this could be the reason. In some isolates, the CRISPR2 array is more than 24 spacers long, and the CRISPR1 array contains over 30 spacers. The largest number of spacers was found in the isolate HN-024: 25 spacers in CRISPR1 and 34 spacers in CRISPR2; some of them were unique.

S and LAM lineages

On the whole, the S and LAM lineages have a canonical *M. tuberculosis* CRISPR-Cas structure (Fig. 2). A certain polymorphism can be observed. For example, one LAM isolate was missing the Sp4-Sp6 spacers in its CRISPR1 array, and another LAM isolate had lost the Sp20 spacer from the same array.

To sum up, the CRISPR1 array of *M. tuberculosis* is highly variable and therefore can be conveniently used in genotyping [8]. Although spacer deletions are common, they almost never occur in 10 highly conserved ancestral CRISPR2 spacers Sp1-Sp10 distal to the leader sequence. The same is true for mutations. Protospacers of Sp1-Sp10 remain unidentified. Although ancient spacers are regarded as barely significant because of their high variability and a rapid evolution of prophages which they protected the bacteria against, they look intact in all analyzed *M. tuberculosis* lineages and do not undergo deletions. This brings in another possible explanation: the Sp1-Sp10 spacers are vital for bacteria, and their role is yet to be elucidated.

THE SEARCH FOR FUNCTIONALLY RELATED PARTNERS AND COMPENSATORY MECHANISMS IN THE BEIJING LINEAGE WITH REDUCED CRISPR-CAS SYSTEMS

The search for functionally related partners and mechanisms compensating for the functions of *cas1*, *cas2*, *csm5*, and *csm6* in the Beijing lineage was conducted using a method of phylogenetic profiling and the genomic sequences of different *M. tuberculosis* lineages (in total, 130 complete genome sequences available in NCBI were analyzed). The phylogenetic profile (PP) is a binary vector determining the presence of a sequence coding for a protein of interest in the genomes of a group of organisms [44]. Hypothetically, the evolution of genes belonging to the same functional pathway happens simultaneously, therefore the genes with similar or inverted PP can be used as functionally related candidate partners or candidate compensatory mechanisms, respectively.

Using phylogenetic profiling we identified orthologous gene groups in different *M. tuberculosis* lineages, constructed binary vectors and a pairwise distance matrix for the vectors, and performed PP clusterization. Construction and visualization of PP were done in OrthoFinder v.2.0.0 [45] and Count [46]. The pairwise distance matrix was constructed based on the mutual information values (MI): DMI=1–MI. Cluster analysis was performed using the unweighted pair group method with arithmetic mean (UPGMA) [47].

The cluster analysis of PP allowed us to identify genes that had undergone evolutionary events similar to those undergone by *cas1*, *cas2*, *csm5*, and *csm6* (Fig. 5, A). The loss of some CRISPR-Cas components in a number of Beijing isolates of *M. tuberculosis* may have been accompanied by at least two evolutionary losses and one acquisition of a genome region (in different regions of a chromosome) (Fig.5 B and C).

The analysis of PP of Beijing *M. tuberculosis* genomes revealed long deletions specific to this lineage. Because of those deletions, the orthologs of Rv0071, Rv0072, Rv0073 and Rv1761c, Rv1760, Rv1758 (identifiers correspond to the genes in the *M. tuberculosis* H37Rv genome; see Table 2) now have similar phylogenetic profiles (partner profiles, Fig. 5B). It should be noted that the chromosomal region harboring

genes Rv1761c, Rv1760 and Rv1758 is flanked with the inverted repeats of IS*6110* IS-elements belonging to the IS3 family. In the second round of the analysis, a long insertion was revealed specific to the Beijing lineage; because of that insertion the orthologs of CFBS_RS10335, CFBS_RS10345, CFBS_RS10350, CFBS_RS10355, CFBS_RS10360, CFBS_RS10365, and CFBS_RS21395 (identifiers correspond to the genes in the *M. tuberculosis* CCDC5079 genome) (Table 2) now have phylogenetic profiles very much resembling inverted profiles (compensator profiles, Fig. 5 C).

To sum up, our PP analysis has identified a number of genes that have undergone similar evolutionary events. The loss of *cas1*, *cas2*, *csm5*, and *csm6* in the Beijing lineage of *M. tuberculosis* was accompanied by the loss and acquisition of other genes (Table 2). Those candidate genes have a potential to participate in the mechanisms of compensation for cas-gene functions or be their functionally related partners in *M. tuberculosis*, creating a subject for further research.

CONCLUSION

The CRISPR-Cas systems of *M. tuberculosis* vary considerably between the lineages: some (EAI) have long arrays, others (Beijing) are partially reduced. Therefore, the presence of an active type III-A CRISPR-Cas system is not an essential prerequisite for the evolutionary success in terms of pathogenicity, virulence, transmissibility and adaptability of the lineage.

The partial loss of the array and a few *cas*-genes in the Beijing lineage of *M. tuberculosis* seems to have resulted in a fully or partially lost ability of their CRISPR-Cas to destroy a foreign DNA. Disturbances in the functioning of the CRISPR-Cas system in one of the most successful *M. tuberculosis* lineages may have been accompanied by the activation of mechanisms compensating for the lost genes (for example, our analysis revealed a long insertion in the Beijing lineage) and by the loss of the functional partners of *cas*-genes; because it is assumed that the gene that has lost its functional partner will not be retained through selection in the genome and will be eliminated, which can be illustrated by the detected long deletions specific to the Beijing lineage. It should be noted that the observed regularities in the pattern of evolutionary losses and acquisitions could be random and require further experimental verification. Phylogenetic profiling provides a basis for generating a hypothesis and material for further research.

Although the CRISPR-Cas system of *M. tuberculosis* Beijing strains can be inactive, it is assumed that in the lineages that have a full set of *cas*-genes and repeats, the CRISPR-Cas system retains its activity and is capable of contributing to the defense against foreign DNA [34]. Considering a short leader sequence typical for all CRISPR-Cas systems of *M. tuberculosis*, it may be more productive to focus on the exploration of their alternative functions, such as regulation of gene expression, DNA repair, virulence formation, etc.

The structure of *M. tuberculosis* CRISPR-Cas systems has been studied and described in great detail [8], but the

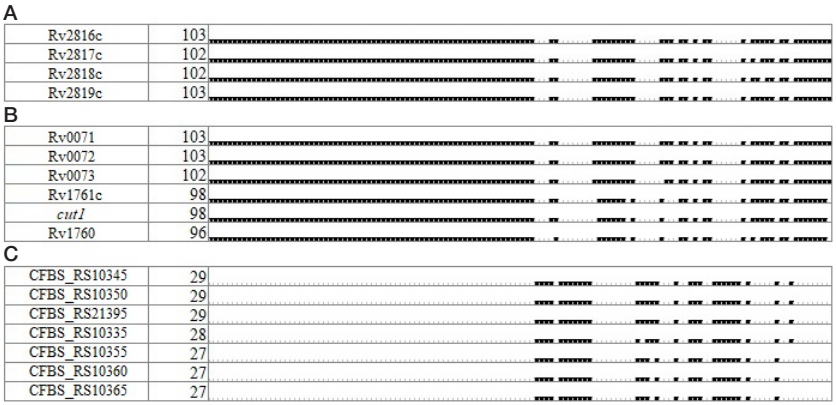

Fig. 5. Phylogenetic profiles of genes found in the genomes of different *M. tuberculosis* lineages and strains. Each line contains gene ID, the number of genomes with an orthologous gene and the PP of the gene; spaces represent missing genes. **A**. PP of *cas*-genes of *M. tuberculosis* H37Rv: *cas2* (Rv2816c), *cas1* (Rv2817c), *csm6* (Rv2818c), and *csm5* (Rv2819c). **B**. PP of candidate functionally related partners of *M. tuberculosis cas*-genes in the genome of the H37Rv strain. **C**. PP of genes putatively involved in the formation of compensatory mechanisms in the genome of the CCDC5079 strain (the Beijing lineage) following the loss of some CRISPR-Cas parts

Table 2. Characteristics of functional partner candidates and genes involved in the compensatory mechanisms for CRISPR-Cas systems*

Evolutionary event	Gene ID	Product (protein)	Protein function
Insertion	CFBS_RS10360 (*tuf*)	Iron-regulated elongation factor Tu Tuf	Participates in protein translation
	CFBS_RS10365	MDR-dehydrogenase	MDR-dehydrogenases exert different activities, such as alcohol dehydrogenase activity, quinone reductase activity, sorbitol dehydrogenase activity, formaldehyde dehydrogenase activity, keto reductase activity, and others
Deletion	Rv1758 (*cut1*)	Cutinase	Enzyme that catalyzes cutin hydrolysis [48]
	Rv1760	Diacylglycerol acyltransferases	Catalyzes final stages of biosynthesis of triacylglycerol and other components of mycobacterial cell wall [49]
	Rv0072	Glutamine ABC transporter permease	ABC transporter, participates in glutamine transport (permease); may be responsible for substrate translocation across the membrane [50]
	Rv0073	Glutamine ABC transporter ATP-binding protein	ABC transporter, participates in glutamine transport (the binding protein); may be responsible for energy coupling to the transport system [50]

Note: * — only annotated genes are presented in this table; other genes code for hypothetical proteins with unknown functions (Rv1761c and CFBS_RS10335, CFBS_RS10345, CFBS_RS10350, CFBS_RS10355, CFBS_RS21395) or, as with Rv0071, are a mobile self-splicing retro-element, the so-called group II intron.

role of these systems is still unclear. For the majority of mycobacterial spacers, no protospacers among the known mycobacteriophage have been identified so far. This is probably because the majority of *M. tuberculosis* bacteriophages have been isolated from *M. smegmatis* and then tested for their ability to invade *M. tuberculosis*. [34]. Different lineages have different sets of spacers and therefore – possibly – different immunity, which means varying degrees of resistance to phages and different regulation of gene expression. Apart from spacers, of interest is the role of the Cas2 protein outside the Cas1-Cas2 complex, in light of the previously proposed hypothesis [15] suggesting that with independent activation this protein can stop translation and drive the cell into the dormant state or promote apoptosis. A search for Cas2 inhibitors also presents a certain interest. Particular attention should be paid to the possible functional link between CRISPR-Cas systems, specifically the *cas*-genes, and TA-systems [38]. Possible participation of CRISPR-Cas systems in virulence formation and drug resistance may allow to develop novel approaches to combating drug-resistant strains of *M. tuberculosis*.

References

1. Marraffini LA, Sontheimer EJ. CRISPR interference: RNA-directed adaptive immunity in bacteria and archaea. Nat Rev Genet. 2010; 11 (3): 181–190.
2. Grissa I, Vergnaud G, Pourcel C. The CRISPRdb database and tools to display CRISPRs and to generate dictionaries of spacers and repeats. BMC Bioinformatics. 2007; 8: 172. DOI: 10.1186/1471-2105-8-172.
3. Ishino Y, Shinagawa H, Makino K, Amemura M, Nakata A. Nucleotide sequence of the iap gene, responsible for alkaline phosphatase isozyme conversion in Escherichia coli, and identification of the gene product. J Bacteriol. 1987; 169 (12): 5429–33.
4. Bolotin A, Quinquis B, Sorokin A, Ehrlich SD. Clustered regularly interspaced short palindrome repeats (CRISPRs) have spacers of extrachromosomal origin. Microbiology. 2005; 151 (8): 2551–61.
5. Barrangou R, Fremaux C, Deveau H, Richards M, Boyaval P, Moineau S, Romero DA, Horvath P. CRISPR provides acquired resistance against viruses in prokaryotes. Science. 2007; 315: 1709–1712.
6. Westra ER, Buckling A, Fineran PC. CRISPR-Cas systems: beyond adaptive immunity. Nat Rev Microbiol. 2014; 12 (5): 317–326. DOI: 10.1038/nrmicro3241.
7. Kamerbeek J, Schouls L, Kolk A, van Agterveld M, van Soolingen D, Kuijper S, et al. Simultaneous detection and strain differentiation of Mycobacterium tuberculosis for diagnosis and epidemiology. J Clin Microbiol. 1997; 35 (4): 907–14.
8. van Embden JD, van Gorkom T, Kremer K, Jansen R, van Der Zeijst BA, Schouls LM. Genetic variation and evolutionary origin of the direct repeat locus of Mycobacterium tuberculosis complex bacteria. J Bacteriol. 2000 May; 182 (9): 2393–401.
9. Haft DH, Selengut J, Mongodin EF, Nelson KE. A guild of 45 CRISPRassociated (Cas) protein families and multiple CRISPR/Cas subtypes exist in prokaryotic genomes. PLoS Comput Biol. 2005; 1 (6): e60.
10. Gogleva AA, Gelfand MS, Artamonova II. Comparative analysis of CRISPR cassettes from the human gut metagenomic contigs. BMC Genomics. 2014; 15 (1): 202. DOI: 10.1186/1471-2164-15-202.
11. Takeuchi N, Wolf YI, Makarova KS, Koonin EV. Nature and Intensity of Selection Pressure on CRISPR-Associated Genes. J Bacteriol. 2012; 194 (5): 1216–25.
12. Makarova KS, Wolf YI, Alkhnbashi OS, et al. An updated evolutionary classification of CRISPR–Cas systems. Nature reviews Microbiology. 2015; 13 (11): 722–36. DOI: 10.1038/nrmicro3569.
13. Makarova KS, Zhang F, Koonin EV. SnapShot: Class 1 CRISPR-Cas Systems. Cell. 2017; 168 (5): 946–46.
14. Goeders N, van Melderen L. Toxin-Antitoxin Systems as Multilevel Interaction Systems. Toxins. 2014; 6 (1): 304–24.
15. Makarova KS, Anantharaman V, Aravind L, Koonin EV. Live virus-free or die: coupling of antivirus immunity and programmed suicide or dormancy in prokaryotes. Biol Direct. 2012; 7: 40.
16. Viswanathan P, Murphy K, Julien B, Garza AG, Kroos L. Regulation of dev, an Operon That Includes Genes Essential for Myxococcus xanthus Development and CRISPR-Associated Genes and Repeats. Journal of Bacteriology. 2007; 189 (10): 3738–50.
17. Babu M, Beloglazova N, Flick R, Graham C, Skarina T, Nocek B, et al. A dual function of the CRISPR-Cas system in bacterial antivirus immunity and DNA repair. Mol Microbiol. 2011; 79 (2): 484–502.
18. Heussler GE, Cady KC, Koeppen K, Bhuju S, Stanton BA, O'Toole GA. Clustered Regularly Interspaced Short Palindromic Repeat-Dependent, Biofilm-Specific Death of Pseudomonas aeruginosa Mediated by Increased Expression of Phage-Related Genes. mBio. 2015; 6 (3): e00129-15.
19. Sampson TR, Saroj SD, Llewellyn AC, Tzeng Y-L, Weiss DS. A CRISPR/Cas system mediates bacterial innate immune evasion and virulence. Nature. 2013; 497: 254–257.
20. Louwen R, Horst-Kreft D, de Boer AG, van der Graaf L, de Knegt G, Hamersma M, et al. A novel link between Campylobacter jejuni bacteriophage defence, virulence and Guillain-Barré syndrome. Eur J Clin Microbiol Infect Dis. 2013; 32 (2): 207–26.
21. Wiedenheft B, Sternberg SH, Doudna JA. RNA-guided genetic silencing systems in bacteria and archaea. Nature. 2012; 482, 331–38.
22. Bhaya D, Davison M, Barrangou R. CRISPR-Cas systems in bacteria and archaea: versatile small RNAs for adaptive defense and regulation. Annu Rev Genet. 2011; 45: 273–97.
23. Makarova KS, Grishin NV, Shabalina SA, Wolf YI, Koonin EV. A putative RNA-interference-based immune system in prokaryotes: computational analysis of the predicted enzymatic machinery, functional analogies with eukaryotic RNAi, and hypothetical mechanisms of action. Biology Direct. 2006; 1: 7.
24. Gagneux S, Small PM. Global phylogeography of Mycobacterium tuberculosis and implications for tuberculosis product development. Lancet Infect Dis. 2007; 7 (5): 328–37.
25. Prozorov AA, Danilenko VN. Mycobacterii tuberculoznogo kompleksa: genomika, molekularnaja epidemiologija, puti evoluzii. Uspehi sovremennoy biologii. 2011; 1 (6): 483–95.
26. Jagielski T, van Ingen J, Rastogi N, Dziadek J, Mazur PK, Bielecki J. Current methods in the molecular typing of Mycobacterium tuberculosis and other Mycobacteria. Biomed Res Int. 2014; 2014:645802.
27. Prozorov AA, Fedorova IA, Bekker OB, Danilenko VN. Faktory virulentnosti Mycobacterium tuberculosis: geneticheskiy kontrol, novie konzepzii. Genetika. 2014; 50 (8): 775–97.
28. Reiling N, Homolka S, Walter K, Brandenburg J, Niwinski L, Ernst M et al. Clade specific virulence patterns of Mycobacterium tuberculosis complex strains in human primarymacrophages and aerogenically infected mice. MBio. 2013; 4 (4): pii: e00250-13.
29. Lasunskaia E, Ribeiro SC, Manicheva O, Gomes LL, Suffys PN, Mokrousov I, et al. Emerging multidrug resistant Mycobacterium tuberculosis strains of the Beijing genotype circulating in Russia express a pattern of biological properties associated with enhanced virulence. Microbes Infect. 2010; 12 (6): 467–75.
30. Hanekom M, Gey van Pittius NC, McEvoy C, Victor TC, Van Helden PD, Warren RM. Mycobacterium tuberculosis Beijing genotype: a template for success. Tuberculosis (Edinb). 2011; 91 (6): 510–23.
31. Wirth T, Hildebrand F, Allix-Béguec C, Wölbeling F, Kubica T,

Kremer K, et al. Origin, spread and demography of the Mycobacterium tuberculosis complex. PLoS Pathog. 2008; 4 (9): e1000160.
32. Mokrousov I. The quiet and controversial: Ural family of Mycobacterium tuberculosis. Infect Genet Evol. 2012; 12 (4): 619–29.
33. Mikheecheva NE, Zaychikova MV, Melerzanov AV, Danilenko VN. A nonsynonymous SNP catalog of Mycobacterium tuberculosis virulence genes and its use for detecting new potentially virulent sublineages. Genome BiolEvol. 2017; 9 (4): 887–99.
34. He L, Fan X, Xie J. Comparative genomic structures of Mycobacterium CRISPR-Cas. J Cell Biochem. 2012; 113 (7): 2464–73.
35. Brosch R, Pym AS, Gordon SV, Cole ST. The evolution of mycobacterial pathogenicity: clues from comparative genomics. Trends Microbiol. 2001; 9 (9): 452–58.
36. Homolka S, Projahn M, Feuerriegel S, Ubben T, Diel R, Nübel U et al. High resolution discrimination of clinical Mycobacterium tuberculosis complex strains based on single nucleotide polymorphisms. PLoS One. 2012; 7 (7): e39855.
37. Merker M, Blin C, Mona S, Duforet-Frebourg N, Lecher S, Willery E, et al. Evolutionary history and global spread of the Mycobacterium tuberculosis Beijing lineage. Nat Genet. 2015; 47 (3): 242–49.
38. Zaychikova MV, Zakharevich NV, Sagaidak MO, Bogolubova NA, Smirnova TG, Andreevskaya SN, et al. Mycobacterium tuberculosis Type II Toxin-Antitoxin Systems: Genetic Polymorphisms and Functional Properties and the Possibility of Their Use for Genotyping. PLoS One. 2015; 10: e0143682
39. Bland C, Ramsey TL, Sabree F, Lowe M, Brown K, Kyrpides NC et al. CRISPR recognition tool (CRT): a tool for automatic detection of clustered regularly interspaced palindromic repeats. BMC Bioinformatics. 2007; 8: 209.
40. Grissa I, Vergnaud G, Pourcel C. CRISPRFinder: a web tool to identify clustered regularly interspaced short palindromic repeats. Nucleic Acids Res. 2007; 35: 52–57.
41. Numata T, Inanaga H, Sato C, Osawa T. Crystal structure of the Csm3-Csm4 subcomplex in the type III-A CRISPR-Cas interference complex. J Mol Biol. 2015; 427 (2): 259–73.
42. Mestre O, Luo T, Dos Vultos T, Kremer K, Murray A, Namouchi A, et al. Phylogeny of Mycobacterium tuberculosis Beijing strains constructed from polymorphisms in genes involved in DNA replication, recombination and repair. PLoS One. 2011; 6 (1): e16020.
43. Freidlin PJ, Nissan I, Luria A, Goldblatt D, Schaffer L, Kaidar-Shwartz H, et al. Structure and variation of CRISPR and CRISPR-flanking regions in deleted-direct repeat region Mycobacterium tuberculosis complex strains. BMC Genomics. 2017; 18 (1): 168.
44. Pellegrini M, Marcotte EM, Thompson MJ, Eisenberg D, Yeates TO. Assigning protein functions by comparative genome analysis: protein phylogenetic profiles. Proc. Natl. Acad. Sci. USA. 1999; 96 (8): 4285–8.
45. Emms DM, Kelly S. OrthoFinder: solving fundamental biases in whole genome comparisons dramatically improves orthogroup inference accuracy. Genome Biology. 2015; 16: 157.
46. Count CM.: evolutionary analysis of phylogenetic profiles with parsimony and likelihood. Bioinformatics. 2010; 26 (15): 1910–2.
47. Sokal R, Michener C. A statistical method for evaluating systematic relationships. University of Kansas Science Bulletin. 1958; 38: 1409–1438.
48. Monu, Meena LS. Roles of Triolein and Lipolytic Protein in the Pathogenesis and Survival of Mycobacterium tuberculosis: a Novel Therapeutic Approach. Appl Biochem Biotechnol. 2016; 178 (7): 1377–89.
49. Deb C, Lee CM, Dubey VS, Daniel J, Abomoelak B, Sirakova TD, et al. A Novel In Vitro Multiple-Stress Dormancy Model for Mycobacterium tuberculosis Generates a Lipid-Loaded, Drug-Tolerant, Dormant Pathogen. PLoS ONE. 2009; 4 (6): e6077.
50. Braibant M, Gilot P, Content J. The ATP binding cassette (ABC) transport systems of Mycobacterium tuberculosis. FEMS Microbiol Rev. 2000; 24 (4): 449–67.

Литература

1. Marraffini LA, Sontheimer EJ. CRISPR interference: RNA-directed adaptive immunity in bacteria and archaea. Nat Rev Genet. 2010; 11 (3): 181–190.
2. Grissa I, Vergnaud G, Pourcel C. The CRISPRdb database and tools to display CRISPRs and to generate dictionaries of spacers and repeats. BMC Bioinformatics. 2007; 8: 172. doi:10.1186/1471-2105-8-172.
3. Ishino Y, Shinagawa H, Makino K, Amemura M, Nakata A. Nucleotide sequence of the iap gene, responsible for alkaline phosphatase isozyme conversion in Escherichia coli, and identification of the gene product. J Bacteriol. 1987; 169 (12): 5429–33.
4. Bolotin A, Quinquis B, Sorokin A, Ehrlich SD. Clustered regularly interspaced short palindrome repeats (CRISPRs) have spacers of extrachromosomal origin. Microbiology. 2005; 151 (8): 2551–61.
5. Barrangou R, Fremaux C, Deveau H, Richards M, Boyaval P, Moineau S, Romero DA, Horvath P. CRISPR provides acquired resistance against viruses in prokaryotes. Science. 2007; 315: 1709–1712.
6. Westra ER, Buckling A, Fineran PC. CRISPR-Cas systems: beyond adaptive immunity. Nat Rev Microbiol. 2014; 12 (5): 317–326. DOI: 10.1038/nrmicro3241.
7. Kamerbeek J, Schouls L, Kolk A, van Agterveld M, van Soolingen D, Kuijper S, et al. Simultaneous detection and strain differentiation of Mycobacterium tuberculosis for diagnosis and epidemiology. Journal of Clinical Microbiology. 1997; 35 (4): 907–14.
8. van Embden JD, van Gorkom T, Kremer K, Jansen R, van Der Zeijst BA, Schouls LM. Genetic variation and evolutionary origin of the direct repeat locus of Mycobacterium tuberculosis complex bacteria. J Bacteriol. 2000 May; 182 (9): 2393–401.
9. Haft DH, Selengut J, Mongodin EF, Nelson KE. A guild of 45 CRISPRassociated (Cas) protein families and multiple CRISPR/Cas subtypes exist in prokaryotic genomes. PLoS Comput Biol. 2005; 1 (6): e60.
10. Gogleva AA, Gelfand MS, Artamonova II. Comparative analysis of CRISPR cassettes from the human gut metagenomic contigs. BMC Genomics. 2014; 15 (1): 202. DOI:10.1186/1471-2164-15-202.
11. Takeuchi N, Wolf YI, Makarova KS, Koonin EV. Nature and Intensity of Selection Pressure on CRISPR-Associated Genes. J Bacteriol. 2012; 194 (5): 1216–25.
12. Makarova KS, Wolf YI, Alkhnbashi OS, et al. An updated evolutionary classification of CRISPR–Cas systems. Nature reviews Microbiology. 2015; 13 (11): 722–36. DOI:10.1038/nrmicro3569.
13. Makarova KS, Zhang F, Koonin EV. SnapShot: Class 1 CRISPR-Cas Systems. Cell. 2017; 168 (5): 946–46.
14. Goeders N, van Melderen L. Toxin-Antitoxin Systems as Multilevel Interaction Systems. Toxins. 2014; 6 (1): 304–24.
15. Makarova KS, Anantharaman V, Aravind L, Koonin EV. Live virus-free or die: coupling of antivirus immunity and programmed suicide or dormancy in prokaryotes. Biol Direct. 2012; 7: 40.
16. Viswanathan P, Murphy K, Julien B, Garza AG, Kroos L. Regulation of dev, an Operon That Includes Genes Essential for Myxococcus xanthus Development and CRISPR-Associated Genes and Repeats . J Bacteriol. 2007; 189 (10): 3738–50.
17. Babu M, Beloglazova N, Flick R, Graham C, Skarina T, Nocek B, et al. A dual function of the CRISPR-Cas system in bacterial antivirus immunity and DNA repair. Mol Microbiol. 2011; 79 (2): 484–502.
18. Heussler GE, Cady KC, Koeppen K, Bhuju S, Stanton BA, O'Toole GA. Clustered Regularly Interspaced Short Palindromic

Repeat-Dependent, Biofilm-Specific Death of Pseudomonas aeruginosa Mediated by Increased Expression of Phage-Related Genes. mBio. 2015; 6 (3): e00129-15.
19. Sampson TR, Saroj SD, Llewellyn AC, Tzeng Y-L, Weiss DS. A CRISPR/Cas system mediates bacterial innate immune evasion and virulence. Nature. 2013; 497: 254–7.
20. Louwen R, Horst-Kreft D, de Boer AG, van der Graaf L, de Knegt G, Hamersma M, et al. A novel link between Campylobacter jejuni bacteriophage defence, virulence and Guillain-Barré syndrome. Eur J Clin Microbiol Infect Dis. 2013; 32 (2): 207–26.
21. Wiedenheft B, Sternberg SH, Doudna JA. RNA-guided genetic silencing systems in bacteria and archaea. Nature. 2012; 482, 331–38.
22. Bhaya D, Davison M, Barrangou R. CRISPR-Cas systems in bacteria and archaea: versatile small RNAs for adaptive defense and regulation. Annu Rev Genet. 2011; 45: 273–97.
23. Makarova KS, Grishin NV, Shabalina SA, Wolf YI, Koonin EV. A putative RNA-interference-based immune system in prokaryotes: computational analysis of the predicted enzymatic machinery, functional analogies with eukaryotic RNAi, and hypothetical mechanisms of action. Biology Direct. 2006; 1: 7.
24. Gagneux S, Small PM. Global phylogeography of Mycobacterium tuberculosis and implications for tuberculosis product development. Lancet Infect Dis. 2007; 7 (5): 328–37.
25. Прозоров А. А., Даниленко В. Н. Микобактерии туберкулезного комплекса: геномика, молекулярная эпидемиология, пути эволюции. Успехи современной биологии. 2011; 131 (3): 227–43.
26. Jagielski T, van Ingen J, Rastogi N, Dziadek J, Mazur PK, Bielecki J. Current methods in the molecular typing of Mycobacterium tuberculosis and other Mycobacteria. Biomed Res Int. 2014; 2014:645802.
27. Прозоров А. А., Федорова И.А., Беккер О. Б., Даниленко В. Н. Факторы вирулентности Mycobacterium tuberculosis: генетический контроль, новые концепции. Генетика. 2014; 50 (8): 885–908.
28. Reiling N, Homolka S, Walter K, Brandenburg J, Niwinski L, Ernst M et al. Clade specific virulence patterns of Mycobacterium tuberculosis complex strains in human primarymacrophages and aerogenically infected mice. MBio. 2013; 4 (4): pii: e00250-13.
29. Lasunskaia E, Ribeiro SC, Manicheva O, Gomes LL, Suffys PN, Mokrousov I, et al. Emerging multidrug resistant Mycobacterium tuberculosis strains of the Beijing genotype circulating in Russia express a pattern of biological properties associated with enhanced virulence. Microbes Infect. 2010; 12 (6): 467–75.
30. Hanekom M, Gey van Pittius NC, McEvoy C, Victor TC, Van Helden PD, Warren RM. Mycobacterium tuberculosis Beijing genotype: a template for success. Tuberculosis (Edinb). 2011; 91 (6): 510–23.
31. Wirth T, Hildebrand F, Allix-Béguec C, Wölbeling F, Kubica T, Kremer K, et al. Origin, spread and demography of the Mycobacterium tuberculosis complex. PLoS Pathog. 2008; 4 (9): e1000160.
32. Mokrousov I. The quiet and controversial: Ural family of Mycobacterium tuberculosis. Infect Genet Evol. 2012; 12 (4): 619–29.
33. Mikheecheva NE, Zaychikova MV, Melerzanov AV, Danilenko VN. A nonsynonymous SNP catalog of Mycobacterium tuberculosis virulence genes and its use for detecting new potentially virulent sublineages. Genome Biol Evol. 2017; 9 (4): 887–99.
34. He L, Fan X, Xie J. Comparative genomic structures of Mycobacterium CRISPR-Cas. J Cell Biochem. 2012; 113 (7): 2464–73.
35. Brosch R, Pym AS, Gordon SV, Cole ST. The evolution of mycobacterial pathogenicity: clues from comparative genomics. Trends Microbiol. 2001; 9 (9): 452–58.
36. Homolka S, Projahn M, Feuerriegel S, Ubben T, Diel R, Nübel U et al. High resolution discrimination of clinical Mycobacterium tuberculosis complex strains based on single nucleotide polymorphisms. PLoS One. 2012; 7 (7): e39855.
37. Merker M, Blin C, Mona S, Duforet-Frebourg N, Lecher S, Willery E, et al. Evolutionary history and global spread of the Mycobacterium tuberculosis Beijing lineage. Nat Genet. 2015; 47 (3): 242–49.
38. Zaychikova MV, Zakharevich NV, Sagaidak MO, Bogolubova NA, Smirnova TG, Andreevskaya SN, et al. Mycobacterium tuberculosis Type II Toxin-Antitoxin Systems: Genetic Polymorphisms and Functional Properties and the Possibility of Their Use for Genotyping. PLoS One. 2015; 10: e0143682.
39. Bland C, Ramsey TL, Sabree F, Lowe M, Brown K, Kyrpides NC, et al. CRISPR recognition tool (CRT): a tool for automatic detection of clustered regularly interspaced palindromic repeats. BMC Bioinformatics. 2007; 8: 209.
40. Grissa I, Vergnaud G, Pourcel C. CRISPRFinder: a web tool to identify clustered regularly interspaced short palindromic repeats. Nucleic Acids Res. 2007; 35: 52–7.
41. Numata T, Inanaga H, Sato C, Osawa T. Crystal structure of the Csm3-Csm4 subcomplex in the type III-A CRISPR-Cas interference complex. J Mol Biol. 2015; 427 (2): 259–73.
42. Mestre O, Luo T, Dos Vultos T, Kremer K, Murray A, Namouchi A, et al. Phylogeny of Mycobacterium tuberculosis Beijing strains constructed from polymorphisms in genes involved in DNA replication, recombination and repair. PLoS One. 2011; 6 (1): e16020.
43. Freidlin PJ, Nissan I, Luria A, Goldblatt D, Schaffer L, Kaidar-Shwartz H, et al. Structure and variation of CRISPR and CRISPR-flanking regions in deleted-direct repeat region Mycobacterium tuberculosis complex strains. BMC Genomics. 2017; 18 (1): 168.
44. Pellegrini M, Marcotte EM, Thompson MJ, Eisenberg D, Yeates TO. Assigning protein functions by comparative genome analysis: protein phylogenetic profiles. Proc Natl Acad Sci USA. 1999; 96 (8): 4285–8.
45. Emms DM, Kelly S. OrthoFinder: solving fundamental biases in whole genome comparisons dramatically improves orthogroup inference accuracy. Genome Biology. 2015; 16: 157.
46. Count CM.: evolutionary analysis of phylogenetic profiles with parsimony and likelihood. Bioinformatics. 2010; 26 (15): 1910–2.
47. Sokal R, Michener C. A statistical method for evaluating systematic relationships. University of Kansas Science Bulletin. 1958; 38: 1409–1438.
48. Monu, Meena LS. Roles of Triolein and Lipolytic Protein in the Pathogenesis and Survival of Mycobacterium tuberculosis: a Novel Therapeutic Approach. Appl Biochem Biotechnol. 2016; 178 (7): 1377–89.
49. Deb C, Lee CM, Dubey VS, Daniel J, Abomoelak B, Sirakova TD, et al. A Novel In Vitro Multiple-Stress Dormancy Model for Mycobacterium tuberculosis Generates a Lipid-Loaded, Drug-Tolerant, Dormant Pathogen. PLoS ONE. 2009; 4 (6): e6077.
50. Braibant M, Gilot P, Content J. The ATP binding cassette (ABC) transport systems of Mycobacterium tuberculosis. FEMS Microbiol Rev. 2000; 24 (4): 449–67.

EXPERIMENTAL APPROACHES TO THE TARGET EDITING OF THE *CFTR* GENE USING CRISPR-CAS9

Smirnikhina SA[1] ✉, Anuchina AA[1], Kochergin-Nikitsky KS[1], Adilgereeva EP[1], Yakushina VD[1], Lavrov AV[1,2]

[1] Laboratory of Mutagenesis, Research Centre for Medical Genetics, Moscow

[2] Department of Molecular and Cellular Genetics,
Pirogov Russian National Research Medical University, Moscow

Cystic fibrosis is a severe autosomal recessive disease caused by mutations in the *CFTR* gene. The most common *CFTR* mutation occurring in the European population is F508del. Advances in the management of patients with cystic fibrosis aimed at blocking disease progression have considerably improved the prognosis, but gene therapy has turned to be less effective than expected. Capable of correcting mutations direct in the cells, genome editing, and specifically the CRISPR-Cas9 technology, raises hope of causal treatment for patients with cystic fibrosis. The aim of this work was to compare and improve the efficacy of F508del editing using different combinations of guide RNAs and Cas9. The study was carried out in HEK293T cells. The efficacy of editing was assessed for both plasmid and genomic sites by T7E1 analysis. The best effect was demonstrated by a combination of SaCas9 and sgRNA targeting F508del: 29% of alleles were successfully edited. A combination of SpCas9 and a similar sgRNA showed low efficacy due to the low expression of this guide RNA. All attempts to improve its expression failed. SgRNA stabilization by introducing a G-quadruplex into the sgRNA sequence and adding GG to the 5′-region also did not work. Perhaps, low performance of this guide RNA is determined by its nucleotide sequence, limiting its use.

Keywords: cystic fibrosis, CRISPR-Cas9, *CFTR*, genome editing, F508del mutation, guide RNA

Funding: the section *Editing of the CFTR locus* was supported by the grant of the Russian Science Foundation (Agreement 17-75-20095), the sections *Increasing the expression of guide RNAs* and *Improving the efficacy of CFTR locus editing* were supported by the Russian Academy of Sciences and the state assignment of FASO Russia.

✉ **Correspondence should be addressed:** Svetlana Smirnikhina
Moskvorechie 1, Moscow, 115522; smirnikhinas@gmail.com

Received: 15.03.2018 **Accepted:** 20.03.2018

DOI: 10.24075/brsmu.2018.022

ЭКСПЕРИМЕНТАЛЬНЫЕ ПОДХОДЫ К ТАРГЕТНОМУ РЕДАКТИРОВАНИЮ ГЕНА *CFTR* С ПОМОЩЬЮ CRISPR-CAS9

С. А. Смирнихина[1] ✉, А. А. Анучина[1], К. С. Кочергин-Никитский[1], Э. П. Адильгереева[1], В. Д. Якушина[1], А. В. Лавров[1,2]

[1] Лаборатория мутагенеза, Медико-генетический научный центр, Москва

[2] Кафедра молекулярной и клеточной генетики, медико-биологический факультет,
Российский национальный исследовательский медицинский университет имени Н. И. Пирогова, Москва

Муковисцидоз — тяжелое аутосомно-рецессивное заболевание, обусловленное мутациями в гене *CFTR*, основной из которых в европейской популяции является F508del. Патогенетическая терапия существенно улучшила прогноз для жизни у пациентов с муковисцидозом, однако генная терапия не оказалась такой эффективной, как ожидалось. Геномное редактирование, в том числе с помощью CRISPR-Cas9, открывает новые возможности для этиотропного лечения, так как позволяет исправить мутации в клетках. Целью исследования было сравнение эффективности коррекции мутации F508del с помощью различных комбинаций направляющих РНК и Cas9 и повышение эффективности редактирования. Работу проводили на культуре клеток HEK293T, эффективность редактирования генома оценивали с помощью анализа T7E1, как на геномном, так и на плазмидном сайтах. Наиболее эффективной оказалась комбинация SaCas9 вместе с РНК на мутацию F508del — произошло редактирование 29% аллелей. Комбинация аналогичной направляющей РНК на F508del для SpCas9 показала небольшую эффективность редактирования, что связано с низкой экспрессией направляющей РНК. Были предприняты попытки увеличения экспрессии данной РНК с помощью разных подходов, однако повышения эффективности ее работы получено не было. Стабилизация направляющей РНК путем добавления в последовательность G-квадруплекса, укорочения и добавления GG в 5′-область также не принесла результатов. Вероятно, низкая эффективность работы использованной направляющей РНК обусловлена ее нуклеотидной последовательностью, что ограничивает ее использование.

Ключевые слова: муковисцидоз, CRISPR-Cas9, *CFTR*, геномное редактирование, мутация F508del, направляющие РНК

Финансирование: раздел «Редактирование *CFTR* локуса» поддержан грантом РНФ (Соглашение № 17-75-20095), разделы «Увеличение экспрессии направляющих РНК» и «Увеличение эффективности редактирования *CFTR* локуса» поддержаны Российской академией наук и государственным заданием ФГБНУ «МГНЦ».

✉ **Для корреспонденции:** Светлана Анатольевна Смирнихина
ул. Москворечье, д. 1, г. Москва, 115522; smirnikhinas@gmail.com

Статья получена: 15.03.2018 **Статья принята к печати:** 20.03.2018

DOI: 10.24075/vrgmu.2018.022

Cystic fibrosis (CF, OMIM#219700) is an autosomal recessive disease caused by mutations in the *CFTR* (cystic fibrosis transmembrane conductance regulator) gene. These mutations result in the impaired transport of chloride and sodium ions across the cell membrane. CF is one of the most common hereditary diseases striking 1 in every 4,500 people. The carrier rate is as high as 1 in 25 [1]. Lung damage is the main clinical symptom of the disease and the major cause of death in patients with CF [2]. Other organs can also be affected, including the pancreas, the liver and the intestines. The most common *CFTR* mutation is F508del. It results in the premature degradation of the encoded protein and its total absence on the cell surface [3]. There have been tremendous advances in the management of CF in the recent decades aimed at blocking disease progression [4–7], but no cure has been found yet.

Genome editing, specifically CRISPR-Cas9, prompts us to take a fresh look at the potential of gene therapies for hereditary conditions [8]. It can be used to correct (or "edit") mutations and eliminate the causes of yet incurable diseases [9–12]. Earlier works describing the attempts of F508del correction by different genome editing techniques [13–20] stimulate discovery of novel approaches to F508del editing. However, a serious drawback of the techniques applied in those studies is their low success rate (<1% cells), which they share with other genome editing tools.

To improve the efficacy of F508del correction, we selected a few guide RNAs specific to the regions flanking the mutation site and introduced a few Cas9 orthologs that had not been used previously for such purposes to design a few combinations of Cas9 + sgRNA and to choose a combination that worked best.

The aim of our study was to compare and improve the efficacy of different combinations of guide RNA and Cas9 in editing the F508del mutation.

METHODS

The initial plasmids for CRISPR-Cas9 were gifts from Feng Zhang (Addgene #71814 and #61591) and Keith Joung (Addgene #72249). Guide RNAs (sgRNAs) for SpCas9, SpCas9(HF4) and SaCas9 were designed using the free-access software developed by Broad Institute (USA; http://portals.broadinstitute.org/gpp/public/analysis-tools/sgrna-design). The cloned plasmids are shown in Fig.1. To test the performance of the obtained constructs, a 400-nucleotide-long sequence flanking the mutation site on both sides and containing the F508del mutation was cloned into the plasmid pGEM-TA-CFTR, which was then transfected into the cell together with the plasmid expressing Cas9 and sgRNA. HEK293T cells (a gift from Skoblov M.Yu., Laboratory of Functional Genomics, Research Centre for Medical Genetics, Moscow) were cultured in DMEM (PanEco, Russia) supplemented with 10% fetal bovine serum (PAA Laboratories GmbH, Austria), 100U/ml/100μg/ml penicillin/streptomycin and 4 mM L-glutamine (PanEco, Russia). To assess the role of temperature, a part of the transfected cells was cultured at standard 37 °C for 72 h; the rest were cultured in two steps: at 37 °C for 24 h followed by 48 h at 30 °C. Calcium-phosphate transfection of HEK293T cells was performed in 12-well plates at 50% confluence as described in [21]. It total, there were 1.5 μg or 5.5 μg of plasmids per well (1 μg or 5 μg, respectively, of the plasmid expressing Cas9 and sgRNA transfected into the cells together with 0.5 μg of the target plasmid). Six hours after transfection, the medium was replaced with a fresh growth medium supplemented with 10% fetal bovine serum. The pEGFP-C1 plasmid (Clontech, USA) served as a reporter. For DNA isolation we used the Genomic DNA-Tissue MiniPrep kit (ZymoResearch, USA) according to the manufacturer's

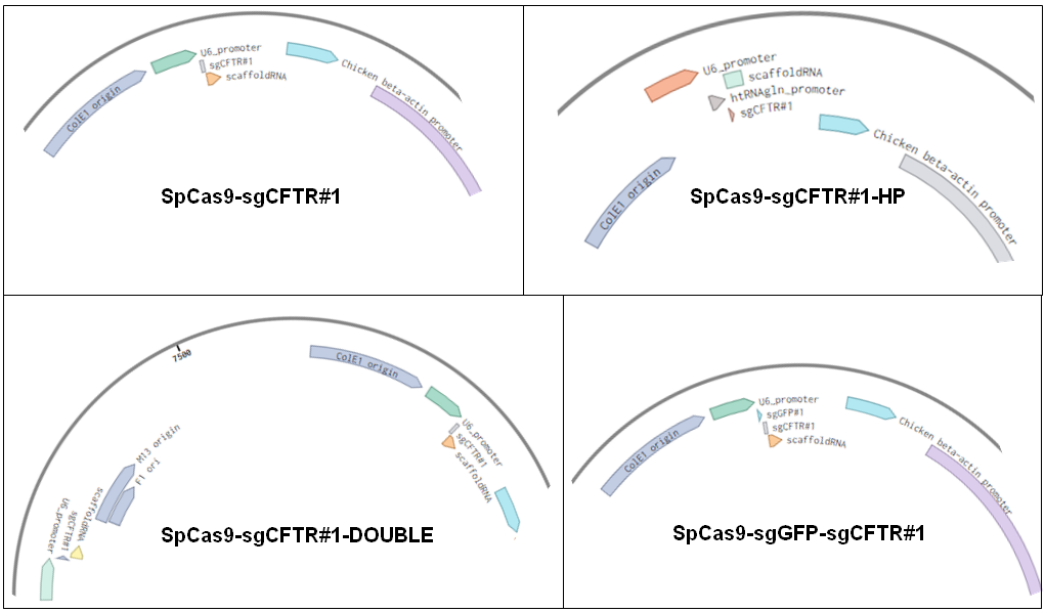

Fig. 1. Maps of synthetic plasmids used for F508del mutation editing in the *CFTR* gene

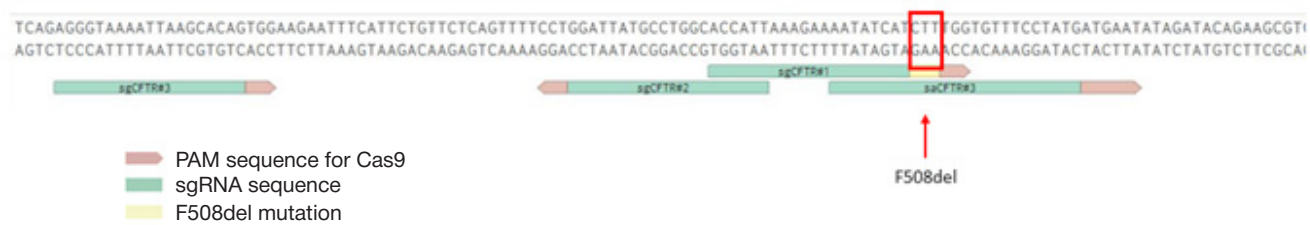

Fig. 2. sgRNAs for the *CFTR* locus used in this study

protocol. T7E1-analysis was carried out as described in [22]: PCR products with anticipated insertions and deletions at the site of a double strand break were heated and immediately cooled down, formation of heteroduplexes was inferred from the presence of extra bands in the electrophoretic gel after the heteroduplexes were treated with endonuclease T7E1.

RESULTS

Editing of the *CFTR* locus

In this work we attempted to compare the efficacy of genomic editing of F508del located in the *CFTR* gene using a few combinations of 2 mutant SpCas9 proteins (eSpCas9(1.1) [23] and SpCas9(HF4) [24]) or SaCas9 [25] and different sgRNAs. For SpCas9 three sgRNAs were selected targeting the sequence of *CFTR* exon 10 harboring F508del (Fig. 2). The first guide RNA sgCFTR#1 precisely targeted the mutation site (in the absence of F508del there was no PAM). The second sgRNA (sgCFTR#2) targeted a region near the mutation and could be used to edit both mutant and wild type alleles. The third sgRNA (sgCFTR#3) was selected for the sequence located 85 nucleotides upstream the mutation [13]. Because SaCas9 requires a different PAM, we selected a different sgRNA (saCFTR#3) for this nuclease, precisely targeting the mutation site. Since HEK293T cells do not have F508del in their genome and the structure of a genomic site presumably affects the efficacy of editing, sgRNAs were tested using a synthetic plasmid containing the *CFTR* locus with the F508del mutation. The synthetic construct was transfected into the HEK293T cells together with the plasmid expressing Cas9 and sgRNA.

The best editing effect was observed for the combination of SaCas9 and saCFTR#3: 29% of alleles were successfully edited (Fig.3). SgCFTR#1 combined with different SpCas9 proteins demonstrated an average success rate of 13%. For sgCFTR#2 the success rate was 18% (16% for the plasmid site and 22% for the genomic site), sgCFTR#3 demonstrated 12% efficacy (6% for the plasmid site and 14% for the genomic site). The editing activity of sgCFTR#1 was comparable to or lower than that exhibited by other guide RNAs, including the control sgGFP targeting the *EGFP* gene (Fig. 3).

Increasing the expression of guide RNAs

Our previous study revealed that low editing efficacy of sgCFTR#1-based systems correlates with its low expression [22]. To improve expression of sgCFTR#1, we inserted an extra cassette consisting of a promoter and sgCFTR#1 (SpCas9–sgCFTR#1–DOUBLE) into the plasmid, but it produced no significant effect on the performance of this guide RNA (Fig. 4). For positive control, we chose sgGFP targeting the *EGFP* gene. Because sgGFP was always known to be expressed vigorously and demonstrated high editing efficacy, we decided to combine it with sgCFTR#1 (SpCas9–sgGFP–sgCFTR#1). Unfortunately, the resulting synthetic sgRNA only negatively affected the efficacy of *CFTR* editing (Fig. 4).

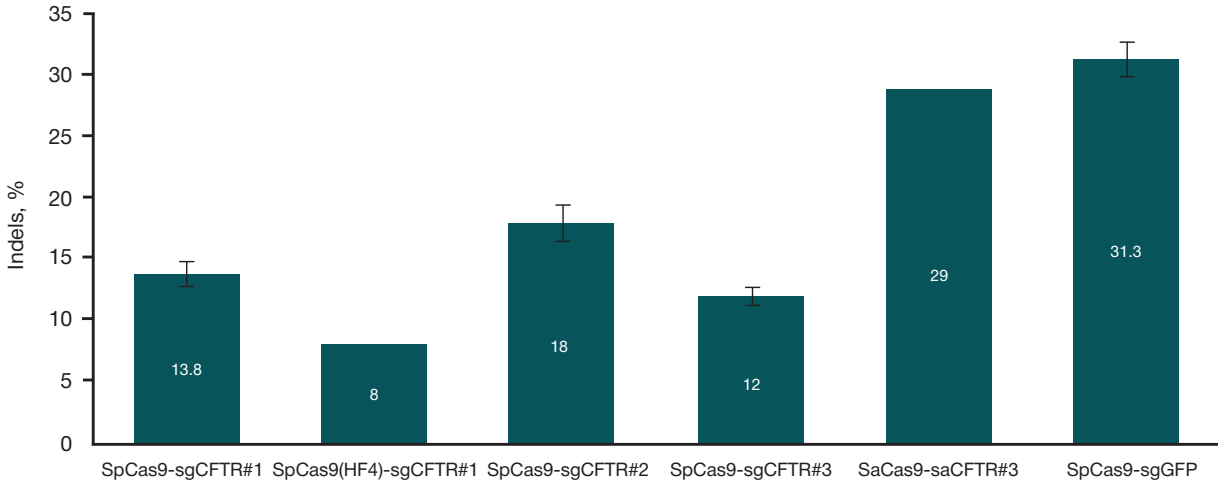

Fig. 3. Efficacy of *CFTR* and *EGFP* editing in HEK293T cells 48–72 hours after transfection. The results are represented as a mean and a standard error of the mean

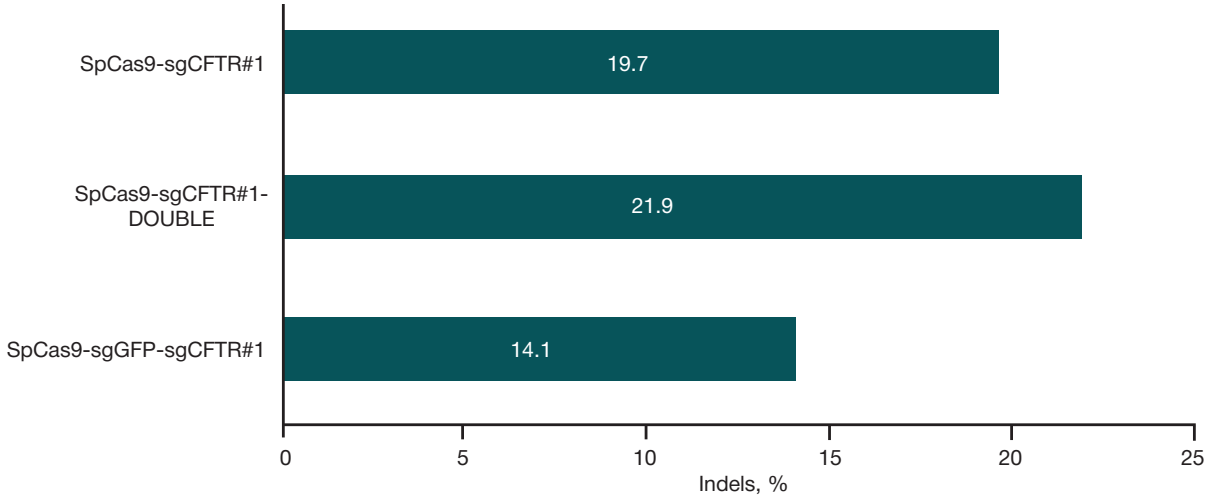

Fig. 4. Comparison of *CFTR* editing efficacy in HEK293T cells. The results are represented as a mean

A number of works have shown that RNA expression can be improved by a synthetic hybrid consisting of two promoters [26]. Perhaps, such effect is achieved because different promoters attract different transcription factors. In our plasmids sgRNA was expressed from U6, a standard promoter for CRISPR-Cas9. A few authors have demonstrated, though, that sgRNA is better expressed from the tRNAgln promoter [26, 27]. Therefore, we decided to clone into the plasmid a hybrid promoter consisting of U6 and tRNAgln (designated as the plasmid's name +HP in the pictures). As shown in Fig. 5, all sgRNAs, except sgCFTR#1, exhibited a poorer performance; sgCFTR#1's activity increased only slightly.

Improving the efficacy of *CFTR* locus editing

It is known that sgRNA molecules shorter than 20 nucleotides in length and starting with the G- or GG-nucleotide produce a better editing outcome [28]. Our sgCFTR#2 and sgCFTR#3 contained two GG nucleotides in their 5′-region, therefore, we shortened them from their 5′-ends down to 17 nucleotides (see SpCas9–sgCFTR#2(GG17) and SpCas9–sgCFTR#3(GG17), respectively). SgCFTR#1 did not have a GG sequence in its 5′-region, so we shortened it down to 19 nucleotides and replaced CC with GG (SpCas9–sgCFTR#1(gg19)). As a result, the activity of the modified sgCFTR#1 and sgCFTR#3 dropped from 20.3% and 11.8% to 8.7% and 0%, respectively (Fig. 6), whereas the modified sgCFTR#2 increased its performance from 10.5% to 22.1%.

Because guide RNA performance is presumably associated with its stability, we attached the sequence CACCGGGAGGGCGGGGAGGG to the 5′-ends of sgCFTR#1 and sgGFP in order to facilitate formation of G-quadruplexes (sgCFTR#1quad and sgGFPquad, respectively) that could improve sgRNA stability [29]. We found that the efficacy of target DNA cleavage using the modified guide RNAs was lower because of their 2- to 16-fold reduced expression, as compared to the unmodified sgRNAs [22].

Lastly, we attempted to stabilize the SpCas9 nuclease by transient hypothermia, i.e. culturing of the transfected cells at 30 °C [14, 30]. As a result, the success rate of *CFTR* editing plunged from 17.6 to 10.9% (Table).

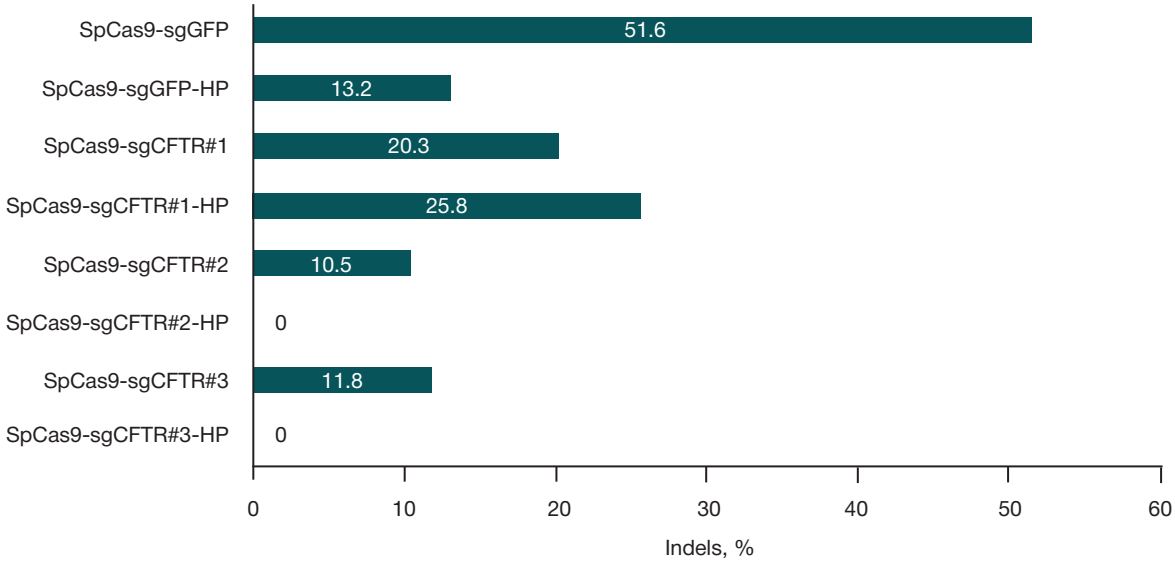

Fig. 5. Efficacy of *CFTR* and *EGFP* editing in HEK293T cells using sgRNA expressed from the standard U6 and the hybrid U6-tRNAgln (plasmid +HP) promoters. The results are represented as a mean

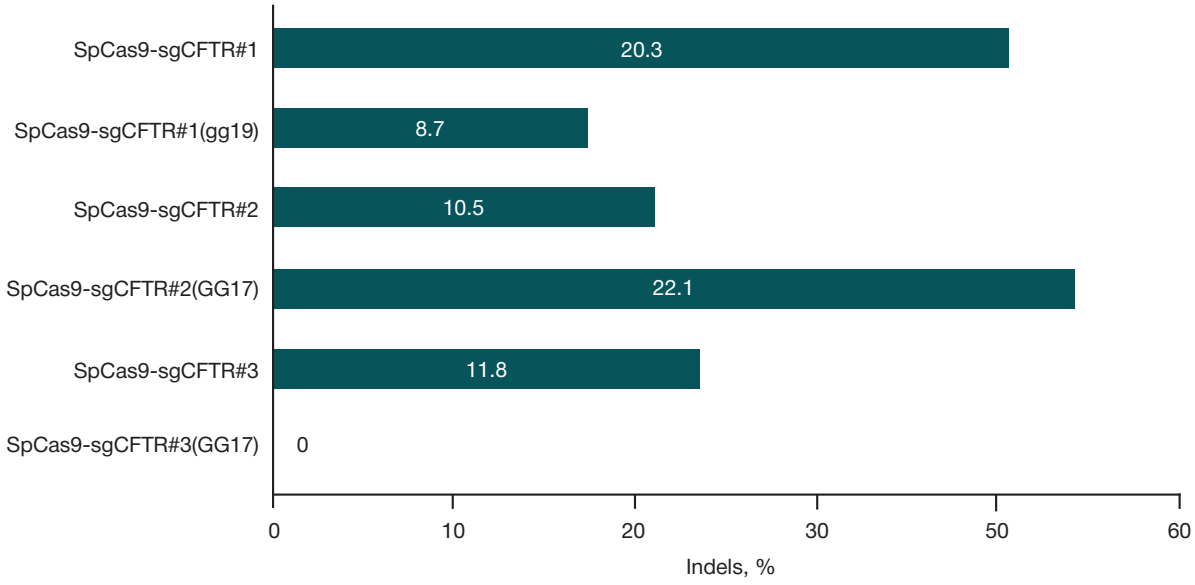

Fig. 6. Comparison of *CFTR* editing efficacy in HEK293T cells using modified sgRNAs. The results are represented as a mean

Table. Comparison of *CFTR* editing efficacy using transient hypothermia of HEK293T cells

Culture conditions	Transfected plasmids	Indels, mean %
72 h at 37 °C	SpCas9-sgCFTR#1+ pGEM-TA-CFTR	17.6
	pGEM-TA-CFTR	0
24 h at 37 °C, 48 h at 30 °C	SpCas9-sgCFTR#1+ pGEM-TA-CFTR	10.9
	pGEM-TA-CFTR	0

DISCUSSION

Attempts to correct *CFTR* mutations by genome editing tools started in 2012 [14], however no effective techniques are yet available. The proposed approaches demonstrate low efficacy, yielding only a small percentage of cells with corrected sequences, which necessitates cell selection [13, 16]. This incurs additional costs and makes the whole cell culture process longer. Besides, such treatment is not systemic.

Evolution of genome editing gives rise to more advanced CRISPR/Cas tools with better efficacy and specificity. The enzymes we use routinely for genome editing are highly specific [23, 24], which improves the safety of the method. Also, we are currently working on the technique that will correct only the mutant site using a guide RNA precisely targeting F508del. This might be a leap to a new level: we expect the technique to work not only in the isolated cells but also in the living organism, since only mutant alleles will be affected. We believe that this approach will prevent repeated cleavage of the already edited sites.

Still, in the course of this experiment we established that the efficacy of sgCFTR#1-based editing of F508del was lower than demonstrated by the majority of other sgRNA used in the study. The underlying reason is low expression of sgCFTR#1 in the cells [22]. We tried a few techniques to stimulate expression of this guide RNA: inserted an extra cassette (promoter + sgCFTR#1) into the plasmid, combined sgCFTR#1 with a more active sgGFP, used the hybrid promoter U6–tRNAgln, but none improved sgCFTR#1 performance.

It was shown previously that transcription from the U6 promoter is initiated in the presence of G or GG nucleotides on the 5′-end of guide RNA [28], therefore we tried shortening sgRNA down to the first G and replacing the initially present nucleotides with G/GG to upregulate sgRNA expression and increase its activity. But this approach did not work.

Given that initially our guide RNAs had one and the same promoter U6, we assumed that transcription of both sgRNAs would be the same. The actual difference in the expression levels may have been the result of a more rapid degradation of sgCFTR#1 in comparison with sgGFP. Screening of a huge guide RNA set [29] showed that sgRNA with G-enriched regions (>8 nucleotides) were more stable because of G-quadruplexes. But G-quadruplexes did not help to increase sgCFTR#1 activity [22].

Some authors report that *Fok*I nuclease has a more stable performance at 30 °C [14, 30]. We hypothesized that exposure of transfected cells to lower temperatures during culture would increase Cas9 activity, but that did not happen [22].

Experiments conducted *in vitro* show that up to 41% of guide RNAs are not active against the target site [31]. The main reason for that is sgRNA nucleotide composition: T- and TT-enriched sequences reduce editing efficacy [32], and the presence of certain nucleotides at certain positions in guide RNA sequences are reliably associated with different degrees of sgRNA activity [31]. Secondary structures formed by guide RNAs may also have a role here [31]. If the low performance of sgRNA is associated with its sequence, then the only solution is to choose a different sgRNA.

CONCLUSIONS

Our attempts to edit the *CFTR* locus in HEK293T cells demonstrate that the most effective combination is SaCas9 + sgRNA selected to precisely target the F508del mutation (the success rate here is 29%). Combinations of sgCFTR#1 targeting the F508del site with two different SpCas9 have the lowest efficacy: 13.8% for Cas9(1.1) and 8% for Cas9(HF4). Such poor outcome is associated with the low expression of the guide RNA. Attempts to improve sgCFTR#1 expression by inserting another expression cassette into the plasmid, fusing sgCFTR#1 with a more active sgGFP or using a hybrid promoter did not result in any significant increase in sgCFTR#1 activity. Stabilization of sgCFTR#1 by introducing a G-quadruplex into its sequence, shortening or adding GG to the 5′-region did not produce a desired effect. Transient hypothermia also did not improve the efficacy of editing. Therefore, the low performance of sgCFTR#1 is probably determined by its nucleotide sequence, and different guide RNAs, different Cas9, such as SaCas9, or different PAM expanding the choice of possible guide RNAs targeting F508del should be used instead.

References

1. Krasovsky SA, Chernyak AV, Voronkov AY, Amelina EL, Kashirskaya NY, Kondratieva EI, i dr. Register of cystic fibrosis patiens in Russian Federation. 2016. Moskva: «MEDPRAKTIKA-M», 2018, 64 s.
2. Burney TJ, Davies JC. Gene therapy for the treatment of cystic fibrosis. Appl Clin Genet. 2012 May 29; 5: 29–36. DOI: 10.2147/TACG.S8873.
3. Amaral MD. Novel personalized therapies for cystic fibrosis: treating the basic defect in all patients. J Intern Med. 2015; 277: 55–166.
4. Cohen-Cymberknoh M, Shoseyov D, Kerem E. Managing cystic fibrosis: strategies that increase life expectancy and improve quality of life. Am J Respir Crit Care Med. 2011 Jun 1; 183 (11): 1463–71. DOI: 10.1164/rccm.201009-1478CI.
5. Whiting P, Al M, Burgers L, Westwood M, Ryder S, Hoogendoorn M, et al. Ivacaftor for the treatment of patients with cystic fibrosis and the G551D mutation: a systematic review and cost-effectiveness analysis. Health Technol Assess. 2014 Mar; 18 (18): 1–106.
6. Mayer M. Lumacaftor-ivacaftor (Orkambi) for cystic fibrosis: behind the 'breakthrough'. Evid Based Med. 2016 Jun; 21 (3): 83–6.
7. Cholon DM, Esther CR Jr, Gentzsch M. Efficacy of lumacaftor-ivacaftor for the treatment of cystic fibrosis patients homozygous for the F508del-CFTR mutation. Expert Rev Precis Med Drug Dev. 2016; 1 (3): 235–43.
8. Zhang F, Wen Y, Guo X. CRISPR/Cas9 for genome editing: progress, implications and challenges. Hum Mol Genet. 2014 Sep 15; 23 (R1): R40–6.
9. Smirnikhina SA, Lavrov AV. Gennaja terapija nasledstvennyh

zabolevanij s pomoshh'ju tehnologii CRISPR/Cas9 in vivo. Medicinskaja genetika. 2016; 15 (9): 3–11.
10. Hockemeyer D, Jaenisch R. Induced pluripotent stem cells meet genome editing. Cell Stem Cell. 2016 May 5; 18 (5): 573–86.
11. Maeder ML, Gersbach CA. Genome-editing Technologies for Gene and Cell Therapy. Mol Ther. 2016 Mar; 24 (3): 430–46.
12. Prakash V, Moore M, Yáñez-Muñoz RJ. Current Progress in Therapeutic Gene Editing for Monogenic Diseases. Mol Ther. 2016 Mar; 24 (3): 465–74.
13. Firth AL, Menon T, Parker GS, Qualls SJ, Lewis BM, Ke E, et al. Functional Gene Correction for Cystic Fibrosis in Lung Epithelial Cells Generated from Patient iPSCs. Cell Rep. 2015 Sep 1; 12 (9): 1385–90.
14. Lee CM, Flynn R, Hollywood JA, Scallan MF, Harrison PT. Correction of the ΔF508 Mutation in the Cystic Fibrosis Transmembrane Conductance Regulator Gene by Zinc-Finger Nuclease Homology-Directed Repair. BioResearch Open Access. 2012; 1 (3): 99–108.
15. Suzuki S, Sargent RG, Illek B, Fischer H, Esmaeili-Shandiz A, Yezzi MJ, et al. TALENs Facilitate Single-step Seamless SDF Correction of F508del CFTR in Airway Epithelial Submucosal Gland Cell-derived CF-iPSCs. Mol Ther Nucleic Acids. 2016 Jan 5; 5: e273.
16. Hollywood JA, Lee CM, Scallan MF, Harrison PT. Analysis of gene repair tracts from Cas9/gRNA double-stranded breaks in the human CFTR gene. Sci Rep. 2016 Aug 25; 6: 32230.
17. Crane AM, Kramer P, Bui JH, Chung WJ, Li XS, Gonzalez-Garay ML, et al. Targeted correction and restored function of the CFTR gene in cystic fibrosis induced pluripotent stem cells. Stem Cell Reports. 2015 Apr 14; 4 (4): 569–77.
18. Bednarski C, Tomczak K, Vom Hövel B, Weber WM, Cathomen T. Targeted Integration of a Super-Exon into the CFTR Locus Leads to Functional Correction of a Cystic Fibrosis Cell Line Model. PLoS One. 2016 Aug 15; 11 (8): e0161072.
19. Camarasa MV, Gálvez VM. Robust method for TALEN-edited correction of pF508del in patient-specific induced pluripotent stem cells. Stem Cell Res Ther. 2016 Feb 9; 7: 26.
20. Schwank G, Koo BK, Sasselli V, Dekkers JF, Heo I, Demircan T, et al. Functional repair of CFTR by CRISPR/Cas9 in intestinal stem cell organoids of cystic fibrosis patients. Cell Stem Cell. 2013 Dec 5; 13 (6): 653–58.
21. Smirnikhina SA, Bannikov AV, Lavrov AV. Optimizacija uslovij transfekcii kletochnoj kul'tury CFTE29o- dlja razrabotki redaktirovanija mutacii F508del v gene CFTR. Medicinskaja genetika. 2016; 15 (8): 36–9.
22. Smirnikhina SA, Bannikov AV, Anuchina AA, Kochergin-Nikitsky KS, Adilgereeva EP, Lavrov AV. Faktory, vlijajushhie na jeffektivnost' CRISPR/Cas9 dlja korrekcii mutacii F508del pri mukoviscidoze. Medicinskaja genetika, 2017; 16 (11) s. 32–7.
23. Slaymaker IM, Gao L, Zetsche B, Scott DA, Yan WX, Zhang F. Rationally engineered Cas9 nucleases with improved specificity. Science. 2016 Jan 1; 351 (6268): 84–8.
24. Kleinstiver BP, Pattanayak V, Prew MS, Tsai SQ, Nguyen NT, Zheng Z, et al. High-fidelity CRISPR–Cas9 nucleases with no detectable genome-wide off-target effects. Nature. 2016; 529: 490–95.
25. Ran FA, Cong L, Yan WX, Scott DA, Gootenberg JS, Kriz AJ, et al. In vivo genome editing using Staphylococcus aureus Cas9. Nature. 2015 Apr 9; 520 (7546): 186–91.
26. Schwartz CM, Hussain MS, Blenner M, Wheeldon I. Synthetic RNA Polymerase III Promoters Facilitate High-Efficiency CRISPR-Cas9-Mediated Genome Editing in Yarrowia lipolytica. ACS Synth Biol. 2016 Apr 15; 5 (4): 356-9. DOI: 10.1021/acssynbio.5b00162.
27. Mefferd AL, Kornepati AV, Bogerd HP, Kennedy EM, Cullen BR. Expression of CRISPR/Cas single guide RNAs using small tRNA promoters. RNA. 2015 Sep; 21 (9): 1683–9. DOI: 10.1261/rna.051631.115.
28. Sander JD, Joung JK. CRISPR-Cas systems for editing, regulating and targeting genomes. Nat Biotechnol. 2014 Apr; 32 (4): 347–55. DOI: 10.1038/nbt.2842.
29. Moreno-Mateos MA, Vejnar CE, Beaudoin JD, Fernandez JP, Mis EK, Khokha MK, et al. CRISPRscan: designing highly efficient sgRNAs for CRISPR-Cas9 targeting in vivo. Nat Methods. 2015 Oct; 12 (10): 982–88.
30. Doyon Y, Choi VM, Xia DF, Vo TD, Gregory PD, Holmes MC. Transient cold shock enhances zinc-finger nuclease-mediated gene disruption. Nat Methods. 2010 Jun; 7 (6): 459–60.
31. Liu X, Homma A, Sayadi J, Yang S, Ohashi J, Takumi T. Sequence features associated with the cleavage efficiency of CRISPR/Cas9 system. Sci Rep. 2016 Jan 27; 6: 19675. DOI: 10.1038/srep19675.
32. Kuan PF, Powers S, He S, Li K, Zhao X, Huang B. A systematic evaluation of nucleotide properties for CRISPR sgRNA design. BMC Bioinformatics. 2017 Jun 6; 18 (1): 297. DOI: 10.1186/s12859-017-1697-6.

Литература

1. Красовский С. А., Черняк А. В., Воронкова А. Ю., Амелина Е. Л., Каширская Н. Ю., Кондратьева Е. И. и др. (редакторы). Регистр больных муковисцидозом в Российской Федерации. 2016 год. М.: ИД «МЕДПРАКТИКА-М», 2018, 64 с.
2. Burney TJ, Davies JC. Gene therapy for the treatment of cystic fibrosis. Appl Clin Genet. 2012 May 29; 5: 29–36. DOI: 10.2147/TACG.S8873.
3. Amaral MD. Novel personalized therapies for cystic fibrosis: treating the basic defect in all patients. J Intern Med. 2015; 277: 55–166.
4. Cohen-Cymberknoh M, Shoseyov D, Kerem E. Managing cystic fibrosis: strategies that increase life expectancy and improve quality of life. Am J Respir Crit Care Med. 2011 Jun 1; 183 (11): 1463–71. DOI: 10.1164/rccm.201009-1478CI.
5. Whiting P, Al M, Burgers L, Westwood M, Ryder S, Hoogendoorn M, et al. Ivacaftor for the treatment of patients with cystic fibrosis and the G551D mutation: a systematic review and cost-effectiveness analysis. Health Technol Assess. 2014 Mar; 18 (18): 1–106.
6. Mayer M. Lumacaftor-ivacaftor (Orkambi) for cystic fibrosis: behind the 'breakthrough'. Evid Based Med. 2016 Jun; 21 (3): 83–6.
7. Cholon DM, Esther CR Jr, Gentzsch M. Efficacy of lumacaftor-ivacaftor for the treatment of cystic fibrosis patients homozygous for the F508del-CFTR mutation. Expert Rev Precis Med Drug Dev. 2016; 1 (3): 235–43.
8. Zhang F, Wen Y, Guo X. CRISPR/Cas9 for genome editing: progress, implications and challenges. Hum Mol Genet. 2014 Sep 15; 23 (R1): R40–6.
9. Смирнихина С. А., Лавров А. В. Генная терапия наследственных заболеваний с помощью технологии CRISPR/Cas9 in vivo. Медицинская генетика. 2016; 15 (9): 3–11.
10. Hockemeyer D, Jaenisch R. Induced pluripotent stem cells meet genome editing. Cell Stem Cell. 2016 May 5; 18 (5): 573–86.
11. Maeder ML, Gersbach CA. Genome-editing Technologies for Gene and Cell Therapy. Mol Ther. 2016 Mar; 24 (3): 430–46.
12. Prakash V, Moore M, Yáñez-Muñoz RJ. Current Progress in Therapeutic Gene Editing for Monogenic Diseases. Mol Ther. 2016 Mar; 24 (3): 465–74.
13. Firth AL, Menon T, Parker GS, Qualls SJ, Lewis BM, Ke E, et al. Functional Gene Correction for Cystic Fibrosis in Lung Epithelial Cells Generated from Patient iPSCs. Cell Rep. 2015 Sep 1; 12 (9): 1385–90.
14. Lee CM, Flynn R, Hollywood JA, Scallan MF, Harrison PT. Correction of the ΔF508 Mutation in the Cystic Fibrosis Transmembrane Conductance Regulator Gene by Zinc-Finger Nuclease Homology-Directed Repair. BioResearch Open Access. 2012; 1 (3): 99–108.
15. Suzuki S, Sargent RG, Illek B, Fischer H, Esmaeili-Shandiz A, Yezzi MJ, et al. TALENs Facilitate Single-step Seamless SDF

Correction of F508del CFTR in Airway Epithelial Submucosal Gland Cell-derived CF-iPSCs. Mol Ther Nucleic Acids. 2016 Jan 5; 5: e273.
16. Hollywood JA, Lee CM, Scallan MF, Harrison PT. Analysis of gene repair tracts from Cas9/gRNA double-stranded breaks in the human CFTR gene. Sci Rep. 2016 Aug 25; 6: 32230.
17. Crane AM, Kramer P, Bui JH, Chung WJ, Li XS, Gonzalez-Garay ML, et al. Targeted correction and restored function of the CFTR gene in cystic fibrosis induced pluripotent stem cells. Stem Cell Reports. 2015 Apr 14; 4 (4): 569–77.
18. Bednarski C, Tomczak K, Vom Hövel B, Weber WM, Cathomen T. Targeted Integration of a Super-Exon into the CFTR Locus Leads to Functional Correction of a Cystic Fibrosis Cell Line Model. PLoS One. 2016 Aug 15; 11 (8): e0161072.
19. Camarasa MV, Gálvez VM. Robust method for TALEN-edited correction of pF508del in patient-specific induced pluripotent stem cells. Stem Cell Res Ther. 2016 Feb 9; 7: 26.
20. Schwank G, Koo BK, Sasselli V, Dekkers JF, Heo I, Demircan T, et al. Functional repair of CFTR by CRISPR/Cas9 in intestinal stem cell organoids of cystic fibrosis patients. Cell Stem Cell. 2013 Dec 5; 13 (6): 653–58.
21. Смирнихина С. А., Банников А. В., Лавров А. В. Оптимизация условий трансфекции клеточной культуры CFTE29o- для разработки редактирования мутации F508del в гене CFTR. Медицинская генетика. 2016; 15 (8): 36–9.
22. Смирнихина С. А., Банников А. В., Анучина А. А., Кочергин-Никитский К. С., Адильгереева Э. П., Лавров А. В. Факторы, влияющие на эффективность CRISPR/Cas9 для коррекции мутации F508del при муковисцидозе. Медицинская генетика, 2017; 16 (11): 32–7.
23. Slaymaker IM, Gao L, Zetsche B, Scott DA, Yan WX, Zhang F. Rationally engineered Cas9 nucleases with improved specificity. Science. 2016 Jan 1; 351 (6268): 84–8.
24. Kleinstiver BP, Pattanayak V, Prew MS, Tsai SQ, Nguyen NT, Zheng Z, et al. High-fidelity CRISPR–Cas9 nucleases with no detectable genome-wide off-target effects. Nature. 2016; 529: 490–95.
25. Ran FA, Cong L, Yan WX, Scott DA, Gootenberg JS, Kriz AJ, et al. In vivo genome editing using Staphylococcus aureus Cas9. Nature. 2015 Apr 9; 520 (7546): 186–91.
26. Schwartz CM, Hussain MS, Blenner M, Wheeldon I. Synthetic RNA Polymerase III Promoters Facilitate High-Efficiency CRISPR-Cas9-Mediated Genome Editing in Yarrowia lipolytica. ACS Synth Biol. 2016 Apr 15; 5 (4): 356-9. DOI: 10.1021/acssynbio.5b00162.
27. Mefferd AL, Kornepati AV, Bogerd HP, Kennedy EM, Cullen BR. Expression of CRISPR/Cas single guide RNAs using small tRNA promoters. RNA. 2015 Sep; 21 (9): 1683–9. DOI: 10.1261/rna.051631.115.
28. Sander JD, Joung JK. CRISPR-Cas systems for editing, regulating and targeting genomes. Nat Biotechnol. 2014 Apr; 32 (4): 347–55. DOI: 10.1038/nbt.2842.
29. Moreno-Mateos MA, Vejnar CE, Beaudoin JD, Fernandez JP, Mis EK, Khokha MK, et al. CRISPRscan: designing highly efficient sgRNAs for CRISPR-Cas9 targeting in vivo. Nat Methods. 2015 Oct; 12 (10): 982–88.
30. Doyon Y, Choi VM, Xia DF, Vo TD, Gregory PD, Holmes MC. Transient cold shock enhances zinc-finger nuclease-mediated gene disruption. Nat Methods. 2010 Jun; 7 (6): 459–60.
31. Liu X, Homma A, Sayadi J, Yang S, Ohashi J, Takumi T. Sequence features associated with the cleavage efficiency of CRISPR/Cas9 system. Sci Rep. 2016 Jan 27; 6: 19675. DOI: 10.1038/srep19675.
32. Kuan PF, Powers S, He S, Li K, Zhao X, Huang B. A systematic evaluation of nucleotide properties for CRISPR sgRNA design. BMC Bioinformatics. 2017 Jun 6; 18 (1): 297. DOI: 10.1186/s12859-017-1697-6.

CAS13A: PURIFICATION AND USE FOR DETECTION OF VIRAL RNA

Savinova AS[1,2], Koptev EYu[1], Usachev EV[1], Tkachuk AP[1], Gushchin VA[1,3] ✉

[1] Laboratory of Translational Biomedicine,
Gamaleya Federal Research Center for Epidemiology and Microbiology, Moscow

[2] Department of Biotechnology, Faculty of Biotechnology and Industrial Ecology,
Mendeleev University of Chemical Technology, Moscow

[3] Department of Virology, Faculty of Biology,
Lomonosov Moscow State University, Moscow

The use of CRIPSR-Cas systems in genome editing has recently become one of the major research areas. Meanwhile, CAS proteins can be employed to develop novel techniques for molecular diagnostics. Traditional approaches to the identification of microorganisms have a few drawbacks: they are time-consuming (microbiological methods), insufficiently sensitive (immunoassays), expensive or labor-intensive (PCR, sequencing). The aim of this work was to obtain a functionally active Cas13a protein that could be used as a diagnostic tool and study its behavior under different conditions and at various target concentrations. We constructed an expression vector with the *cas13a* gene of *Leptotrichia wadei* under the control of T7 promoter. We obtained a functionally active Cas13a RNAse with pre-programmed activity, guide RNA, and a fragment of influenza B RNA sequence serving as a target. The functional activity of Cas13 RNAse was assessed by fluorescence in the reaction mix containing guide RNA, target RNA, and a molecular RNA beacon. The obtained protein Cas13a was able to specifically recognize the target and did not exhibit any non-specific RNAse activity. This study can become a basis for developing a novel, rapid, specific and sensitive method for pathogen detection.

Keywords: PCR, diagnostics, infectious diseases, CRISPR-Cas system, Cas13a

✉ **Correspondence should be addressed:** Vladimir Gushchin
Gamalei 18, Moscow, 123098; wowaniada@gmail.com, vladimir.a.gushchin@gamaleya.org

Received: 31.05.2018 **Accepted:** 07.06.2018

DOI: 10.24075/brsmu.2018.021

CAS13A: ПОЛУЧЕНИЕ И ИСПОЛЬЗОВАНИЕ ДЛЯ ОПРЕДЕЛЕНИЯ ВИРУСНОЙ РНК

А. С. Савинова[1,2], Е. Ю. Коптев[1], Е. В. Усачев[1], А. П. Ткачук[1], В. А. Гущин[1,3] ✉

[1] Лаборатория трансляционной медицины,
Национальный исследовательский центр эпидемиологии и микробиологии имени Н. Ф. Гамалеи, Москва

[2] Кафедра биотехнологии, факультет биотехнологии и промышленной экологии,
Российский химико-технологический факультет имени Д. И. Менделеева, Москва

[3] Кафедра вирусологии, биологический факультет,
Московский государственный университет имени М. В. Ломоносова, Москва

Использование CRISPR-Cas систем для редактирования геномов организмов в последнее время стало одним из магистральных научных направлений. Между тем белки системы CAS можно применять для разработки методов молекулярной диагностики. Традиционные подходы к идентификации микроорганизмов имеют ряд недостатков: они времязатратны (культуральные методы диагностики), недостаточно чувствительны (иммунологические методы), имеют высокую себестоимость и методически сложны (ПЦР, секвенирование). Целью работы было получение функционально активного препарата белка Cas13a и изучение его поведения в различных условиях, в том числе при изменении концентрации мишени, для дальнейшего использования в диагностических целях. Была создана генетическая экспрессионная конструкция, имеющая на 5′-конце Т7-промотер и ген *cas13a* бактерии *Leptotrichia wadei*. Получены препараты функционально активной программируемой РНКазы белка Cas13a, направляющей РНК, а также РНК вируса гриппа Б (РНК-мишень). Функциональную активность РНКазы белка Cas13a определяли по появлению флуоресцентного сигнала в реакционной смеси, содержащей направляющую РНК, РНК-мишень, молекулярный РНК-маячок. Показано, что полученный препарат белка Cas13a способен специфически выявлять мишень на примере фрагментов РНК вируса гриппа Б и не обладает неспецифическими видами РНКазной активности. Данное исследование может стать основой для создания нового быстрого специфичного и чувствительного метода идентификации микроорганизмов.

Ключевые слова: ПЦР, диагностика, инфекционные заболевания, CRISPR-Cas система, Cas13a

✉ **Для корреспонденции:** Владимир Алексеевич Гущин
ул. Гамалеи, д. 18, г. Москва, 123098; wowaniada@gmail.com, vladimir.a.gushchin@gamaleya.org

Статья получена: 31.05.2018 **Статья принята к печати:** 07.06.2018

DOI: 10.24075/vrgmu.2018.021

Mankind has been fighting infectious diseases for many decades now. A serious threat is posed by those infections that cause outbreaks or epidemics [1]. Because a successful treatment outcome depends in the first place on the accuracy of the diagnosis, a search for novel diagnostic approaches continues. Unlike classical microbiological methods of pathogen identification based on the use of differential culture media, polymerase chain reaction (PCR) ensures rapid detection of microorganisms regardless of the specifics of their life cycle. Evolution of sequencing techniques and free access to public databases containing sequencing data encourage a more active use of PCR [2].

Still, there is a need for novel molecular diagnostic techniques. There are a few obstacles preventing a wider application of PCR, including high equipment costs and a lack of laboratory facilities and qualified personnel. Among the proposed alternatives to PCR are mobile biosensors based on a combination of physical and biological approaches [3–5] and techniques that do not rely on complex equipment [6, 7]. We believe that the most promising technique that provides high specificity and sensitivity for single molecule detection is Specific High-Sensitivity Enzymatic Reporter Unlocking, or SHERLOCK [8, 9].

SHERLOCK combines isothermal amplification of total nucleic acids and Cas13a activity, allowing detection of both DNA and RNA molecules. Isothermal amplification ensures accumulation of target molecules, while Cas13a acts as a sensor capable of accurate target recognition, including single nucleotide polymorphisms [9].

Cas13a nuclease activity is initiated when CRIPSR guide RNA (crRNA) binds to Cas13a entailing significant conformational changes in the protein structure aimed to form a channel for the binding of a target RNA [10]. When Cas13a "meets" target RNA, a guide crRNA/target RNA duplex is formed in a positively charged NUC lobe channel. The target RNA serves as an activator: duplex formation catalyzes the movement of catalytic domains towards each other, followed by the formation of an RNA cleavage site. The use of RNA probes enables a visual representation of fluorescence signal accumulation as Cas13 exerts its activity.

The aim of this work was to obtain a functionally active Cas13a protein and study its behavior under different conditions, including varying concentrations of a target molecule represented by an RNA fragment of the influenza B virus.

METHODS

Synthesis of the recombinant protein LwCas13a

To obtain the recombinant protein Cas13a of *Leptotrichia wadei* (LwCas13a), a codon-optimized gene synthesized *de novo* by Evrogen, Russia, was incorporated into the gene expression vector pET42b(+) under the control of *lacT7* promotor. Gene expression was induced in the cells of *Escherichia coli* BL21(DE3) pLysS, driven by isopropyl β-D-1-thiogalactopyranoside (IPTG). The resulting Cas13a protein was tagged with octo-histidine on its C-terminus. The frozen bacterial cells were resuspended in the lysing buffer (20 mM Tris HCl, pH of 8.8, 500 mM NaCl, 5 mM β-mercaptoethanol) and lysed by exposure to cyclic pulsed ultrasound. The lysate was centrifuged for clarification at 15,000 g for 20 min; the supernatant was then used for the affinity chromatography on automated medium-pressure system NGC Discover™ 10 (Bio-Rad, USA) with the 20 ml HisPrep FF 16/10 column (GE, Germany) pre-charged with Ni^{2+} ions. To remove non-specifically bound impurities, Triton X-100 was added to the buffer solutions at a final concentration of 0.1%. The protein was eluted using a linear imidazole gradient (the final concentration was 0.5M). After chromatography, Cas13a-containing fractions were combined and dialyzed against a storage buffer (20 mM Tris HCl, pH of 8.0, 200 mM NaCl, 0.1 mM EDTA). Protein concentrations were measured spectrophotometrically at 280 nm wavelength using Implen NanoPhotometer (IMPLEN, Germany). Concentrations were calculated accounting for the extinction coefficient [11, 12].

Acquisition of target and guide RNAs

Guide and target RNAs were obtained through PCR followed by the transcription of PCR products using the qPCRmix-HS SYBR kit (Evrogen, Russia) according to the manufacturer's protocol. Guide RNA was obtained using artificially synthesized oligonucleotide primers with self-complementary regions. To get a target RNA molecule, we amplified a plasmid fragment carrying a sequence of the influenza B virus and a sequence of the MS2 phage. *In vitro* transcription of the amplicons was aided by the MEGAscript® T7 Kit (Thermo Fisher Scientific, USA).

Testing LwCas13a for non-specific nuclease activities

To test LwCas13a for non-specific nuclease activities, we measured fluorescence. Briefly, the fluorescence signal is emitted when the reporter RNA molecule RNAseAlert v2 Substrate (Thermo Fisher Scientific, USA) is cleaved. The reporter RNA molecule is an oligonucleotide beacon with a fluorescent dye sitting on its 5′-end and a quencher on its 3′-end. When the molecule is cleaved, the dye is separated from the quencher emitting light in the green spectrum at 520 nm wavelength. The final LwCas13a concentration of 450 nM was incubated at 37 °C for 2 hours in the reaction mix containing a nuclease buffer and the reporter RNA (40 mM Tris HCl, pH of 7.3, 60 mM NaCl, 6 mM $MgCl_2$, 125 nM RNAseAlert v2 Substrate); fluorescence was measured in real time on the QuantStudio 5 Real-Time PCR System (Applied Biosystems, USA). RNAse A (Thermo fisher scientific, USA) was was used for positive control; pure reporter RNA, for negative.

Testing LwCas13a endonuclease activity

The reaction mix for testing LwCas13a endonuclease activity consisted of a nuclease buffer (40 mM Tris HCl, pH of 7.3,

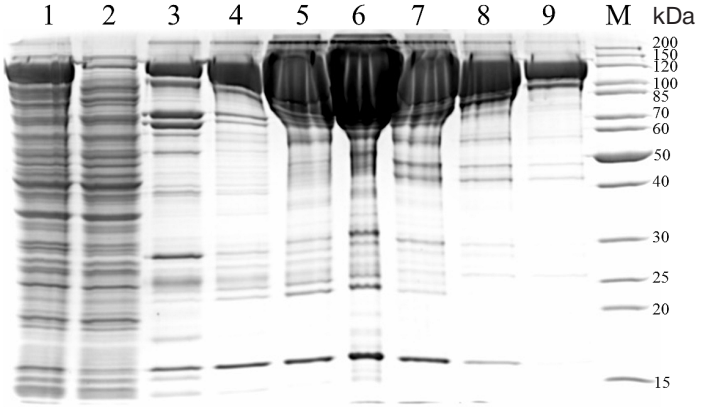

Fig. 1. SDS-PAGE of recombinant LwCas13a. Fraction analysis after IMAC: 1 — total protein; 2 — flow through; 3–9 — eluted fractions; M — molecular weight markers

60 mM NaCl, 6 mM $MgCl_2$), 450 mM LwCas13a, 22.5 nM crRNA, 125 мМ RNAseAlert v2 Substrate, 2 µl RiboLock RNAse Inhibitor, 100 ng RNA of a tobacco mosaic virus (for the background), and different concentrations of target RNA. Fluorescence was measured in real time for 2 hours at 37 °C using the QuantStudio 5 Real-Time PCR System (Applied Biosystems, USA).

RESULTS

Purification of the recombinant LwCas13a

The recombinant protein LwCas13a was obtained using affinity chromatography. Chromatography products were analyzed by denaturing electrophoresis, which revealed that induced *E. coli* cells had produced a water-soluble protein with a molecular weight comparable with the predicted LwCas13a weight (139.8 kDa) (Fig. 1).

Optimization of reporter RNA (RNAseAlert) concentrations in the reaction mix

To achieve optimal fluorescence intensity, we conducted a series of model tests using RNAse A (Fig. 2) and selected the substrate concentration of 125 nM for further experiments. At this particular value the maximal dynamic range of 100, 000 arbitrary fluorescence units was provided.

Testing LwCas13a for non-specific RNAse activities

The obtained LwCas13a protein was tested for non-specific RNAse activities by 2-h incubation with the fluorescent RNAseAlert v2 Substrate in the absence of crRNA and target RNA. The fluorescence signal was not changed during incubation. For positive control, we incubated the fluorescent substrate with RNAse A; for negative control, the reporter RNA was incubated without any additives (Fig. 3). We found that our method yielded the LwCas13a protein that did not exhibit any non-specific RNAse activity, which allowed us to proceed to the study of characteristics of its pre-programmed RNAse activity.

Testing method sensitivity using the influenza B virus

Our LwCas13a-based detection method was tested for sensitivity in a series of model tests, for which we employed a fragment of influenza B viral RNA sequence, which served as a target. The lower sensitivity threshold observed was 10^7 molecules of viral RNA (Fig. 4 and fig. 5).

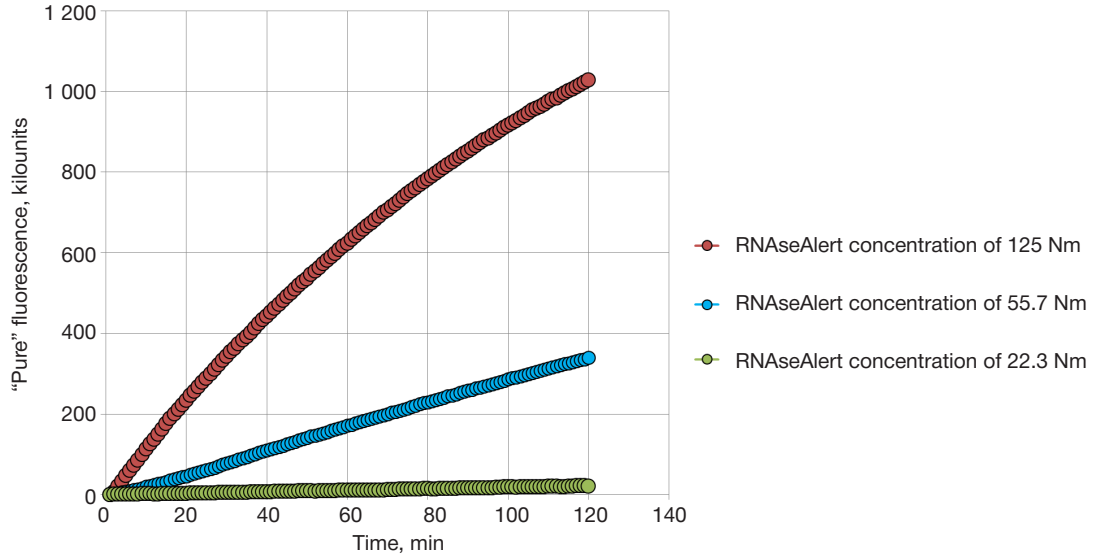

Fig. 2. Fluorescence kinetics during incubation of different RNAseAlert

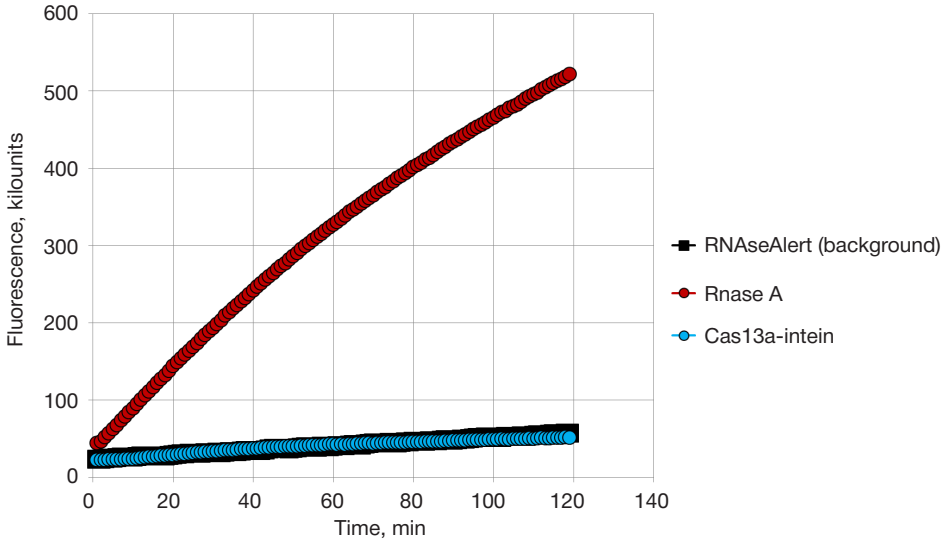

Fig. 3. Fluorescence kinetics during the study of non-specific RNAse activities of LwCas13a

DISCUSSION

LwCas13a-based pathogen detection opens up new diagnostic horizons. In 2017 Cas13 was adapted for the use in a platform called SHERLOCK [7, 9]. The latter combines Cas13a-based detection of RNA targets pre-amplified by recombinase polymerase amplification (RPA) and T7-transcription. All reactions take place in the same reaction mix. Using this approach, the researchers were able to design a diagnostic platform for Zika detection. Its attomolar sensitivity and specificity proved to be no less inferior to those of quantitative PCR (qRT-PCR) and droplet digital PCR. The researchers studied Cas13a orthologs to obtain a stable and reliable fluorescent signal emitted when Cas13a started to exert its RNAse activity. They found that Cas13a of *Leptotrichia wadei* was capable of detecting up to 50 pM of target RNA [7]. So, this enzyme served as a basis for the SHERLOCK platform. Although the sensitivity demonstrated by Cas13-based detection was high, the researchers decided to investigate a possibility of combining it with different types of isothermal amplification and established that RPA combined with transcription and the effect of Cas13a RNAse activity could improve the sensitivity of the method even more. SHERLOCK is able to discriminate between target RNAs that differ in only one nucleotide and are present in the solution at very low concentrations; the platform can also be used as a portable tool [7, 9].

In our research work we have synthesized a codon-optimized variant of LwCas13a. Unlike the previously described protein [7, 9], our protein had a different sequence changed for more effective expression in *E. Coli* cells. The protein yield was up to 10 mg from 1L of culture (Fig. 1). We have also elaborated a method for Cas13a purification and tested it to discover that programmed RNAse does not exhibit any non-specific RNAse activity. We ran a few *in vitro* tests to evaluate the specificity of Cas13 RNase activity against the fragments of viral RNA. Without target pre-amplification by previously described RPA and T7-transcription [7, 9], the sensitivity of our technique was 10^7 molecules per reaction.

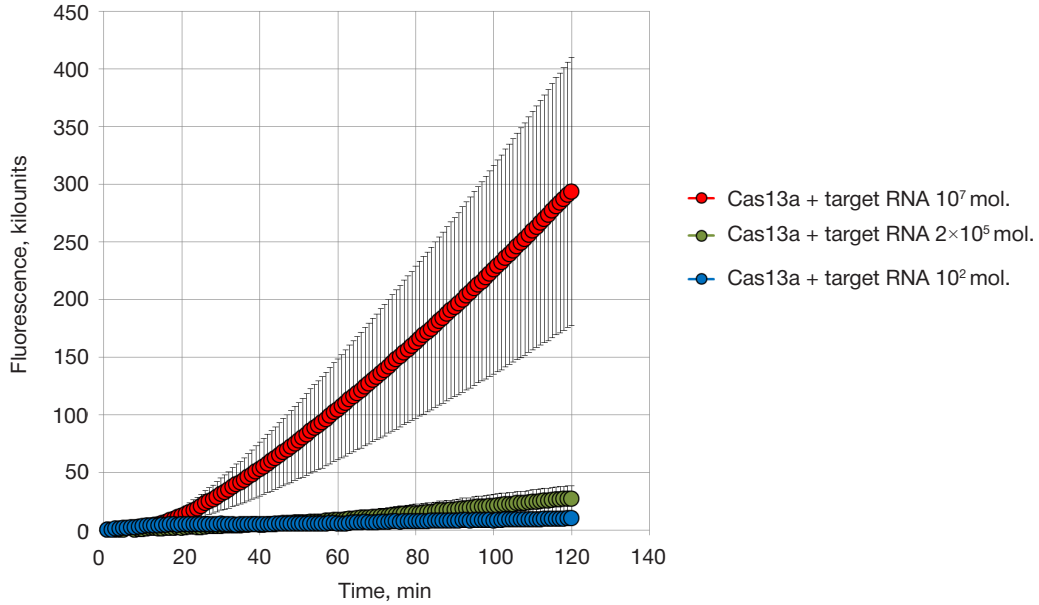

Fig. 4. Fluorescence kinetics at different concentrations of target RNA

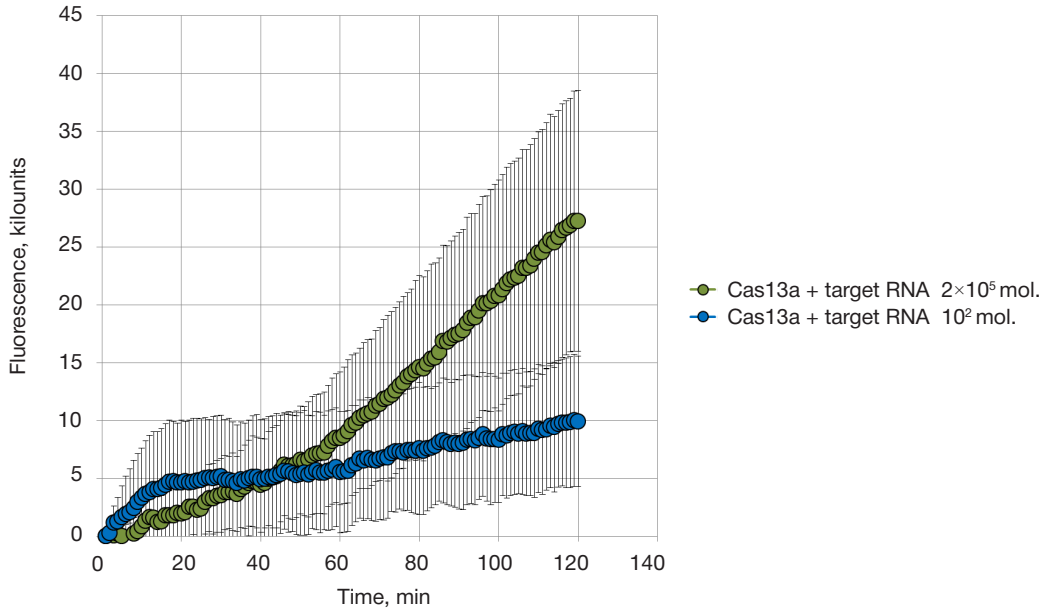

Fig. 5. Fluorescence kinetics at small concentrations of target RNA of the influenza B virus

CONCLUSIONS

In the course of this work we synthesized a codon-optimized variant of *Leptotrichia wadei* Cas13a that exhibits specific RNAse activity in *E. coli* cells. The obtained protein is deprived of non-specific nuclease activities and can specifically detect the target, which in our case was a fragment of influenza RNA.

Further research will be aimed at perfecting the technique, improving its sensitivity, studying programmed RNAse specificity, and increasing multiplexity. Besides, we will attempt to create a Cas13a-based diagnostic system for portable use. Field diagnostic tools can be of great assistance in monitoring the agents of infection in their natural reservoirs, preventing the invasion of pathogens into the human population [13–15].

References

1. Makarov VV, Khromov AV, Gushchin VA, Tkachuk AP. Emergence Of New Infections In The 21st Century And Identification Of Pathogens Using Next Generation Sequencing. Bulletin of Russian State Medical University. 2017; 01: 5–25.
2. Fournier PE, Dubourg G, Raoult D. Clinical detection and characterization of bacterial pathogens in the genomics era. Genome medicine. 2014; 6 (11): 114.
3. Karadeema RJ, Stancescu M, Steidl TP, Bertot SC, Kolpashchikov DM. The owl sensor: a 'fragile' DNA nanostructure for the analysis of single nucleotide variations. Nanoscale. 2018; 10: 10116–22.
4. Durmanov NN, Guliev RR, Eremenko AV, Boginskaya IA, Ryzhikov IA, Trifonova EA, et al. Non-labeled selective virus detection with novel SERS-active porous silver nanofilms fabricated by Electron Beam Physical Vapor Deposition. Sensors Actuators B: Chemical. 2018; 257: 37–47.
5. Pachauri V, Ingebrandt S. Biologically sensitive field-effect transistors: from ISFETs to NanoFETs. Essays Biochemistry. 2016; 60 (1): 81–90.
6. Stein V, Alexandrov K. Synthetic protein switches: Design principles and applications. Trends in Biotechnology. 2015; 33 (2): 101–10.
7. Gootenberg JS, Abudayyeh OO, Kellner MJ, Joung J, Collins JJ, Zhang F. Multiplexed and portable nucleic acid detection platform with Cas13, Cas12a, and Csm6. Science. 2018; 360 (6387): 439–44.
8. East-Seletsky A, O'Connell MR, Knight SC, Burstein D, Cate JHD, Tjian R, et al. Two distinct RNase activities of CRISPR-C2c2 enable guide-RNA processing and RNA detection. Nature. 2016; 538 (7624): 270–73.
9. Gootenberg JS, Abudayyeh OO, Lee JW, Essletzbichler P, Dy AJ, Joung J, et al. Nucleic acid detection with CRISPR-Cas13a/C2c2. Science. 2017; 356 (6336): 435–42.
10. Liu L, Li X, Wang J, Wang M, Chen P, Yin M, et al. Two Distant Catalytic Sites Are Responsible for C2c2 RNase Activities. Cell. 2017; 168 (1–2): 121–34.
11. Gill SC, von Hippel PH. Calculation of protein extinction coefficients from amino acid sequence data. Analitical Biochemistry. 1989; 182 (2): 319–26.
12. Pace CN, Vajdos F, Fee L, Grimsley G, Gray T. How to measure and predict the molar absorption coefficient of a protein. Protein Science. 1995; 4 (11): 2411–23.
13. Li CX, Shi M, Tian JH, Lin XD, Kang YJ, Chen LJ, et al. Unprecedented genomic diversity of RNA viruses in arthropods reveals the ancestry of negative-sense RNA viruses. Elife. 2015; 4: 1–26.
14. Shi M, Lin XD, Tian JH, Chen LJ, Chen X, Li CX, et al. Redefining the invertebrate RNA virosphere. Nature. 2016; 540 (7634): 539–43.
15. Gao GF. Commentary From " A " IV to " Z " IKV: Attacks from Emerging and Re-emerging Pathogens. Cell. 2018; 172 (6): 1157–59.

Литература

1. Makarov VV, Khromov AV, Gushchin VA, Tkachuk AP. Emergence Of New Infections In The 21st Century And Identification Of Pathogens Using Next Generation Sequencing. Bulletin of Russian State Medical University. 2017; 01: 5–25.
2. Fournier PE, Dubourg G, Raoult D. Clinical detection and characterization of bacterial pathogens in the genomics era. Genome medicine. 2014; 6 (11): 114.
3. Karadeema RJ, Stancescu M, Steidl TP, Bertot SC, Kolpashchikov DM. The owl sensor: a 'fragile' DNA nanostructure for the analysis of single nucleotide variations. Nanoscale. 2018; 10: 10116–22.
4. Durmanov NN, Guliev RR, Eremenko AV, Boginskaya IA, Ryzhikov IA, Trifonova EA, et al. Non-labeled selective virus detection with novel SERS-active porous silver nanofilms fabricated by Electron Beam Physical Vapor Deposition. Sensors Actuators B: Chemical. 2018; 257: 37–47.
5. Pachauri V, Ingebrandt S. Biologically sensitive field-effect transistors: from ISFETs to NanoFETs. Essays Biochemistry. 2016; 60 (1): 81–90.
6. Stein V, Alexandrov K. Synthetic protein switches: Design principles and applications. Trends in Biotechnology. 2015; 33 (2): 101–10.
7. Gootenberg JS, Abudayyeh OO, Kellner MJ, Joung J, Collins JJ, Zhang F. Multiplexed and portable nucleic acid detection platform with Cas13, Cas12a, and Csm6. Science. 2018; 360 (6387): 439–44.
8. East-Seletsky A, O'Connell MR, Knight SC, Burstein D, Cate JHD, Tjian R, et al. Two distinct RNase activities of CRISPR-C2c2 enable guide-RNA processing and RNA detection. Nature. 2016; 538 (7624): 270–73.
9. Gootenberg JS, Abudayyeh OO, Lee JW, Essletzbichler P, Dy AJ, Joung J, et al. Nucleic acid detection with CRISPR-Cas13a/C2c2. Science. 2017; 356 (6336): 435–42.
10. Liu L, Li X, Wang J, Wang M, Chen P, Yin M, et al. Two Distant Catalytic Sites Are Responsible for C2c2 RNase Activities. Cell. 2017; 168 (1–2): 121–34.
11. Gill SC, von Hippel PH. Calculation of protein extinction coefficients from amino acid sequence data. Analitical Biochemistry. 1989; 182 (2): 319–26.
12. Pace CN, Vajdos F, Fee L, Grimsley G, Gray T. How to measure and predict the molar absorption coefficient of a protein. Protein Science. 1995; 4 (11): 2411–23.
13. Li CX, Shi M, Tian JH, Lin XD, Kang YJ, Chen LJ, et al. Unprecedented genomic diversity of RNA viruses in arthropods reveals the ancestry of negative-sense RNA viruses. Elife. 2015; 4: 1–26.
14. Shi M, Lin XD, Tian JH, Chen LJ, Chen X, Li CX, et al. Redefining the invertebrate RNA virosphere. Nature. 2016; 540 (7634): 539–43.
15. Gao GF. Commentary From " A " IV to " Z " IKV: Attacks from Emerging and Re-emerging Pathogens. Cell. 2018; 172 (6): 1157–59.

THE SEARCH AND ANALYSIS OF A CRISPR-CAS SYSTEM IN *ESCHERICHIA COLI* HS WITH SUBSEQUENT SCANNING FOR THE CORRESPONDING PHAGE RACES BASED ON THE SPACERS OF THE DETECTED CRIPSR ARRAY USING BIOINFORMATIC METHODS

Ivanova EI[1]✉, Dzhioev YuP[2], Borisenko AYu[2], Peretolchina NP[2], Stepanenko LA[2], Paramonov AI[1], Grigorova EV[1], Nemchenko UM[1], Tunik TV[1], Kungurtseva EA[1]

[1] Scientific Center for Family Health and Human Reproduction Problems, Irkutsk

[2] Research Institute for Biomedical Technologies of Irkutsk State Medical University, Irkutsk

CRISPR-Cas is an immune system of prokaryotes that protects them against alien replicons, mainly viruses and plasmids. Short sequences (spacers) complementary to the regions of a viral or plasmid genome are inserted into a CRISPR array conferring resistance to reinfection. Infections caused by *Escherichia coli* still present a serious challenge for clinical medicine. The aim of this study was to scan the genome of *Escherichia coli* HS for CRISPR-Cas components. The search was conducted using MacSyFinder (Macromolecular System Finder, ver. 1.0.2.), a program for bioinformatic modelling. Sequence homology searches were done using makeblastdb (ver. 2.2.28) and HMMER (ver. 3.0) tools. Bioinformatics-based methods allowed us to detect one CRISPR-Cas system in the studied genome of *Escherichia coli* HS and read the spacer sequences of its CRIPSR array. The protospacer regions complementary to the spacer sequences of the detected CRISPR array are typical for a few types of phages. Based on these findings, one can assess the degree of bacterial resistance to alien genetic elements.

Keywords: bioinformatics, CRISPR-Cas system, *Escherichia coli* HS, bacteriophage

✉ **Correspondence should be addressed:** Elena Ivanova
Timiryazeva 16, Irkutsk, 664003; ivanova.iem@gmail.com

Received: 15.03.18 **Accepted:** 24.03.18

DOI: 10.24075/brsmu.2018.019

ПОИСК И АНАЛИЗ CRISPR-CAS СИСТЕМЫ В ШТАММЕ *ESCHERICHIA COLI* HS И ДЕТЕКТИРУЕМЫХ СПЕЙСЕРАМИ ЕГО CRISPR-КАССЕТЫ ФАГОВЫХ РАС МЕТОДАМИ БИОИНФОРМАТИКИ

Е. И. Иванова[1]✉, Ю. П. Джиоев[2], А. Ю. Борисенко[2], Н. П. Перетолчина[2], Л. А. Степаненко[2], А. И. Парамонов[1], Е. В. Григорова[1], У. М. Немченко[1], Т. В. Туник[1], Е. А. Кунгурцева[1]

[1] Научный центр проблем здоровья семьи и репродукции человека, Иркутск

[2] Институт биомедицинских технологии, Иркутский государственный медицинский университет, Иркутск

CRISPR-Cas система — это иммунная система прокариот, обеспечивающая защиту от чужеродных репликонов, в первую очередь вирусов и плазмид. Устойчивость к повторным инфекциям приобретается в результате включения в состав CRISPR-кассет коротких последовательностей, или спейсеров, комплементарных участкам соответствующих вирусных или плазмидных геномов. В настоящее время эшерихиозные инфекции остаются серьезной проблемой практической медицины. Вследствие их крайней устойчивости к терапии с использованием антибиотиков необходима разработка новых подходов лечения. Целью исследования был поиск структур CRISPR-Cas систем в геномной последовательности штамма *Escherichia coli* HS. Использовали методы программного моделирования MacSyFinder (Macromolecular System Finder, ver. 1.0.2.). Поиск точной гомологии последовательностей осуществляли посредством установленных вспомогательных пакетов makeblastdb (ver. 2.2.28), HMMER (ver. 3.0). В результате методами биоинформатики была выявлена одна CRISPR-Cas система и расшифрованы спейсерные последовательности CRISPR-кассеты у штамма *Escherichia coli* HS. С помощью последовательностей спейсеров CRISPR-кассеты были определены комплементарные им протоспейсерные участки нескольких типов фагов, что позволяет оценить степень их устойчивости к этим чужеродным генетическим элементам.

Ключевые слова: биоинформатика, CRISPR-Cas система, *Escherichia coli* HS, бактериофаги

✉ **Для корреспонденции:** Елена Иннокентьевна Иванова
ул. Тимирязева, д. 16, г. Иркутск, 664003; ivanova.iem@gmail.com

Статья получена: 15.03.18 **Статья принята к печати:** 24.03.18

DOI: 10.24075/vrgmu.2018.019

The *Escherichia coli* species comprises multiple biotypes. Some of them are commensal colonizers of the mammalian (including human) gut. Others are pathogenic and cause disease. One of the most significant causative agents of intestinal infections is enterohemorrhagic *Escherichia coli* O157:H7, whereas an important representative of commensals is *E. coli* HS. Infection caused by *E. coli* O157:H7 can provoke hemolytic uremic syndrome (HUS) characterized by progressive renal failure. *E. coli* O157:H7 is a serotype capable of producing Shiga toxins [1–3]. No specific treatment has yet proved effective against this syndrome. Only supportive care is recommended during the acute stage of the disease. The use of antibiotics for treating

infections caused by Shiga-toxin-producing *E. coli* (Stx-E. *coli*) is very debatable [4, 5]. It has been shown that antibiotic therapy prescribed to patients with acute gastrointestinal infection caused by Stx-E. *coli* increases the risk of developing HUS 17-fold [6]. Disruption of the bacterial membrane by antibiotics can stimulate progression to the acute stage because the bacteria start to release the toxin in large quantities [7].

Therefore, we need novel alternatives to antibiotics to combat pathogenic bacteria. Phage therapy holds great promise here [8–10]. The evolution of this approach relies on the fundamental knowledge about the genetic basis underlying the interactions between bacteria and bacteriophages. This knowledge, in turn, can be obtained only if bacterial and phage genomes, as well as new analytical methods, are at the researcher's disposal. Currently available bioinformatics software allows the researcher to manipulate huge arrays of genomic data, extracting new information about bacterial genomes [11].

Besides the advances in bioinformatics, another significant event of the past few years is discovery of specific adaptive immunity in prokaryotes. It was long believed that bacteria could not resist phage attacks, but in 1987 a strange region was discovered in the *E. coli* genome that consisted of multiple repeats [12]. However, it was not until 2005 that it became clear that the sequences alternating with those repeats were often identical to the sequences found in bacterial and plasmid genomes [13, 14]. The discovered structures were termed CRISPR-Cas (Clustered Regularly Interspaced Short Palindromic Repeats — CRISPR-associated proteins). They are a specific adaptive defense of bacteria and archaea against alien genetic material mostly derived from phages and plasmids [15–18]. CRISPR arrays are a unique set of palindromic repeats of 21–47 base pairs separated by unique spacers. Spacers are complementary to the regions in phage or plasmid genomes the bacterium is immune against [13]. In close proximity to a CRISPR locus are *cas*-genes. Their products ensure proper functioning of a CRISPR locus. According to the current classification, CRISPR-Cas systems are grouped into 3 types based on their mechanism of action and the *cas*- proteins present in the genome [19].

Bioinformatic methods are employed to detect and identify CRISPR-Cas systems in bacterial genomes [20, 21]. For example, they can help to identify bacteriophage races by bacterial spacer sequences and, therefore, to assess bacterial resistance to certain phages or plasmids [22–24]. This is an important research field, because such screening can provide a solution to the practical challenges faced in the therapy of infections and contribute to the study of evolution across and between bacterial species [17, 22]. For many bacterial species, however, the mechanism of interactions between them and their phages mediated by CRISPR-Cas and anti-CRISPR-Cas systems remains totally understudied. Therefore, it is wise to start with the development of an efficient algorithm for the bioinformatics-based search and analysis of bacterial CRISPR-Cas loci and their structural components and then proceed to the screening of phage races using bacterial CRIPSR arrays. Considering the abovesaid, we aimed to search the genome of *Escherichia coli* HS for CRIPSR-Cas loci, study the detected components and then identify the corresponding bacteriophage races through screening using bacterial CRISPR arrays and an original bioinformatics-based search algorithm.

METHODS

The object of our study was the strain *Escherichia coli* HS. GenBank stores two of its genomes: NC_009800.1 sequenced in 2017 and CP000802 sequenced in 2014. *E. coli* HS represented in GenBank by the genome NC_009800.1 was cultured using a reference strain from the collection of the Center for Vaccine Development (USA) [25]. For our study we selected the genome CP000802 of a reference strain [26] isolated from the gastrointestinal tract of a healthy human who showed no clinical symptoms of colonization [25].

To detect CRISPR-Cas loci in the bacterial genome, we used MacSyFinder (Macromolecular System Finder, ver. 1.0.2.), a program for bioinformatic modelling [27]. This software requires a protein profile of genomic sequences encoded as hidden Markov models (HMM) available in PFAM, TIGRFAM and PRODOM databases. Sequence homology searches were conducted using makeblastdb (ver. 2.2.28) and HMMER (ver. 3.0); the same software allowed us to obtain structural and functional characteristics of *cas*-proteins detected in each analyzed genome [28]. Visual representation of the results returned by MacSyFinder was generated in MacSyView. The programming language used was Python (ver. 2.7) [29].

The obtained CRISPR arrays were run against the online database *CRISPI*: a *CRISPR Interactive database* (Gen Ouest BioInformatics Platform, http://genouest.org/) for structural analysis. Bacterial and archaeal genomes were downloaded from the NCBI FTP Server and processed in C and Java (ver. 1.5.0.12.) [30]. The detection algorithm was based on imposing a limitation on the number of closest matches. To avoid detection of unrelated structures, the minimally required percent identity was set to 60%. The web-page was implemented in PHP (ver. 4.3.9) and Java (ver. 1.5.0.12). For phage identification, the obtained spacer sequences were run against the GenBank-Phage database using the search algorithm BLASTn [31]. The following online services were used: CRISPRTarget (http://bioanalysis.otago.ac.nz/CRISPRTarget/crispr_analysis.html) and Mycobacteriophage Database (http://phagesdb.org/blast/).

RESULTS

The screening of the *E. coli* HS genome CP000802 revealed a presence of a CRISPR-Cas system at positions 2920652-2921839, i.e. its length was 1,187 b.p. Structurally, this CRISPR-Cas system belonged to CAS-Type-IE.

Using MacSyFinder, we identified and visualized the following regions of the *E. coli* HS genome coding for Cas proteins:

– mandatory genes, whose presence in the genome indicates the presence of a CRISPR-Cas system (Fig. 1);

– accessory genes that may be found in more than one system and are hard to identify using only one protein profile; however, they also signal the presence of a CRISPR-Cas system in a bacterial genome.

Using MacSyFinder, we were able to detect *cas*-genes in the CRISPR-Cas system of the analyzed *E. coli* HS genome and get a visual representation of the obtained XML in MacSyView. Examples of *cas*-genes and their location in the genome of the studied strain are shown in Fig. 1.

Using HMMER (ver. 3.0) and makeblastdb (ver. 2.2.28), we obtained structural and functional characteristics of *cas*-proteins detected in each analyzed genome, namely: gene (the gene corresponding to the profile), system (the system the gene belongs to), hitid (the sequence identifier), hit seq length (length of the sequence), replicon name (the name of the replicon), position hit (the rank of the sequence matched in the input dataset file), i-eval (independent evalue), score (the score of the hit), profile coverage (percentage of the profile that matches the hit sequence), sequence coverage (percentage of the hit

sequence that matches the profile), begin match (the position in the sequence where the profile match begins), and end match (the position in the sequence where the profile match ends) (Fig. 2).

The obtained CRISPR arrays were analyzed in real time in *CRISPI*: a *CRISPR Interactive database*, which basically uses homology of repeated regions to return information about the sequence structure. Using this online tool, 11 repeats were identified in the CRISPR array of the studied strain. The consensus view is provided in Fig. 3. After repeats were detected, 10 spacers were identified in the CRISPR array (Table 1). Visual representations of the CRISPR array and *cas*-genes detected in the studied bacterial genome was implemented in Java (Fig. 4).

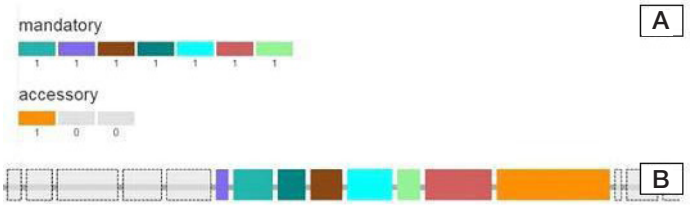

Fig. 1. *Cas*-genes (**A**) and their location in the genome (**B**) of *E. coli* HS (CP000802) detected by MacSyFinder and visualized in MacSyView

Color	Sequence Id	Position	Profile Match	Function	Gene status	System	Protein length (aa)	Score	i-evalue	Profile coverage	Sequence coverage	Begin match	End match
	lcl|NC_002695.1_prot_NP_311635.1_3467	3467	cas2_TypeIE		mandatory	CAS-TypeIE	97	133.6	5.5e-40	1.00	0.89	3	88
	lcl|NC_002695.1_prot_NP_311636.1_3468	3468	cas1_TypeIE		mandatory	CAS-TypeIE	307	380.1	1.4e-114	0.99	0.86	8	272
	lcl|NC_002695.1_prot_NP_311637.1_3469	3469	cas6_TypeIE		mandatory	CAS-TypeIE	216	292.6	7e-88	1.00	0.98	1	212
	lcl|NC_002695.1_prot_NP_311638.1_3470	3470	cas5_TypeIE		mandatory	CAS-TypeIE	248	159.4	3e-47	0.99	0.93	3	233
	lcl|NC_002695.1_prot_NP_311639.1_3471	3471	cas7_TypeIE		mandatory	CAS-TypeIE	351	447.9	9.3e-135	1.00	0.92	3	324
	lcl|NC_002695.1_prot_NP_311640.1_3472	3472	cse2_TypeIE		mandatory	CAS-TypeIE	178	127.7	1.3e-37	1.00	0.89	12	169
	lcl|NC_002695.1_prot_NP_311641.1_3473	3473	cse1_TypeIE		mandatory	CAS-TypeIE	520	620.3	7.7e-187	1.00	0.97	5	509
	lcl|NC_002695.1_prot_NP_311642.1_3474	3474	cas3_TypeI		accessory	CAS	885	216.2	1.9e-64	0.90	0.42	292	662

Fig. 2. Structural and functional characteristics of Cas proteins of *E. coli* HS (CP000802) obtained in MacSyFinder

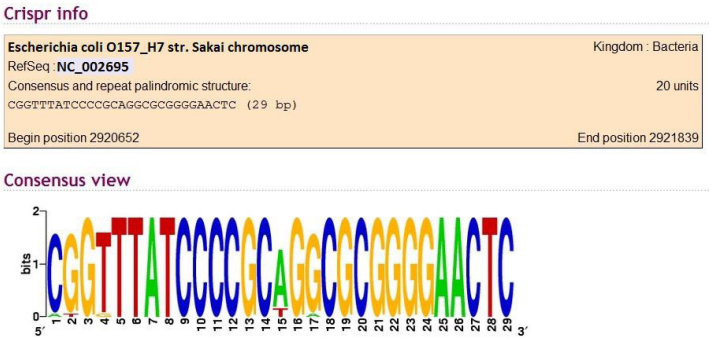

Fig. 3. The consensus view of the alternating repeats in the genome of *E. coli* HS (CP000802) generated in *CRISPI*: a *CRISPR Interactive database*. The size of nucleotide letter codes shows a degree of nucleotide variability in the repeat: the taller the letter, the more variable the nucleotide

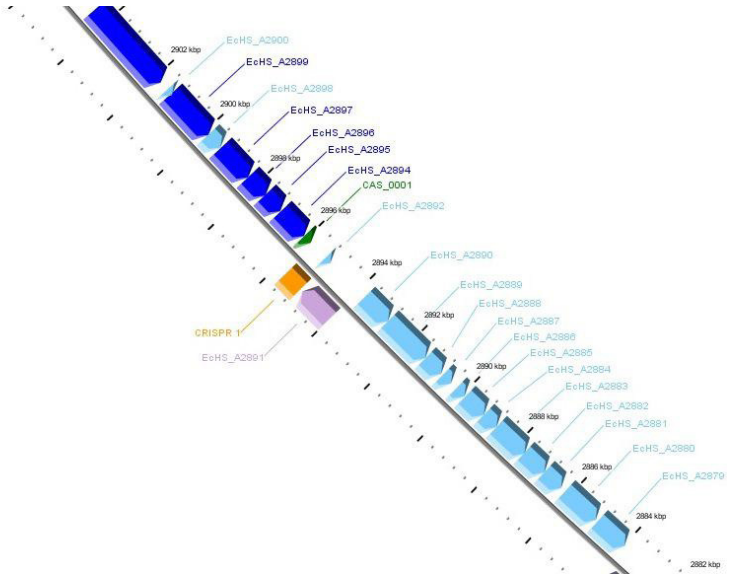

Fig. 4. Location of *cas*-genes and the CRISPR array in the genome of *E. coli* HS (CP000802)

Table 1. The list of nucleotide sequences in the CRIPSR array: spacers separated by repeat units detected in *CRISPI*: a *CRISPR Interactive database* in the genome of *E. coli* HS (CP000802)

Spacers/repeats	Begin	End	Nucleotide sequences	Size
unit 1	2920652	2920680	ATGGTTATCCCCGCTGACGCGGGGAACTC	29
spacer 1	2920681	2920712	TCGTCCAGACTGAATACGTTGTCCCAAAATCT	31
unit 2	2920713	2920741	CGGTTTATCCCCGCTGGCGCGGGGAACTC	29
spacer 2	2920742	2920773	CTATTGATGAGGTGCACCATCAGAAGCGAGAT	31
unit 3	2920774	2920802	CGGTTTATCCCCGCTGGCGCGGGGAACTC	29
spacer 3	2920803	2920834	GACGTACAGATTGGCTGCGGCACCTCAAACAC	31
unit 4	2920835	2920863	CGGTTTATCCCCGCAGGCGCGGGGAACTC	29
spacer 4	2920864	2920895	TTAATTCGCGTACCTGCGCATCCATTGCCGCG	31
unit 5	2920896	2920924	CGGTTTATCCCCGCAGGCGCGGGGAACTC	28
spacer 5	2920925	2920956	CGCAATCATGTTTTTCATTGGGTTTACGTCCT	31
unit 6	2920957	2920985	CGGTTTATCCCCGCAGGCGCGGGGAACTC	28
spacer 6	2920986	2921017	TTTTTATGACTGAATCCACTACGCCTTCATAG	31
unit 7	2921018	2921046	CGGTTTATCCCCGCAGGCGCGGGGAACTC	28
spacer 7	2921047	2921078	TTTACGTCGTTGATGACATCGTTCAGGTGTTT	31
unit 8	2921079	2921107	CGGTTTATCCCCGCAGGCGCGGGGAACTC	28
spacer 8	2921108	2921139	GTGATTTTCGTACCCGGCGCGATCGCGATATG	31
unit 9	2921140	2921168	CGGTTTATCCCCGCAGGCGCGGGGAACTC	28
spacer 9	2921169	2921200	GATAACCGCTTCGCGGTCAATATCTGCCGCAC	31
unit 10	2921201	2921229	CGGTTTATCCCCGCAGGCGCGGGGAACTC	28
spacer 10	2921230	2921261	GCCCATCGCCTGCGCCACACTGTTAAAAAGTT	31
unit 11	2921262	2921290	CGGTTTATCCCCGCAGGCGCGGGGAACTC	28
spacer 11	2921291	2921322	TCATTCGCAATCATCCACTGACTCAGGGGCTG	31

Table 2. Spectrum of the phage races revealed by the complementary structures of the spacer sequences of the CRISPR cassette of *E. coli* HS strain (No. CP000802)

№	Spacer	Bacteriophages	Number of substitutions
1	spacer 1 (2920681-2920712)	**Aeromonas phage phiAS4**, (HM452125) positions: 100313-100337, **Cronobacter phage vB_CsaP_Ss1**, (KM058087) positions: 19880-19863	8 10
2	spacer 5 (2920925-2920956)	**Salmonella phage PVP-SE1**, (GU070616) positions: 124932-124959 **Salmonella phage SSE-121**, (JX181824) positions: 87806-87779 **Bacillus phage Bp8p-T**, (KJ010548) positions: 144792-144820 **Bacillus phage Bp8p-C**, (KJ010547) positions: 144790-144818	7 7 8 8
3	spacer 7 (2921047-2921078)	**Rhizobium phage vB_RleM_P10VF**, (KM199770) positions: 93101-93076 **Burkholderia phage phiE255**, (CP000622) positions: 17180-17211 **Burkholderia cenocepacia phage BcepMu**, (AY539836) positions: 30887-30918 **Gordonia phage GTE5**, (JF923796) positions: 49708-49734 **Dickeya phage vB_DsoM_LIMEstone1** (HE600015) positions: 52018-52038 **Dickeya phage RC-2014**, (KJ716335) positions: 27496-27516 **Synechococcus phage S-CAM1** (HQ634177) positions: 189041-189018 **Cyanophage S-SSM6b** (HQ316603) positions: 161353-161374 **Cyanophage S-SSM4** (HQ316583) positions: 103276-103255	8 7 7 8 8 8 9 10 10
4	spacer 10 (2921230-2921261)	**Bacteriophage RTP**, (AM156909) positions: 34535-34554	10

DISCUSSION

Last year the *Escherichia coli* HS genome NC_009800.1 was annotated in the GenBank database. The annotation contained information about three CRISPR-Cas loci in this genome. In the CRISPR-Cas database (http://crispr.i2bc.paris-saclay.fr/crispr/) these loci are represented by a few variants. Our study demonstrates that, on the whole, the structural units of the CRISPR array detected in the *E. coli* HS genome (CP000802, sequenced in 2014) coincide with the structural units of the *E. coli* HS strain (NC_009800_6, sequenced in 2017).

Using the spacer sequences detected in the CRIPSR array of the studied strain, we attempted to identify the phages (Table 2). Of 10 spacer sequences only 4 spacers (1, 5, 7, and 10) were complementary to the protospacers of phage races presented in the table. The identified phage races are typical for a wide range of bacterial hosts. Perhaps, this is a result of the horizontal transfer of CRIPSR-Cas systems between different types of bacteria throughout a long history of development of their adaptive immunity. Further research will definitely yield new knowledge of the nature of the antagonistic relationship between bacteria and their phages. Based on the detected phage races, one can infer the degree of immune protection and the viability of bacteria throughout their evolution.

CONCLUSIONS

The successful detection of a CRISPR-Cas array in the genome of the *E. coli* HS strain (CP000802, sequenced in 2014) and its structural analysis render bioinformatics-based methods effective for the search of CRISPR-Cas structures in the sequenced bacterial genomes. Such type of search

yields valuable information. The presence of "mandatory" Cas proteins suggest high anti-phage activity of the CRISPR-Cas system of the studied strain. The number of detected spacers reflect the duration of the strain's evolution. The comparative analysis of spacers in two CRISPR arrays detected in the CP000802 genome of *E. coli* HS sequenced in 2014 and in the NC_009800.1 genome of the same strain sequenced in 2017 demonstrates that the number of spacers in the CRIPSR array detected in NC_009800.1 has increased to 19. The number of spacers in CP000802 is only 10. We assume that such increase in the number of spacers was possible due to their accumulation following frequent passaging or because of frequent contamination by phages. In any case, it can be indicative of high CRIPSR-Cas activity in *E. coli* HS.

References

1. Trachtman H, Austin C, Lewinski M, Stahl R. A. Renal and neurological involvement in typical Shiga toxin-associated HUS. Nature Reviews Nephrology. 2012; (8): 658–69.
2. Croxen MA, Law RJ, Scholz R, Keeney KM, Wlodarska M, Finlay BB. Recent advances in understanding enteric pathogenic Escherichia coli. Clinical Microbiology Reviews. 2013; (26): 822–80.
3. Tarr G, Shringi S, Phipps AI, Besser TE, Mayer J, Oltean HN, et. al. Geogenomic Segregation and Temporal Trends of Human Pathogenic Escherichia coli O157:H7, Washington, USA, 2005–2014. Emerg Infect Dis. 2018; 24 (1): 32–9.
4. Ivanova EI, Rychkova LV, Nemchenko UM, Bukharova EV, Savelkaeva MV, Dzhioeva YuP. The Structure of the Intestinal Microbiota of the Intestine and the Frequency of Detection of Pathogenicity Genes (stx1, stx2, bfp) in Escherichia coli with Normal Enzymatic Activity Isolated from Children during the First Year of Life. Molecular Genetics, Microbiology and Virology. 2017; 32 (1): 42–8.
5. Holmes A, Dallman TJ, Shabaan S, Hanson M, Allison L. Validation of Whole-Genome Sequencing for Identification and Characterization of Shiga Toxin-Producing Escherichia coli To Produce Standardized Data To Enable Data Sharing. J Clin Microbiol. 2018; 56 (3): e01388-17.
6. Wong CS, Mooney JC, Brandt JR, Staples AO, Jelacic S, Boster DR, et al. Risk factors for the hemolytic uremic syndrome in children infected with Escherichia coli O157:H7: a multivariable analysis. Clin Infect Dis. 2012; 55 (1): 33–41.
7. Freedman SB, Xie J, Neufeld MS, Hamilton WL, Hartling L, Tarr PI. Shiga toxin-producing Escherichia coli infection, antibiotics, and risk of developing hemolytic uremic syndrome: A meta-analysis. Clinical Infectious Diseases. 2016; (62): 1251–58.
8. Pirnay JP, Blasdel BG, Bretaudeau L, Buckling A, Chanishvili N, Clark JR, et.al. Quality and safety requirements for sustainable phage therapy products. Pharm Res. 2015; 32 (7): 2173–79.
9. Qadir MI. Review: phage therapy: a modern tool to control bacterial infections. Pak J Pharm Sci. 2015; 28 (1): 265–70.
10. Nazarov PA. Al'ternativy antibiotikam: liticheskie fermenty bakteriofagov i fagovaja terapija. Vestnik RGMU. 2018; (1).
11. Rusconi B, Sanjar F, Koenig SS, Mammel MK, Tarr PI, Eppinger M. Whole Genome Sequencing for Genomics-Guided Investigations of Escherichia coli O157:H7 Outbreaks. Front Microbiol. 2016; 7: 985.
12. Nakata A, Amemura M, Makino KJ. Unusual nucleotide arrangement with repeated sequences in the Escherichia coli K-12 chromosome. Bacteriol. 1989; 171 (6): 3553–56.
13. Bolotin A, Quinquis B, Sorokin A, Ehrlich SD. Clustered regularly interspaced short palindrome repeats (CRISPRs) have spacers of extrachromosomal origin. Microbiology 2005; 151: 2551–61.
14. Brouns SJ, Jore MM, Lundgren M, Westra ER, Slijkhuis RJ, Snijders AP, et al. CRISPR RNAs guide antiviral defense in prokaryotes. Science. 2008; (321): 960–4.
15. Dzhagarov DJe. Umnye nozhnicy dlja DNK. Himija i zhizn'. 2014; 7: 6–9.
16. Westra ER, Buckling A, Fineran PC. CRISPR-Cas systems: beyond adaptive immunity. Nat Rev Microbiol. 2014; 12 (5): 317–26.
17. Makarova KS, Koonin EV. Annotation and Classification of CRISPR-Cas Systems. Methods Mol Biol. 2015; (1311): 47–75.
18. Modell JW, Jiang W, Marraffini LA. CRISPR-Cas systems exploit viral DNA injection to establish and maintain adaptive immunity. Nature. 2017; 544 (7648): 101–4.
19. Gasiunas G, Sinkunas T, Siksnys V. Molecular mechanisms of CRISPR-mediated microbial immunity. Cellular and Molecular Life Sciences. 2014; 71 (3): 449–65.
20. Peretolchina NP, Dzhioev YP, Boricenko AY, Paramonov AI, Voskresenskaya EA, Stepanenko LA, et al. Bioinformatic search and screening of phages and plasmids via spaser sites of Yersinia pseudotuberculosis YPIII CRISPR/Cas System. Materials 15th Medical Biodefence Conference, 26–29 April 2016; Minich: 43–44.
21. Zlobin VI, Dzhioev YuP, Peretolchina NP, Borisenko AY, Stepanenko LA, Yingchen Wang, et.al. Prospects to Enhance Phage Therapy by Looking At CRISP Fingerprints in Bacterial Populations. Current Trends in Biomedical Engineering & Biosciences. 2018; 10 (5): 1–3.
22. Abedon S, Kuhl S, Blasdel B. Phage treatment of human infections. Bacteriophage. 2011; (1): 66–85.
23. Stepanenko LA, Dzhioev JuP, Borisenko AJu, Kolbaseeva OV, Zlobin VI, Malov IV. Poisk fagov i plazmid cherez spejsernye sajty CRISPR/CAS-sistemy Neisseria meningitides fdaargos_214. Zhurnal infektologii. 2018; 10 (S1): 30–31.
24. Borisenko AJu, Dzhioev JuP, Peretolchina NP, Stepanenko LA, Kuz'minova VM, Kolbaseeva OV i dr. Bioinformacionnyj poisk i skrining bakteriofagov cherez spejsery CRISPR/CAS-sistemy shtamma Staphylococcus aureus Mu3. Aktual'nye problemy nauki pribajkal'ja. 2017; 2: 45–9.
25. Levine M. M., Rennels M. B. E. coli colonization factor antigen in diarrhoea. Lancet. 1978; 2 (8088): 534.
26. Rasko DA, Rosovitz MJ, Myers GSA, Mongodin EF, Fricke WF, Gajer P, et al. The Pangenome Structure of Escherichia coli: Comparative Genomic Analysis of E. coli Commensal and Pathogenic Isolates. J Bacteriol. 2008; 190 (20): 6881–93.
27. Abby SS, Néron B, Ménager H, Touchon M, Rocha Eduardo PC. MacSyFinder: A Program to Mine Genomes for Molecular Systems with an Application to CRISPR-Cas Systems. PLoS One. 2014; 9 (10): e110726.
28. Gaj T, Gersbach CA, Barbas CF. ZFN, TALEN and CRISPR/Cas-based methods for genome engineering. Trends Biotechnol. 2013; 31: 397–405.
29. Qi LS, Larson MH, Gilbert LA, Doudna JA, Weissman JS, Arkin AP, et al. Repurposing CRISPR as an RNA guided platform for sequence-specific control of gene expression. Cell. 2013; 152 (5): 1173–83.
30. Grissa I, Vergnaud G, Pourcel C. CRISPRFinder: a web tool to identify clustered regularly interspaced short palindromic repeats. Nucleic Acids Res. 2007; (35) (Web Server issue): W52-7.
31. Johnson M, Zaretskaya I, Raytselis Y, Merezhuk Y, McGinnis S, Madden TL. NCBI BLAST: a better web interface. NCBI BLAST: a better web Interface. Nucleic Acids Res. 2008; (1); 36 (Web Server issue): W5-9.

Литература

1. Trachtman H, Austin C, Lewinski M, Stahl R. A. Renal and neurological involvement in typical Shiga toxin-associated HUS. Nature Reviews Nephrology. 2012; (8): 658–69.
2. Croxen MA, Law RJ, Scholz R, Keeney KM, Wlodarska M, Finlay BB. Recent advances in understanding enteric pathogenic Escherichia coli. Clinical Microbiology Reviews. 2013; (26): 822–80.
3. Tarr G, Shringi S, Phipps AI, Besser TE, Mayer J, Oltean HN, et. al. Geogenomic Segregation and Temporal Trends of Human Pathogenic Escherichia coli O157:H7, Washington, USA, 2005–2014. Emerg Infect Dis. 2018; 24 (1): 32–9.
4. Ivanova EI, Rychkova LV, Nemchenko UM, Bukharova EV, Savelkaeva MV, Dzhioeva YuP. The Structure of the Intestinal Microbiota of the Intestine and the Frequency of Detection of Pathogenicity Genes (stx1, stx2, bfp) in Escherichia coli with Normal Enzymatic Activity Isolated from Children during the First Year of Life. Molecular Genetics, Microbiology and Virology. 2017; 32 (1): 42–8.
5. Holmes A, Dallman TJ, Shabaan S, Hanson M, Allison L. Validation of Whole-Genome Sequencing for Identification and Characterization of Shiga Toxin-Producing Escherichia coli To Produce Standardized Data To Enable Data Sharing. J Clin Microbiol. 2018; 56 (3): e01388-17.
6. Wong CS, Mooney JC, Brandt JR, Staples AO, Jelacic S, Boster DR, et al. Risk factors for the hemolytic uremic syndrome in children infected with Escherichia coli O157:H7: a multivariable analysis. Clin Infect Dis. 2012; 55 (1): 33–41.
7. Freedman SB, Xie J, Neufeld MS, Hamilton WL, Hartling L, Tarr PI. Shiga toxin-producing Escherichia coli infection, antibiotics, and risk of developing hemolytic uremic syndrome: A meta-analysis. Clinical Infectious Diseases. 2016; (62): 1251–58.
8. Pirnay JP, Blasdel BG, Bretaudeau L, Buckling A, Chanishvili N, Clark JR, et.al. Quality and safety requirements for sustainable phage therapy products. Pharm Res. 2015; 32 (7): 2173–79.
9. Qadir MI. Review: phage therapy: a modern tool to control bacterial infections. Pak J Pharm Sci. 2015; 28 (1): 265–70.
10. Назаров П. А. Альтернативы антибиотикам: литические ферменты бактериофагов и фаговая терапия. Вестник РГМУ. 2018; (1).
11. Rusconi B, Sanjar F, Koenig SS, Mammel MK, Tarr PI, Eppinger M. Whole Genome Sequencing for Genomics-Guided Investigations of Escherichia coli O157:H7 Outbreaks. Front Microbiol. 2016; 7: 985.
12. Nakata A, Amemura M, Makino KJ. Unusual nucleotide arrangement with repeated sequences in the Escherichia coli K-12 chromosome. Bacteriol. 1989; 171 (6): 3553–56.
13. Bolotin A, Quinquis B, Sorokin A, Ehrlich SD. Clustered regularly interspaced short palindrome repeats (CRISPRs) have spacers of extrachromosomal origin. Microbiology 2005; 151: 2551–61.
14. Brouns SJ, Jore MM, Lundgren M, Westra ER, Slijkhuis RJ, Snijders AP, et al. CRISPR RNAs guide antiviral defense in prokaryotes. Science. 2008; (321): 960–4.
15. Джагаров Д. Э. Умные ножницы для ДНК. Химия и жизнь. 2014; (7): 6–9.
16. Westra ER, Buckling A, Fineran PC. CRISPR-Cas systems: beyond adaptive immunity. Nat Rev Microbiol. 2014; 12 (5): 317–26.
17. Makarova KS, Koonin EV. Annotation and Classification of CRISPR-Cas Systems. Methods Mol Biol. 2015; (1311): 47–75.
18. Modell JW, Jiang W, Marraffini LA. CRISPR-Cas systems exploit viral DNA injection to establish and maintain adaptive immunity. Nature. 2017; 544 (7648): 101–4.
19. Gasiunas G, Sinkunas T, Siksnys V. Molecular mechanisms of CRISPR-mediated microbial immunity. Cellular and Molecular Life Sciences. 2014; 71 (3): 449–65.
20. Peretolchina NP, Dzhioev YP, Boricenko AY, Paramonov AI, Voskresenskaya EA, Stepanenko LA, et al. Bioinformatic search and screening of phages and plasmids via spaser sites of Yersinia pseudotuberculosis YPIII CRISPR/Cas System. Materials 15th Medical Biodefence Conference, 26–29 April 2016; Minich: 43–44.
21. Zlobin VI, Dzhioev YuP, Peretolchina NP, Borisenko AY, Stepanenko LA, Yingchen Wang, et.al. Prospects to Enhance Phage Therapy by Looking At CRISP Fingerprints in Bacterial Populations. Current Trends in Biomedical Engineering & Biosciences. 2018; 10 (5): 1–3.
22. Abedon S, Kuhl S, Blasdel B. Phage treatment of human infections. Bacteriophage. 2011; (1): 66–85.
23. Степаненко Л. А., Джиоев Ю. П., Борисенко А. Ю., Колбасеева О. В., Злобин В. И., Малов И. В. Поиск фагов и плазмид через спейсерные сайты CRISPR/CAS-системы Neisseria meningitides fdaargos_214. Журнал инфектологии. 2018; 10 (S1): 30–31.
24. Борисенко А. Ю., Джиоев Ю. П., Перетолчина Н. П., Степаненко Л. А., Кузьминова В. М., Колбасеева О. В. и др. Биоинформационный поиск и скрининг бактериофагов через спейсеры CRISPR/CAS-системы штамма Staphylococcus aureus Mu3. Актуальные проблемы науки прибайкалья. 2017; (2): 45–9.
25. Levine M. M., Rennels M. B. E. coli colonization factor antigen in diarrhoea. Lancet. 1978; 2 (8088): 534.
26. Rasko DA, Rosovitz MJ, Myers GSA, Mongodin EF, Fricke WF, Gajer P, et al. The Pangenome Structure of Escherichia coli: Comparative Genomic Analysis of E. coli Commensal and Pathogenic Isolates. J Bacteriol. 2008; 190 (20): 6881–93.
27. Abby SS, Néron B, Ménager H, Touchon M, Rocha Eduardo PC. MacSyFinder: A Program to Mine Genomes for Molecular Systems with an Application to CRISPR-Cas Systems. PLoS One. 2014; 9 (10): e110726.
28. Gaj T, Gersbach CA, Barbas CF. ZFN, TALEN and CRISPR/Cas-based methods for genome engineering. Trends Biotechnol. 2013; 31: 397–405.
29. Qi LS, Larson MH, Gilbert LA, Doudna JA, Weissman JS, Arkin AP, et al. Repurposing CRISPR as an RNA guided platform for sequence-specific control of gene expression. Cell. 2013; 152 (5): 1173–83.
30. Grissa I, Vergnaud G, Pourcel C. CRISPRFinder: a web tool to identify clustered regularly interspaced short palindromic repeats. Nucleic Acids Res. 2007; (35) (Web Server issue): W52-7.
31. Johnson M, Zaretskaya I, Raytselis Y, Merezhuk Y, McGinnis S, Madden TL. NCBI BLAST: a better web interface. NCBI BLAST: a better web Interface. Nucleic Acids Res. 2008; (1); 36 (Web Server issue): W5-9.

CONSERVED SEQUENCES OF GENES CODING FOR THE MULTIDRUG RESISTANCE PUMP ACRAB-TOLC OF *ESCHERICHIA COLI* SUGGEST THEIR INVOLVEMENT INTO PERMANENT CELL "CLEANING"

Karakozova MV[1] ✉, Nazarov PA[2]

[1] Research Centre of Medical Genetics, Moscow

[2] Belozersky Institute of Physico-Chemical Biology, Lomonosov Moscow State University, Moscow

Multidrug resistance pumps (MDR pumps) of bacteria confer protection against aggressive environmental factors. The genes coding for MDR pumps are thought to be variable. They belong to the group of the so-called contingency genes, i.e are necessary for bacterial adaptation to the changing environment. The aim of the present work was to establish how conserved are the sequences of genes coding for MDR pumps. We analyzed the sequences of AcrA, AcrB and TolC proteins of different *Escherichia coli* strains. Using sequence alignment tools, we demonstrated that strains originating in different countries and cultured in the labs for a long time are amazingly conserved in terms of AcrAB-TolC sequences. They resemble housekeeping genes, suggesting the involvement of the AcrAB-TolC pump into permanent "cleaning" of various biotic and abiotic agents.

Keywords: multidrug resistance, antibiotic, AcrAB-TolC, sequence alignment, *Escherichia coli*, pump, transporter, biocide, contingency genes, housekeeping genes

Acknowledgement: the authors wish to thank students (Dzhafarova T, Mamedova D, Maushev F, Miranian K, Omarova D and Rodionova E) and the Department of Morphology and Pathology of Medical Institute REAVIZ for the provided data, their analysis and discussion.

✉ **Correspondence should be addressed:** Marina Karakozova
Microrayon 1, d.15, kv. 43, Zaraisk, Zaraiski r-n, Moscow region, 140601; mvk752002@gmail.com

Received: 19.02.2018 **Accepted:** 30.03.2018

DOI: 10.24075/brsmu.2018.024

КОНСЕРВАТИВНОСТЬ ПОСЛЕДОВАТЕЛЬНОСТЕЙ ГЕНОВ ПОМПЫ МНОЖЕСТВЕННОЙ ЛЕКАРСТВЕННОЙ УСТОЙЧИВОСТИ ACRAB-TOLC *ESCHERICHIA COLI* КАК ПРИЗНАК ВОВЛЕЧЕННОСТИ В ПЕРМАНЕНТНУЮ «УБОРКУ» БАКТЕРИАЛЬНОЙ КЛЕТКИ

М. В. Каракозова[1] ✉, П. А. Назаров[2]

[1] Медико-генетический научный центр, Москва

[2] Научно-исследовательский институт физико-химической биологии имени А. Н. Белозерского, Московский государственный университет имени М. В. Ломоносова, Москва

Помпы множественной лекарственной устойчивости (МЛУ) помогают бактериям защищаться от неблагоприятного воздействия окружающей среды. Считается, что гены, кодирующие помпы МЛУ, вариабельны и относятся к так называемым генам «роскоши», т. е. предназначены для адаптации бактерий к изменению окружающих условий. Целью работы было проверить насколько консервативны последовательности генов помпы МЛУ. Для этого проводили анализ последовательностей белков AcrA, AcrB и TolC для различных лабораторных штаммов *Escherichia coli*. Методом выравнивания последовательностей было показано, что штаммы из разных стран, культивируемые в лабораториях уже долгое время, имеют удивительную консервативность последовательностей белков помпы AcrAB-TolC. Она напоминает консервативность генов «домашнего хозяйства», что, по-видимому, говорит о вовлеченности помпы МЛУ AcrAB-TolC в перманентную «уборку» клетки от различных веществ биотического и абиотического происхождения.

Ключевые слова: множественная лекарственная устойчивость, антибиотик, AcrAB-TolC, выравнивание последовательностей, *Escherichia coli*, помпа, транспортер, биоцид, гены «роскоши», гены «домашнего хозяйства»

Благодарности: авторы благодарят студентов (Джафарову Т., Мамедову Д., Маушева Ф., Миранян К., Омарову Д. и Родионову Э.) и сотрудников кафедры морфологии и патологии Московского медицинского университета «Реавиз» за предварительные данные, их анализ и дискуссию.

✉ **Для корреспонденции:** Марина Викторовна Каракозова
Микрорайон 1-й, д. 15, кв. 43, г. Зарайск, Зарайский р-н, Московская обл., 140601; mvk752002@gmail.com

Статья получена: 19.02.2018 **Статья принята к печати:** 30.03.2018

DOI: 10.24075/vrgmu.2018.024

The gram-negative gammaproteobacterium *Escherichia coli* (*E. coli*) was first discovered by Theodor Escherich in the stool samples of healthy individuals in 1885 [1]. *E. coli* naturally inhabits the lower intestines of warm-blooded species and is an important object of research. Four strains of *E. coli*, including K-12, B, W and C, are now used as model organisms. Strain K-12 was first isolated at Stanford university in 1922 [2]. Strain B was described by d'Herelle at the Pasteur Institute in Paris in 1918 [3]. The other 2 strains are less common. Strain C was discovered by Margaret Lieb in 1951 [4, 5], and strain W was originally reported by Selman Waksman in 1943 [6]. Strains comprising groups K-12 and B are the most widespread and best known. Laboratory strains have "evolved" to lose some of their properties, such as the ability to form biofilms on abiotic surfaces, and therefore can be advantageously used in research studies, especially for the discovery of novel antibiotics [7].

The pressure of both natural and artificial selection existing in laboratories has produced numerous derivatives of K-12 and B that are now used all over the world (Table 1). Among the derivatives of strain B are BL21 and BL21(DE3); DH5α, JM109, W3110, XL-1 Blue, and MG1655 are examples of strain K-12 derivatives.

Discovery of novel antibiotics or their effective alternatives is a pressing challenge. One of the most promising areas of research is identification of multidrug resistance (MDR) pump inhibitors. MDR pumps are responsible for removing antibiotics from the bacterial cell. Studies of deletion mutants with knocked-out genes coding for MDR pumps demonstrate that minimum effective inhibitory concentrations of antibiotics in their case are several times lower than usual [8]. This may help to reduce both treatment costs and the toxic effect of antibiotic therapies on the patient. Although effects of MDR pumps on antibacterial agents are actively studied, there is an extensive list of objective factors preventing cross-study comparisons, such as different genetic backgrounds of the strains. Even for such closely related strains as W3110 and MG1655 [9], the number of differences at genomic sites can be over 200, impeding comparison. Because bacterial resistance to drugs depends on the presence or absence of efflux pumps, we hypothesized that *E. coli* strains with identical sequences of MDR pumps might have comparable or equal resistance. To check this supposition, we selected the AcrAB-TolC pump. We aimed to compare sequences of AcrA, AcrB and TolC proteins obtained from different laboratory strains of *E. coli* and to study the associations between drug resistance and possible mutations if such were present in a sequence.

METHODS

Selecting an object

For our study we selected a few K-12 strains: W3110, MG1655, NEB 5-alpha, MDS42, GM4792, AG100, MC4100, DH10B, ER3413, HMS174, BW2952, and BW25113, as well as strain BL21(DE3) from group B. Their *acrA*, *acrB* and *tolC* sequences are known and stored in databases (Table 2).

Selecting a reference sequence

When selecting a reference sequence, we bore in mind a large number of deletion mutants in *E. coli* K-12 BW25113. It is a parent strain for the Keio collection, which comprises *E. coli* strains with 3,985 deletions (of 4,288 total *E. coli* genes) [10]. Sequence AIN30961.1 was selected as a reference sequence for AcrA; AIN30960.1, as a reference sequence for AcrB, and AIN33386.1, as a reference sequence for TolC.

Sequence alignment

Sequences were analyzed using a standard local alignment tool NCBI BLASTp, which allows comparison of multiple alignments [11], and the STRING database [12]. Visual representation of the results was done in NCBI MSA Viewer [13]. Each protein sequence was aligned against its reference sequence.

RESULTS

It is known that bacterial resistance can be a product of: 1) accumulation of resistance genes in plasmids; 2) increased expression of genes coding for MDR pumps; 3) gene duplication; 4) accumulation of mutations [14, 15]. Increased expression and accumulation of mutations in the genes coding for MDR pumps can result in single nucleotide polymorphisms (SNPs) in the amino acid sequences of proteins. Therefore, bacterial resistance can be predicted by sequence analysis.

Bacterial genes are subdivided into housekeeping genes, which support vital functions of the cell, and contingency genes, which play an important role in bacterial adaptation to the changing environment. Housekeeping genes usually have a low mutation rate, while contingency genes tend to demonstrate a high mutation rate [16]. It is believed that genes coding for multidrug efflux pumps are contingency genes; therefore, the proteins they encode are expected to have variable primary structures. Because laboratory strains are usually subject to the pressure of natural selection induced by various biocides and mutagens, the strains that have been cultured in world laboratories for over 100 years, as well as their derivatives, might be different in terms of their amino acid polymorphisms. The strains compared in this work originate from different countries and continents (Table 1), so we can infer the presence of mutations in one of the AcrAB-TolC-encoding genes.

However, the analysis of aligned sequences of AcrA (Fig. 1), AcrB (Fig. 2) and TolC (Fig. 3) proteins (substrain BW25113), those of strain K-12 (substrains W3110, MG1655, NEB 5-alpha, MDS42, GM4792, AG100, MC4100, DH10B,

Table 1. Geographic origin of *E. coli* strains used in this work

Strain	Institution	City, country
MG1655	University of Wisconsin	Milwaukee, USA
W3110	Nara Institute of Science and Technology	Ikoma, Japan
BL21(DE3)	Korea Research Institute of Bioscience and Biotechnology	Daejeon, South Korea
MDS42	Osaka University	Osaka, Japan
MC4100	University of Kiel, Germany	Kiel, Germany
BW25113	Universite de Sherbrooke, Canada	Sherbrooke, Canada
ER3413	New England Biolabs	Ipswich, USA
AG100	University of Exeter	Exeter, UK
NEB 5-alpha	New England Biolabs	Ipswich, USA
HMS174	Austrian Centre of Industrial Biotechnology	Graz, Austria
BW2952	Nankai University	Nankai, China
DH10B	University of Wisconsin-Madison	Madison, USA
GM4792	Beijing Normal University	Beijing, China

Table 2. Accession numbers for the stored protein sequences of *acrA*, *acrB* and *tolC* genes

Substrain	Strain	AcrA	AcrB	TolC
MG1655	*K-12*	NP_414996.1	NP_414995.1	NP_417507.2
W3110	*K-12*	BAE76242.1	BAE76241.1	BAE77091.1
NEB 5-alpha	*K-12*	AOO68785.1	AOO68784.1	AOO71261.1
MDS42	*K-12*	BAL37669.1	BAL37668.1	BAL39694.1
GM4792	*K-12*	AKK16793.1	AKK13611.1	AKK18828.1
AG100	*K-12*	CQR80062.1	CQR80061.1	CQR82466.1
MC4100	*K-12*	CDJ70932.1	CDJ70931.1	CDJ73817.1
DH10B	*K-12*	ACB01590.1	ACB01589.1	ACB04120.1
ER3413	*K-12*	AIZ54314.1	AIZ54313.1	AIZ52829.1
HMS174	*K-12*	CDY55568.1	CDY55565.1	CDY61615.1
BW2952	*K-12*	ACR63806.1	ACR63808.1	ACR65687.1
BW25113	*K-12*	AIN30961.1	AIN30960.1	AIN33386.1
BL21(DE3)	*B*	ACT42313.1	ACT42312.1	ACT44711.1

ER3413, HMS174, and BW2952) and those of strain B (substrain BL21(DE3)) reveals the absence of polymorphisms in all three proteins constituting the AcrAB-TolC efflux pump, regardless of whether the strain belongs to the derivatives of K-12 or B.

Considering the fact that *E. coli* mutation rate is ~1×10^{-3} per genome per generation [17] or even higher ($3–4\times10^{-3}$ per genome per generation) [18], we hypothesize that the AcrAB-TolC pump sequence is conserved. Given the same sequence coverage for all studied proteins (397 amino acid residues for AcrA, 1049 amino acid residues for AcrB and 493 amino acid residues for TolC), the sequence identity was 100%.

DISCUSSION

According to the currently existing classification, strains from group B and K-12 belong to phylogroup A [19], which may explain the similarity of amino acid sequences between all three proteins but not their identity. Our findings allow us to conclude the presence of a consensus sequence of a highly conserved AcrAB-TolC ensemble. Thus, the selected protein reference sequences AcrA (AIN30961.1 for AcrA, AIN30960.1 for AcrB and AIN33386.1 for TolC, respectively) are consensus for the studied *E. coli* strains.

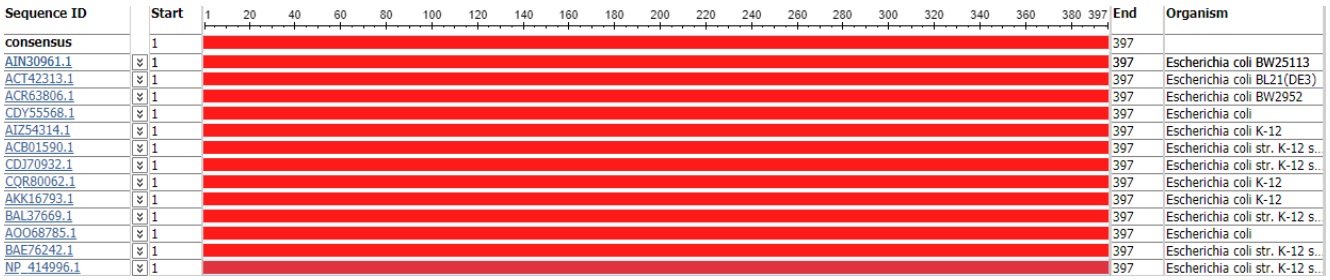

Fig. 1. Alignment of AcrA sequences for strains K-12 and B against the reference AcrA sequence of substrain BW25113

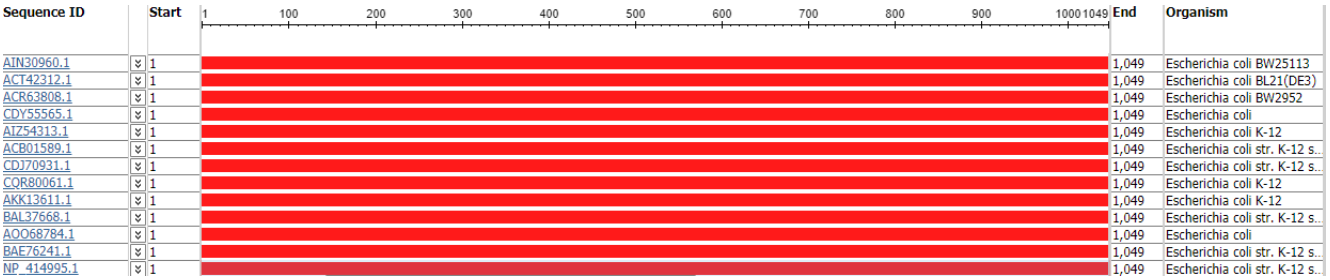

Fig. 2. Alignment of AcrB sequences for strains K-12 and B against the reference AcrB sequence of substrain BW25113

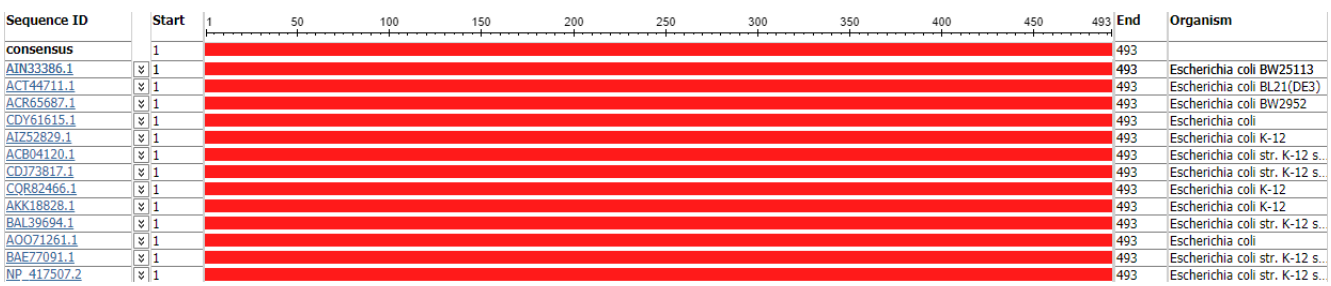

Fig. 3. Alignment of TolC sequences for strains K-12 and B against the reference TolC sequence of substrain BW25113

The discovered sequences are consensus for all representatives of group A and possibly other phylogroups, including B1, B2, D, and E, which can facilitate normalization of sequences against their consensus counterparts.

The absence of point mutations in the genes coding for protein components of the AcrAB-TolC pump in all studied strains is indicative of the strict selection control, as is the case with housekeeping genes. Such control is particularly important for the major multidrug efflux pump of *E. coli* (AcrAB-TolC) responsible for removing benzalkonium chloride, ethidium bromide, indole, hexane, antibiotics (erythromycin, ciprofloxacin, etc.), rhodamine, berberine and also triphenylphosphonium and its derivatives from the cell [20–21].

It would be wrong to see genes coding for MDR pumps as responsible for biocide resistance only. They have a role in bacterial colonization and persistence [22], so it is not limited to defense against antibiotics. It appears that proteins produced by MDR pump-encoding genes routinely protect bacterial cells from various biotic and abiotic agents and can be regarded as housekeeping genes engaged in permanent cell "cleaning", unlike contingency genes that get involved only at certain times.

CONCLUSION

Our findings suggest a unique role of the AcrAB-TolC multidrug resistance pump in *E. coli*. The protein sequence of AcrAB-TolC has turned to be surprisingly conserved. This provides a fresh look at AcrAB-TolC from a different angle: this pump ensures permanent protection against aggressive environment, determines bacterial resistance to antibiotics or their alternatives and even ensures bacterial survival.

References

1. Escherich T. Die Darmbakterien des Neugeborenen und Säuglinge. Fortschr. Med. 1885; 3: 515–522.
2. Daegelen P, Studier FW, Lenski RE, Cure S, Kim JF. Tracing ancestors and relatives of Escherichia coli B, and the derivation of B strains REL606 and BL21(DE3). J Mol Biol. 2009; 394 (4): 634–43.
3. Bachmann BJ. Pedigrees of Some Mutant Strains of Escherichia coli K-12. Bacteriological Reviews, 1972; 36 (4): 525–557.
4. Lieb M, Weigle JJ, Kellenberger E. A study of hybrids between two strains of Escherichia coli. Journal of Bacteriology. 1955; 69 (4): 468–471.
5. Lieb M. Forward and Reverse Mutation in a Histidine-Requiring Strain of Escherichia Coli Genetics. 1951; 36 (5): 460–477.
6. Archer CT, Kim JF, Jeong H, Park JH, Vickers CE, Lee SY, et al. The genome sequence of E. coli W (ATCC 9637): comparative genome analysis and an improved genome-scale reconstruction of E. coli. BMC Genomics. 2011; 12: 9.
7. Vidal O, Longin R, Prigent-Combaret C, Dorel C, Hooreman M, Lejeune P. Isolation of an Escherichia coli K-12 mutant strain able to form biofilms on inert surfaces: involvement of a new ompR allele that increases curli expression. J Bacteriol. 1998; 180 (9): 2442–2449.
8. Sulavik MC, Houseweart C, Cramer C, Jiwani N, Murgolo N, Greene J, et al. Antibiotic susceptibility profiles of Escherichia coli strains lacking multidrug efflux pump genes. Antimicrob Agents Chemother. 2001; 45 (4): 1126–1136.
9. Hayashi K, Morooka N, Yamamoto Y, Fujita K, Isono K, Choi S, et al. Highly accurate genome sequences of Escherichia coli K-12 strains MG1655 and W3110. Mol Syst Biol. 2006; 2: 2006.0007.
10. Baba T, Ara T, Hasegawa M, Takai Y, Okumura Y, Baba M, et al. Construction of Escherichia coli K-12 in-frame, single-gene knockout mutants: the Keio collection. Mol Syst Biol. 2006; 2: 2006.0008.
11. BLASTp (https://blast.ncbi.nlm.nih.gov/Blast.cgi?PROGRAM=blastp&PAGE_TYPE=BlastSearch&LINK_LOC=blasthome)
12. Szklarczyk D, Morris JH, Cook H, Kuhn M, Wyder S, Simonovic M, et al. The STRING database in 2017: quality-controlled protein-protein association networks, made broadly accessible. Nucleic Acids Res. 2017; 45: D362–68.
13. Multiple Sequence Alignment Viewer v. 1.7.7 (https://www.ncbi.nlm.nih.gov/tools/msaviewer/about/)
14. Nikaido H. Multidrug Resistance in Bacteria. Annu Rev Biochem. 2009; 78: 119–146.
15. Martinez JL, Baquero F Mutation frequencies and antibiotic resistance. Antimicrob Agents Chemother. 2000; 44 (7): 1771–1777.
16. Moxon ER, Rainey PB. Nowak MA. Lenski RE. Adaptive evolution of highly mutable loci in pathogenic bacteria. Curr Biol. 1994; 4: 24–33.
17. Lee H, Popodi E, Tang H, Foster PL. Rate and molecular spectrum of spontaneous mutations in the bacterium Escherichia coli as determined by whole-genome sequencing. Proc Natl Acad Sci USA, 2012; 109 (41): E2774–E2783.
18. Drake JW. A constant rate of spontaneous mutation in DNA-based microbes. Proc Natl Acad Sci USA, 1991; 88: 7160–7164.
19. Sims GE, Kim S.-H. Whole-genome phylogeny of Escherichia coli/Shigella group by feature frequency profiles (FFPs) Proc Natl Acad Sci U S A. 2011; 108 (20): 8329–8334.
20. Pos KM. Drug transport mechanism of the AcrB efflux pump. Biochim Biophys Acta. 2009; 1794 (5): 782–793.
21. Nazarov PA, Osterman IA, Tokarchuk AV, Karakozova MV, Korshunova GA, Lyamzaev KG et al. Mitochondria-targeted antioxidants as highly effective antibiotics. Sci Rep. 2017; 7 (1): 1394.
22. Piddock LJ Multidrug-resistance efflux pumps — not just for resistance. Nat Rev Microbiol. 2006; 4 (8): 629–36.

Литература

1. Escherich T. Die Darmbakterien des Neugeborenen und Säuglinge. Fortschr. Med. 1885; 3: 515–522.
2. Daegelen P, Studier FW, Lenski RE, Cure S, Kim JF. Tracing ancestors and relatives of Escherichia coli B, and the derivation of B strains REL606 and BL21(DE3). J Mol Biol. 2009; 394 (4): 634–43.
3. Bachmann BJ. Pedigrees of Some Mutant Strains of Escherichia coli K-12. Bacteriological Reviews, 1972; 36 (4): 525–557.
4. Lieb M, Weigle JJ, Kellenberger E. A study of hybrids between two strains of E. coli. Journal of Bacteriology. 1955; 69 (4): 468–471.
5. Lieb M. Forward and Reverse Mutation in a Histidine-Requiring Strain of Escherichia Coli Genetics. 1951; 36 (5): 460–477.
6. Archer CT, Kim JF, Jeong H, Park JH, Vickers CE, Lee SY, et al. The genome sequence of E. coli W (ATCC 9637): comparative genome analysis and an improved genome-scale reconstruction of E. coli. BMC Genomics. 2011; 12: 9.
7. Vidal O, Longin R, Prigent-Combaret C, Dorel C, Hooreman M, Lejeune P. Isolation of an Escherichia coli K-12 mutant strain able

to form biofilms on inert surfaces: involvement of a new ompR allele that increases curli expression. J Bacteriol. 1998; 180 (9): 2442–2449.
8. Sulavik MC, Houseweart C, Cramer C, Jiwani N, Murgolo N, Greene J, et al. Antibiotic susceptibility profiles of Escherichia coli strains lacking multidrug efflux pump genes. Antimicrob Agents Chemother. 2001; 45 (4): 1126–1136.
9. Hayashi K, Morooka N, Yamamoto Y, Fujita K, Isono K, Choi S, et al. Highly accurate genome sequences of Escherichia coli K-12 strains MG1655 and W3110. Mol Syst Biol. 2006; 2: 2006.0007.
10. Baba T, Ara T, Hasegawa M, Takai Y, Okumura Y, Baba M, et al. Construction of Escherichia coli K-12 in-frame, single-gene knockout mutants: the Keio collection. Mol Syst Biol. 2006; 2: 2006.0008.
11. BLASTp (https://blast.ncbi.nlm.nih.gov/Blast.cgi?PROGRAM=blastp&PAGE_TYPE=BlastSearch&LINK_LOC=blasthome)
12. Szklarczyk D, Morris JH, Cook H, Kuhn M, Wyder S, Simonovic M, et al. The STRING database in 2017: quality-controlled protein-protein association networks, made broadly accessible. Nucleic Acids Res. 2017; 45: D362–68.
13. Multiple Sequence Alignment Viewer v. 1.7.7 (https://www.ncbi.nlm.nih.gov/tools/msaviewer/about/)
14. Nikaido H. Multidrug Resistance in Bacteria. Annu Rev Biochem. 2009; 78: 119–146.
15. Martinez JL, Baquero F Mutation frequencies and antibiotic resistance. Antimicrob Agents Chemother. 2000; 44 (7): 1771–1777.
16. Moxon ER, Rainey PB. Nowak MA. Lenski RE. Adaptive evolution of highly mutable loci in pathogenic bacteria. Curr Biol. 1994; 4: 24–33.
17. Lee H, Popodi E, Tang H, Foster PL. Rate and molecular spectrum of spontaneous mutations in the bacterium Escherichia coli as determined by whole-genome sequencing. Proc Natl Acad Sci USA, 2012; 109 (41): E2774–E2783.
18. Drake JW. A constant rate of spontaneous mutation in DNA-based microbes. Proc Natl Acad Sci USA, 1991; 88: 7160–7164.
19. Sims GE, Kim S.-H. Whole-genome phylogeny of Escherichia coli/Shigella group by feature frequency profiles (FFPs) Proc Natl Acad Sci U S A. 2011; 108 (20): 8329–8334.
20. Pos KM. Drug transport mechanism of the AcrB efflux pump. Biochim Biophys Acta. 2009; 1794 (5): 782–793.
21. Nazarov PA, Osterman IA, Tokarchuk AV, Karakozova MV, Korshunova GA, Lyamzaev KG et al. Mitochondria-targeted antioxidants as highly effective antibiotics. Sci Rep. 2017; 7 (1): 1394.
22. Piddock LJ Multidrug-resistance efflux pumps — not just for resistance. Nat Rev Microbiol. 2006; 4 (8): 629–36.

CHANGES IN THE SENSITIVITY OF HUMAN GLIOBLASTOMA CELLS TO ONCOLYTIC ENTEROVIRUSES INDUCED BY PASSAGING

Soboleva AV[1,2], Lipatova AV[1], Kochetkov DV[1], Chumakov PM[1,2] ✉

[1] Engelhardt Institute of Molecular Biology, Moscow

[2] Chumakov Federal Scientific Center for Research and Development of Immune-and-Biological Products, Moscow

Existing therapies for glioblastoma multiforme do not ensure patient's recovery. Oncolytic viruses (OV) represent a promising alternative as they can destroy glioblastoma-initiating stem cells, the major cause of relapses. However, while individual OV strains are effective for some patients, they could be ineffective for others. To achieve a predictable therapeutic effect, live tumor cells of the patient need to be tested for their sensitivity to different viruses. The aim of this study was to assess how sensitivity of tumor cells to viruses changes with passaging in the cell culture. Primary glioblastoma cell cultures were prepared from excised tumors. We compared the sensitivity of the cells to four non-pathogenic enteroviruses (type 1 poliovirus, Coxsackie virus A7, Echoviruses 1 and 12) for freshly explanted primary tumor cell cultures and for those that had undergone 700 divisions during passaging. Cell sensitivity was assessed by the MTT assay based on the proportion of viable cells 72 hours after the cells were inoculated with serial 10-fold dilutions of virus preparations. Cells isolated from the tumors of 3 patients exhibited varying sensitivity to the used viral strains. Differences in the lowest virus dose required for the successful infection of the cell cultures were as high as 10^5. Passaging induced sensitivity shifts, such as increased or decreased sensitivity to individual viruses. Differences in the sensitivity correlated with the ability of the infected cells to produce the virus. Based on our findings, we conclude that the sensitivity of cancer cells to viruses should be tested at very early stages of passaging, preferably in primary cultures.

Keywords: oncolytic viruses, non-pathogenic human enteroviruses, glioblastoma multiforme, cell culture, viral infection, sensitivity to viruses, viral oncolysis, virotherapy

Funding: this work was supported by the Ministry of Education and Science of the Russian Federation (Project ID RFMEFI60714X0014).

✉ **Correspondence should be addressed:** Peter M. Chumakov
Vavilova 32, Moscow, 119991; chumakovpm@yahoo.com

Recieved: 16.06.2018 **Accepted:** 22.06.2018

DOI: 10.24075/brsmu.2018.025

ИЗМЕНЕНИЯ ЧУВСТВИТЕЛЬНОСТИ КЛЕТОК ГЛИОБЛАСТОМ ЧЕЛОВЕКА К ОНКОЛИТИЧЕСКИМ ЭНТЕРОВИРУСАМ ПРИ ПАССИРОВАНИИ В КУЛЬТУРЕ

А. В. Соболева[1,2], А. В. Липатова[1], Д. В. Кочетков[1], П. М. Чумаков[1,2] ✉

[1] Институт молекулярной биологии имени В. А. Энгельгардта, Москва

[2] Федеральный научный центр исследований и разработки иммунобиологических препаратов имени М. П. Чумакова, Москва

Современная терапия мультиформных глиобластом не приводит к излечению пациентов. В качестве альтернативы перспективны онколитические вирусы (ОВ): они способны уничтожать опухолевые стволовые клетки, источники рецидивов. Однако каждый отдельный штамм ОВ эффективен только в ряде случаев. Для подбора подходящего штамма требуется тестирование чувствительности на живых опухолевых клетках пациента. Целью исследования было изучение изменения чувствительности к вирусам в процессе пассирования опухолевых клеток пациента в культуре. Органные и первичные культуры клеток глиобластом получали из операционного материала больных. Проводили сравнение чувствительности к четырем штаммам непатогенных энтеровирусов (вакцинный штамм полиовируса 1 типа, вирус Коксаки А7, Эховирусы 1 и 12) на первичных культурах, и на клетках, прошедших около 700 удвоений при пассировании. Чувствительность к вирусам оценивали по измерению доли жизнеспособных клеток с помощью МТТ теста через 72 ч после заражения серийными десятикратными разведениями вирусных препаратов. Клетки каждого из четырех пациентов имели строго индивидуальные спектры чувствительности к испытанным вирусным штаммам. Различия в минимальной инфекционной дозе, необходимой для заражения культур, составляли до 10^5. При пассировании происходили изменения в чувствительности, которые могли приводить к повышению чувствительности к одному вирусу, и понижению — к другому. Различия в чувствительности коррелировали со способностью зараженных клеток продуцировать инфекционный вирус. На основании полученных данных можно заключить, что испытание индивидуальной чувствительности опухолевых клеток пациентов следует проводить на как можно более ранних этапах пассирования, предпочтительно — на первичных культурах.

Ключевые слова: онколитические вирусы, непатогенные энтеровирусы человека, мультиформная глиобластома, культура клеток, вирусная инфекция, чувствительность к вирусам, вирусный онколиз, виротерапия

Финансирование: работа выполнена при финансовой поддержке Министерства образования и науки РФ, уникальный код проекта RFMEFI60714X0014.

✉ **Для корреспонденции:** Петр Михайлович Чумаков
ул. Вавилова, д. 32, г. Москва, 119991; chumakovpm@yahoo.com

Статья получена: 16.06.2018 **Статья принята к печати:** 22.06.2018

DOI: 10.24075/vrgmu.2018.025

Glioblastoma multiforme is the most aggressive and still incurable form of brain tumors. The median survival time after the diagnosis and treatment is only 15 months [1, 2]. Treatment is complicated by the blood-brain barrier that limits access of chemotherapy drugs to the tumor and by the ability of glioblastoma stem cells to migrate far from the tumor into brain tissues, evading surgical resection. Recently, a hope has emerged that this desperate therapeutic situation can be overcome by using oncolytic viruses. There have been reports of successful treatment outcomes and long-lasting remissions in patients with glioblastomas who received oncolytic virotherapy [3–8]. Moreover, oncolytic viruses have demonstrated the ability to kill glioblastoma stem cells [9–14]. However, virotherapies work only for some patients because the molecular genetic defects in tumors that affect their sensitivity to different viral strains vary between individuals. Therefore, it is wise to use panels of viruses with overlapping specificity against individual tumor cells in order to achieve the desired therapeutic effect. This approach can be more effective if cancer cells of the patient are tested for the sensitivity to a wide range of oncolytic viruses prior to treatment. To run such tests, viable cancer cells from excised tumor fragments are required. Once the cells are obtained, they need to be cultured and passaged to study the underlying cause of their varying sensitivity to different viruses. To test this approach, we optimized protocols for cell culture, cryopreservation and passaging that yielded viable glioblastoma cells. We aimed to determine the extent to which the subcultured cells can retain their original sensitivity to a certain virus type. The cells were cultured from the specimens obtained from different patients. We compared the response of glioblastoma cells from different passages (from primary tissue culture to passage 10) to infection with a few strains of oncolytic enteroviruses.

METHODS

Cell lines of glioblastoma multiforme

Glioblastoma cell lines U87MG and A172 from the American Type Culture Collection (ATCC) were cultured in DMEM (PanEco, Moscow) supplemented with 10% fetal bovine serum (FBS), 4 mM L-glutamine, 100 un/ml penicillin, and 100 μg/ml streptomycin at 5% CO_2 and 37 °C. Primary tissue cultures were prepared from fragments of freshly resected tumors.

Tissue and primary glioblastoma cultures

Tumor samples were collected at Burdenko Neurosurgery Research Institute according to the protocol approved by the Institute's Ethics Committee. The samples were collected into sterile tubes filled with DMEM and stored at +4 °C for no more than 24 h. Tissue cultures were prepared from tumor fragments washed in PBS and placed onto sterile culture plates; necrotic tissue and blood vessels were excised using a pair of tweezers and a scalpel. Cell suspensions were prepared from tumor fragments stirred through a sterile nylon mesh with 50-micron pores, purified by centrifugation at 800 g for 5 min 3 times, suspended in the growth medium, and carefully pipetted until a homogeneous suspension of single cells and cell aggregates was obtained. For cryogenic preservation of viable tissue cultures at liquid nitrogen temperature, cell suspensions were placed into DMEM containing 50% serum and 7% dimethyl sulfoxide and aliquoted into cryogenic vials at 1 ml per vial. The vials were kept in a well-insulated container at –80 °C for the first 24 h and then transferred to a liquid nitrogen tank. Dispersed cells were grown to reach the density of 2×10^4 in 1 ml DMEM-F12 (PanEco, Moscow) supplemented with 10% FBS and antibiotics, seeded onto 6-cm plastic culture plates and incubated at 37 °C in a humidified atmosphere containing 5% CO_2. The medium was replaced every 3 days. Cell growth was monitored twice a week. When a monolayer of cells was formed on days 6–15 of culturing, the cells were either cryopreserved in liquid nitrogen as described above or passaged further.

Passaging of glioblastoma cultures

About one third of primary cultures demonstrated a stable growth and formed a monolayer. The rest stopped dividing, perhaps due to the lack of favorable conditions. For passaging, monolayers of washed cultured cells were treated with a trypsin solution and plated onto new dishes at a ratio of 1:2–1:3. Passaging was repeated multiple times. With each passage, a portion of cells was cryopreserved.

Strains of oncolytic viruses

In our study we used non-pathogenic strains of human enteroviruses: type 1 poliovirus (Sabin vaccine strain), Coxsackie virus A7 (LEV8), Echovirus 1 (LEV4), and Echovirus 12 (LEV7) [4, 15]. The enteroviruses were propagated in Vero cells (permanent African green monkey kidney cells) at a multiplicity of infection of < 1 PFU per cell and harvested 24 h later. Virus titers were measured using the endpoint dilution assay.

Analysis of viability of infected cells

96-well plates containing primary and continuous cell lines were infected with viruses in a series of 10-fold virus dilutions at a multiplicity of infection from 10^{-5} to 1 PFU per cell in 4 replicates. After one hour of adsorption, the virus-containing fluid was removed, the cells were washed in PBS and cultured in the growth medium supplemented with FBS. In 72 h cell viability was measured by MTT and CellTiter 96® Non-Radioactive Cell Proliferation assays (Promega, USA) according to the manufacturer's protocol.

Analysis of viral replication in the infected cells

Five days after viral infection, we identified the wells in which the cells had been completely lysed by the lowest infectious dose. Following three cycles of freezing and thawing, supernatants were clarified by centrifugation (10 min at 1000 g) and used for virus titration as described above.

RESULTS

In this study we assessed the sensitivity of cancer cells obtained from three patients with glioblastoma and maintained in the culture for different number of passages to a few non-pathogenic strains of human enteroviruses. We compared responses to viral infection between freshly explanted primary glioblastoma cultures and those that had undergone six passages. Passaging lasted for about 2 months and by that time the cells had undergone about 700 division cycles. To determine the lowest effective dose of the viruses, glioblastoma cultures were incubated with serial tenfold dilutions of standard virus preparations; cell viability was measured 72 h after infection. Fig. A shows sensitivity profiles of primary cell cultures prepared from tumor fragments of 3 patients (in the pictures

the profiles are designated as GM-3564-0, GM-3876-0 and GM-3912-0) in response to infection with 4 strains of human enteroviruses. Standard Vero cell cultures routinely used for the propagation of viruses served as the control. Fig. 1B shows the sensitivity of glioblastoma cells from passage 6 (designated in the picture as GM-3564-6, GM-3876-6 and GM-3912-6) to the same viral strains. Vero cells were again used as the control; their sensitivity was measured in a replicate (Vero-2).

The cell sensitivity to 4 enteroviral strains varied significantly between 3 studied primary glioblastoma cell cultures. Culture GM-3564 was most sensitive to Coxsackie virus A7 (the cells were successfully infected using a 10^{-6}-fold dilution of this virus); it was less sensitive to poliovirus (a 10^{-4}-fold dilution was effective) and only slightly sensitive to Echoviruses 1 and 12 (10^{-3}-fold dilutions were effective). Culture GM-3876 was most sensitive to poliovirus (the cells were successfully infected with a 10^{-6}-fold dilution of this virus) and less sensitive to Coxsackie virus A7 (a 10^{-5}-fold dilution), Echovirus 12 (a 10^{-4}-fold dilution) and Echovirus 1 (a 10^{-3}-fold dilution). Culture GM-3912 was most sensitive to Coxsackie virus A7 (a 10^{-7}-fold dilution), poliovirus (a 10^{-5}-fold dilution) and Echoviruses 1 and 12 (a 10^{-4}-fold dilution). Experiments conducted on Vero cells demonstrated that the highest activity was exerted by Echovirus 1 (a 10^{-7}-fold dilution), followed by poliovirus (a 10^{-6}-fold dilution), Coxsackie virus A7 (a 10^{-6}-fold dilution), and Echovirus 12 (a 10^{-5}-fold dilution). Apparently, the passaging affected the sensitivity of cells to certain viruses. GM-3564 cells demonstrated an increased sensitivity to type 1 poliovirus and reduced sensitivity to Coxsackie virus A7, while their sensitivity to Echoviruses 1 and 12 remained unchanged. The sensitivity of GM-3876 cells to poliovirus also increased, while the sensitivity to Coxsackie virus A7 decreased; these cells also exhibited a slight increase in the sensitivity to Echovirus 12, but their sensitivity to Echovirus 1 remained unchanged and low. GM-3912 cells showed a slight increase in the sensitivity to Echovirus 12 and an unchanged sensitivity to the rest 3 viruses.

Different sensitivity of glioblastoma cells to different viruses and the changes induced by passaging may be associated with altered rates of viral replication. To qualitatively assess the replication of viruses, we measured their infectivity titers in the supernatants of cell cultures infected with a penultimate dilution that caused a cytopathic effect. The viral dose in that dilution was about 10 infectious units per each well of a 96-well plate, which is an optimal dose ensuring successful infection of a cell culture. This dose precludes the accumulation of defective interfering particles. The table below presents viral titers in every primary and passaged glioblastoma cell cultures.

Titration results confirm the supposition that changing sensitivity to viral infection during passaging can be associated with a more or less effective replication of a virus. During GM3564 passaging, poliovirus increased its replication over 30-fold, while production of Coxsackie virus A7 decreased 3-fold; replication of Echoviruses 1 and 12 remained unchanged. Different sensitivity ranges were also observed for two other cell cultures.

DISCUSSION

Glioblastoma multiforme is a highly aggressive type of brain tumors. Its genome is very unstable and the cell population is

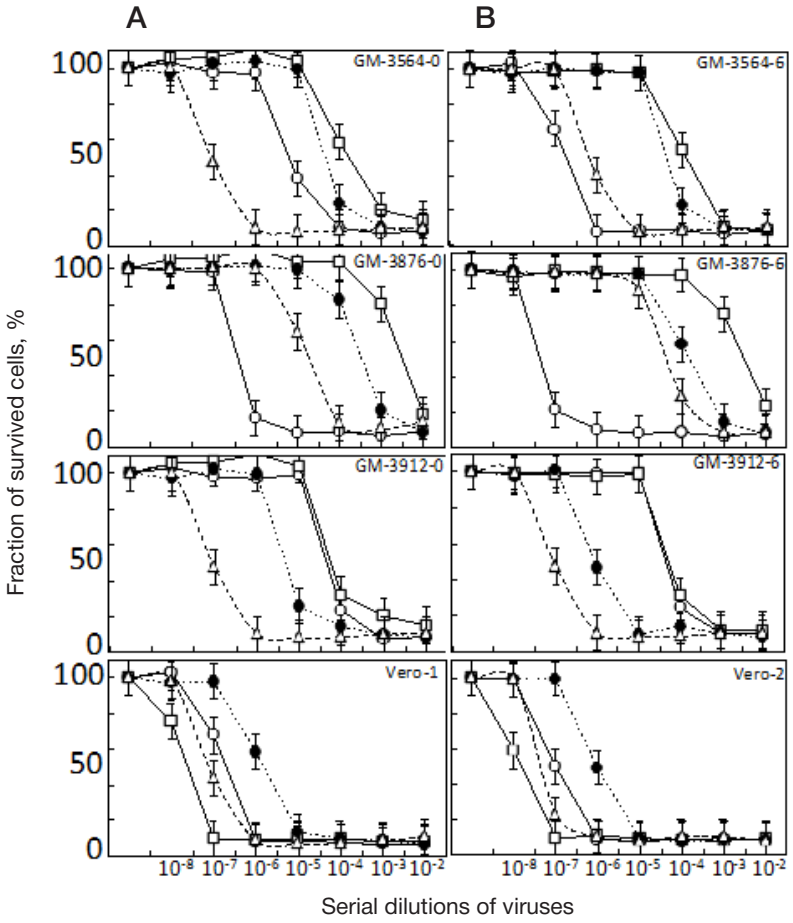

Fig. 1. Sensitivity of primary glioblastoma cell cultures obtained from 3 patients (**A**) and the same cells from passage 6 (**B**) to 4 strains of non-pathogenic oncolytic enteroviruses: —○— — type 1 poliovirus; - -Δ- - — Coxsackie virus A7; —□— — Echovirus 1; ….●…. — Echovirus 12. The horizontal scale (10^{-8}–10^{-2}) shows 10-fold dilutions of virus preparations

Table 1. Infectious titers of viruses produced in primary and passaged glioblastoma cell cultures infected at a low multiplicity of infection (<0.001 infectious units per cell)

Cell culture	Poliovirus 1	Coxsackie virus A7	Echovirus 1	Echovirus 12
GM3564-0	4×10^5	3×10^7	5×10^3	6×10^4
GM3564-6	2×10^7	1×10^7	6×10^3	4×10^4
GM3876-0	1×10^6	2×10^4	1×10^3	3×10^2
GM3876-6	1×10^7	8×10^3	2×10^3	4×10^2
GM3912-0	1×10^4	3×10^7	8×10^3	1×10^4
GM3912-6	1×10^4	4×10^7	8×10^3	8×10^5
Vero-1	5×10^7	8×10^7	2×10^8	5×10^6
Vero-2	4×10^7	1×10^8	1×10^8	5×10^6

heterogenous and continuously changing. Although a certain equilibrium is maintained in the tumor in terms of its cellular composition, supported by local conditions, this balance is shifted when cells are transferred to a culture flask. As a result, cells that are better adapted to *in vitro* conditions may overgrow. Therefore, one can assume that selection of certain cell types can be accompanied by shifts in the sensitivity to oncolytic viruses.

Our findings suggest that passaging of a primary glioblastoma cell culture is accompanied by certain changes leading to an increased or decreased sensitivity to individual viruses. This may be a result of the initial population heterogeneity of cancer cells that, due to a number of causes, have different sensitivity to viruses. Certain cell types tend to thrive excessively in the culture, affecting the overall sensitivity to viruses.

CONCLUSION

We have tested glioblastoma cells obtained from 3 patients for their sensitivity to 4 oncolytic enteroviral strains. We conclude that initial tumor cells differ in their sensitivity to different viruses and passaging may induce qualitative changes in the cell sensitivity to individual viral strains. Our study demonstrates the need for sensitivity tests at the very early stages of *in vitro* cell cultures.

References

1. Wen PY, Kesari S. Malignant gliomas in adults. N Engl J Med. 2008; 359 (5): 492–507.
2. Mirimanoff RO, Gorlia T, Mason W, Van den Bent MJ, Kortmann RD, Fisher B, et al. Radiotherapy and temozolomide for newly diagnosed glioblastoma: recursive partitioning analysis of the EORTC 26981/22981-NCIC CE3 phase III randomized trial. J Clin Oncol. 2006; 24 (16): 2563–2569. DOI: 10.1200/JCO.2005.04.5963. PubMed PMID: 16735709.
3. Sosnovtceva AO, Grinenko NF, Lipatova AV, Chumakov PM, Chekhonin VP. Onkoliticheskie virusy v terapii zlokachestvennih gliom. Biomeditsinskaia khimiia. 2016; 62 (4): 376–90. DOI: 10.18097/pbmc20166204376. PubMed PMID: 27562991.
4. Gubanova NV, Gaytan AS, Razumov IA, Mordvinov VA, Krivoshapkin AL, Netesov SV, et al. Onkoliticheskie virusy v terapii gliom. Molecular Biology. 2012; 46 (6): 726–38.
5. Csatary LK, Bakacs T. Use of Newcastle disease virus vaccine (MTH-68/H) in a patient with high-grade glioblastoma. JAMA. 1999; 281 (17): 588–589.
6. Markert JM, Medlock MD, Rabkin SD, Gillespie GY, Todo T, Hunter WD, et al. Conditionally replicating herpes simplex virus mutant, G207 for the treatment of malignant glioma: results of a phase I trial. Gene Ther. 2000; 7 (10): 867–874.
7. Csatary LK, Gosztonyi G, Szeberenyi J, Fabian Z, Liszka V, Bodey B, et al. MTH-68/H oncolytic viral treatment in human high-grade gliomas. J Neurooncol. 2004; 67 (1–2): 83–93.
8. Iwadate Y, Inoue M, Saegusa T, Tokusumi Y, Kinoh H, Hasegawa M, et al. Recombinant Sendai virus vector induces complete remission of established brain tumors through efficient interleukin-2 gene transfer in vaccinated rats. Clin Cancer Res. 2005; 11 (10): 3821–27.
9. Allen C, Opyrchal M, Aderca I, Schroeder MA, Sarkaria JN, Domingo E, et al. Oncolytic measles virus strains have significant antitumor activity against glioma stem cells. Gene Ther. 2012; 23 (10): 62.
10. Alonso MM, Jiang H, Gomez-Manzano C, Fueyo J. Targeting brain tumor stem cells with oncolytic adenoviruses. Methods Mol Biol. 2012; 797: 111–125.
11. Dey M, Ulasov IV, Lesniak MS. Virotherapy against malignant glioma stem cells. Cancer Lett. 2010; 289 (1): 1–10.
12. Kanai R, Rabkin SD, Yip S, Sgubin D, Zaupa CM, Hirose Y, et al. Oncolytic virus-mediated manipulation of DNA damage responses: synergy with chemotherapy in killing glioblastoma stem cells. J Natl Cancer Inst. 2012; 104 (1): 42–55.
13. van den Hengel SK, Balvers RK, Dautzenberg IJ, van den Wollenberg DJ, Kloezeman JJ, Lamfers ML, et al. Heterogeneous reovirus susceptibility in human glioblastoma stem-like cell cultures. Cancer Gene Ther. 2013; 20(9): 507–513. DOI: 10.1038/cgt.2013.47. PubMed PMID: 23907517.
14. Zhu Z, Gorman MJ, McKenzie LD, Chai JN, Hubert CG, Prager BC, et al. Zika virus has oncolytic activity against glioblastoma stem cells. J Exp Med. 2017; 214 (10): 2843–57. DOI: 10.1084/jem.20171093. PubMed PMID: 28874392; PubMed Central PMCID: PMCPMC5626408.
15. Voroshilova MK. Potential use of nonpathogenic enteroviruses for control of human disease. Prog Med Virol. 1989; 36: 191–202. PubMed PMID: 2555836.

Литература

1. Wen PY, Kesari S. Malignant gliomas in adults. N Engl J Med. 2008; 359 (5): 492–507.
2. Mirimanoff RO, Gorlia T, Mason W, Van den Bent MJ, Kortmann RD, Fisher B, et al. Radiotherapy and temozolomide for newly diagnosed glioblastoma: recursive partitioning analysis of the EORTC 26981/22981-NCIC CE3 phase III randomized trial.

J Clin Oncol. 2006; 24 (16): 2563–9. Epub 2006/06/01. DOI: 24/16/2563 [pii] 10.1200/JCO.2005.04.5963. PubMed PMID: 16735709.
3. Сосновцева А. О., Гриненко Н. Ф., Липатова А. В., Чумаков П. М., Чехонин В. П. Онколитические вирусы в терапии злокачественных глиом. Биомедицинская химия. 2016 (4): 376–90.
4. Губанова Н. В., Гайтан А. С., Разумов И. А., Мордвинов В. А., Кривошапкин А. Л., Нетесов С. В., et al. Онколитические вирусы в терапии глиом. Молекулярная биология. 2012; 46 (6): 726–38.
5. Csatary LK, Bakacs T. Use of Newcastle disease virus vaccine (MTH-68/H) in a patient with high-grade glioblastoma. JAMA. 1999; 281 (17): 588–9.
6. Markert JM, Medlock MD, Rabkin SD, Gillespie GY, Todo T, Hunter WD, et al. Conditionally replicating herpes simplex virus mutant, G207 for the treatment of malignant glioma: results of a phase I trial. Gene Ther. 2000; 7 (10): 867–74.
7. Csatary LK, Gosztonyi G, Szeberenyi J, Fabian Z, Liszka V, Bodey B, et al. MTH-68/H oncolytic viral treatment in human high-grade gliomas. J Neurooncol. 2004; 67 (1–2): 83–93.
8. Iwadate Y, Inoue M, Saegusa T, Tokusumi Y, Kinoh H, Hasegawa M, et al. Recombinant Sendai virus vector induces complete remission of established brain tumors through efficient interleukin-2 gene transfer in vaccinated rats. Clin Cancer Res. 2005; 11 (10): 3821–7.
9. Allen C, Opyrchal M, Aderca I, Schroeder MA, Sarkaria JN, Domingo E, et al. Oncolytic measles virus strains have significant antitumor activity against glioma stem cells. Gene Ther. 2012; 23 (10): 62.
10. Alonso MM, Jiang H, Gomez-Manzano C, Fueyo J. Targeting brain tumor stem cells with oncolytic adenoviruses. Methods Mol Biol. 2012; 797: 111–25.
11. Dey M, Ulasov IV, Lesniak MS. Virotherapy against malignant glioma stem cells. Cancer Lett. 2010; 289 (1): 1–10.
12. Kanai R, Rabkin SD, Yip S, Sgubin D, Zaupa CM, Hirose Y, et al. Oncolytic virus-mediated manipulation of DNA damage responses: synergy with chemotherapy in killing glioblastoma stem cells. J Natl Cancer Inst. 2012; 104 (1): 42–55.
13. van den Hengel SK, Balvers RK, Dautzenberg IJ, van den Wollenberg DJ, Kloezeman JJ, Lamfers ML, et al. Heterogeneous reovirus susceptibility in human glioblastoma stem-like cell cultures. Cancer Gene Ther. 2013; 20(9): 507–13. Epub 2013/08/03. DOI: 10.1038/cgt.2013.47. PubMed PMID: 23907517.
14. Zhu Z, Gorman MJ, McKenzie LD, Chai JN, Hubert CG, Prager BC, et al. Zika virus has oncolytic activity against glioblastoma stem cells. J Exp Med. 2017; 214 (10): 2843–57. Epub 2017/09/07. doi: 10.1084/jem.20171093. PubMed PMID: 28874392; PubMed Central PMCID: PMCPMC5626408.
15. Voroshilova MK. Potential use of nonpathogenic enteroviruses for control of human disease. Prog Med Virol. 1989; 36: 191–202. Epub 1989/01/01. PubMed PMID: 2555836.

HUMAN ENTEROVIRUSES EXHIBIT SELECTIVE ONCOLYTIC ACTIVITY IN THE MODEL OF HUMAN GLIOBLASTOMA MULTIFORME XENOGRAFTS IN IMMUNODEFICIENT MICE

Zheltukhin AO[1], Soboleva AV[1,2], Sosnovtseva AO[1,3], Le TH[1], Ilyinskaya GV[1,4], Kochetkov DV[1], Lipatova AV[1], Chumakov PM[1,2] ✉

[1] Engelhardt Institute of Molecular Biology, Russian Academy of Sciences, Moscow

[2] Chumakov Federal Scientific Center for Research and Development of Immune-and-Biological Products, Moscow

[3] Pirogov Russian National Research Medical University, Moscow

[4] Blokhin National Medical Research Center of Oncology, Moscow

Stem cells that penetrated deeply into the brain tissue are the main reason behind the relapses of glioblastoma multiforme after surgery. Finding new approaches to counter such relapses, including those that make use of oncolytic viruses, is a pressing issue. This study aimed to determine the sensitivity of cells of human glioblastoma multiforme to non-pathogenic enteroviruses, in vitro and *in vivo* (mice xenografts model). Glioblastoma tumor cells were exposed to type 1 poliovirus (Sabin vaccine strain), Coxsackie virus A7 (strain LEV8), Coxsackie virus A9 (strain LEV9) and Coxsackie virus B5 (strain LEV14). The virus reproduction intensity and cytolytic activity were assessed through infection of monolayered glioblastoma cell cultures. The ability of glialoblastoma cell cultures (enriched with tumor stem cells) to build subcutaneous tumors in immunodeficient mice after those cultures were exposed to viruses signaled the effectiveness of glioblastoma stem cells destruction. The study revealed that Coxsackie virus A7 and type 1 poliovirus possess the most pronounced oncolytic and replicative properties when tested on gliblastoma cells infected with viruses *in vitro* and on subcutaneous tumor xenografts in immunodeficient mice (*in vivo*). Type 1 poliovirus and Coxsackie virus A7 virus prevented development of tumors when glioblastoma neurospheric cell cultures were preincubated with viruses before subcutaneous implantation. Coxsackie virus B5 only managed to reduce the number of tumors developed, and Coxsackie virus A9 did not affect the tumor development at all. Thus, a number of non-pathogenic enteroviruses strains can destroy glioblastoma's stem cells, i.e. they show promise in the context of development of therapeutic agents for relapse-free treatment of glioblastomas.

Keywords: glioblastoma multiforme, oncolytic virus, non-pathogenic enteroviruses, personalized medicine, tumor relapse, experimental cancer therapy

Funding: the study was supported by the Ministry of Education and Science of the Russian Federation; project code RFMEFI60714X0014.

✉ **Correspondence should be addressed:** Peter M Chumakov
Vavilova, 32, Moscow, 119991; chumakovpm@yahoo.com

Received: 26.06.2018 **Accepted:** 30.06.18

DOI: 10.24075/brsmu.2018.026

ЭНТЕРОВИРУСЫ ЧЕЛОВЕКА ПРОЯВЛЯЮТ ИЗБИРАТЕЛЬНУЮ ОНКОЛИТИЧЕСКУЮ АКТИВНОСТЬ НА МОДЕЛИ КСЕНОТРАНСПЛАНТАТОВ МУЛЬТИФОРМНОЙ ГЛИОБЛАСТОМЫ ЧЕЛОВЕКА В ИММУНОДЕФИЦИТНЫХ МЫШАХ

А. О. Желтухин[1], А. В. Соболева[1,2], А. О. Сосновцева[1,3], Т. Х. Ле[1], Г. В. Ильинская[1,4], Д. В. Кочетков[1], А. В. Липатова[1], П. М. Чумаков[1,2] ✉

[1] Институт молекулярной биологии имени В. А. Энгельгардта, Москва

[2] Федеральный научный центр исследований и разработки иммунобиологических препаратов имени М. П. Чумакова, Москва

[3] Российский национальный исследовательский медицинский университет имени Н. И. Пирогова, Москва

[4] Российский онкологический центр имени Н. Н. Блохина, Москва

Основным источником возникновения рецидивов мультиформной глиобластомы после хирургического вмешательства являются стволовые клетки, успевающие проникнуть глубоко в ткани мозга. В настоящее время актуален поиск новых подходов для борьбы с ними, в том числе с помощью онколитических вирусов. Целью работы было определение чувствительности к непатогенным энтеровирусам клеток мультиформной глиобластомы человека, поддерживаемых *in vitro* и в модели мышиных ксенотрансплантатов. Культуры опухолевых клеток глиобластом испытывали на чувствительность к полиовирусу 1 типа (штамм вакцины Сэбина), вирусу Коксаки А7 (штамм ЖЭВ8), Коксаки А9 (штамм ЖЭВ9) и Коксаки В5 (Штамм ЖЭВ12). Количественную оценку репродукции вирусов и их цитолитическую активность проводили заражением монослойных культур клеток глиобластомы. Эффективность уничтожения стволовых клеток глиобластомы определяли по способности клеточных культур глиобластом, обогащенных опухолевыми стволовыми клетками, формировать подкожные опухоли у иммунодефицитных мышей после обработки вирусами. По результатам исследования наиболее выраженная онколитическая и репликационная активность выявлена у вируса Коксаки А7 и полиовируса 1 типа при тестировании в модели культур клеток глиобластом, инфицированных вирусами *in vitro*, а также *in vivo*, в модели подкожных опухолевых ксенотрансплантатов на иммунодефицитных мышах. Полиовирус 1 типа и вирус Коксакси А7 предотвращали образование опухолей после того как нейросферные культуры клеток глиобластом преинкубировали с вирусами перед подкожным введением. Вирус Коксаки В5 вызывал лишь частичное сокращение числа опухолей, а Коксаки А9 не влиял на опухолеобразование. Таким образом, ряд штаммов непатогенных энтеровирусов способен уничтожать стволовые клетки глиобластом и представляется перспективным при разработке терапевтических средств для безрецидивного лечения глиобластом.

Ключевые слова: мультиформная глиобластома, онколитический вирус, непатогенные энтеровирусы, персонифицированная медицина, рецидив опухоли, экспериментальная терапия рака

Финансирование: работа выполнена при финансовой поддержке Министерства образования и науки РФ, уникальный код проекта RFMEFI60714X0014.

✉ **Для корреспонденции:** Петр Михайлович Чумаков
ул. Вавилова, д. 32, г. Москва, 119991; chumakovpm@yahoo.com

Статья получена: 26.06.2018 **Статья принята к печати:** 30.06.18

DOI: 10.24075/vrgmu.2018.026

Brain tumors remain hard to treat, especially when they take form of a glioblastoma multiforme, which is the most malignant and practically incurable [1]. Such tumors grow and infiltrate functionally important areas of the brain, making surgery extremely difficult. Often, the risk of neurological disorders dictates minimal invasion, i.e. only partial removal of the tumor. However, even when it is removed completely, a relapse is imminent: glioblastoma stem cells that ignite the development of such tumors migrate deeply into the healthy areas of the brain and cannot be removed [2–4]. Chemotherapy and radiotherapy result in short-term remissions only; when they are over, the tumor resumes its growth [4]. Modern medicine is almost out of options when dealing with glioblastomas, which justifies the search for alternative approaches to targeted and effective destruction of malignant cells. Significant progress in understanding the mechanisms of malignant growth and specific properties of glioblastoma cells is a good basis for development of innovative therapies. The particularly promising one implies using non-pathogenic oncolytic viruses that recognize and destroy glioblastoma cells [5, 6].

Members of various virus families are used to design oncolytic viruses to treat human gliomas. Among these are herpes viruses, Newcastle Disease virus [7–11], adenoviruses [12–16], parvoviruses [17–19], reoviruses [20–23] , enteroviruses [24–27] etc [1]. Numerous clinical trials have shown that oncolytic virus preparations are non-toxic [28–31]. In addition, unlike chemo- and targeted therapy, many oncolytic viruses can effectively kill tumor-initiating stem cells [16, 32–37], which is crucial for the complete recovery of patients. Today, there is a wide range of potentially therapeutic virus strains that can be used in further clinical trials. Properties of non-pathogenic strains of Coxsackie viruses (A7, A9 and B5 in particular) are being studied actively, and preliminary data suggest that they can potentially form therapeutic agents [38].

This study aimed at evaluating the response of glioblastoma tumor cells to oncolytic action of a number of non-pathogenic enteroviruses in in vitro and in vivo models in order to uncover and assess their therapeutic potentials for a treatment of glioblastomas.

MATERIALS AND METHODS

Obtaining primary cell cultures from glioblastoma tumors

Fragments of the freshly removed tumors were stored for up to 12 hours in ice-cold sterile culture medium. Pieces of tumors were mechanically separated from necrotic tissue, stroma, blood vessels, and then gently pushed through a nylon mesh (pore size — 50 μm). The tumor cell aggregate suspension was washed with PBS and incubated in 25 volumes of collagenase 4 solution (PanEco, Moscow) for 25 minutes at 30 °C. To obtain monolayer glioblastoma cells cultures, the suspension treated with collagenase was washed twice with DMEM (PanEco, Moscow) and placed in DMEM-F12 supplemented with 10% fetal bovine serum and 100 μg/ml of penicillin and streptomycin at the density of 10^5 cells/ml. The incubation was at 37 °C in the atmosphere of 5% CO_2; the medium was replaced every 4 days up until the monolayers formed. 18–25 days after the incubation, monolayer cultures were placed to 10 cm culture dishes.

Growth of tumor xenografts in immunodeficient mice

We obtained the xenografts of subcutaneous tumors by injecting neurospheres, which were obtained by the alternative method of plating cells from glioblastomas after treating tumor fragments with collagenase 4 (PanEco, Moscow). The plating conditions were as follows: density — 10^4 cells/ml; medium — DMEM-F12; supplements — 100 μg/ml penicillin and streptomycin; growth factor — 20 ng/ml EGF and 10 ng/ml bFGF. The cultures stayed in a CO_2 incubator at 37 °C for 2 weeks; the medium was replaced every 4 days until visible neurospheres appeared. The neurospheres enriched with glioblastoma stem cells are highly tumorigenic when injected to immunodeficient mice. For implantation purposes, the neurospheres were washed twice with PBS, their numbers counted with a hemocytometer. 3–5-week-old athymic Balb/c mice received 200 neurospheres subcutaneously, injection location — shoulder. The tumor growth was monitored every 3 days; the total number of tumors was assessed on the day 21.

Strains of oncolytic viruses

We used non-pathogenic strains of human enteroviruses from the laboratory's collection: type 1 poliovirus (Sabin vaccine strain), Coxsackie virus A7 (strain LEV8), Coxsackie virus A9 (strain LEV9) and Coxsackie virus B5 (strain LEV14) [38, 39]. Enteroviruses were grown in Vero cells. Viral titres as TCID50/ml were determined by infecting Vero cells with serial dilutions of the virus-containing liquid.

Testing sensitivity of glioblastomas cells to viruses

We used the tumor material from two patients with glioblastomas to determine the differential sensitivity of cells (after a minimal number of passages in the culture) to the panel of oncolytic enteroviruses. The cultures obtained from these patients were named GM-3564 and GM-3876. 96-well culture plates (SPL Lifesciences, Republic of Korea) were used to infect the cultures. Subconfluent one-day monolayers of GM-3564 and GM-3876 cell cultures, as well as Vero control cells, were incubated with 0.1 ml serial virus dilutions. We measured cell viability seven hours after infecting the cultures with serial tenfold dilutions of viral preparations (four non-pathogenic enteroviruses). After 72 hours, we evaluated the cytopathic activity using the CellTiter-Glo® Luminescent Cell Viability Assay kit (Promega, USA).

In vivo virus introduction

To measure the ability of viruses to prevent formation of tumors with neurospheres injected, we incubated neurospheres with viruses prior to subcutaneous administration (2×10^6 virus infectious units (i.u.), volume 0.1 ml, for 30 minutes at 37 °C).

RESULTS

We tested sensitivity of the monolayer glioblastoma cultures (obtained from tumors in two patients) to four strains of enteroviruses. GM-3564 cells were most susceptible to Coxsackie virus A7 and slightly less so to type I poliovirus (Fig. 1). GM-3876 culture showed quite the opposite: type I poliovirus was the strongest agent in its case and Coxsackie virus A7 produced a similar effect only when the dose was about ten times larger. Both cultures were relatively resistant to Coxsackie virus B5 and almost completely resistant to Coxsackie virus A9. The latter produced a slight toxic effect only at maximum doses. At the same time, all for strains were cytotoxic to the Vero cells (control) at approximately the same dosage. Thus, the two cultures of glioblastomas are apparently selective in their sensitivity to virus strains, and the lysing activity of those

strains depends on that sensitivity. The probable explanation is the differing ability to support replication of viruses the cultures exhibit.

In order to establish the ability of viral strains to prevent formation of subcutaneous tumors following introduction of xenografts into immunodeficient mice, we obtained cultures of neurospheres from tumor material of glioblastoma patients. The neurospheres received tumor-forming stem cells, which made their tumorigenicity significantly greater than that of monolayer glioblastoma cell cultures. Obtaining neurosphere cultures requires medium with specific growth factors, EGF and bFGF. In addition, the cells should be plated to a non-adhering plastic surface preventing attachment of cells. In such conditions, glioblastoma cells form spheroid aggregates, or neurospheres, which are enriched in tumor-forming stem cells. Since counting the number of individual cells in spheroids is difficult, in order to standardize the procedure of subcutaneous injections aiming tumor development we counted the number of neurospheres. In our preliminary study, we found that injecting 200 neurospheres leads to the formation of tumors within 1–2.5 weeks. The control group of five mice received 200 neurospheres in a volume of 0.5 ml subcutaneously in the shoulder region. We used the same number of mice to test the effect produced by viruses on tumor formation. Thus, each group of mice could develop up to 10 tumors. To test the ability of viruses to prevent formation of tumors from the injected neurospheres, the latter were incubated with viruses (see Materials and Methods). We used five mice for each type of virus; they were injected with a suspension containing virus-treated neurospheres (two injection points). The resulting tumors were counted 21 days after the injection. Assessing the tumors, we did not take into account their size (Fig. 2). 9 tumors (out of 10) developed in the control group injected with GM-5564 neurospheres. Treatment with type 1 poliovirus completely suppressed the formation of the tumors; Coxsackie virus A7 showed a less prominent result: one tumor did develop, but at a later date. Treatment with the Coxsackie virus B5 lead to the formation of three tumors, while Coxsackie virus A9 showed almost no anti-tumor effect (8 tumors). Groups of mice that received the GM-3876 neurospheres showed principally similar results: 8 tumors in the control group (out of 10 possible), no tumors after treatment with poliovirus and Coxsackie virus A7, 4 tumors in the group treated with the Coxsackie virus B5, 8 tumors in the Coxsackie virus A9 group.

DISCUSSION

Neurosphere cultures are the most adequate model for analyzing the therapeutic potential of anti-glioblastoma agents [40]. This is due to the fact that neurospheres carry tumor stem cells, which are the main cause of relapses: they are very resistant to most therapeutic agents [41]. In this study,

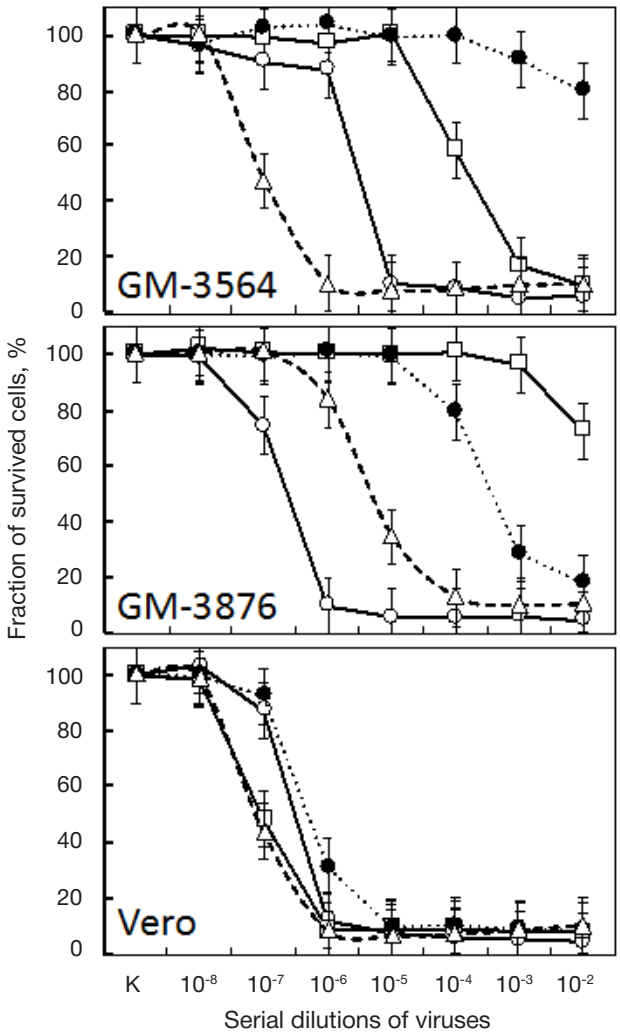

Fig. 1. Sensitivity of early-passage monolayer cell cultures obtained from two glioblastoma patients to four strains oncolytic enteroviruses: —○— Type 1 Poliovirus; - -Δ- - Coxsackie virus A7; —□— Coxsackie virus A9; ….●…. Coxsackie virus B5. Horizontal scale: 10^{-8}–10^{-2} — ten-fold serial dilutions of viral stocks used for the infections. Vero — control cell line that is sensitive to all four types of viruses used

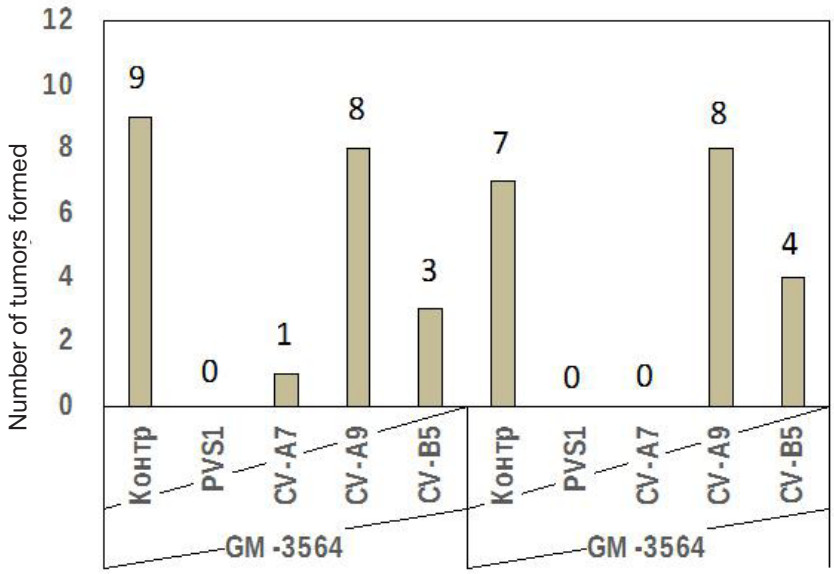

Fig. 2. Tumorigenicity-inhibition assay with glioblastoma neurosheres pretreated with each f the four viruses before being injected subcutaneously into nude mice. Bars reflect number of tumors formed in each treated and untereated (Contr) group of mice. PVS1 — Type 1 Poliovirus; CV-A7 — Coxsackie virus A7; CV-A9 — Coxsackie virus A9; CV-B5 — Coxsackie virus B5

we analyzed the ability of four non-pathogenic oncolytic enteroviruses to prevent the formation of subcutaneous tumor xenografts obtained through injecting neurospheres that were developed from the tumor material of two glioblastoma patients. The results of the study indicate that two viral strains, type 1 poliovirus and Coxsackie virus A7 were the most effective. However, neurospheres from the two different patients reacted to those viruses differently, which points to the need for a personalized selection of the most effective therapeutic strains after preliminary analysis of biopsy or surgical material taken from the patients' tumors. The recently published results of clinical trials of recombinant poliovirus PVSRIPO prove its ability to initiate prolonged remissions in 21% of glioblastoma patients, while the remaining patients saw no therapeutic effect from the virus [42]. Adding more therapeutic virus strains to the range available will significantly increase the percentage of successfully treated glioblastoma cases.

CONCLUSIONS

Based on the results of the study, we conclude that each of the four strains of non-pathogenic oncolytic enteroviruses produces cytolitic effect on monolayer cell cultures of human glioblastomas, and that the effect correlates well with the ability of the same strains to prevent tumor formation in xenografts transplanted to immunodeficient mice. Thus, there is a clear relationship between the effects produced by the viruses *in vitro* and their oncolytic activity *in vivo*. Besides, it was found that viruses that can efficiently replicate in monolayer glioblastoma cell cultures can effectively kill tumor-initiating glioblastoma stem cells, which signals the high oncolytic potential of the viruses in preventing tumor relapses. The differences in reaction to viruses that tumor cells from two patients have shown indicate the need for personalized selection of therapeutic strains.

References

1. Gubanova NV, Gaytan AS, Razumov IA, Mordvinov VA, Krivoshapkin AL, Netesov SV, i dr. Onkoliticheskie virusy v terapii gliom. Molekuljarnaja biologija. 2012; 46 (6): 726–38.
2. Greenberg MS. Handbook of Neurosurgery. 7th ed. New York: Thieme Publishers; 2010.
3. Park DM, Rich JN. Biology of glioma cancer stem cells. Molecules and cells. 2009; 28 (1): 7–12. DOI: 10.1007/s10059-009-0111-2. PubMed PMID: 19655094.
4. Claes A, Idema AJ, Wesseling P. Diffuse glioma growth: a guerilla war. Acta Neuropathol. 2007; 114 (5): 443–58. DOI: 10.1007/s00401-007-0293-7. PubMed PMID: 17805551; PubMed Central PMCID: PMCPMC2039798.
5. Buonaguro FM, Tornesello ML, Izzo F, Buonaguro L. Oncolytic virus therapies. Pharmaceutical patent analyst. 2012; 1 (5): 621–27. DOI: 10.4155/ppa.12.65. PubMed PMID: 24236929.
6. Parker JN, Bauer DF, Cody JJ, Markert JM. Oncolytic viral therapy of malignant glioma. Neurotherapeutics. 2009; 6 (3): 558–69.
7. Zulkifli MM, Ibrahim R, Ali AM, Aini I, Jaafar H, Hilda SS, et al. Newcastle diseases virus strain V4UPM displayed oncolytic ability against experimental human malignant glioma. Neurological research. 2009; 31 (1): 3–10. DOI: 10.1179/174313208x325218. PubMed PMID: 18937888.
8. Wagner S, Csatary CM, Gosztonyi G, Koch HC, Hartmann C, Peters O, et al. Combined treatment of pediatric high-grade glioma with the oncolytic viral strain MTH-68/H and oral valproic acid. Apmis. 2006; 114 (10): 731–43.
9. Freeman AI, Zakay-Rones Z, Gomori JM, Linetsky E, Rasooly L, Greenbaum E, et al. Phase I/II trial of intravenous NDV-HUJ oncolytic virus in recurrent glioblastoma multiforme. Mol Ther. 2006; 13 (1): 221–28.
10. Csatary LK, Gosztonyi G, Szeberenyi J, Fabian Z, Liszka V, Bodey B, et al. MTH-68/H oncolytic viral treatment in human high-grade gliomas. J Neurooncol. 2004; 67 (1–2): 83–93.
11. Csatary LK, Bakacs T. Use of Newcastle disease virus vaccine (MTH-68/H) in a patient with high-grade glioblastoma. JAMA. 1999; 281 (17): 588–89.
12. Tsamis KI, Alexiou GA, Vartholomatos E, Kyritsis AP. Combination treatment for glioblastoma cells with tumor necrosis factor-related apoptosis-inducing ligand and oncolytic adenovirus delta-24. Cancer Invest. 2013; 31 (9): 630–38. DOI: 10.3109/07357907.2013.849724. PubMed PMID: 24164301.
13. Li X, Mao Q, Wang D, Xia H. A novel Ad5/11 chimeric oncolytic

adenovirus for improved glioma therapy. Int J Oncol. 2012; 41 (6): 2159–65. DOI: 10.3892/ijo.2012.1674. PubMed PMID: 23117867.
14. Alonso MM, Jiang H, Gomez-Manzano C, Fueyo J. Targeting brain tumor stem cells with oncolytic adenoviruses. Methods Mol Biol. 2012; 797: 111–25.
15. Ahmed AU, Ulasov IV, Mercer RW, Lesniak MS. Maintaining and loading neural stem cells for delivery of oncolytic adenovirus to brain tumors. Methods Mol Biol. 2012; 797: 97–109.
16. Gomez-Manzano C, Fueyo J. Oncolytic adenoviruses for the treatment of brain tumors. Curr Opin Mol Ther. 2010; 12 (5): 530–37.
17. Lacroix J, Schlund F, Leuchs B, Adolph K, Sturm D, Bender S, et al. Oncolytic effects of parvovirus H-1 in medulloblastoma are associated with repression of master regulators of early neurogenesis. Int J Cancer. 2014; 134 (3): 703–16. DOI: 10.1002/ijc.28386. PubMed PMID: 23852775.
18. Paglino JC, Ozduman K, van den Pol AN. LuIII parvovirus selectively and efficiently targets, replicates in, and kills human glioma cells. J Virol. 2012; 86 (13): 7280–91.
19. Geletneky K, Huesing J, Rommelaere J, Schlehofer JR, Leuchs B, Dahm M, et al. Phase I/IIa study of intratumoral/intracerebral or intravenous/intracerebral administration of Parvovirus H-1 (ParvOryx) in patients with progressive primary or recurrent glioblastoma multiforme: ParvOryx01 protocol. BMC cancer. 2012; 12: 99.
20. Kicielinski KP, Chiocca EA, Yu JS, Gill GM, Coffey M, Markert JM. Phase 1 clinical trial of intratumoral reovirus infusion for the treatment of recurrent malignant gliomas in adults. Mol Ther. 2014; 22 (5): 1056–62. DOI: 10.1038/mt.2014.21. PubMed PMID: 24553100; PubMed Central PMCID: PMCPMC4015229.
21. van den Wollenberg DJ, Dautzenberg IJ, van den Hengel SK, Cramer SJ, de Groot RJ, Hoeben RC. Isolation of reovirus T3D mutants capable of infecting human tumor cells independent of junction adhesion molecule-A. PLoS One. 2012; 7 (10): e48064. DOI: 10.1371/journal.pone.0048064. PubMed PMID: 23110175; PubMed Central PMCID: PMCPMC3480499.
22. Forsyth P, Roldan G, George D, Wallace C, Palmer CA, Morris D, et al. A phase I trial of intratumoral administration of reovirus in patients with histologically confirmed recurrent malignant gliomas. Mol Ther. 2008; 16 (3): 627–32.
23. Wilcox ME, Yang W, Senger D, Rewcastle NB, Morris DG, Brasher PM, et al. Reovirus as an oncolytic agent against experimental human malignant gliomas. J Natl Cancer Inst. 2001; 93 (12): 903–12. PubMed PMID: 11416111.
24. Goetz C, Dobrikova E, Shveygert M, Dobrikov M, Gromeier M. Oncolytic poliovirus against malignant glioma. Future Virol. 2011; 6 (9): 1045–58.
25. Goetz C, Gromeier M. Preparing an oncolytic poliovirus recombinant for clinical application against glioblastoma multiforme. Cytokine Growth Factor Rev. 2010; 21 (2–3): 197–203. DOI: 10.1016/j.cytogfr.2010.02.005. PubMed PMID: 20299272; PubMed Central PMCID: PMCPMC2881183.
26. Dobrikova EY, Broadt T, Poiley-Nelson J, Yang X, Soman G, Giardina S, et al. Recombinant oncolytic poliovirus eliminates glioma in vivo without genetic adaptation to a pathogenic phenotype. Mol Ther. 2008; 16 (11): 1865–72.
27. Gromeier M, Lachmann S, Rosenfeld MR, Gutin PH, Wimmer E. Intergeneric poliovirus recombinants for the treatment of malignant glioma. Proc Natl Acad Sci USA. 2000; 97 (12): 6803–08.
28. Lawler SE, Speranza MC, Cho CF, Chiocca EA. Oncolytic Viruses in Cancer Treatment: A Review. JAMA oncology. 2017; 3 (6): 841–49. DOI: 10.1001/jamaoncol.2016.2064. PubMed PMID: 27441411.
29. Pol J, Buque A, Aranda F, Bloy N, Cremer I, Eggermont A, et al. Trial Watch-Oncolytic viruses and cancer therapy. Oncoimmunology. 2016; 5 (2): e1117740. DOI: 10.1080/2162402x.2015.1117740. PubMed PMID: 27057469; PubMed Central PMCID: PMCPMC4801444.
30. Taguchi S, Fukuhara H, Homma Y, Todo T. Current status of clinical trials assessing oncolytic virus therapy for urological cancers. Int J Urol. 2017; 24 (5): 342–51. DOI: 10.1111/iju.13325. PubMed PMID: 28326624.
31. Warner SG, O'Leary MP, Fong Y. Therapeutic oncolytic viruses: clinical advances and future directions. Curr Opin Oncol. 2017; 29 (5): 359–65. DOI: 10.1097/cco.0000000000000388. PubMed PMID: 28678032.
32. Bach P, Abel T, Hoffmann C, Gal Z, Braun G, Voelker I, et al. Specific elimination of CD133+ tumor cells with targeted oncolytic measles virus. Cancer Res. 2013; 73 (2): 865–74. DOI: 10.1158/0008-5472.can-12-2221. PubMed PMID: 23293278.
33. Berghauser Pont LM, Balvers RK, Kloezeman JJ, Nowicki MO, van den Bossche W, Kremer A, et al. In vitro screening of clinical drugs identifies sensitizers of oncolytic viral therapy in glioblastoma stem-like cells. Gene Ther. 2015. DOI: 10.1038/gt.2015.72. PubMed PMID: 26196249.
34. Dey M, Ulasov IV, Lesniak MS. Virotherapy against malignant glioma stem cells. Cancer Lett. 2010; 289 (1): 1–10.
35. Liu J, Ma L, Xu J, Liu C, Zhang J, Liu J, et al. Spheroid body-forming cells in the human gastric cancer cell line MKN-45 possess cancer stem cell properties. Int J Oncol. 2013; 42 (2): 453–59. DOI: 10.3892/ijo.2012.1720. PubMed PMID: 23229446; PubMed Central PMCID: PMCPMC3583623.
36. Sgubin D, Wakimoto H, Kanai R, Rabkin SD, Martuza RL. Oncolytic herpes simplex virus counteracts the hypoxia-induced modulation of glioblastoma stem-like cells. Stem cells translational medicine. 2012; 1 (4): 322–32. DOI: 10.5966/sctm.2011-0035. PubMed PMID: 23197811; PubMed Central PMCID: PMCPMC3659700.
37. van den Hengel SK, Balvers RK, Dautzenberg IJ, van den Wollenberg DJ, Kloezeman JJ, Lamfers ML, et al. Heterogeneous reovirus susceptibility in human glioblastoma stem-like cell cultures. Cancer Gene Ther. 2013; 20 (9): 507–13. DOI: 10.1038/cgt.2013.47. PubMed PMID: 23907517.
38. Chumakov PM, Morozova VV, Babkin IV, Baykov IK, Netesov SV, Tikunova NV. Onkoliticheskie enterovirusy. Molekuljarnaja biologija. 2012; 46 (6): 712–25.
39. Voroshilova MK, Magazanik SS, Chumakov PM. Poleznye virusy cheloveka. Aktual'nye voprosy epidemiologii, mikrobiologii i infekzionnyh zabolevaniy. Tashkent: Medicina; 1980. p. 227–29.
40. Wang X, Yang K, Xie Q, Wu Q, Mack SC, Shi Y, et al. Purine synthesis promotes maintenance of brain tumor initiating cells in glioma. Nature neuroscience. 2017; 20 (5): 661–73. DOI: 10.1038/nn.4537. PubMed PMID: 28346452; PubMed Central PMCID: PMCPMC6015494.
41. Lathia JD, Mack SC, Mulkearns-Hubert EE, Valentim CL, Rich JN. Cancer stem cells in glioblastoma. Genes Dev. 2015; 29 (12): 1203–17. DOI: 10.1101/gad.261982.115. PubMed PMID: 26109046; PubMed Central PMCID: PMCPMC4495393.
42. Desjardins A, Gromeier M, Herndon JE, 2nd, Beaubier N, Bolognesi DP, Friedman AH, et al. Recurrent Glioblastoma Treated with Recombinant Poliovirus. N Engl J Med. 2018; DOI: 10.1056/NEJMoa1716435. PubMed PMID: 29943666.

Литература

1. Губанова Н. В., Гайтан А. С., Разумов И. А., Мордвинов В. А., Кривошапкин А. Л., Нетесов С. В., и др. Онколитические вирусы в терапии глиом. Молекулярная биология. 2012; 46 (6): 726–38.
2. Greenberg MS. Handbook of Neurosurgery. 7th ed. New York: Thieme Publishers; 2010.
3. Park DM, Rich JN. Biology of glioma cancer stem cells. Molecules and cells. 2009; 28 (1): 7–12. DOI: 10.1007/s10059-009-0111-2. PubMed PMID: 19655094.
4. Claes A, Idema AJ, Wesseling P. Diffuse glioma growth: a guerilla

war. Acta Neuropathol. 2007; 114 (5): 443–58. DOI: 10.1007/s00401-007-0293-7. PubMed PMID: 17805551; PubMed Central PMCID: PMCPMC2039798.
5. Buonaguro FM, Tornesello ML, Izzo F, Buonaguro L. Oncolytic virus therapies. Pharmaceutical patent analyst. 2012; 1 (5): 621–27. DOI: 10.4155/ppa.12.65. PubMed PMID: 24236929.
6. Parker JN, Bauer DF, Cody JJ, Markert JM. Oncolytic viral therapy of malignant glioma. Neurotherapeutics. 2009; 6 (3): 558–69.
7. Zulkifli MM, Ibrahim R, Ali AM, Aini I, Jaafar H, Hilda SS, et al. Newcastle diseases virus strain V4UPM displayed oncolytic ability against experimental human malignant glioma. Neurological research. 2009; 31 (1): 3–10. DOI: 10.1179/174313208x325218. PubMed PMID: 18937888.
8. Wagner S, Csatary CM, Gosztonyi G, Koch HC, Hartmann C, Peters O, et al. Combined treatment of pediatric high-grade glioma with the oncolytic viral strain MTH-68/H and oral valproic acid. Apmis. 2006; 114 (10): 731–43.
9. Freeman AI, Zakay-Rones Z, Gomori JM, Linetsky E, Rasooly L, Greenbaum E, et al. Phase I/II trial of intravenous NDV-HUJ oncolytic virus in recurrent glioblastoma multiforme. Mol Ther. 2006; 13 (1): 221–28.
10. Csatary LK, Gosztonyi G, Szeberenyi J, Fabian Z, Liszka V, Bodey B, et al. MTH-68/H oncolytic viral treatment in human high-grade gliomas. J Neurooncol. 2004; 67 (1–2): 83–93.
11. Csatary LK, Bakacs T. Use of Newcastle disease virus vaccine (MTH-68/H) in a patient with high-grade glioblastoma. JAMA. 1999; 281 (17): 588–89.
12. Tsamis KI, Alexiou GA, Vartholomatos E, Kyritsis AP. Combination treatment for glioblastoma cells with tumor necrosis factor-related apoptosis-inducing ligand and oncolytic adenovirus delta-24. Cancer Invest. 2013; 31 (9): 630–38. DOI: 10.3109/07357907.2013.849724. PubMed PMID: 24164301.
13. Li X, Mao Q, Wang D, Xia H. A novel Ad5/11 chimeric oncolytic adenovirus for improved glioma therapy. Int J Oncol. 2012; 41 (6): 2159–65. DOI: 10.3892/ijo.2012.1674. PubMed PMID: 23117867.
14. Alonso MM, Jiang H, Gomez-Manzano C, Fueyo J. Targeting brain tumor stem cells with oncolytic adenoviruses. Methods Mol Biol. 2012; 797: 111–25.
15. Ahmed AU, Ulasov IV, Mercer RW, Lesniak MS. Maintaining and loading neural stem cells for delivery of oncolytic adenovirus to brain tumors. Methods Mol Biol. 2012; 797: 97–109.
16. Gomez-Manzano C, Fueyo J. Oncolytic adenoviruses for the treatment of brain tumors. Curr Opin Mol Ther. 2010; 12 (5): 530–37.
17. Lacroix J, Schlund F, Leuchs B, Adolph K, Sturm D, Bender S, et al. Oncolytic effects of parvovirus H-1 in medulloblastoma are associated with repression of master regulators of early neurogenesis. Int J Cancer. 2014; 134 (3): 703–16. DOI: 10.1002/ijc.28386. PubMed PMID: 23852775.
18. Paglino JC, Ozduman K, van den Pol AN. LuIII parvovirus selectively and efficiently targets, replicates in, and kills human glioma cells. J Virol. 2012; 86 (13): 7280–91.
19. Geletneky K, Huesing J, Rommelaere J, Schlehofer JR, Leuchs B, Dahm M, et al. Phase I/IIa study of intratumoral/intracerebral or intravenous/intracerebral administration of Parvovirus H-1 (ParvOryx) in patients with progressive primary or recurrent glioblastoma multiforme: ParvOryx01 protocol. BMC cancer. 2012; 12: 99.
20. Kicielinski KP, Chiocca EA, Yu JS, Gill GM, Coffey M, Markert JM. Phase 1 clinical trial of intratumoral reovirus infusion for the treatment of recurrent malignant gliomas in adults. Mol Ther. 2014; 22 (5): 1056–62. DOI: 10.1038/mt.2014.21. PubMed PMID: 24553100; PubMed Central PMCID: PMCPMC4015229.
21. van den Wollenberg DJ, Dautzenberg IJ, van den Hengel SK, Cramer SJ, de Groot RJ, Hoeben RC. Isolation of reovirus T3D mutants capable of infecting human tumor cells independent of junction adhesion molecule-A. PLoS One. 2012; 7 (10): e48064. DOI: 10.1371/journal.pone.0048064. PubMed PMID: 23110175; PubMed Central PMCID: PMCPMC3480499.
22. Forsyth P, Roldan G, George D, Wallace C, Palmer CA, Morris D, et al. A phase I trial of intratumoral administration of reovirus in patients with histologically confirmed recurrent malignant gliomas. Mol Ther. 2008; 16 (3): 627–32.
23. Wilcox ME, Yang W, Senger D, Rewcastle NB, Morris DG, Brasher PM, et al. Reovirus as an oncolytic agent against experimental human malignant gliomas. J Natl Cancer Inst. 2001; 93 (12): 903–12. PubMed PMID: 11416111.
24. Goetz C, Dobrikova E, Shveygert M, Dobrikov M, Gromeier M. Oncolytic poliovirus against malignant glioma. Future Virol. 2011; 6 (9): 1045–58.
25. Goetz C, Gromeier M. Preparing an oncolytic poliovirus recombinant for clinical application against glioblastoma multiforme. Cytokine Growth Factor Rev. 2010; 21 (2–3): 197–203. DOI: 10.1016/j.cytogfr.2010.02.005. PubMed PMID: 20299272; PubMed Central PMCID: PMCPMC2881183.
26. Dobrikova EY, Broadt T, Poiley-Nelson J, Yang X, Soman G, Giardina S, et al. Recombinant oncolytic poliovirus eliminates glioma in vivo without genetic adaptation to a pathogenic phenotype. Mol Ther. 2008; 16 (11): 1865–72.
27. Gromeier M, Lachmann S, Rosenfeld MR, Gutin PH, Wimmer E. Intergeneric poliovirus recombinants for the treatment of malignant glioma. Proc Natl Acad Sci USA. 2000; 97 (12): 6803–08.
28. Lawler SE, Speranza MC, Cho CF, Chiocca EA. Oncolytic Viruses in Cancer Treatment: A Review. JAMA oncology. 2017; 3 (6): 841–49. DOI: 10.1001/jamaoncol.2016.2064. PubMed PMID: 27441411.
29. Pol J, Buque A, Aranda F, Bloy N, Cremer I, Eggermont A, et al. Trial Watch-Oncolytic viruses and cancer therapy. Oncoimmunology. 2016; 5 (2): e1117740. DOI: 10.1080/2162402x.2015.1117740. PubMed PMID: 27057469; PubMed Central PMCID: PMCPMC4801444.
30. Taguchi S, Fukuhara H, Homma Y, Todo T. Current status of clinical trials assessing oncolytic virus therapy for urological cancers. Int J Urol. 2017; 24 (5): 342–51. DOI: 10.1111/iju.13325. PubMed PMID: 28326624.
31. Warner SG, O'Leary MP, Fong Y. Therapeutic oncolytic viruses: clinical advances and future directions. Curr Opin Oncol. 2017; 29 (5): 359–65. DOI: 10.1097/cco.0000000000000388. PubMed PMID: 28678032.
32. Bach P, Abel T, Hoffmann C, Gal Z, Braun G, Voelker I, et al. Specific elimination of CD133+ tumor cells with targeted oncolytic measles virus. Cancer Res. 2013; 73 (2): 865–74. DOI: 10.1158/0008-5472.can-12-2221. PubMed PMID: 23293278.
33. Berghauser Pont LM, Balvers RK, Kloezeman JJ, Nowicki MO, van den Bossche W, Kremer A, et al. In vitro screening of clinical drugs identifies sensitizers of oncolytic viral therapy in glioblastoma stem-like cells. Gene Ther. 2015. DOI: 10.1038/gt.2015.72. PubMed PMID: 26196249.
34. Dey M, Ulasov IV, Lesniak MS. Virotherapy against malignant glioma stem cells. Cancer Lett. 2010; 289 (1): 1–10.
35. Liu J, Ma L, Xu J, Liu C, Zhang J, Liu J, et al. Spheroid body-forming cells in the human gastric cancer cell line MKN-45 possess cancer stem cell properties. Int J Oncol. 2013; 42 (2): 453–59. DOI: 10.3892/ijo.2012.1720. PubMed PMID: 23229446; PubMed Central PMCID: PMCPMC3583623.
36. Sgubin D, Wakimoto H, Kanai R, Rabkin SD, Martuza RL. Oncolytic herpes simplex virus counteracts the hypoxia-induced modulation of glioblastoma stem-like cells. Stem cells translational medicine. 2012; 1 (4): 322–32. DOI: 10.5966/sctm.2011-0035. PubMed PMID: 23197811; PubMed Central PMCID: PMCPMC3659700.
37. van den Hengel SK, Balvers RK, Dautzenberg IJ, van den Wollenberg DJ, Kloezeman JJ, Lamfers ML, et al. Heterogeneous reovirus susceptibility in human glioblastoma stem-like cell cultures. Cancer Gene Ther. 2013; 20 (9): 507–13. DOI: 10.1038/cgt.2013.47. PubMed PMID: 23907517.
38. Чумаков П. М., Морозова В. В., Бабкин И. В., Байков И. К., Нетесов С. В., Тикунова Н. В. Онколитические энтеровирусы. Молекулярная биология. 2012; 46 (6): 712–25.
39. Ворошилова М. К., Магазаник С. С., Чумаков П. М. Полезные вирусы человека. Актуальные вопросы эпидемиологии, микробиологии и инфекционных заболеваний. Ташкент: Медицина; 1980. p. 227–29.
40. Wang X, Yang K, Xie Q, Wu Q, Mack SC, Shi Y, et al. Purine synthesis promotes maintenance of brain tumor initiating cells in glioma. Nature neuroscience. 2017; 20 (5): 661–73. DOI:

10.1038/nn.4537. PubMed PMID: 28346452; PubMed Central PMCID: PMCPMC6015494.

41. Lathia JD, Mack SC, Mulkearns-Hubert EE, Valentim CL, Rich JN. Cancer stem cells in glioblastoma. Genes Dev. 2015; 29 (12): 1203–17. DOI: 10.1101/gad.261982.115. PubMed PMID: 26109046; PubMed Central PMCID: PMCPMC4495393.

42. Desjardins A, Gromeier M, Herndon JE, 2nd, Beaubier N, Bolognesi DP, Friedman AH, et al. Recurrent Glioblastoma Treated with Recombinant Poliovirus. N Engl J Med. 2018; DOI: 10.1056/NEJMoa1716435. PubMed PMID: 29943666.

UTERINE HEMODYNAMICS AND OVARIAN RESERVE QUALITY IN THE PREDICTION OF IN VITRO FERTILIZATION OUTCOMES

Rabadanova AK, ✉ Shalina RI, Gugushvili NA

Department of Obstetrics and Gynecology, Faculty of Pediatrics,
Pirogov Russian National Research Medical University, Moscow

There are a few major factors determining the success of in vitro fertilization (IVF), including the potential of embryos to implant and the receptivity of the endometrium, which, in turn, are directly dependent on the ovarian reserve, i.e. the quality and quantity of oocytes. Diminished ovarian reserve can be inferred from reduced blood flow to the uterus on Doppler sonography. Based on the results of 3D power Doppler imaging of uterine blood flow on the day of ET and Virtual Organ Computer-aided AnaLysis (VOCAL), we attempted to predict the outcomes of IVF and embryo transfer (ET) in 56 female patients with different ovarian reserves. Blood flow was measured in the uterus, subendometrial region and endometrium, and IVF cycle outcomes were subsequently assessed. We have established an association between the characteristics of uterine and subendometrial blood flow and the outcomes of IVF cycles and ET. No such association has been established for the endometrium, though. Therefore, a 3D power Doppler examination on the day of embryo transfer provides valuable information on the endometrium receptivity and can be used as a prognostic marker of IVF success.

Keywords: IVF, 3D power Doppler, diminished ovarian reserve, poor ovarian response, uterine blood flow

✉ **Correspondence should be addressed:** Asiyat Rabadanova
Mnevniki 23, k. 254, Moscow, 123423; asyakubataeva@gmail.com

Received: 15.03.2018 **Accepted:** 20.03.2018

DOI: 10.24075/brsmu.2018.015

ГЕМОДИНАМИКА МАТКИ И СОСТОЯНИЕ ОВАРИАЛЬНОГО РЕЗЕРВА В ОЦЕНКЕ ЭФФЕКТИВНОСТИ ЭКСТРАКОРПОРАЛЬНОГО ОПЛОДОТВОРЕНИЯ

А. К. Рабаданова, ✉ Р. И. Шалина, Н. А. Гугушвили

Кафедра акушерства и гинекологии, педиатрический факультет,
Российский национальный исследовательский медицинский университет имени. Н. И. Пирогова

Эффективность программы экстракорпорального оплодотворения (ЭКО) зависит от ряда факторов, среди которых большое значение имеют эмбриональный и эндометриальный. Каждый из этих факторов напрямую зависит от овариального резерва, определяющего качество ооцитов и изменение допплерометрических показателей в матке, которые отражают снижение внутриматочной перфузии. Целью исследования было прогнозирование эффективности циклов ЭКО и переноса эмбрионов (ПЭ) у пациенток с различным овариальным резервом на основании определения объемного кровотока в матке в день переноса эмбриона с помощью 3D-УЗИ с функцией энергетической допплерографии. У 56 пациенток с различным овариальным резервом произведено измерение параметров кровотока с помощью 3D-УЗИ и прикладной программы VOCAL (Virtual Organ Computer-aided AnaLysis) в матке, субэндометриальной зоне и в эндометрии в день переноса эмбриона с последующей оценкой эффективности циклов ЭКО. В ходе работы установлена зависимость между параметрами 3D-кровотока в матке и субэндометриальной зоне и эффективностью циклов ЭКО и ПЭ. При исследовании кровотока в эндометрии такая зависимость не выявлена. Таким образом, использование 3D-УЗИ с функцией энергетической допплерографии в день переноса эмбриона позволяет судить о степени выраженности рецептивности эндометрия и может быть использовао в качестве прогностического критерия для определения вероятности наступления беременности в цикле ЭКО.

Ключевые слова: экстракорпоральное оплодотворение, сниженный овариальный резерв, маточный кровоток, 3D-УЗИ с функцией энергетической допплерографии

✉ **Для корреспонденции:** Асият Рабаданова
ул. Мнёвники, д. 23, к. 254, г. Москва, 123423; asyakubataeva@gmail.com

Статья получена: 15.03.2018 **Статья принята к печати:** 20.03.2018

DOI: 10.24075/vrgmu.2018.015

Today, the success of in vitro fertilization (IVF) is seen as a combination of two major factors: the ability of embryos to implant and the receptivity of the endometrium [1]. These two factors are directly dependent on the ovarian reserve of the female patient. In patients with diminished ovarian reserve the quality of oocytes tends to degrade [2] and Doppler ultrasonography reveals decreased uterine perfusion. In the study presented below we chose to focus on the endometrial blood flow as the quality of transferred embryos was good; so their ability to implant is not discussed here.

In 2013 the Russian Association of Human Reproduction (RAHR) reported that the use of cryopreserved donor eggs

in females over 40 years of age improves the outcome of IVF cycles by as little as 4.8% [3]. The figures published in the report suggest that better IVF outcomes in patients with diminished ovarian reserve are largely determined by the receptive quality of the endometrium. In this light, the discovery of robust methods for its assessment and enhancement should receive special attention. Conveniently, three-dimensional power Doppler ultrasonography can be a perfect non-invasive tool for predicting endometrial receptivity [4, 5].

Proliferation and differentiation of endometrial cells is controlled by ovarian steroid hormones promoting angiogenesis [6], which plays a crucial role in stimulating endometrial growth and ensures good implantation of the embryo [7, 8]. Sufficient blood supply to the endometrial and subendometrial regions is an essential prerequisite for successful implantation.

The study conducted in 2012 [8] compared the prognostic value of 2D and 3D ultrasonography in the assessment of endometrial receptivity, which signals the opening or closure of the implantation window. The data on the endometrial blood flow obtained during the scans were compared to the findings of endometrial biopsy. It was established that 3D ultrasonography is a more accurate prognostic tool than 2D ultrasonography. The lack of correlation between 2D ultrasonography findings and IVF outcomes was also reported by other researchers [9].

Unfortunately, few authors have studied the uterine blood flow as a predictor of the outcomes of infertility treatment with embryo transfer in patients with different ovarian reserves, so the literature on this problem is scarce.

In our study we attempted to establish a correlation between the outcome of an IVF cycle and the findings of a 3D power Doppler examination of uterine blood flow in patients with different ovarian reserves on the day of embryo transfer.

METHODS

The study was carried out at the facilities of the Center for Family Planning and Reproductive Health (Department of Reproduction) between 2015 and 2017.

As part of the study, we conducted a prospective analysis of standard IVF cycles in 56 female patients with different ovarian reserves. The treatment included transfer of no more than 2 blastocysts on day 5 after oocyte retrieval. Based on the outcome of the IVF cycle we distributed the patients into 2 groups. The first group included 21 patients who became pregnant after IVF, and the second group consisted of 35 patients whose IVF cycle failed. Among the patients who achieved pregnancy, 13 (61.9%) had been previously diagnosed with tuboperitoneal infertility and 8 (38.1%) had a diminished ovarian reserve. Twenty-three (65.7%) of all patients who did not achieve pregnancy had been diagnosed with tuboperitoneal infertility, and in 12 (34.2%) females the ovarian reserve was diminished.

Our study was conducted in the females between 30 and 40 years of age diagnosed with diminished ovarian reserve and tuboperitoneal infertility.

Patients with ovarian neoplasms, myomas, adenomyosis, and those who had previously undergone a therapy to improve their uterine blood flow or had an infertile partner were excluded from the study.

The loss of ovarian reserve was assessed by measuring the levels of the follicle stimulating hormone (FSH) and the anti-Müllerian hormone (AMH), and by counting antral follicles less than 10 mm in size identified during the ultrasound scan on days 2–3 of treatment. If FSH levels exceeded 8 IU/l and AMH levels were lower than 1 ng/ml and the number of retrieved oocytes was < 3, then the ovarian reserve was considered diminished.

In the course of treatment, patients' ovaries were stimulated by gonadotropin-releasing hormone antagonists. Ovulation was induced by a recombinant FSH.

The starting dose of FSH (75 to 275 IU/24 hours) was individually selected for each patient depending on her age, body mass index (BMI), FSH and AMH levels, and ovarian response to previous treatment cycles. Follicle development was monitored by ultrasonography. Once a leading follicle had reached 18–20 mm in diameter, we introduced an ovulation trigger (human chorionic gonadotropin HCG) and 34–36 hours later performed a transvaginal puncture of follicles of >15 mm in size. Oocyte retrieval, insemination, culture, ET and lutein phase support by progesterone administration in the post-transfer period were performed according to standard protocols [2].

On the day of embryo transfer the patients underwent an ultrasound examination; a 3D image of the uterus was reconstructed in a 3D power Doppler mode. The procedure was performed on Voluson 730 Expert (GE Healthcare, Austria) equipped with an endovaginal transducer (frequency range from 5 to 9 MHz). Because blood flow characteristics are sensitive to varying frequencies, we used the following settings: Gn of 9.0, Frq, low; Qual, norm; WMF, low1; PRF, 0.9 kHz.

The original 2D image for further 3D reconstruction represented the central plane of the volume of interest [10, 11]; the scan swept through the volume from one of its borders to another. The scan angle was 120°; the rotation step was exactly 15°, because otherwise the vessels located in close proximity to the uterus could have been captured into the reconstructed volume.

The contours of the endometrium and the uterus were manually delineated using the VOCAL software. Blood flow was assessed in 1) the endometrial region with the contour drawn along its basal layer and in 2) the endometrium and a 5-mm shell area around its basal layer which included the subendometrium with its basal and radial arteries [12]. Jagged contours after contouring were regarded as an error.

After the reconstruction, the volumes of the uterus, endometrium and subendometrium were computed. A few important histogram indices were also computed, including the vascularization index (VI), which represents the percentage of blood vessels in a given tissue volume; the flow index (FI), which represents the blood volume moving through the vessels during the scan, and the vascularization-flow index (VFI), which provides information on the organ perfusion.

The data were processed in Excel 7.0 and Statistica 6.0. The parameters analyzed were compared pairwise; differences were considered significant at $p < 0.05$. We also used the AUC ROC analysis. Generally, the higher is AUC, the better is the performance of the model. The performance scale used in our study was as follows: 0.9–1.0, excellent; 0.8–0.9, very good; 0.7–0.8, good; 0.6–0.7, fair; 0.5–0.6, poor.

RESULTS

Patients' age varied between 30 and 42 years (mean age was 34.27 ± 3.98 years). There were 17 patients under 35 and 39 patients between 35 and 42 years of age. The mean age of the patients who achieved pregnancy after ET (group 1) was 34.27 ± 3.98 years. The mean age of the patients whose IVF failed (group 2) was 36.00 ± 3.74 years ($p > 0.05$). Although IVF tended to fail in older patients, especially in those with diminished ovarian reserve, no significant differences were

revealed between the groups with regard to this parameter (Table 1).

Because candidates for the infertility treatment with assisted reproductive technologies (AST) were selected very carefully, the rate of extragenital pathologies fell within the population range.

A relatively big number of patients (40%) with diminished ovarian reserve whose IFV treatment failed had previously undergone an ovarian surgery (Table 1). Of them 5 patients (31.2%) had received surgical treatment for cystadenomas and 11 patients (68.8%) for endometroid cysts.

About half of our patients (48.6%, or 17 individuals with different ovarian reserves) whose IVF failed had a previous history of dilation and curettage. Of them 14 had received treatment for uterine polyps and 3 for endometrial hyperplasia. In patients who achieved pregnancy after IVF endometrial pathologies were 1.7 times less frequent (Table 1).

The duration of infertility ranged from 1 to 11 years. The patients with diminished ovarian reserve had a longer history of infertility than those with normal ovarian reserve, but the difference between those two groups was insignificant (Table 1).

The majority of the patients who achieved pregnancy had been previously diagnosed with primary sterility. The same was true for 20 patients (57.1%) whose IVF failed.

FSH and AMH levels regulating the ovarian function differed significantly between the patients with different ovarian reserves. Low AMH and high FSH were observed in the patients with diminished ovarian reserve (Table 1).

Doses of rFSH administered to the patients and the number of transferred embryos did not differ significantly between the groups.

On day 5 after oocyte retrieval and before embryo transfer, the patients underwent 2D and 3D power Doppler ultrasonography.

Endometrial thickness measured on the day of embryo transfer varied from 8.0 to 14.5 mm in the patients who achieved pregnancy after IVF. The endometrium was the thickest (14.5 mm) in the patient who later gave birth to twins. In the females whose IVF failed the thickness of the endometrium varied from 7.0 to 10.6 mm. The differences in the endometrial thickness were significant between the patients whose IVF was successful and those whose IVF was ineffective, for both good and bad ovarian reserves ($p = 0.003$; $p = 0.05$) (Table 1).

Therefore, endometrial thickness measured on the day of embryo transfer can be a good prognostic marker of the IVF cycle outcome regardless of the quality of ovarian reserve.

The uterine volume measured by 3D Doppler varied from 31.7 to 83.3 mm^3 in group 1 (successful IVF) and from 21.0 to 90.3 mm^3 in group 2 (failed IVF). The analysis revealed that the uterine volume tended to depend on whether the patient had given birth in the past. In group 1 there were 87.5% of females who had given birth before, and in group 2 such patients made 65.7%. The uterine volume in such patients was over 58 mm^3. No association between the uterine volume and the ovarian reserve or IVF success was established during the study ($p > 0.05$) (Table 2).

On average, the volume of the endometrium ranged from 3.5 to 13.9 mm^3 in women who achieved pregnancy after IFV. In women whose IVF failed this parameter varied from 4 to 14 mm^3. No significant differences ($p > 0.05$) in the endometrial volume were observed between the groups with different ovarian reserves or different IVF outcomes (Table 2).

This means that myometrial and subendometrial volumes have no significant prognostic value for IVF success regardless of the quality of patient's ovarian reserve.

In contrast, the data on the endometrial volume available in the literature demonstrate its strong correlation with IVF success. Unlike thickness (midline echo), the endometrial volume is recommended as a predictor of an IVF cycle outcome [12]. Our study shows that the volume of the endometrium was significantly larger in patients who achieved pregnancy, regardless of their ovarian reserve, than in those whose IVF failed ($p = 0.003$; see Table 2). The endometrial volume was 1.4

Table 1. Characteristics of female patients with different ovarian reserves and the IVF outcome

	Successful IVF cycle (n = 21)		Failed IVF cycle (n = 35)		p
	Good ovarian reserve (n = 13) p^1	Diminished ovarian reserve (n = 8) p^2	Good ovarian reserve (n = 23) p^3	Diminished ovarian reserve (n = 12) p^4	
Age. years	33.27 ± 4.98	35.45 ± 2.98	35.09 ± 3.46	37.02 ± 2.87	–
Body mass index	24.36 ± 1.98	24.76 ± 1.43	25.02 ± 1.17	25.32 ± 1.87	–
History of infertility. years	4.16 ± 2.54	5.26 ± 3.54	5.98 ± 2.07	5.41 ± 3.07	–
Primary sterility	3 14.3%	6 28.6%	5 14.3%	10 28.6%	–
Secondary sterility	10 47.6%	2 9.5%	18 51.4%	2 5.7%	–
FSH levels. mIU/ml	6.8 ± 1.56	11.99 ± 7.03	7.18 ± 1.79	12.29 ± 5.99	$p^1/p^2 = 0.001$* $p^3/p^4 = 0.002$*
AMH levels. ng/ml	3.26 ± 1.27	0.61 ± 0.42	3.57 ± 2.43	0.65 ± 0.37	$p^1/p^3 = 0.021$* $p^2/p^4 = 0.001$*
rFSH dose. IU	2202.5 ± 986.8	1602.9 ± 796.8	2309.2 ± 862.2	1809.2 ± 987.8	–
Endometrial thickness on the day of ET. mm	10.4 ± 2.6	10.60 ± 1.94	8.4 ± 0.9	8.31 ± 1.28	$p^1/p^3 = 0.05$* $p^2/p^4 = 0.003$*
Number of transferred embryos	1.49 ± 0.21	1.59 ± 0.29	1.76 ± 0.68	1.32 ± 0.43	–
Ovarian surgeries	1 4.8%	3 14.9%	5 14.9%	7 40%	–
Number of ovarian pathologies in the patient's medical history	4 19.0%	2 9.5%	9 25.7%	8 22.9%	–

Note: * — represents significant differences.

Table 2. Volumes of the myometrium, subendometrium and endometrium measured by 3D power Doppler

	Successful IVF cycle (n = 21)		Failed IVF cycle (n = 35)		p
	Good ovarian reserve (mm^3) (n = 13) p^1	Diminished ovarian reserve (mm^3) (n = 8) p^2	Good ovarian reserve (mm^3) (n = 25) p^3	Diminished ovarian reserve (mm^3) (n = 12) p^4	
Volume of myometrium	49.4 ± 5.01	47.2 ± 4.98	49.2 ± 3.67	48.6 ± 5.12	–
Volume of subendometrium	10.0 ± 1.1	9.8 ± 0.8	8.9 ± 0.8	8.7 ± 0.7	–
Volume of endometrium	2.53 ± 0.19	1.38 ± 0.31	1.79 ± 0.38	0.82 ± 0.25	$p^1/p^2 = 0.004^*$ $p^3/p^4 = 0.008^*$ $p^1/p^3 = 0.05^*$ $p^2/p^4 = 0.02^*$

Note: * — represents significant differences.

and 1.7 times bigger, respectively, in patients whose IVF was effective and ovarian reserve was good than in those whose IVF failed (p = 0.004, p = 0.008; see Table 2). This confirms that the volume of the endometrium can be used for predicting the success of IVF cycles.

The endometrial volume was relatively small on the day of embryo transfer in the patients who had undergone endometrial curettage in the past, in contrast to those who had not had a prior surgery. This was true for all patients regardless of their IVF outcome.

To predict the success of IVF cycles, we used 3D power Doppler ultrasonography which helps to measure the parameters of the low-velocity blood flow typical for the myometrium and endometrium. Some authors point out that 3D power Doppler is more effective for the imaging of blood vessels with low-velocity blood flow [11].

Histogram indices of myometrial and subendometrial blood flow presented in Table 3 were significantly higher in the patients who achieved pregnancy after ET. VI and VFI computed for the myometrium were 1.6 and 2.0 times higher, respectively, in the patients whose IVF was successful than in those whose IVF failed. A similar tendency was observed for the subendometrial region where VI and VFI were 2.6 and 2.5 times higher, respectively, in the patients whose IVF was successful than in those whose IVF failed.

In the patients with diminished ovarian reserve whose IVF was ineffective, the myometrial VI and VFI were 1.6 and 1.5 times lower, respectively, and the subendometrial VFI was 2.5 lower than in the females with normal ovarian reserve whose IVF was also ineffective (p < 0.05; see Table 3). This suggests poor uterine blood supply in the patients with diminished ovarian reserve.

In contrast, the patients who achieved pregnancy after IVF showed no differences in the blood flow indices, regardless of the ovarian reserve quality.

To compare the approaches to the assessment of the endometrial blood flow (the subendometrium excluded and included into the studied volume; see Fig.1), we used the ROC-AUC analysis (Fig.2); it revealed no associations between the studied blood flow indices and the success of IVF (Fig. 2 A; AUC for VI was 0.49, for FI, 0.50, for VFI, 0.49).

For the reconstructed images that included the 5-mm shell around the basal layer (the subendometrium), an association was established between the studied blood flow indices and the outcome of IVF cycles (Fig. 2 B) (AUC for VI was 0.88, for FI, 0.66; for VFI, 0.91).

Using the data obtained with 2D and 3D ultrasonography, we identified 3 major parameters that showed a reliable correlation with IVF success regardless of the patient's ovarian reserve: the volume of the endometrium, myometrial VI and subendometrial VFI. The prognostic value of these parameters was demonstrated using the ROC-curve (Fig. 3). For the endometrial volume sensitivity was 74.8%; specificity 60.6%; AUC 0.851; for the myometrial VI these values were 86.4%, 69.4%, and 0.857, respectively, and for the subendometrial VFI they were 90.4%, 79.4% and 0.916, respectively.

Table 3. Uterine hemodynamics in patients with different ovarian reserve and IVF outcomes

Groups	Effect/ 3D Doppler parameters	Uterus			Subendometrium			Endometrium		
		VI	FI	VFI	VI	FI	VFI	VI	FI	VFI
Good ovarian reserve	Successful cycle (n = 13) p^1	11.41 ± 2.19	16.16 ± 2.90	1.77 ± 0.35	6.13 ± 4.23	10.0 ± 1.17	0.92 ± 0.64	3.41 ± 2.82	11.60 ± 1.61	0.32 ± 0.33
	Failed cycle (n = 25) p^2	7.45 ± 0.97	12.75 ± 1.68	0.94 ± 0.05	3.19 ± 2.57	10.55 ± 1.90	0.25 ± 0.15	2.5 ± 2.22	11.38 ± 2.76	0.27 ± 0.21
Diminished ovarian reserve	Successful cycle (n = 8) p^3	10.56 ± 2.57	17.68 ± 3.44	1.92 ± 0.75	3.52 ± 1.09	11.12 ± 1.03	0.39 ± 0.16	2.40 ± 1.84	10.69 ± 1.68	0.22 ± 0.20
	Failed cycle (n = 12) p^4	4.47 ± 2.30	14.05 ± 3.32	0.62 ± 0.28	1.23 ± 1.27	8.61 ± 3.95	0.10 ± 0.08	1.82 ± 1.49	11.17 ± 2.16	0.19 ± 0.16
p		$p^1/p^2 = 0.007^{**}$ $p^3/p^4 = 0.003^{**}$ $p^1/p^3 = 0.62$ $p^2/p^4 = 0.014^*$	$p^1/p^2 = 0.06$ $p^3/p^4 = 0.35$ $p^1/p^3 = 0.52$ $p^2/p^4 = 0.41$	$p^1/p^2 = 0.23$ $p^3/p^4 = 0.009^{**}$ $p^1/p^3 = 0.78$ $p^2/p^4 = 0.011^*$	$p^1/p^2 = 0.24$ $p^3/p^4 = 0.014^*$ $p^1/p^3 = 0.27$ $p^2/p^4 = 0.12$	$p^1/p^2 = 0.58$ $p^3/p^4 = 0.18$ $p^1/p^3 = 0.19$ $p^2/p^4 = 0.30$	$p^1/p^2 = 0.013^*$ $p^3/p^4 = 0.007^{**}$ $p^1/p^3 = 0.12$ $p^2/p^4 = 0.04^*$	$p^1/p^2 = 0.34$ $p^3/p^4 = 0.82$ $p^1/p^3 = 0.21$ $p^2/p^4 = 0.41$	$p^1/p^2 = 0.83$ $p^3/p^4 = 0.65$ $p^1/p^3 = 0.37$ $p^2/p^4 = 0.85$	$p^1/p^2 = 0.57$ $p^3/p^4 = 0.77$ $p^1/p^3 = 0.57$ $p^2/p^4 = 0.32$

Note: * — difference significant at p < 0.05; ** — difference significant at p < 0.01.

DISCUSSION

The thickness of the endometrium (midline echo) was measured by 2D ultrasonography. There is no consensus in the literature on the minimal endometrial thickness necessary for achieving pregnancy. The majority of the researchers report failed IVF in patients with endometrial thickness less than 7 mm [7, 13, 14]. However, there are reports of pregnancy in patients with 6-mm- or even 4-mm-thick endometrium [15]. Endometrial thickness over 14 mm is associated with a high risk of miscarriage [7].

Our study reveals that endometrial thickness measured by 2D ultrasonography in patients with different ovarian reserve correlates with the outcomes of IVF cycles. The differences were more significant (p = 0.003), though, for the patients with good ovarian reserve than for those with diminished ovarian reserve (p = 0.05). Some researchers have demonstrated

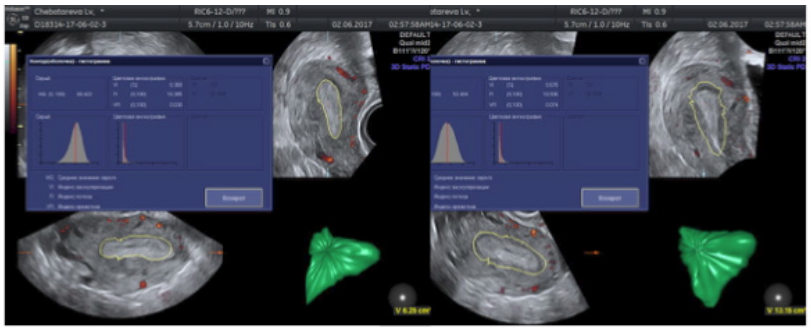

A Blood flow in the endometrium

B Blood flow in the subendometrium

Fig. 1. Blood flow assessment in the endometrium (the subendometrial region excluded and included)

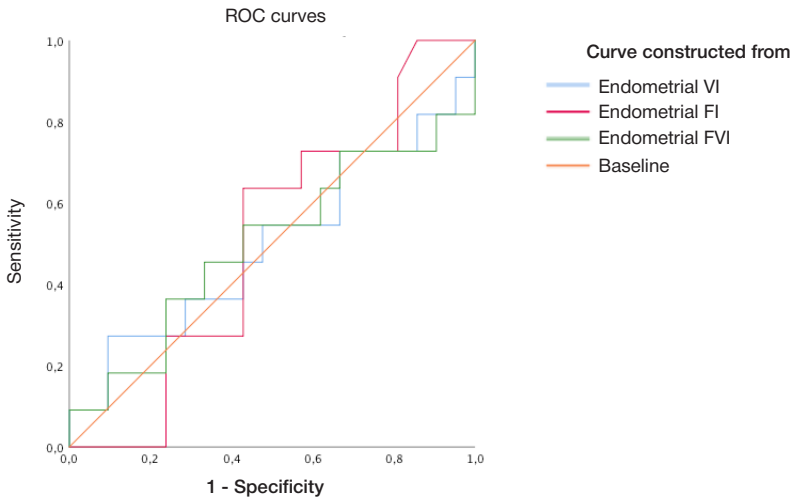

A Blood flow in the endometrium

Diagonal segments generated by the associations

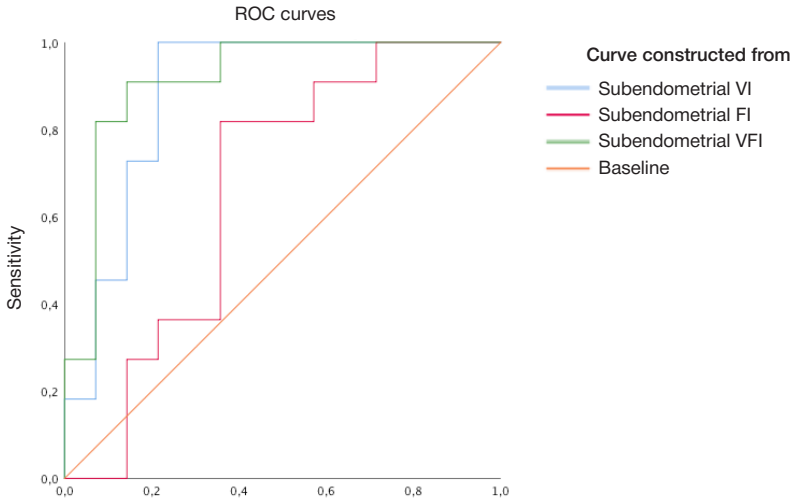

B Blood flow in the subendometrial region

Fig. 2. ROC-analysis of the associations between IVF outcomes and the blood flow in the endometrium (**A**) and the subendometrial region (**B**)

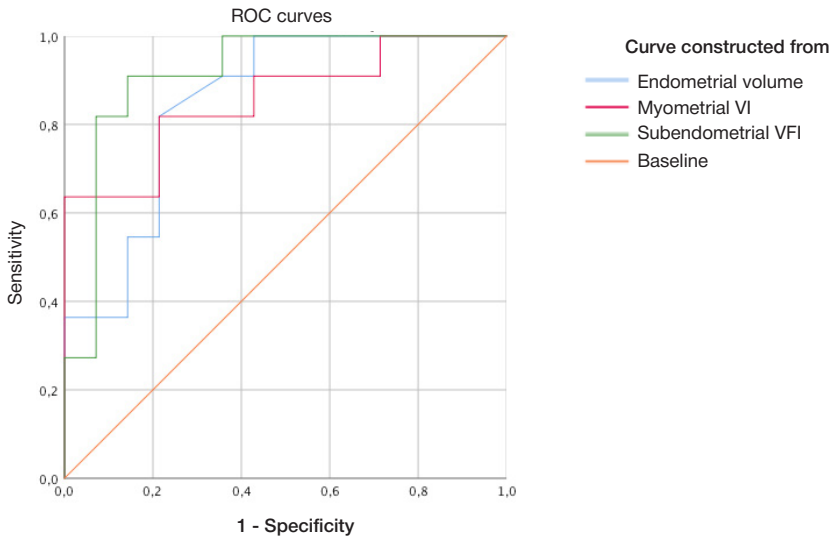

Fig. 3. ROC-analysis of the associations between IVF outcomes and the endometrial volume, myometrial VI and subendometrial VFI

the lack of associations between the success of IVF and the thickness of the endometrium [14]. It has been also reported that patients older than 40 tend to have thinner endometrium, which is a consequence of lower estradiol levels [12]. A few authors believe that endometrial thickness is a subjective parameter, so 3D sonography appears to be a more reliable tool for measuring the endometrial volume and establishing an association between this parameter and the success of IVF [9]. The use of 3D ultrasonography allowed us to reveal significant differences in the endometrial volume in the patients whose IVF outcomes were different ($p = 0.05$; $p = 0.02$). The endometrial volumes were also significantly different in the patients who achieved pregnancy but had different ovarian reserves ($p = 0.004$); however, no significant difference was observed between the patients with regard to their endometrial thickness.

Uterine blood flow plays an important role in the prediction of IVF outcomes. The meta-analysis of the literature has demonstrated that indices of subendometrial and endometrial blood flows can indirectly reflect endometrial receptivity [5]. It is known that blood is supplied to the endometrium mainly by spiral arteries which are a continuation of the basal arteries located in the subendometrium [11]. The subendometrial region should be included in the studied volume because the subendometrial blood flow indices show the intensity of blood flow in the arcuate artery and its radial branches.

Due to a high risk of injury to the endometrium, invasive techniques cannot be used on the day of embryo transfer for the assessment of endometrial receptivity. Non-invasive techniques are recommended instead. Ultrasonography of the myometrial and subendometrial blood flows has revealed significant differences between the patients regardless of the quality of their ovarian reserve in the myometrial IV ($p = 0.007$ for the patients with normal ovarian reserve; $p = 0.003$ for the patients with diminished ovarian reserve) and the subendometrial VFI ($p = 0.013$ for the patients with normal ovarian reserve and $p = 0.007$ for the patients with diminished ovarian reserve). The lowest values were observed in the patients with low ovarian reserve who failed to achieve pregnancy. It is believed that in patients with decreased ovarian reserve reduced blood flow indices result from the impaired growth of blood vessels in the functional endometrial layer due to the insufficient effect of estrogen during the proliferative stage [16].

Our findings are consistent with the results of the study [17] suggesting that estrogen content in the serum can be reliably associated with the intensity of the uterine blood flow during IVF cycles in patients who receive gonadotropins and gonadotropin-releasing hormone antagonists. It has been proved that hormone replacement therapy considerably improves the uterine blood flow (as and its indices measured by Doppler sonography) in patients with premature ovarian insufficiency [18].

Thus, our findings suggest that the use of 3D power Doppler ultrasonography on the day of embryo transfer can be an effective technique for the indirect assessment of endometrial receptivity, which is consistent with the data obtained by other researchers [5], and a good tool for predicting the outcome of an IVF cycle after embryo transfer.

Once we know myometrial and subendometrial blood flow characteristics, we can avoid useless embryo transfers. Patients with diminished ovarian reserve are recommended to undergo uterine flow examinations and therapies aimed at improving uterine perfusion (should there be any deviations from the norm) before starting IVF.

CONCLUSIONS

We have demonstrated that 3D power Doppler ultrasonography is a reliable method for the assessment of uterine perfusion on the day of embryo transfer in patients undergoing infertility treatment. Myometrial and subendometrial blood flow indices are better predictors of IVF success than characteristics of the endometrial blood flow which showed no correlation with the IVF outcomes in our study. Endometrial volume measured by 3D Doppler has a higher prognostic value than endometrial thickness measured by 2D ultrasound. Considering very low values of blood flow indices in patients with diminished ovarian reserve whose IVF was ineffective, we recommend 3D Doppler scans for such patients before embryo transfer.

References

1. Anshina MB, Isakova EHV, Kalinina EAnat, Kalinina EAndr, Korsak VS, Krasnopolskaya KV i dr. Priemenie estrogenov v programmach WPT. Nachno-practicheskie rekomendacii. M.: Rossiyskaja associaacija reprodukcii sheloveka. 2015; 80 s.
2. Nazarenko TA, Krasnoposkaya KV. «Poor response.» Tactica vedenija pacientok so snijennoy reacciej a stimuljaciju gonadotropinami v programmach EKO. M. : MEDpress-inform, 2013. 80 s.
3. Korsak VS, Smirnova AA, Shurygina OV. VRT v Rossii. Otchet za 2013 g. Problemy reprodukcii. 2015; 21 (6): 17–19 .
4. Mishra VV, Agarwal R, Sharma U, Aggarwal R, Choudhary S, Bandwal P. Endometrial and Subendometrial Vascularity by Three-Dimensional (3D) Power Doppler and Its Correlation with Pregnancy Outcome in Frozen Embryo Transfer (FET) Cycles. J of Obstetrics and Gynaecology of India. 2016; 66 (Suppl 1): 521–527. DOI: 10.1007/s13224-016-0871-5.
5. Jianing Wang, Fei Xia, Ying Zhou, Xuedong Wei, Yanyan Zhuang, Yingxue Huang. Association Between Endometrial/Subendometrial Vasculature and Embryo Transfer Outcome: A Meta-analysis and Subgroup Analysis. J Ultrasound Med. 2018 Jan; 37 (1): 149-163. DOI: 10.1002/jum.14319. Epub 2017 Jul 17.
6. Lecce G, Meduri G, Ancelin M. Presence of estrogen receptor bin the human endometrium through the cycle: expression inglandular, stromal, and vascular cells. J Clin Endocrinol Metab. 2001; 86: 1379–86.
7. Amir W, Micha B, Ariel H, Liat LG, Jehoshua D, Adrian S. Predicting factors for endometrial thickness during treatment with assisted reproductive technology. Fertil Steril 2007; 87 (4): 799–804.
8. Kalmantis K, Loutradis D, Lymperopoulos E, Beretsos P, Bletsa R, Antsaklis A. Three Dimensional Power Doppler evaluation of human endometrium after administration of oxytocine receptor antagonist (OTRa) in an IVF program., Arch Gynecol Obstet. 2012 Jan; 285 (1): 265–70. DOI: 10.1007/s00404-011-2019-2. Epub 2011 Aug 7.
9. Prasad S, Goyal R, Kumar Y, et al. The Relationship Between Uterine Artery two-dimensional Color Doppler Measurement and Pregnancy Outcome: A Prospective Observational Study. Journal of Reproduction & Infertility. 2017; 18 (2): 251–6.
10. Krylova YuS, Kvetnoj IM, Ajlamazyan EK. Receptivnost' endometrija: moleculjarnye mechanizmy eguljacii implantacii. J akusherstva i jenskich boleznej. 2013; 62 (2): 63–74. DOI: http://dx.doi.org/10.17816/JOWD62263-74.
11. Ozerskaja IA. Atlas ginekologischeskoj ul'trazvukovoj normy. M.: Vidar-M; 2010. 225 s.
12. Ari Kim, Hyuk Jung, Won June Choi, Sung Nam Hong, Heung Yeol Kim. Detection of endometrial and subendometrial vasculature on the day of embryo transfer and prediction of pregnancy during fresh in vitro fertilization cycles Taiwanese. Journal of Obstetrics & Gynecology. 2014; 53 (3): 360–5.
13. Krasnopol'skaya KV, Nazarenko TA, Sesina NI, Ershova IYu, Aleksandrova VR. Rezul'taty programmy EKO s donorskimi oocitami u pacientok s ul'trazvukovymi prinakami "tonkogo" endometrija. Medicinskij alfavit. M.: Al'famed. 2017; 1 (12) (309) : 34–8.
14. Kasius A, Smit JG, Torrance HL et al. Endometrial thickness and pregnancy rates after IVF: a systematic review and meta-analysis. Hum Reprod Update. 2014; 20 (4): 530–41.
15. Weiss NS, van Vliet MN, Limpens J, Hompes PGA et al. Endometrial thickness in women undergoing IUI with ovarian stimulation. How thick is too thin? A systematic review and meta-analysis. Hum Reprod Update. 2017; 32 (5): 1009–18.
16. Jayaprakasan K, Hopkisson JF, Campbell BK, Clewes J, Johnson IR, Raine-Fenning NJ. Quantification of the effect of pituitary down-regulation on 3D ultrasound predictors of ovarian response. Human Reproduction. 2008; 23 (7): 1538–44.
17. Bassil S. Changes in endometrial thickness, width, length and pattern in predicting pregnancy outcome during ovarian stimulation in in vitro fertilization. Ultrasound Obstet Gynecol. 2001 Sep; 18 (3): 258–63.
18. Mayra PR, Rosalina VL, López G, Iruretagoyena J, Magness R. Regulation of uterine blood flow. I. Functions of estrogen and estrogen receptor α/β in the uterine vascular endothelium during pregnancy. Rev Chil Obstet Ginecol. 2014; 79 (2): 129–39.

Литература

1. Аншина М. Б., Исакова Э. В., Калинина Е. Анат., Калинина Е. Андр., Корсак В. С., Краснопольская К. В. и др. Применение эстрогенов в программах ВРТ. Научно-практические рекомендации. М.: Российская ассоциация репродукции человека. 2015, 80 с.
2. Назаренко Т. А, Краснопольская К. В. «Бедный ответ». Тактика ведения пациенток со сниженной реакцией на стимуляцию гонадотропинами в программах ЭКО. М.: МЕДпресс-информ; 2013, 80 с.
3. Корсак В. С., Смирнова А. А., Шурыгина О. В. ВРТ в России. Отчет за 2013 г. Проблемы репродукции. 2015; 21 (6): 17–19.
4. Mishra VV, Agarwal R, Sharma U, Aggarwal R, Choudhary S, Bandwal P. Endometrial and Subendometrial Vascularity by Three-Dimensional (3D) Power Doppler and Its Correlation with Pregnancy Outcome in Frozen Embryo Transfer (FET) Cycles. J of Obstetrics and Gynaecology of India. 2016; 66 (Suppl 1): 521–527. DOI: 10.1007/s13224-016-0871-5.
5. Jianing Wang, Fei Xia, Ying Zhou, Xuedong Wei, Yanyan Zhuang, Yingxue Huang. Association Between Endometrial/Subendometrial Vasculature and Embryo Transfer Outcome: A Meta-analysis and Subgroup Analysis. J Ultrasound Med. 2018 Jan; 37 (1): 149-163. DOI: 10.1002/jum.14319. Epub 2017 Jul 17.
6. Lecce G, Meduri G, Ancelin M. Presence of estrogen receptor bin the human endometrium through the cycle: expression inglandular, stromal, and vascular cells // J Clin Endocrinol. Metab. 2001; 86: 1379–86.
7. Amir W, Micha B, Ariel H, Liat LG, Jehoshua D, Adrian S. Predicting factors for endometrial thickness during treatment with assisted reproductive technology. Fertil Steril 2007; 87 (4): 799–804.
8. Kalmantis K, Loutradis D, Lymperopoulos E, Beretsos P, Bletsa R, Antsaklis A. Three Dimensional Power Doppler evaluation of human endometrium after administration of oxytocine receptor antagonist (OTRa) in an IVF program., Arch Gynecol Obstet. 2012 Jan; 285 (1): 265–70. DOI: 10.1007/s00404-011-2019-2. Epub 2011 Aug 7.
9. Prasad S, Goyal R, Kumar Y, et al. The Relationship Between Uterine Artery two-dimensional Color Doppler Measurement and Pregnancy Outcome: A Prospective Observational Study. Journal of Reproduction & Infertility. 2017; 18 (2): 251–6.
10. Крылова Ю. С, Кветной И. М., Айламазян Э. К. Рецептивность эндометрия: молекулярные механизмы регуляции имплантации. Журнал акушерства и женских болезней. 2013; 62 (2): 63–74. DOI: http://dx.doi.org/10.17816/JOWD62263-74.
11. Озерская И. А. Атлас гинекологической ультразвуковой нормы. М.: Видар-М; 2010. 225 с.
12. Ari Kim, Hyuk Jung, Won June Choi, Sung Nam Hong, Heung Yeol Kim. Detection of endometrial and subendometrial vasculature on the day of embryo transfer and prediction of pregnancy during fresh in vitro fertilization cycles Taiwanese. Journal of Obstetrics & Gynecology. 2014; 53 (3): 360–5.
13. Краснопольская К. В., Назаренко Т. А., Сесина Н. И., Ершова И. Ю., Александрова В. Р. Результаты программ ЭКО с донорскими ооцитами у пациенток с ультразвуковыми признаками "тонкого" эндометрия. Медицинский алфавит. М.: Альфмед. 2017; 1 (12) (309) : 34–8.

14. Kasius A, Smit JG, Torrance HL et al. Endometrial thickness and pregnancy rates after IVF: a systematic review and meta-analysis. Hum Reprod Update. 2014; 20 (4): 530–41.
15. Weiss NS, van Vliet MN, Limpens J, Hompes PGA et al. Endometrial thickness in women undergoing IUI with ovarian stimulation. How thick is too thin? A systematic review and meta-analysis. Hum Reprod Update. 2017; 32 (5): 1009–18.
16. Jayaprakasan K, Hopkisson JF, Campbell BK, Clewes J, Johnson IR, Raine-Fenning NJ. Quantification of the effect of pituitary down-regulation on 3D ultrasound predictors of ovarian response. Human Reproduction. 2008; 23 (7): 1538–44.
17. Bassil S. Changes in endometrial thickness, width, length and pattern in predicting pregnancy outcome during ovarian stimulation in in vitro fertilization. Ultrasound Obstet Gynecol. 2001 Sep; 18 (3): 258–63.
18. Mayra PR, Rosalina VL, López G, Iruretagoyena J, Magness R. Regulation of uterine blood flow. I. Functions of estrogen and estrogen receptor α/β in the uterine vascular endothelium during pregnancy. Rev Chil Obstet Ginecol. 2014; 79 (2): 129–39.

NON-THERMAL ATMOSPHERIC-PRESSURE PLASMA IN THE ANTI-AGE THERAPY OF FACIAL SKIN

Shemshuk MI[1], Korotky VN[1]✉, Serov DN[2], Kochetkov MA[2], Stenko AG[3], Korotky NG[1]

[1] Department of Dermatology and Venerology, Pirogov Russian National Research Medical University, Moscow

[2] Moscow Research and Medical Center of Dermatology and Cosmetology, Moscow

[3] Institute of Plastic Surgery and Cosmetology, Moscow

Traditionally, anti-age therapies employ ultraviolet radiation and exposure to ozone, nitric oxide and electromagnetic fields. Non-thermal atmospheric-pressure plasma (NTAPP) combines the effects of all those techniques. The aim of our study was to assess the feasibility of low-dose NTAPP application in anti-age facial skin therapy. Ten female patients aged 50 to 55 years were examined and three facial zones were chosen for the experiment: the T-zone (the central part of the forehead) and the "crow's feet" areas on the right and left sides of the face. Ultrasonography was performed on the DUB SkinScaner before the treatment course and 24 hours after the last treatment. Cleansed skin was exposed to a low-energy NTAPP helium jet generated by the HELIOS system (Plasma Research and Production, Russia). Exposure time was 5 min per zone. Each participant received 10 NTAPP procedures on alternate days. Before therapy, the skin condition in all participants fitted into morphotype 3. Ultrasonography of the studied zones revealed a considerable deformation of the skin surface, a thickening of the epidermis with a distinct border between the epidermis and the dermis, a slight thinning of the dermis, its relatively homogenous echogenicity, and a blurred border between the dermis and the hypodermis. After the course was completed, all patients demonstrated an evener skin surface, reduced epidermal thickness and reduced acoustic density of the epidermis and the dermis; the dermis tended to have above average thickness. The most significant changes were observed for the wrinkles: they became less pronounced in the "crow's feet" area. Exposure to NTAPP caused the epidermal corneum to diminish in thickness; it also stimulated microcirculation and improved the condition of the hydrolipidic film, all of which ultimately led to the effacement of wrinkles. Treatment produced no adverse effects on the skin or its appendages.

Keywords: skin aging, non-thermal atmospheric-pressure plasma, wrinkles

✉ **Correspondence should be addressed:** Vladimir Korotky
Leninsky 117, bl. 6, Moscow, 119571; vkbknk@gmail.com

Received: 15.03.18 **Accepted:** 22.03.18

DOI: 10.24075/brsmu.2018.018

НИЗКОТЕМПЕРАТУРНАЯ АТМОСФЕРНАЯ ПЛАЗМА В КОРРЕКЦИИ ВОЗРАСТНЫХ ИЗМЕНЕНИЙ КОЖИ ЛИЦА

М. И. Шемшук[1], В. Н. Короткий[1]✉, Д. Н. Серов[2], М. А. Кочетков[2], А. Г. Стенько[3], Н. Г. Короткий[1]

[1] Кафедра дерматовенерологии, Российский национальный исследовательский медицинский университет им. Н. И. Пирогова, Москва

[2] Московский научно-практический центр дерматологии и косметологии, Москва

[3] Институт пластической хирургии и косметологии, Москва

В антивозрастной терапии кожи лица стандартно используют ультрафиолетовое облучение, обработку поверхности кожи озоном и оксидом азота и воздействие электромагнитным полем. Низкотемпературная атмосферная плазма (НТП) способна оказать все эти воздействия. Целью работы было оценить эффективность НТП низкой интенсивности в качестве антивозрастной терапии кожи лица. Десяти пациенткам в возрасте 50–55 лет проводили исследование состояния кожи лица (Т-зону (центр лба), области «гусиных лапок» справа и слева) на аппарате DUB SkinScaner до начала применения НТП и через сутки после 10 процедур. После очищения кожи ее обработали НТП низкой интенсивности, которую генерировали в среде гелия в виде плазменного факела на приборе «ГЕЛИОС» («НПЦ Плазма», Россия). Время экспозиции НТП составило 5 мин на каждую зону, процедуры проводили через день. До лечения состояние кожи лица всех участниц соответствовало третьему морфотипу инволюционных изменений. Ультразвуковое исследование (УЗИ) всех зон показало значительную деформацию микрорельефа, утолщение эпидермиса при сохранении четкой границы эпидермиса и дермы, некоторое снижение толщины дермы с однородной эхоструктурой, смазанное отграничение дермы от гиподермы. После завершения курса у всех пациенток отмечено уменьшение деформации микрорельефа, средней толщины эпидермиса и ультразвуковой плотности эпидермиса и дермы, тенденция к увеличению средней толщины дермы. Наибольшие изменения коснулись морщин: наблюдалось их сглаживание в области «гусиных лапок». Таким образом, использование НТП вызвало уменьшение толщины рогового слоя эпидермиса, улучшение микроциркуляции и улучшение качества гидролипидной мантии кожи, что сопровождалось сглаживанием морщин. Нежелательных явлений со стороны кожного покрова и придатков кожи не было отмечено.

Ключевые слова: возрастные изменения кожи, низкотемпературная атмосферная плазма, морщины

✉ **Для корреспонденции:** Владимир Николаевич Короткий
Ленинский пр-т, д. 117, корп. 6, г. Москва, 119571; vkbknk@gmail.com

Статья получена: 15.03.18 **Статья принята к печати:** 22.03.18

DOI: 10.24075/vrgmu.2018.018

Skin aging is the first visible sign of changes occurring in the body as it grows old. There are two types of aging: chronological (intrinsic) and sun-induced (extrinsic, also called photoaging) [1]. Typical features of chronological aging include a 10% to 50% loss of the epidermal thickness, atrophy of the prickle cell layer, shrinking and flattening of basal cells, decreased mitotic activity of basal keratinocytes, slow lipid renewal, flattening of the dermal-epidermal junction, and progressive loss of melanocytes, Langerhans cells and melanocyte heterogeneity. Dermal fibroblasts of the aging skin become less abundant, the extracellular matrix atrophies, collagen and elastic fibers degrade and shrink, and amyloids deposit. Such involution causes skin deformation and wrinkles. The second type of aging, photoaging, is an inevitable result of skin exposure to the hostile environment that causes skin withering. Its symptoms can be noticed long before the first wrinkles appear. Morphological and functional signs of photoaging are traditionally categorized into dermal and epidermal. Visible manifestations of photoaging include telangiectasias and pigment spots (lentigines).

The main differences between photoaging and intrinsic aging include epidermal thickening caused by the thickening of the stratum corneum and accumulation of atypical amorphous elastin in the dermal extracellular matrix. However, in photoaging the dermis retains its ability to synthesize collagen and other components of the extracellular matrix; therefore, some of its manifestations can be reversed.

Visible signs of aging vary and can be grouped into five morphological types [2]:

• morphotype 1 referred to as “the tired face”; the face looks puffy, with drooping mouth corners;

• morphotype 2 known as “the wrinkled face”; it is characterized by the pronounced wrinkles around the eyes (“crow’s feet”) and on the upper and lower eyelids; vertical upper lip wrinkles are also visible;

• morphotype 3, which refers to age-related facial and neck deformities, namely excess skin on the upper and lower eyelids, sagging cheeks, and a double chin;

• morphotype 4 is the combined type; it brings together the age-related changes mentioned above, lack of skin firmness, deep wrinkles, and overall skin deformation;

• morphotype 5 is the muscular type characterized by the folds on the lower and upper eyelids, pronounced expression wrinkles, and loss of facial contours; this type is most often seen in Asian and Japanese people who have well developed facial muscles and not so much subcutaneous fat.

As we grow older, our skin becomes thinner and paler, loses its elasticity and firmness, and the texture of its surface changes. Age affects all skin layers, including the epidermis, the dermis, and the subcutis. In young people these layers are visually distinct; dermal papillae create a very clear pattern showing on the epidermis, the dermis is firm, the subcutaneous tissue is well-pronounced [2]. As we age, the skin thins out and loses its well-defined structure [2]. The pattern on the skin surface fades out and the interface contact between the epidermis and the dermis shrinks in size [2]. The fibrous support of the dermis becomes lax, the signs of edema are observed [2]. Wrinkles start to show. The subcutaneous tissue looks fibrotic and the border between the subcutis and the dermis becomes very blurred.

Skin aging is an issue for many patients and a challenge for a cosmetic dermatologist. Treatments invented to combat skin aging are abounding and based on the use of special cosmetic products, chemical peeling and other non-surgical procedures used alone or in combination [3–5]. All of them serve to restore the hydrolipidic film of the skin, maintain adequate water content in the epidermis and dermis, and improve microcirculation in all skin layers, promoting synthesis of collagen fibers [3]. However, these therapies often have unpleasant or even severe adverse effects. Treatments for the aging face, neck or décolleté area may provoke allergies [5]; chemical peelings can cause skin flaking, edema and/or pigmentation of the treated areas [5]; laser treatments, electrical stimulation or the like may result in demarcation lines, hyper- or hypopigmentation, scarring, thermal burns, pain, loss of skin tone, or electric injury [6]. Therefore, the search for effective and safe treatments against skin aging is still ongoing. So far, a number of experiments have shown that low-dose non-thermal atmospheric-pressure plasma (NTAPP) can improve tissue nutrition and the ability of skin to rejuvenate [7–10].

NTAPP is a novel noninvasive method that combines the effects of ultraviolet light and exposure to ozone, nitric oxide, and the electromagnetic field [8–12]. In its essence, plasma is a partially or fully ionized gas, the so-called fourth state of matter. NTAPP is generated when the electromagnetic field is applied to the gas at atmospheric pressure. When the field is strong enough, gas molecules start releasing electrons, turning into gas ions. Free electrons are accelerated by the electromagnetic field and move to the anode colliding with gas molecules, generating more gas ions and more free electrons (ionization by collision). The process goes on and on, resulting in the generation of plasma. Plasma properties are determined not only by the electromagnetic field, but also by gas pressure, gas type and the radiation source geometry [12, 13]. Conveniently, NTAPP lacks the main drawback of other therapies: high concentrations of toxic chemicals.

The main components of NTAPP are electrons, ions, free radicals, and light [13]. Free radicals are particularly important for cell and tissue physiology. Reactive oxygen and nitrogen species have a crucial role in cellular health and pathology [14–16]. In the recent decade new devices have been invented for NTAPP production [17, 18]. NTAPP’s direct effects on lipids, proteins, and nucleic acids of living cells, as well as its indirect impact on signaling pathways, are well studied [15, 19].

Recently, NTAPP has been introduced into regenerative medicine. Low-dose NTAPP stimulates cell growth and proliferation, while high-dose NTAPP is capable of inducing apoptosis or necrosis, confirming the dose-dependent effect of oxidative stress [13, 20, 22]. Studies of the effects of different NTAPP energies applied to mammalian cells have demonstrated that low doses (under 0.2 J/cm^2) stimulate cell proliferation, medium doses (0.2 to 0.6 J/cm^2) do not have any effect on mammalian cells, whereas high doses (over 0.6 J/ cm^2) induce apoptosis [19, 22]. Multiple *ex vivo* and *in vivo* experiments described in the literature prove antiseptic [22–28] and wound-healing [9, 10, 29, 30] effects of NTAPP. High-dose NTAPP has found its application in cancer treatment [20, 31] and is employed to fight pathogens [21–28]. Low-dose NTAPP is used in regenerative medicine [9, 10, 20, 29, 30].

In the present work we study the feasibility of low-dose NTAPP for improving the condition of aging facial skin.

METHODS

The study was conducted in September through November 2017 at the Department of Dermatology and Venerology (Pirogov Russian National Medical Research University) in 10 healthy female volunteers aged 50 to 55 years who gave informed consent to participate. The study was approved by the independent ethics committee (Protocol 2 dated February 8, 2017) and the Academic Council of the Research

and Medical Center of Dermatology and Cosmetology of the Department of Healthcare, Moscow (Protocol 3 dated March 2, 2017). The study included only females between 50 and 55 years of age without facial inflammation or infection and normal sugar levels. Females who had facial inflammation or infection, diabetes mellitus, chronic kidney or liver diseases, vasculitis or decompensated cardiovascular diseases and those who had undergone a previous anti-age therapy less than 3 months before the study were excluded.

All study participants had their facial skin examined; 3 facial zones were selected for the experiment: zone 1, or the T-zone, covered the central part of the forehead; zone 2 included the "crow's feet" area on the right side of the face; zone 3, "crow's feet" on the left. We used the DUB SkinScaner (Digital Ultraschall Bildisystem, Germany) equipped with two 22 MHz and 75 MHz applicators with an axial resolution of 72 μm and 21 μm, respectively; the applicator with 75 MHz center frequency (frequency range of 65 MHz to 85 MHz) was used. The participants were examined twice: before NTAPP therapy was started and 24 hours after the last treatment. A standard ultrasound conductive gel was used for ultrasound examinations. The obtained data were interpreted and analyzed using the original software for the DUB SkinScaner according to the manufacturer's guidelines. Ultrasound examinations were performed at room temperature, with the patients lying in the supine position. We measured the average thickness of the epidermis and the dermis, the acoustic density of the epidermis and the dermis, assessed the microtopography of the skin (length of the epidermal external surface contour), calculated the index of epidermal deformation and the coefficient of acoustic density distribution in the dermis (ADDD), i.e. the ratio of the acoustic density of lower dermal layers to the acoustic density of upper dermal layers; the reference interval for the coefficient ranged from 0.75 to 1.70 units [33, 34].

After cleansing the face was exposed to the non-thermal atmospheric pressure helium plasma jet (HELIOS, Plasma Research and Production, Russia; see Fig. 1). Helium, the inert gas, was released from the tank at 1.5 l/min on the rotameter scale at moderate jet intensity. Exposure time was 10 min for the "crow's feet" areas and 5 min for the T-zone (the region of the procerus muscle). Every participant received 10 procedures in total with a one-day interval between successive procedures.

RESULTS

Before the experiment all participants were ascribed to morphotype 3 based on their skin condition (puffy face, drooping mouth corners, pronounced "crow's feet", wrinkles on the upper and lower eyelids, vertical lip wrinkles, excess skin on the upper and lower eyelids); one participant had a deep furrow between the brows. Figures 2A and 3A show photos of the participants with typical signs of skin aging.

The ultrasound examination (Table 1) revealed a considerable deformation of the skin surface in all participants, a thickening of the epidermis with a distinct border between the epidermis and the dermis, a slight thinning of the dermis, its relatively homogenous echogenicity, and a blurred border between the dermis and the hypodermis. In one case (a 50-year-old female) a deep wrinkle was observed in the T-zone (width of 2, 867 μm, depth of 250 μm; see Fig. 2A).

After completing the procedures, we observed improvements of skin condition in all participants (Table 1, Fig. 2B and 3B). Epidermal deformation decreased by 35% in the T-zone, by 58% and 30% in the "crow's feet" area on the right and left sides of the face, respectively. Average thickness of the epidermis decreased by 13.3%, 5.0% and 6.3%, respectively. The acoustic density of the epidermis was 20% in the T-zone, 46.6% and 35.6%, respectively, in the "crow's feet" areas on the right and left sides of the face, demonstrating improved epidermal nutrition. Positive changes were also observed for the dermis. Its average thickness increased in the T-zone by 6%, in the "crow's feet" area by 1.2% and 2.7% on the right and left sides, respectively. The acoustic density of the dermis decreased by 37.7%, 20.6% and 52.2%, respectively. The observed changes indicate better nutrition and better tissue hydration. On the whole, the skin structure in the studied zones became considerably healthier, which was confirmed by the increase in the ADDD value by 27.1%, 11.9% and 30.3%, respectively. The deep wrinkle between the eyebrows in one of the participants became narrower, though its depth remained unchanged (Fig. 2B).

The most pronounced changes were observed for the microtopography of the skin surface in the "crow's feet" area: the skin became smother, and the wrinkles shallower.

DISCUSSION

It is known that exposure to NTAPP induces production of reactive oxygen and nitrogen species, UV-protons, electrons and ions [32]. Experiments have demonstrated improved skin microcirculation and, therefore, better hydration and activation of collagen synthesis after exposure to low-dose NTAPP [33–35]. In another study conducted in healthy male and female volunteers over 18 years of age, changes in microcirculation and the lowering of skin pH depended on the duration of exposure to NTAPP [36]. It has been shown that nitric oxide generated by low-dose NTAPP triggers β-catenin activation by epidermal cells, stimulating the renewal of the epidermis [37].

For normal epidermal function, proliferation of keratinocytes and their apoptosis (programmed cell death) need to be well balanced. Repeated exposure to NTAPP helps to achieve normal epidermal thickness and better regeneration [37]. At present NTAPP is used for microbial decontamination; it is also employed to promote wound or venous ulcer healing. Currently, the feasibility of NTAPP application in regenerative medicine is being explored. Our study proves that NTAPP is safe for the skin. We have shown that after 10 procedures of facial skin exposure to NTAPP, epidermal acoustic density decreases significantly, suggesting the loss of excess corneum thickness, better microcirculation and improved quality of the hydrolipidic film. Our findings are consistent with the published experimental data [7, 12, 17, 33, 34]. Decreased acoustic density of the dermis can be the result of good hydration of deep

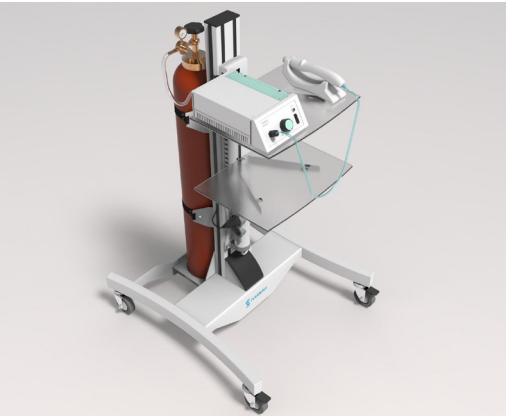

Fig. 1. Low-dose non-thermal atmospheric-pressure helium plasma jet generator (HELIOS, Plasma Research and Production, Russia)

Table 1. Ultrasonography of different facial skin zones before and after exposure to NTAPP (M±σ)

Parameter	Before exposure to NTAPP			After exposure to NTAPP		
	Zone 1	Zone 2	Zone 3	Zone 1	Zone 2	Zone 3
Microtopography, mm	13.2 ± 0.1	13.2 ± 0.3	13.1 ± 0.2	13.1 ± 0.1	12.9 ± 0.08	13.02 ± 0.13
Epidermal deformation, un.	0.416 ± 0.07	0.43 ± 0.26	0.33 ± 0.18	0.27 ± 0.09*	0.18 ± 0.08*	0.23 ± 0.13*
Epidermal thickness, μm	72.9 ± 12.3	64.3 ± 10.0	65.1 ± 7.8	63.3 ± 8.2*	61.1 ± 8.7*	61.0 ± 9.8*
Acoustic density of the epidermis, un.	142.1 ± 12.8	106.6 ± 7.2	125.6 ± 28.7	113.7 ± 24.0*	56.9 ± 21.0*	82.1 ± 33.7*
Dermal thickness, μm	1521.6 ± 249.8	1313.4 ± 121.1	1292.4 ± 106.1	1612.4 ± 168.0*	1329.1 ± 136.4*	1326.4 ± 92.4*
Acoustic density of the dermis, un.	11.4 ± 6.7	19.9 ± 14.6	20.7 ± 10.8	7.1 ± 4.7	15.8 ± 14.8	9.9 ± 5.1
ADDD	0.70 ± 0.11	1.09 ± 0.16	0.944 ± 0.191	0.89 ± 0.14*	1.22 ± 0.18*	1.23 ± 0.28*

Note: ADDD is distribution of acoustic density in the dermis; * shows statistically significant differences between the parameters before and after exposure to NTAPP ($p < 0.05$).

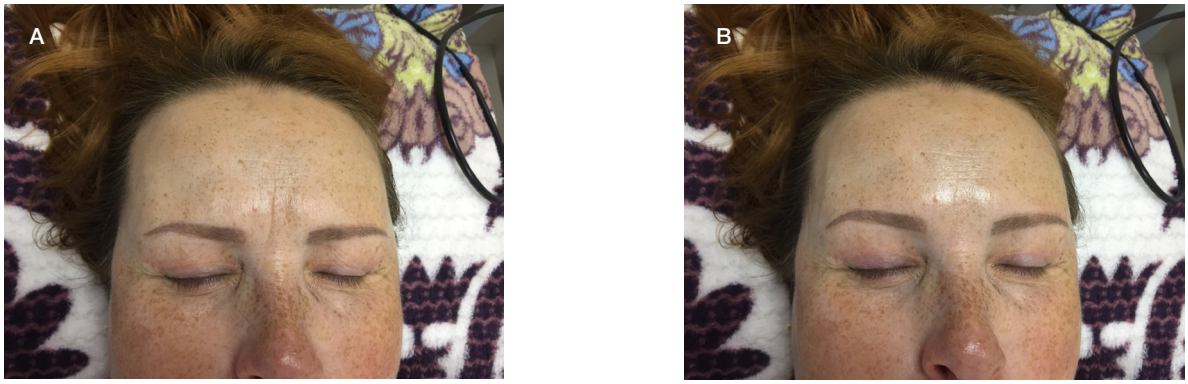

Fig. 2. The area between the eyebrows before (**A**) and after 10 procedures of exposure to NTAPP (**B**)

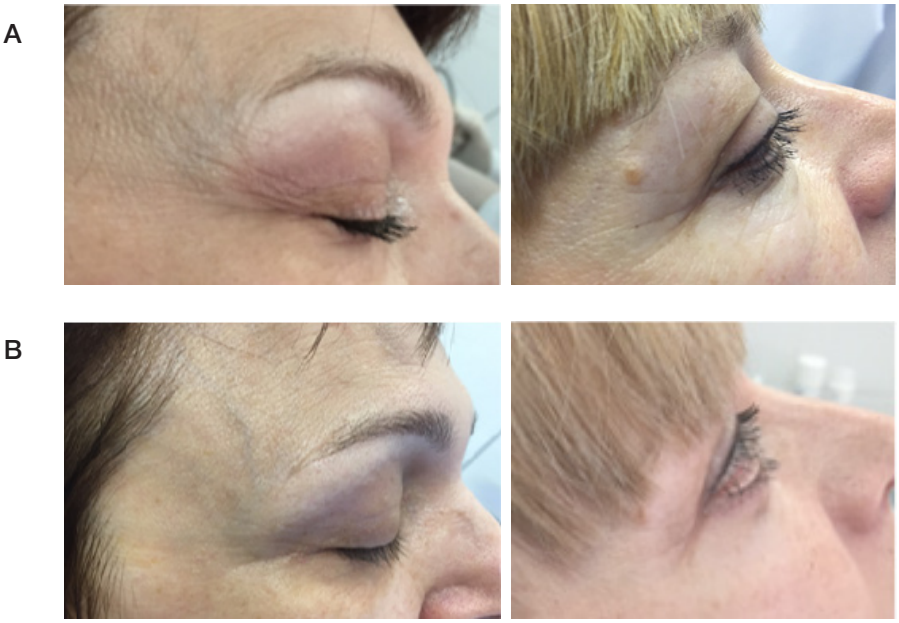

Fig. 3. The "crow's feet" area before (**A**) and after 10 procedures of exposure to NTAPP (**B**)

skin structures. The structural changes in the skin following the treatment course demonstrate the anti-age effect of NTAPP. All study participants noticed changes in their skin appearance (fewer and shallower wrinkles in the areas of interest). It is still unclear, though, how many procedures need to be performed and at what interval in order to achieve the best possible effect. Perhaps, structural improvements would have been more pronounced if the number of exposures had been higher. This question requires further investigation.

CONCLUSION

Exposure to low-dose NTAPP can significantly improve the condition of the epidermis, smoothing out the wrinkles that negatively affect women's emotional state. No adverse effects on the skin or its appendages have been observed. Further clinical studies of NTAPP application in cosmetology are necessary to perfect the technique and define the optimal duration of the treatment course for the best anti-age effect.

References

1. Zouboulis C, Makrantonaki E. Clinical aspect and molecular diagnostics of skin aging. Clinics in dermatology, 2011; 29: 3–14.
2. Borhunova EN, Taganov FV. Novaya kosmetologia. Mikroskopicheskoe izmenenie koghi pri starenii. M.: ID "Kosmetica i meditsina", 2017; s. 74–102.
3. Asher B. Kosmetologicheskie protseduri v oblasti litsa. In'ektsionnie metody v kosmetologii. Izd. «MEDpress-Inform», 2014; s. 179–215.
4. Trufanov VD, Kogan EA, Yutskovskaya JaA, Faizulina NM, Ivanov SYu. Radiovolni visokoy chastoti – innovatsionnii podhod k korrektsii vozrastnih izmenenii koghi; klinicheskoe, immunogistohimicheskoe issledovanie. STM. 2016; 8 (1); 106–16.
5. Margolina A, Aernandes E. Novaya kosmetologiya. M.: ID «Kosmetika i meditsina», 2015.
6. Saromitskaya AN. Sochetannoe primenenie fraktsionirovannogo fototermoliza i botylinoterapii v korrektsii gipertroficheskih i keloidnih rubtsovyh deformatsij koghi. M.: ID «Kosmetica i meditsina», 2016; s. 278–86.
7. Heinlin J, Morfill G, Landthaler M, Stolz W, Isbary G, Zimmermann J, Shimizu T, Karrer S. Plasma medicine: possible applications in dermatology. JDDG. 2010; 12: 968–976.
8. Okazaki Y, Wang Y, Tanaka H, et al. Direct exposure of non-equilibrium atmospheric pressure plasma confers simultaneous oxidative and ultraviolet modifications in biomolecules. J Clin Biochem Nutr. 2014; 55: 207–15.
9. Brehmer F, Haenssle HA, Daeschlein G, Ahmed R, Pfeiffer S, Gorlitz A, et al. Alleviation of chronic venous leg ulcers with a hand-held dielectric barrier discharge plasma generator (PlasmaDerm(®) VU-2010): results of monocentric, two-armed, open, prospective, randomized and controlled trial (NCTO1415622). J Eur Acad Dermatol Venereol. 2015; 29(1): 148–55.
10. Haertel B, von Woedtke Th, Weltmann K-D, Lindequist U. Non-Thermal Atmospheric-Pressure Plasma Possible Application in Wound Healing. Biol Therapeutics. 2014; 22: 477–90.
11. Akishev Y. Atmospheric pressure non-thermal plasma sterilization of microorganisms in liquids and on the surfaces. Pure and Applied Chemistry. 2008; 80 (9): 1953–69.
12. Laroussi M, Kong M, Morfill G, Stolz W (eds). Plasma medicine: application of low-temperature gas plasmas in medicine and biology. Cambridge University Press, 2012.
13. Korotky VN. Nizkotemperaturnaya atmosfernaya plasma v dermatologii. Klinicheskaya dermatologiya i venerologiya. 2017; 16 (5): 4–11.
14. Toyokuni S. The origin and future of oxidative stress pathology: from the recognition of carcinogenesis as an iron addiction with ferroptosis-resistance to non-thermal plasma therapy. Pathol Int. 2016; 66: 245–59.
15. Hybertson BM, Gao B, Bose SK, McCord JM. Oxidative stress in health and disease: the therapeutic potential of Nrf2 activation. Mol Aspects Med 2011; 32: 234–46.
16. Uttara B, Singh AV, Zamboni P, Mahajan RT. Oxidative stress and neurodegenerative diseases: a review of upstream and downstream antioxidant therapeutic options. Curr Neuropharmacol. 2009; 7: 65–74.
17. Yousfi M, Merbahi N, Pathak A, Eichwald O. Low-temperature plasmas at atmospheric pressure: toward new pharmaceutical treatments in medicine. Fundamental & Clinical Pharmacology. 2014; 28: 123–35.
18. Kalghatgi S, Friedman G, Fridman A, Clyne AM. Endothelial cell proliferation is enhanced by low dose non-thermal plasma through fibroblast growth factor-2 release. Ann Biomed Eng. 2010; 38: 748–57.
19. Kalghatgi S, Kelly CM, Cerchar E, Torabi B, Alekseev O, Fridman A, et al. Effects of non-thermal plasma on mammalian cells. PLoS ONE. 2011; 6: e16270.
20. Moureau M, Orange N, Feuilloley MGL. Non-thermal plasma technologies: new tools for bio-decontamination. Biotechnol Adv. 2008; 26: 610–17.
21. Shimizu T, Zimmermann JL, Morfill GE. The bactericidal effect of surface micro-discharge plasma under different ambient conditions. New Journal of Physics 2011; 13: 1–7.
22. Ermolaeva SA, Varfolomeev AF, Chernukha MY, Yurov DS, Vasiliev MM, Kaminskaya AA, et al. Bactericidal effects of non-thermal argon plasma in vitro, in biofilms and in the animal model of infected wounds. J Med Microbiol. 2011; 60: 75–83.
23. Ehlbeck J, Schnabel U, Polak M, Winter J, von Woedtke Th, Brandenburg R, et al. Low temperature atmospheric pressure plasma sources for microbial decontamination. J Phys D: Appl Phys. 2011; 44: 013002.
24. Lademann O, Kramer A, Richter H, Patzelt A, Meinke MC, et al. Skin disinfection by plasma-tissue interaction: comparison of the effectivity of tissue-tolerable plasma and a standard antiseptic. Skin Pharmacol Physiol. 2011; 24: 284–88.
25. Maisch T, Shimizu T, Li Y-F, Heinlin J, Karrer S, Morfill G, et al. Decolonisation of MRSA, S. aures and E. Coli by cold-atmospheric plasma using a porcine skin model in vitro. PLoS ONE. 2012; 7: e34610.
26. Daeschlein G, Scholz S, Emmert S, von Podewils S, Haase H, von Woedtke Th. Plasma medicine in dermatology: basic antimicrobial efficacy testing as prerequisite to clinical plasma therapy. Plasma Med. 2012; 2 (1–3): 33–69.
27. Daeschlein G, Napp M, von Podewils S, Lutze S, Emmert S., Lange A, et al. In vitro susceptibility of multidrug resistant skin and wound pathogens against low temperature atmospheric pressure plasma jet (APPJ) and dielectric barrier discharge plasma (DBD). Plasma Process Polymers. 2014; 11: 175–183.
28. Bekeschus S, Masur K, Kolata J, Wende K, Schmidt A, Bundscherer L, et al. Human mononuclear cell survival and proliferation is modulated by cold atmospheric plasma jet. Plasma Process Polym. 2013; 10: 706–13.
29. Korotky VN. Vozmoghnosti primenenija kholodnoy amosernoy plazmy v onkologii (obzor literatury). Sibirskiy onkologicheskiy ghurnal. 2018; 17 (1): 72–81.
30. Bezuglii AP, Bikbulatova NN, Shuginina EA, Belkov PA, Habutdinova NR. Ul'trazvukovoe issledovanie koghi v praktike vracha-kosmetologa. Vestnik Dermatologii I venerologii. 2011; 3: 142–152.
31. Bezuglii AP, Potekaev NN, Sapoghnikova YuA. Ul'trazvukovoe skanirovanie visokogo razresheniya v dermatologii i meditsinskoi kosmetologii. Eksperimental'naya i klinicheskaya dermatovenerologiya. 2014; 2: 20–25.
32. Bibinov N, Knake N, Bahre H, Awakowicz P, von der Gathen VS. Spectroscopic characterization of an atmospheric pressure μ-jet plasma source. J Phys D: Appl Phys. 2011; 44 (34): 345204.
33. Heuer K, Hoffmanns MA, Demir E, Baldus S, Volkmar CM, Röhle M, et al. The topical use of non-thermal dielectric barrier discharge (DBD): nitric oxide related effects on human skin. Nitric Oxide. 2015; 44: 52–60.
34. Kisch T, Helmke A, Schleusser S, Song J, Liodaki E, Stang FH, Mailaender P, Kraemer R. Improvement of cutaneous microcirculation by cold atmospheric plasma (CAP): results of a controlled, prospective cohort study. Microvasc Res. 2016; 104: 55–62.
35. Kisch T, Schleusser S, Helmke A, Mauss KL, Wenzel ET, Hasemann B, et al. The repetitive use of non-thermal dielectric barrier discharge plasma boosts cutaneous micro- circulatory effects. Microvasc Res. 2016; 106: 8–13.
36. Borchardt T, Ernst J, Helmke A, Tanyeli M, Schilling AF, Felmerer G, et al. Effect of direct cold atmospheric plasma (diCAP) on microcirculation of intact skin in a controlled mechanical environment. Microcirculation. 2017; 24: e12399.
37. Blanpain C, Fuchs E. Epidermal homeostasis: a balancing act of stem cells in the skin. Nat Rev Mol Cell Biol. 2009; 10: 207–17.

Литература

1. Zouboulis C, Makrantonaki E. Clinical aspect and molecular diagnostics of skin aging. Clinics in dermatology, 2011; 29: 3–14.
2. Борхунова Е. Н., Таганов А. В. Новая косметология. Микроскопические изменения кожи при старении. М.: ИД «Косметика и медицина», 2017. с. 74–102.
3. Ашер Б. Косметологические процедуры в области лица. Иньекционные методы в косметологии. М.: Изд. «МЕДпресс-Информ», 2014; с. 179–215.
4. Труфанов В. Д., Коган Е. А., Юцковская Я. А., Файзулина Н. М., Иванов С. Ю. Радиоволны высокой частоты — инновационный подход к коррекции возрастных изменений кожи; клиническое, иммуногистохимическое исследование. СТМ. 2016; 8 (1): 106–16.
5. Марголина А., Эрнандес Е.. Новая косметология. М.: ИД «Косметика и медицина», 2015.
6. Саромыцкая А. Н.. Сочетанное применение фракционного фототермолиза и ботулинотерапии в коррекции гипертрофических и келоидных рубцовых деформаций кожи. М.: ИД «Косметика и медицина», 2016; с. 278–86.
7. Heinlin J, Morfill G, Landthaler M, Stolz W, Isbary G, Zimmermann J, Shimizu T, Karrer S. Plasma medicine: possible applications in dermatology. JDDG. 2010; 12: 968–76.
8. Okazaki Y, Wang Y, Tanaka H, et al. Direct exposure of non-equilibrium atmospheric pressure plasma confers simultaneous oxidative and ultraviolet modifications in biomolecules. J Clin Biochem Nutr. 2014; 55: 207–15.
9. Brehmer F, Haenssle HA, Daeschlein G, Ahmed R, Pfeiffer S, Gorlitz A, et al. Alleviation of chronic venous leg ulcers with a hand-held dielectric barrier discharge plasma generator (PlasmaDerm(®) VU-2010): results of monocentric, two-armed, open, prospective, randomized and controlled trial (NCTO1415622). J Eur Acad Dermatol Venereol. 2015; 29(1): 148–55.
10. Haertel B, von Woedtke Th, Weltmann K-D, Lindequist U. Non-Thermal Atmospheric-Pressure Plasma Possible Application in Wound Healing. Biol Therapeutics. 2014; 22: 477–90.
11. Akishev Y. Atmospheric pressure non-thermal plasma sterilization of microorganisms in liquids and on the surfaces. Pure and Applied Chemistry. 2008; 80 (9): 1953–69.
12. Laroussi M, Kong M, Morfill G, Stolz W (eds). Plasma medicine: application of low-temperature gas plasmas in medicine and biology. Cambridge University Press, 2012.
13. Короткий В. Н. Низкотемпературная атмосферная плазма в дерматологии. Клиническая дерматология и венерология. 2017; 16 (5): 4-11.
14. Toyokuni S. The origin and future of oxidative stress pathology: from the recognition of carcinogenesis as an iron addiction with ferroptosis-resistance to non-thermal plasma therapy. Pathol Int. 2016; 66: 245–59.
15. Hybertson BM, Gao B, Bose SK, McCord JM. Oxidative stress in health and disease: the therapeutic potential of Nrf2 activation. Mol Aspects Med 2011; 32: 234–46.
16. Uttara B, Singh AV, Zamboni P, Mahajan RT. Oxidative stress and neurodegenerative diseases: a review of upstream and downstream antioxidant therapeutic options. Curr Neuropharmacol. 2009; 7: 65–74.
17. Yousfi M, Merbahi N, Pathak A, Eichwald O. Low-temperature plasmas at atmospheric pressure: toward new pharmaceutical treatments in medicine. Fundamental & Clinical Pharmacology. 2014; 28: 123–35.
18. Kalghatgi S, Friedman G, Fridman A, Clyne AM. Endothelial cell proliferation is enhanced by low dose non-thermal plasma through fibroblast growth factor-2 release. Ann Biomed Eng. 2010; 38: 748–57.
19. Kalghatgi S, Kelly CM, Cerchar E, Torabi B, Alekseev O, Fridman A, et al. Effects of non-thermal plasma on mammalian cells. PLoS ONE. 2011; 6: e16270.
20. Moureau M, Orange N, Feuilloley MGL. Non-thermal plasma technologies: new tools for bio-decontamination. Biotechnol Adv. 2008; 26: 610–17.
21. Shimizu T, Zimmermann JL, Morfill GE. The bactericidal effect of surface micro-discharge plasma under different ambient conditions. New Journal of Physics 2011; 13: 1–7.
22. Ermolaeva SA, Varfolomeev AF, Chernukha MY, Yurov DS, Vasiliev MM, Kaminskaya AA, et al. Bactericidal effects of non-thermal argon plasma in vitro, in biofilms and in the animal model of infected wounds. J Med Microbiol. 2011; 60: 75–83.
23. Ehlbeck J, Schnabel U, Polak M, Winter J, von Woedtke Th, Brandenburg R, et al. Low temperature atmospheric pressure plasma sources for microbial decontamination. J Phys D: Appl Phys. 2011; 44: 013002.
24. Lademann O, Kramer A, Richter H, Patzelt A, Meinke MC, et al. Skin disinfection by plasma-tissue interaction: comparison of the effectivity of tissue-tolerable plasma and a standard antiseptic. Skin Pharmacol Physiol. 2011; 24: 284–88.
25. Maisch T, Shimizu T, Li Y-F, Heinlin J, Karrer S, Morfill G, et al. Decolonisation of MRSA, S. aures and E. Coli by cold-atmospheric plasma using a porcine skin model in vitro. PLoS ONE. 2012; 7: e34610.
26. Daeschlein G, Scholz S, Emmert S, von Podewils S, Haase H, von Woedtke Th. Plasma medicine in dermatology: basic antimicrobial efficacy testing as prerequisite to clinical plasma therapy. Plasma Med. 2012; 2 (1–3): 33–69.
27. Daeschlein G, Napp M, von Podewils S, Lutze S, Emmert S., Lange A, et al. In vitro susceptibility of multidrug resistant skin and wound pathogens against low temperature atmospheric pressure plasma jet (APPJ) and dielectric barrier discharge plasma (DBD). Plasma Process Polymers. 2014; 11: 175–83.
28. Bekeschus S, Masur K, Kolata J, Wende K, Schmidt A, Bundscherer L, et al. Human mononuclear cell survival and proliferation is modulated by cold atmospheric plasma jet. Plasma Process Polym. 2013; 10: 706–13.
29. Короткий В. Н. Возможности применения холодной атмосферной плазмы в онкологии (обзор литературы). Сибирский онкологический журнал. 2018; 17 (1): 72–81.
30. Безуглый А. П., Бикбулатова Н. Н., Шугинина Е. А., Белков П. А., Хабутдинова Н. Р. Ультразвуковое исследование кожи в практике врача-косметолога. Вестник Дерматологии Венерол. 2011; 3: 142–152.
31. Безуглый А. П., Потекаев Н. Н., Сапожникова Ю. А. Ультразвуковое сканирование высокого разрешения в дерматологии и медицинской косметологии. Экспериментальная и клиническая дерматокосметология. 2014; 2: 20–25.
32. Bibinov N, Knake N, Bahre H, Awakowicz P, von der Gathen VS. Spectroscopic characterization of an atmospheric pressure μ-jet plasma source. J Phys D: Appl Phys. 2011; 44 (34): 345204.
33. Heuer K, Hoffmanns MA, Demir E, Baldus S, Volkmar CM, Röhle M, et al. The topical use of non-thermal dielectric barrier discharge (DBD): nitric oxide related effects on human skin. Nitric Oxide. 2015; 44: 52–60.
34. Kisch T, Helmke A, Schleusser S, Song J, Liodaki E, Stang FH, Mailaender P, Kraemer R. Improvement of cutaneous microcirculation by cold atmospheric plasma (CAP): results of a controlled, prospective cohort study. Microvasc Res. 2016; 104: 55–62.
35. Kisch T, Schleusser S, Helmke A, Mauss KL, Wenzel ET, Hasemann B, et al. The repetitive use of non-thermal dielectric barrier discharge plasma boosts cutaneous micro- circulatory effects. Microvasc Res. 2016; 106: 8–13.
36. Borchardt T, Ernst J, Helmke A, Tanyeli M, Schilling AF, Felmerer G, et al. Effect of direct cold atmospheric plasma (diCAP) on microcirculation of intact skin in a controlled mechanical environment. Microcirculation. 2017; 24: e12399.
37. Blanpain C, Fuchs E. Epidermal homeostasis: a balancing act of stem cells in the skin. Nat Rev Mol Cell Biol. 2009; 10: 207–17.

THE COMPETENCE OF PLASTIC SURGEONS

Manturova NE[1], Kochubey VV[2]✉, Kochubey AV[3]

[1] Department of Plastic and Reconstructive Surgery, Cosmetology and Cell Technologies, Pirogov Russian National Research Medical University, Moscow

[2] Department of faculty surgery №1, Faculty of Medicine, Yevdokimov Moscow State University of Medicine and Dentistry, Moscow

[3] Department of Public health and Healthcare Management, Institution of Advanced Training FMBA, Moscow

Russian system of continuous medical education does not guarantee professional development of its participants: doctors do not report the number and specifics of the operations performed, self-assess their competence and compile individual professional development plans, and the professional community does not take part in these processes. Therefore, there is a need for accurate assessment of competence of plastic surgeons and objectivity of their self-assessment. We have conducted a study in the form of a single-stage questionnaire filled by the surgeons in person. The questionnaire contained two sections. The first section offered a competence self-assessment table listing 9 plastic surgery specialties; the participants used a 5-point scoring system to state their level, where 1 meant "no experience", 2 — "beginner", 3 — "specialist", 4 — "knowledgeable", 5 — "expert". The second section contained 9 test tasks (closed, univariate) used to objectively assess the level of competence of the participants. Each correct answer added 1 point to the participant's score, wrong answers added nothing. 162 people took part in the survey. The average age of the participants was 31.5 ± 6.9 years; average length of service — 4.0 ± 4.8 years. Analyzing the data, we applied the Kolmogorov-Smirnov test, Mann-Whitney test, Kruskal-Wallis test, Spearman's coefficient, used ANOVA, Levene's test, Duncan test. The values were considered statistically significant at $p < 0.05$. The overall self-assessment score was 2.1 ± 0.92 points. We have discovered a statistically significant ($p < 0.001$) correlation of the length of service with the level of self-assessment ($r_s = 0.72$). The average score for the second section, the tests, was 2.6 ± 1.76 points (out of 9). The correlation between the test score and the length of service was insignificant ($r_s = –0.08$, $p = 0.3$); same is true for the self-assessment ($r_s = –0.006$, $p = 0.9$).

Keywords: competence of plastic surgeons, self-assessment of competence by plastic surgeons, objectivity of self-assessment of competence

✉ **Correspondence should be addressed:** Valentin Vladimirovich Kochubey
Delegatskaya, 20/1, Moscow, 127473; kochoubey@gmail.com

Received: 24.04.2018 **Accepted:** 23.05.2018

DOI: 10.24075/brsmu.2018.023

КОМПЕТЕНТНОСТЬ ПЛАСТИЧЕСКИХ ХИРУРГОВ

Н. Е. Мантурова[1], В. В. Кочубей[2]✉, А. В. Кочубей[3]

[1] Кафедра пластической, реконструктивной хирургии, косметологии и клеточных технологий, факультет дополнительного профессионального образования, Российский национальный исследовательский медицинский университет имени Н. И. Пирогова, Москва

[2] Кафедра факультетской хирургии № 1, лечебный факультет, Московский государственный медико-стоматологический университет имени А. И. Евдокимова, Москва

[3] Кафедра общественного здоровья и здравоохранения, Институт повышения квалификации Федерального медико-биологического агентства, Москва

Отечественная система непрерывного медицинского образования (НМО) не гарантирует ежегодного прогресса профессиональной компетентности у всех ее участников: врачами не предоставляются отчеты о количестве и спектре проделанных операций, оценка компетентности и создание планов индивидуального обучения проводятся ими самостоятельно без участия профессионального сообщества. В этой связи актуальным является изучение компетентности пластических хирургов и объективности ее самооценки. Изучение проводили с помощью очного одноэтапного анкетирования. Анкета содержала два раздела. Первый раздел включал тесты для самооценки компетентности по 9 трудовым функциям пластического хирурга, где 1 означало, что нет опыта, 2 — новичок, 3 — специалист, 4 — знаток, 5 — эксперт. Во второй раздел входили тестовые задания закрытого типа простого одновариантного выбора для объективной оценки знаний респондентов. Правильный ответ оценивали в 1 балл, неверный — 0. В анкетировании приняли участие 162 человека. Средний возраст респондентов был 31,5 ± 6,9 года, средний стаж работы 4,0 ± 4,8 года. Для статистического анализа рассчитывали критерии Колмогорова–Смирнова, Манна–Уитни, Краскела–Уоллиса, коэффициент Спирмена, использовали однофакторный дисперсионный анализ (ANOVA), тест Левена, тест Дункана. Статистически значимыми считали значения при $p < 0,05$. По результатам исследования общий уровень самооценки всех респондентов составил 2,1 ± 0,92 балла. Обнаружена статистически значимая ($p < 0,001$) корреляция стажа с уровнем самооценки ($r_s = 0,72$). Средняя оценка по тестам составила 2,6 ± 1,76 баллов из 9 максимально возможных. Незначимой оказалась корреляция тестовой оценки со стажем работы ($r_s = –0,08$, $p = 0,3$) и с самооценкой ($r_s = –0,006$, $p = 0,9$).

Ключевые слова: компетентность пластических хирургов, самооценка компетентности пластическими хирургами, объективность самооценки компетентности

✉ **Для корреспонденции:** Кочубей Валентин Владимирович
ул. Делегатская, д. 20/1, г. Москва, 127473; kochoubey@gmail.com

Статья получена: 24.04.2018 **Статья принята к печати:** 23.05.2018

DOI: 10.24075/vrgmu.2018.023

Russian legislation obliges each medical doctor to constantly improve professional expertise through participation in additional professional education programs [1]. One of the goals of modernization of the national medical education system is introduction of the continuous professional development principle [2]. For this purpose, there was built a continued medical and pharmaceutical education web portal, which is maintained by the Center for Scientific and Methodological Support of Transition to Continuous Medical and Pharmaceutical Education System under the Russian National Research Medical University named after N. Pirogov [3, 4]. This portal hosts continued education programs and educational activities approved by the Commission for Development of Continued Medical and Pharmaceutical Education of the Ministry of Health of the Russian Federation [5]. This is the factor that guarantees high quality of content provided in the context of the CME (continued medical education) system. The portal also allows practitioners to compile individual training plans [3], which means that a doctor's professional level depends on his or her own attitude, personal desire to develop and master a wider range of professional skills, and, most importantly, objectivity of self-assessment.

Today, testing in the context of periodic accreditation is the only tool to "weed out" unqualified specialists. At the same time, it encourages professional growth [6]. But periodic accreditation only takes place once every 5 years; it is a checkpoint through which a doctor gets permission to practice. During those 5 years, the Russian continued medical education system does not oblige practitioners to develop their professional skills, as opposed to the like systems active abroad, which do [7–10]. The latter prove that their mechanisms designed to annually assess a doctor's professional progress are effective, with such assessment comprising a portfolio of reports stating number and specifics of operations, peer reviews and an individual training plan (developed jointly with the organization administrating the system) listing mandatory subjects [11–14].

This study aimed to learn the level of competence of plastic surgeons, as well as objectivity of their self-assessment, in certain modules of plastic surgery.

MATERIALS AND METHODS

The study started with a one-time surveying of medical doctors carrying plastic surgeon certificates (which was the inclusion criterion). The questionnaire contained two sections. First section offered a competence self-assessment table listing 9 plastic surgery modules; the participants used a 5-point scoring system to state their level, where 1 point meant "no experience" and 5 points — "expert". Each score tier for each specialty defined one of five groups a doctor could belong to: 1 — no experience, 2 — beginner, 3 — knowledgeable, 4 — specialist, 5 — expert.

The mean of all points a participant assigned to each specialty was his or her overall self-assessment level. This level could bring the participant into one of three groups: mean from 0 to 2 — low self-assessment level; mean from 2 to 4 — average self-assessment level; mean from 4 to 5 — high self-assessment level.

Second section contained 9 test tasks (closed, univariate) used to objectively assess the level of competence of the participants. The tasks were taken from a collection of tests used at the final certification exam plastic surgeons take [15]. Each correct answer added 1 point to the participant's score, while wrong answers added nothing. The total number of points was the overall assessment level of each participant; the values ranged from 0 to 9.

162 people took part in the survey. The survey was anonymous. Respondents indicated their age, sex and length of service in the field of plastic surgery.

The average age of the participants was 31.5 ± 6.9 years, average length of service — 4.0 ± 4.8 years. There were 63 women (mean age 32.1 ± 8.6 years, average length of service 4.5 ± 0.8 years) and 99 men (mean age 31.2 ± 5.5 years, average length of service 3.7 ± 0.4 years). Length of service defined 4 groups of participants: 0 years of experience — 14.2% of respondents, 1–5 years — 58.0%, 6–10 years — 20.4%, over 10 years — 7.4 %. Distribution by age, length of service and variants of respondents' self-assessment was irregular ($p < 0.001$).

We applied the Kolmogorov–Smirnov test to assess uniformity of distribution; any deviation at $p < 0.05$ was considered statistically significant. Differences between the two groups were assessed with the help of the Mann–Whitney test (U), that among multiple groups — through ANOVA with simultaneous assessment of the equality of variances (Levene's test) and application of the Kruskal–Wallis test (chi-square). Duncan test allowed isolation of the homogeneous groups. Spearman's coefficient (r_s) was used to confirm correlation between attributes. The criteria and coefficients were considered statistically significant at $p < 0.05$. Average, standard deviations, percentages were calculated.

IBM SPSS Statistics software (version 23) was used for statistical processing of the data.

RESULTS

The most popular competence level for all plastic surgery modules was "no experience" (Table 1).

Table 1. Competence level of plastic surgeons: self-assessment

Specialty	Competence levels				
	no experience	beginner	knowledgeable	specialist	expert
Otoplasty	37%	27.8%	16.7%	18.5%	-
Rhinoplasty	38.9%	27.8%	18.5%	14.8%	-
Blepharoplasty	40.7%	22.2%	14.8%	13.0%	9.3%
Cheiloplasty	40.7%	33.3%	13.0%	7.4%	5.6%
Mammaplasty	33.3%	29.6%	13.0%	14.8%	9.3%
Urogenital plastic surgery	68.5%	20.4%	5.6%	1.9%	3.7%
Cutaneous plastic surgery	31.5%	25.9%	20.4%	16.7%	5.6%
Craniofacial plastic surgery	50.0%	29.6%	9.3%	5.6%	5.6%
Arm and hand plastic surgery	57.4%	24.1%	5.6%	11.1%	1.9%

The greater the competence level, the less respondents picked it throughout all specialties, the only exception being "arm and hand surgery". In this specialty, the share of self-assessed "specialists" was greater than that of "knowledgeable". The participants of the study picked the lower competence levels in the "arm and hand surgery", "urogenital plastic surgery", "craniofacial plastic surgery" specialties.

The overall self-assessment score was 2.1 ± 0.92 points. For the "otoplasty" specialty, the figure was 2.2 ± 1.12 points; for the "rhinoplasty" — 2.1 ± 1.08; "blepharoplasty" — 2.3 ± 1.36; "cheiloplasty" — 2.0 ± 1.16; "mammaplasty" — 2.4 ± 1.32; "urogenital plastic surgery" — 1.5 ± 0.96; "cutaneous plastic surgery" — 2.4 ± 1.24; "craniofacial plastic surgery" — 1.9 ± 1.14; "arm and hand surgery" — 1.8 ± 1.09.

Analysis of the self-assessment scores against length of service (0 years, 1–5 years, 6–10 years, over 10 years) has shown that the level of self-assessed competence level differs in all specialties (chi-square 66.9; $p < 0.001$). The average self-assessment score grows together with the length of service (Table 2).

The results received and the fact that the greater the length of service the more participants consider themselves "experts" and "specialists" lead us to look into the relationship of experience and self-assessment. We have found a statistically significant ($p < 0.001$) correlation between length of service, overall ($r_s = 0.72$) and specialty-specific self-assessment levels: "otoplasty" $r_s = 0.64$, "rhinoplasty" $r_s = 0.52$, "blepharoplasty" $r_s = 0.57$, "cheiloplasty" $r_s = 0.66$, "mammaplasty" $r_s = 0.72$, "urogenital plastic surgery" $r_s = 0.35$, "cutaneous plastic surgery" $r_s = 0.62$, "craniofacial plastic surgery" $r_s = 0.46$, "arm and hand surgery " $r_s = 0.42$.

As for the second part of the study, the tests, 7.4% of participants gave no correct answers, 22.8% gave one correct answer, 20.4% — two correct answers, 17.9% — three correct answers, 20.4% — five correct answers, 3.7% — six correct answers, 1.9% — nine correct answers. Specialty-wise, the distribution of correct answers was as follows: "otoplasty" — 53.1% (of respondents answered correctly); "rhinoplasty" — 46.9%, "blepharoplasty" — 21%, "cheiloplasty" — 20.4%, "mammaplasty" — 20.4%, "urogenital plastic surgery" — 24.1%, "cutaneous plastic surgery" — 34%, "craniofacial plastic surgery" — 32.1%, "arm and hand surgery" — 13%.

The overall average score was 2.6 ± 1.76 points. There was no correlation found between the overall score (all test tasks) and length of service ($r_s = –0.08$, $p = 0.3$). As for the specialties, no correlation between length of service and the amount of correct answers was established for "rhinoplasty" ($r_s = –0.03$, $p = 0.7$), "blepharoplasty" ($r_s = –0.05$, $p = 0,5$), "urogenital plastic surgery" ($r_s = –0.09$, $p = 0.2$), "cutaneous plastic surgery" ($r_s = –0.05$, $p = 0.5$). A statistically significant but inverse correlation was found between the length of service and the number of correct answers for "mammaplasty" ($r_s = –0.2$, $p = 0.01$) and "craniofacial plastic surgery" ($r_s = –0.05$, $p = 0.01$). "Rhinoplasty" and "cheiloplasty" were the only modules where experience directly affects the number of correct answers: $r_s = 0.27$, $p = 0.001$ and $r_s = 0.19$, $p = 0.02$, respectively. It should be noted that the correlation, although statistically significant, was quite weak.

The distribution of correct answers among the 4 length of service groups was uneven (chi-square 12.1, $p = 0.007$).

The "overall assessment level" in the three groups that were defined during the study (low, medium and high self-assessment levels) showed no statistically significant differences: 2.6 ± 1.63, 2.8 ± 2.0, 1.5 ± 0.55, respectively, chi-square 3.3, $p = 0.20$. Table 2 shows collates the overall average assessment score by length of service and self-assessment level.

The correlation between overall self-assessment level and overall assessment level was not statistically significant ($r_s = –0.006$, $p = 0.9$). In some specialties, the distribution of correct answers considered from the point of view of 5 proficiency groups (no experience, beginners, knowledgeable, specialists, experts) was quite even: "rhinoplasty" ($p = 0.36$), "blepharoplasty" ($p = 0.31$), mammaplasty ($p = 0.11$), "urogenital plastic surgery" ($p = 0.45$). In other specialties, on the contrary, it was uneven: "rhinoplasty" ($p = 0.0001$), "cheiloplasty" ($p = 0.015$), "cutaneous plastic surgery" ($p = 0.018$), "craniofacial plastic surgery" ($p = 0.002$), "arm and hand plastic surgery" ($p = 0.005$).

The Duncan's test allowed singling out groups with homogeneous distribution of correct answers. In "rhinoplasty", the correct answers were distributed similarly in "no experience" ($M = 0.25$) and "specialist" ($M = 0.29$) ($p = 0.74$) proficiency

Table 2. Overall assessment score by length of service and self-assessment level

Length of service	Self-assessment level	Overall average assessment score
0 years	low	2.6 ± 1.64
	total	2.6 ± 1.64
1–5 years	low	2.8 ± 1.61
	medium	2.1 ± 1.48
	high	1.0 ± 0.00
	total	2.6 ± 1.59
6–10 years	low	2.0 ± 1.09
	medium	3.8 ± 2.24
	total	3.5 ± 2.18
Over 10 years	low	0.0 ± 0.00
	medium	1.7 ± 0.51
	high	2.0 ± 0.00
	total	1.3 ± 0.88
Total	low	2.6 ± 1.63
	medium	2.9 ± 2.01
	high	1.5 ± 0.55
	total	2.7 ± 1.76

Table 3. Competence level: results of the testing

Modules	Average number of correct answers in groups	
	"no experience"	"expert"
Otoplasty	0.47 + 0.50	-
Rhinoplasty	0.29 + 0.46	-
Blepharoplasty	**0.18 + 0.39**	**0.20 + 0.41**
Cheiloplasty	**0.09 + 0.29**	**0.33 + 0.50**
Mammaplasty	0.28 + 0.45	0.00 + 0.00
Urogenital plastic surgery	0.26 + 0.44	0.00 + 0.00
Cutaneous plastic surgery	0.35 + 0.48	0.00 + 0.00
Craniofacial plastic surgery	0.33 + 0.47	0.00 + 0.00
Arm and hand plastic surgery	0.16 + 0.37	0.00 + 0.00

groups, as well as in "knowledgeable" (M = 0.60) and "beginner" (M = 0.76) (p = 0.15). As for the cheiloplasty specialty, there were no statistically significant differences in distribution of correct answers: "no experience" (M = 0.09) and "knowledgeable" (M = 0.14) (p = 0.1), "specialist" (M = 0.25), "beginner" (M = 0.33), "experts" (M = 0.33) (p = 0.26). In cutaneous plastic surgery, homogeneity in distribution of correct answers was registered in groups "expert" (M = 0.00) and "beginner" (M = 0.21) (p = 0.12), as well as groups "no experience" (M = 0.35), "specialist" (M = 0.44), "knowledgeable" (M = 0.48) (p = 0.07). In craniofacial plastic surgery we have also detected two groups with expressed correct answers homogeneity, one comprised of "knowledgeable" (M = 0.00), "expert" (M = 0.00), "no experience" (M = 0.33) (p = 0.05), the other including "beginner" (M = 0.40) and "specialist" (M = 0.67) (p = 0.05). In arm and hand surgery, homogeneous groups were "beginner", "knowledgeable", "expert" (M = 0.00 for each) (p = 0.34) and groups "no experience" (M = 0.20) and "specialist" (M = 0.33) (p = 0.26).

As this data describing homogeneity of distribution of correct answers in groups shows, self-assessment does not match scores received through testing. Moreover, in most specialty groups those respondents that claimed to have "no experience" gave more correct answers than those who placed themselves on the "expert" tier (Table 3).

In blepharoplasty the average number of correct answers was higher in the "expert" group, but the difference was non statistically significant (U = 486, p = 0.88). Only in the cheiloplasty specialty the average number of correct answers given by "experts" was higher than that seen in the "no experience" group (U = 225, p = 0.04).

DISCUSSION

Our survey has shown that plastic surgeons generally believe their level of competence to be quite low. This is especially so in such modules as urogenital plastic surgery (1.5 ± 0.96), arm and hand surgery (1.8 ± 1.09), craniofacial plastic surgery (1.9 ± 1.14). It should be noted that according to a study we have conducted earlier [16], these are the modules where surgeries are most seldom.

However, in most cases plastic surgeons assess their own proficiency objectively. The level of objective assessment is low: the average is 2.6 ± 1.76 with the top being 9 points.

We have established that practitioners tend to self-assess their proficiency level higher as their length of service increases. Unfortunately, testing — objective competency level assessment — does not confirm that correlation. Self-assessment (r_s = –0.006, p = 0.9) has no statistically significant relation to length of service (rs = –0.08, p = 0.3). It should be noted that in rhinoplasty and cheiloplasty there was some weak correlation registered between length of service and number of correct answers given; however, comparison of "no experience" and "expert" groups and calculation of testing homogeneity in the proficiency level groups show no proof of length of service being the factor directly and positively affecting level of competence. Even in the cheiloplasty specialty, where "experts" have given more correct answers than respondents belonging to the "no experience" proficiency group (U = 225, p = 0.04), calculations of homogeneity brought "beginners" together with "experts", and "no experience" joined "knowledgeable". At that, overall self-assessment and specialty-specific self-assessment show statistically significant correlation with the length of service (p < 0.001).

The fact that those participants that have no or minimal practical experience have done better in testing than surgeons who have been practicing for over 10 years may probably be the result of the former being fresh out of medical schools. Practitioners whose length of service ranges between 6 and 10 years have shown the highest average score, 3.8 ± 2.24 points, which reflects the level of activity of their practice.

CONCLUSIONS

The present study has shown that the level of competence of plastic surgeons is low; self-assessment does not match the results of objective testing; after 10 years of practice, surgeons tend to regress. Thus, we believe that our findings back the suggestions to limit access to reconstructive plastic surgery practice by introducing discrete training and support opinions of our continuous medical education system being ineffective in allowing doctors to draw up training plans themselves.

References

1. Federal'nyy zakon ot 21.11.2011 N 323-FZ «Ob osnovakh okhrany zdorov'ya grazhdan v Rossiyskoy Federatsii», stat'ya 73. Russian.
2. Prikaz Minzdrava Rossii ot 02.06.2016 N334n «Ob utverzhdenii Polozheniya ob akkreditatsii spetsialistov». Russian.
3. Portal nepreryvnogo medicinskogo i farmacevticheskogo

obrazovanija Available at: https://edu.rosminzdrav.ru/o-portale Russian.
4. Portal nepreryvnogo medicinskogo obrazovaniya. Zamestitel' glavnogo vracha. 2016; 1: 81. Russian.
5. Prikaz Minzdrava Rossii ot 18.02.2013 N82 «O Koordinacionnom sovete po razvitiyu nepreryvnogo medicinskogo i farmacevticheskogo obrazovaniya Ministerstva zdravoohraneniya Rossijskoj Federacii» Russian.
6. Petrova I. A. Akkreditatsiya meditsinskikh rabotnikov: pol'za i riski. Byulleten' Natsional'nogo nauchno-issledovatel'skogo instituta obshchestvennogo zdorov'ya imeni N.A. Semashko. 2015; (4–5): 180–6. Russian.
7. Kochubey V. V. Nepreryvnoe medicinskoe obrazovanie plasticheskogo hirurga v Velikobritanii. Moskovskiy khirurgicheskiy zhurnal. 2017; 1: 56 –9. Russian.
8. Conntinuing Professional Development (CPD) [Elektronniy resurs] https://www.rcseng.ac.uk/careers-in-surgery/surgeons/practicing-as-a-surgeon/continuing-professional-development Data obraschenija 25 dekabrja.
9. Shojania KG, Silver I, Levinson W. Continuing medical education and quality improvement: a match made in heaven? Ann Intern Med. 2012 Feb 21; 156 (4): 305–8. DOI: 10.7326/0003-4819-156-4-201202210-00008.
10. Zolotor AJ, Randolph GD, Johnson JK, Wegner S, Edwards L, Powell C, et al. Effectiveness of a practice-based, multimodal quality improvement intervention for gastroenteritis within a Medicaid managed care network. Pediatrics. 2007; 120: e644–50. [PMID: 17766504].
11. Esposito P, Dal Canton A. Clinical audit, a valuable tool to improve quality of care. General methodology and applications in nephrology. World J Nephrol. 2014 Nov 6; 3 (4): 249–55. DOI: 10.5527/wjn.v3.i4.249.
12. GMC. Licence to practise withdrawal appeals [Elektronniy resurs] http://www.gmc-uk.org/doctors/14008.asp Data obraschenija 25 dekabrja.
13. Ericsson KA. Acquisition and Maintenance of Medical Expertise: A Perspective From the Expert-Performance Approach With Deliberate Practice. Acad Med. 2015; 90 (11): 1471–86. [PMID: 26375267].
14. Van de Wiel MW, Van den Bossche P. Deliberate practice in medicine: The motivation to engage in work-related learning and its contribution to expertise. Vocat Learn. 2013; 6 (1): 135–58.
15. Enoch S, Jagadeesan J, Jose RM, Chan WY, McGrouth G. Plastic Surgery Exam Questions and Answers: A Guide to the Plastic Surgery exit exam, 2 ed. UK: Doctors Academy Publications, 2012. 498 ps.
16. Manturova N. E., Kochubey V. V., Kochubei A. V. Harakteristiki deyatel'nosti plasticheskih hirurgov. Vestnik RGMU. 2017; 6: 47–51.

Литература

1. Федеральный закон от 21.11.2011 № 323-ФЗ «Об основах охраны здоровья граждан в Российской Федерации». Ст. 73 «Обязанности медицинских работников и фармацевтических работников».
2. Приказ Минздрава России от 02.06.2016 №334н «Об утверждении Положения об аккредитации специалистов».
3. Портал непрерывного медицинского и фармацевтического образования [Электронный ресурс] https://edu.rosminzdrav.ru/o-portale/ Дата обращения 25 декабря 2017.
4. Портал непрерывного медицинского образования. Заместитель главного врача. 2016; 1: 81.
5. Приказ Минздрава России от 18.02.2013 N82 «О Координационном совете по развитию непрерывного медицинского и фармацевтического образования Министерства здравоохранения Российской Федерации».
6. Петрова И. А. Аккредитация медицинских работников: польза и риски. Бюллетень Национального НИИ общественного здоровья имени Н. А. Семашко. 2015; (4–5): 180-6.
7. Кочубей В. В. Непрерывное медицинское образование пластического хирурга в Великобритании. Московский хирургический журнал. 2017; 1: 56–9.
8. Continuing Professional Development (CPD) [Электронный ресурс] https://www.rcseng.ac.uk/careers-in-surgery/surgeons/practicing-as-a-surgeon/continuing-professional-development Дата обращения 25 декабря 2017.
9. Shojania KG, Silver I, Levinson W. Continuing medical education and quality improvement: a match made in heaven? Ann Intern Med. 2012 Feb 21; 156 (4): 305–8. DOI: 10.7326/0003-4819-156-4-201202210-00008.
10. Zolotor AJ, Randolph GD, Johnson JK, Wegner S, Edwards L, Powell C, et al. Effectiveness of a practice-based, multimodal quality improvement intervention for gastroenteritis within a Medicaid managed care network. Pediatrics. 2007; 120: e644–50. [PMID: 17766504].
11. Esposito P, Dal Canton A. Clinical audit, a valuable tool to improve quality of care. General methodology and applications in nephrology. World J Nephrol. 2014 Nov 6; 3 (4): 249–55. DOI: 10.5527/wjn.v3.i4.249.
12. GMC. Licence to practise withdrawal appeals [Электронный ресурс] http://www.gmc-uk.org/doctors/14008.asp Дата обращения 25 декабря 2017/.
13. Ericsson KA. Acquisition and Maintenance of Medical Expertise: A Perspective From the Expert-Performance Approach With Deliberate Practice. Acad Med. 2015; 90 (11): 1471–86. [PMID: 26375267].
14. Van de Wiel MW, Van den Bossche P. Deliberate practice in medicine: The motivation to engage in work-related learning and its contribution to expertise. Vocat Learn. 2013; 6 (1): 135–58
15. Enoch S, Jagadeesan J, Jose RM, Chan WY, McGrouth G. Plastic Surgery Exam Questions and Answers: A Guide to the Plastic Surgery exit exam, 2 ed. UK: Doctors Academy Publications, 2012. 498 ps.
16. Мантурова Н. Е., Кочубей В. В., Кочубей А. В. Характеристики деятельности пластических хирургов. Вестник РГМУ. 2017; 6: 47–51.

CLINICAL AND RADIOGRAPHIC CHARACTERISTICS OF PATIENTS WITH CERVICALGIA AFTER PREVIOUS INJURY TO THE PECTORAL GIRDLE

Kalinsky EB[1]✉, Chernyaev AV[1], Slinyakov LYu[1], Lychagin AV[1], Kalinsky BM[2], Goncharuk YuR[1]

[1] Chair of Trauma, Orthopedics and Disaster Surgery, Faculty of Medicine, Sechenov First Moscow State Medical University (Sechenov University), Moscow

[2] Botkin Moscow State Clinical Hospital, Moscow

The health of the cervical spine (CS) and the functional state of the pectoral girdle are interdependent. Injuries to the pectoral girdle can be an underlying cause of CS pain, including cervicalgia. The aim of this study was to evaluate the condition of the cervical spine in patients with cervicalgia developed after a pectoral girdle injury using radiographic and physical examinations. The study included 400 patients complaining of cervicalgia. Pain intensity was evaluated on the visual analog scale (VAS); the impact of the condition on patients' lives was assessed using the Neck Disability Index (Russian language). During physical examinations, the general health of the spine was evaluated and abnormalities in the cervical spine were noted. All participants underwent a radiographic scan of the cervical spine in the lateral and anterior-posterior projections; 49.5% of patients underwent postural digital radiography to evaluate their CS sagittal profile. All patients received an MRI scan. Based on the results, we identified certain functional changes in the cervical spine which possibly caused cervicalgia. Structurally and functionally, the changes were divided into static and dynamic. We conclude that cervical spinal pain is a common problem among patients with previous pectoral girdle injury.

Keywords: cervicalgia, sagittal balance, spine, cone of economy, radiography, pectoral girdle injury, cervical spine, global alignment

✉ **Correspondence should be addressed:** Evgeny Kalinsky, Trubetskaya 8, bl. 2, Moscow, 119991; eugene_kalinsky@mail.ru

Received: 15.03.2018 **Accepted:** 24.03.2018

DOI: 10.24075/brsmu.2018.017

КЛИНИКО-РЕНТГЕНОЛОГИЧЕСКАЯ ХАРАКТЕРИСТИКА ПАЦИЕНТОВ С ЦЕРВИКАЛЬНЫМ СИНДРОМОМ ПОСЛЕ ТРАВМЫ НАДПЛЕЧЬЯ

Е. Б. Калинский[1]✉, А. В. Черняев[1], Л. Ю. Слиняков[1], А. В. Лычагин[1], Б. М. Калинский[2], Ю. Р. Гончарук[1]

[1] Кафедра травматологии, ортопедии и хирургии катастроф, лечебный факультет Первый Московский государственный медицинский университет им. И. М. Сеченова (Сеченовский университет), Москва

[2] Городская клиническая больница им. С. П. Боткина, Москва

Состояние шейного отдела позвоночника (ШОП) находится во взаимосвязи с функциональным состоянием пояса верхней конечности. Повреждения пояса верхней конечности могут лежать в основе болевых ощущений в ШОП, в том числе вызывать цервикалгию. Целью исследования было оценить клинико-рентгенологическую картину ШОП у пациентов с цервикалгией, перенесших травму плечевого пояса. В исследование вошли 400 пациентов с жалобами на цервикалгию. Интенсивность боли оценивали по визуально-аналоговой шкале (VAS), ограничения жизнедеятельности — по опроснику NDI-RU (The Neck Disability Index, Russian language). При осмотре пациентов проводили оценку профиля позвоночника и локальных изменений в ШОП. Всем лицам, включенным в исследование, было выполнено рентгенологическое обследование ШОП в боковой и передне-задней проекциях, у 49,5% пациентов проведена постуральная цифровая рентгенография позвоночника для оценки сагиттального профиля ШОП. Всем пациентам была сделана магнитно-резонансная томография (МРТ). По результатам комплексного клинико-лучевого обследования у пациентов были отмечены функциональные изменения, которые можно трактовать как причину развития цервикалгии. С точки зрения структурно-функционального диагноза определены различные статико-динамические нарушения. Таким образом, было выявлено, что болевой синдром в области ШОП является часто встречающейся проблемой у пациентов, перенесших травму надплечья.

Ключевые слова: цервикалгия, сагиттальный баланс, позвоночник, конус экономии, рентгенография, травма верхней конечности, шейный отдел позвоночника, общее строение

✉ **Для корреспонденции:** Калинский Евгений Борисович ул. Трубецкая, д. 8, стр. 2, г. Москва, 119991; eugene_kalinsky@mail.ru

Статья получена: 15.03.2018 **Статья принята к печати:** 24.03.2018

DOI: 10.24075/vrgmu.2018.017

In the recent decade structural deformities and functional impairments of the spine have been deemed increasingly important as an underlying cause of both axial and peripheral pain syndromes. Biomechanically, the spine and the pectoral and pelvic girdles resemble an intricate rigging system [1, 2]; the spine, its central component, is a "mast" supported by "shrouds", i.e. the pectoral girdle, pelvis, and spinal and limb muscles. In this biomechanical system, a change in the spatial orientation of one component will entail adaptive shifts or functional adjustments of others. Through such adaptation energy-efficient performance is achieved, meaning that the body can maintain its postural balance within the cone of

economy, as described by Dubousset (Fig.1) [3–6]. Thus, functional statuses of the cervical spine (CS) and the shoulder girdle should be seen as interdependent [1, 3, 7, 8].

Injuries to the pectoral girdle are very common and nowadays account for 15% of all skeletal injuries [9]. They are most often seen in young patients of working age and are a result of household, sport-related and road accidents.

Based on the analysis of treatment outcomes in patients with pectoral girdle injuries, we can isolate a group of patients with cervicalgia. This group is heterogenous and includes differently aged individuals who previously received operative or non-operative treatment for their condition. Of particular interest here are young and middle-aged patients who had no clinical signs of cervicalgia before the injury. Neck pain entails functional limitations and slows down rehabilitation, affecting its intensity; it also deteriorates the patient's quality of life [7]. It is worth noting that there are no reliable data in the literature on the prevalence of cervicalgia in patients with previous injuries to the pectoral girdle or on its possible causes.

The aim of our study was to evaluate the condition of the cervical spine in patients with cervicalgia after a pectoral girdle injury based on radiographic and physical examinations.

METHODS

The study was conducted in 400 patients undergoing treatment at the facilities of the Trauma Unit (Botkin City Clinical Hospital, Sechenov First Moscow State Medical University, Department of Traumatology, Orthopedics and Disaster Surgery) between 2015 and 2018. The study included male and female individuals aged from 18 to 59 years (mean age was 41.3 ± 1.1 years) with localized neck pain (suggestive of cervicalgia) and an isolated unilateral injury of the pectoral girdle received at least 6 weeks before the study.

Patients with clinical signs of cervical radiculopathy, any previous injury to the spine, the narrowing of the cervical spinal cord of any etiology and multiple injuries were excluded from the study.

Age- and sex-based distribution of patients is shown in Table 1.

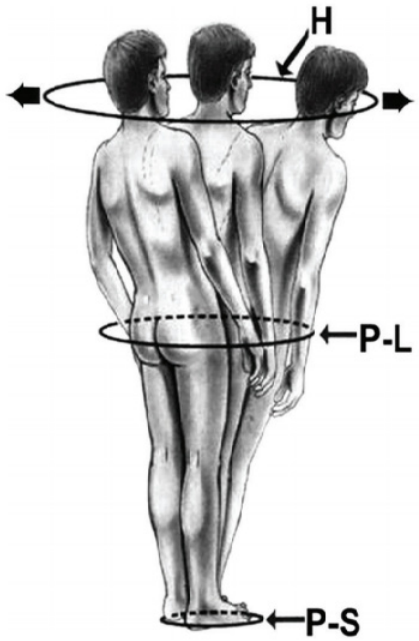

Fig. 1. The picture of the optimal standing posture of the human body as proposed by the "cone of economy" concept [3]

Of all selected patients, 276 (69%) received surgical treatment, 124 (31%) received non-operative treatment.

Clinical evaluation of the orthopedic status was performed in all patients. Pain intensity was evaluated on the visual analog scale (VAS) [10, 11].

The impact of neck pain on the patients' lives was assessed using the NDI-RU questionnaire [12–14].

CS radiography was performed in standard anterior-posterior and lateral projections (100%). Functional radiography of the cervical spine was not ordered: it would have provided no valuable information because of the pain syndrome the patients suffered from and because it would have been impossible to maintain identical conditions during each examination.

To investigate the sagittal profiles of CS, we performed postural digital radiography of the spine in the lateral and anterior-posterior projections in 198 patients (49.5%) [5]. This type of imaging allows to evaluate both cervical spinal balance and the so-called global alignment (Fig. 2) [7, 15–20].

To understand the condition of intervertebral discs and to exclude cervical spinal stenosis, an MRI examination was ordered for all the patients (T1/T2-weighted and STIR scans in closed 1.5 Tesla machines with standard Pfirrmann grading) [21].

RESULTS

All patients complained of neck pain. Pain intensity on the VAS scale was mild in 18 patients (4.5%), moderate in 312 patients (78%), fairly severe and severe in 70 patients (17.5%). Average score for pain intensity was 5.6 ± 0.45 points.

The NDI-RU questionnaire revealed mild self-measured disabilities in 85 patients (21.3%), moderate, in 290 patients (72.5%) and severe, in 25 (6.2%) patients.

Physical examinations were carried out to assess the overall condition of the spine, search for the abnormalities in the cervical spine, and estimate the range of motion in the latter (Table 2).

Radiography detected the following local symptoms (Table 3).

In the frontal plane the cervical spinal axis looked undeformed.

Table 4 shows the findings of postural digital radiography performed to assess cervical sagittal balance.

MRI scans were suggestive of intervertebral disc degeneration in the studied zone in all the patients (Pfirrmann's types I and II) [21]; their vertebral bodies were intact. No signs of cervical spinal stenosis were observed.

DISCUSSION

Our study was conducted in 400 patients with previous injury to the pectoral girdle who had developed clinical signs of cervicalgia in the post-injury period. The symptoms included local pain, myofascial pain, and the restricted range of motion in the cervical spine. Radiography did not detect severe degeneration or dystrophic changes in the spine. The sagittal balance profile obtained for 198 patients (49.5%) did not reveal severe biological or mechanical damage to the

Table 1. Distribution of patients based on sex and age

	Male	Female
18–44	125 (31.3%)	101 (25.2%)
45–59	88 (22%)	86 (21.5%)
Total	213 (53.3%)	187 (46.7%)

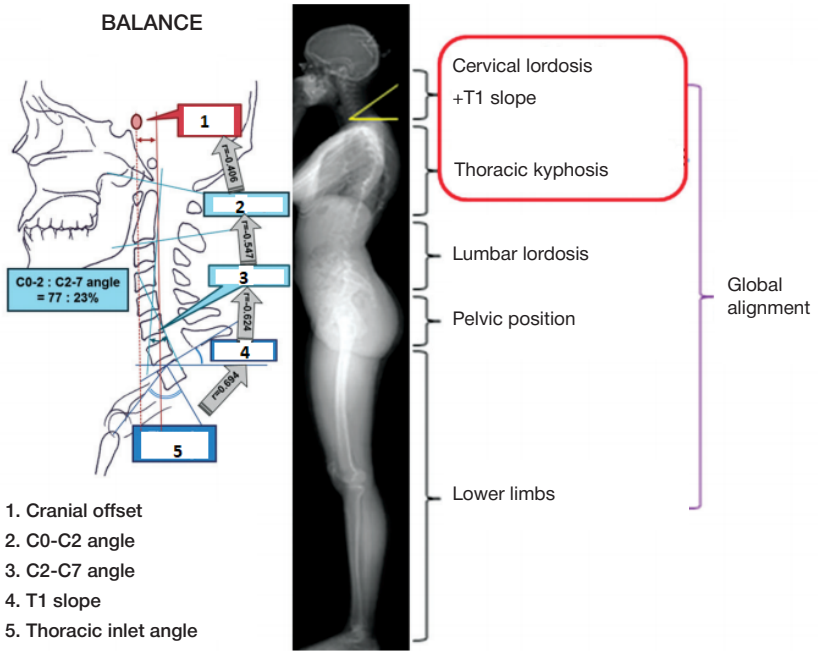

Fig. 2. Radiographic parameters of sagittal balance [15, 19, 20]

Table 2. Results of clinical examinations

Symptom	Number of patients
General health of the spine	
Flat back (loss of cervical and lumbar lordosis or thoracic kyphosis)	98 (24.5%)
Round back (thoracic hyperkyphosis)	47 (11.7%)
Flat-concave back (thoracic hyperkyphosis and lumbar lordosis)	29 (7.3%)
Thoracolumbar scoliosis	247 (61.8%)
Pelvic misalignment	198 (49.5%)
Changes in the cervical spine	
Cervical hyperlordosis	186 (46.5%)
Loss of cervical lordosis	199 (49.8%)
Hypertonia of paraspinal muscles	359 (89.3%)
Restricted flexion	373 (93.3%)
Restricted extension	340 (85%)
Restricted rotation	381 (95.3%)
Restricted lateral flexion	391 (97.8%)

Table 3. Radiographic findings

Symptom	Number (%)
Loss of disc height (relative to neighboring discs)	49 (12.3%)
Stepladder instability of vertebral bodies (the posterior vertebral body line is interrupted)	273 (68.3%)
Facet joint arthrosis	23 (5.8%)
Local deviation of the spinous process	379 (94.8%)
Inclination of zygapophyses (facet subluxation. broken Hadley's S curve)	367 (91.8%)
Spondylosis	12 (3%)

Table 4. Parameters of cervical sagittal balance

Parameter	Value	Mean [1, 15, 18]
C0-C2 angle	–29° ± 1.3°	–30°
C2-C7 angle	–9.8° ± 0.9°	–9.6
T1 slope	38.9° ± 1.2°	40°
C2-C7 SVA (sagittal vertical axis)	3.9 ± 0.5 cm	4 cm
TIA (thoracic inlet angle)	43° ± 1.4°	44°

spine, suggesting that pain originated in the neck. MRI data are suggestive of the initial stage of degenerative dystrophic changes in the functional spinal units but show no disc-root conflicts and central or lateral canal stenosis.

Therefore, the changes detected in the cervical spine are not structural, but functional, implying static and dynamic impairments, such as hypermobility or hypomobility of spinal units, which can be interpreted as a functional dislocation within the facet joint syndrome [22, 23].

Based on the static and dynamic changes detected, patients can be recommended an adequate plan of rehabilitation to alleviate cervical pain. However, further research is necessary to understand a correlation between those changes and different types of injuries to the pectoral girdle, types of surgical treatment applicable and other structural and functional impairments of the spine and pelvis.

CONCLUSIONS

Cervical spinal pain is a common problem in patients with previous injuries to the pectoral girdle. Girdle injuries can entail functional damage to the cervical spine, causing cervicalgia. Further exploration of cervical spine dysfunctions in patients with previous pectoral girdle injuries will help to develop methods for their prevention and elaborate adequate rehabilitation plans.

References

1. Kapandzhi AI. Pozvonochnik. Fiziologiya sustavov. 6 izd. M.: Izdatel'stvo Eksmo; 2009: 327 s.
2. Dubousset J, Challier V, Farcy JP, Schwab FJ, Lafage V. Spinal alignment versus spinal balance. In: Haid RW, Schwab FJ, Shaffrey CI, Youssef JA (ed.). Global Spinal Alignment: Principles, Pathologies, and Procedures St. Louis, MO: Quality Medical Publishing, 2014. p. 3–9.
3. Dubousset J. Three-dimensional analysis of the scoliotic deformity. In: The pediatric spine: principles and practice. New York: Raven Press; 1994: 479–496.
4. Hasegawa K, Okamoto M, Hatsushikano S, Shimoda H, Ono M, Watanabe K. Normative values of spino-pelvic sagittal alignment, balance, age, and health-related quality of life in a cohort of healthy adult subjects. Eur Spine J. 2016; 25 (11): 3675–86. https://doi.org/10.1007/s00586-016-4702-2
5. Mac-Thiong JM, Roussouly P, Berthonnaud E, Guigui P. Sagittal parameters of global spinal balance: normative values from a prospective cohort of seven hundred nine Caucasian asymptomatic adults. Spine. 2010; 35 (22): E1193–E1198. https://doi.org/10.1097/brs.0b013e3181e50808
6. Ames CP, Smith JS, Scheer JK, Bess S, Bederman SS, Deviren V et al. Shaffrey Impact of spinopelvic alignment on decision making in deformity surgery in adults: A review. J Neurosurg Spine. 2012; 16 (6): 547–64. https://doi: 10.3171/2012.2.SPINE11320
7. Burtsev AV, Ryabykh SO, Kotel'nikov AO, Gubin AV. Klinicheskie aspekty sagittal'nogo balansa u vzroslykh. Genii ortopedii. 2017; 23 (2): 228–35. https://doi.org/10.18019/1028-4427-2017-23-2-228-235
8. Kalinsky EB, Kalinsky BM, Goncharuk JuR, Usmanova NH. Podhody k lecheniju povrezhdenij akromial'no-kljuchichnogo sustava III tipa (po Rockwood). Manual'naja terapija. 2017; 66 (2): 65–8.
9. Kotel'nikov GP, Mironov SP, redactory. Travmatologiya. Natsional'noe rukovodstvo. M.: GEOTAR-Media; 2008: 808.
10. Scott J, Huskisson EC. Vertical or horizontal visual analogue scales. Ann Rheum Dis. 1979; 38: 560.
11. Gould D et al. Visual Analogue Scale (VAS). Journal of Clinical Nursing 2001; 10: 697–706.
12. Vernon H, Mior S. (1991). The Neck Disability Index: A study of reliability and validity. Journal of Manipulative and Physiological Therapeutics. 14 (7): 409–15.
13. Bakhtadze MA, Vernon H, Zakharova OB, Kuzminov KO, Bolotov DA. The Neck Disability Index-Russian Language Version (NDI-RU): A Study of Validity and Reliability. Spine (Phila Pa 1976). 2015 Jul 15; 40 (14): 1115–1. DOI: 10.1097/BRS.0000000000000880.
14. Bivaltsev VA, Belikh EG, Alekseeva NV, Sorokovikov VA. Primenenie shkal I anket v obsledovanii patsientov s degenerativnim porazheniem poyasnichnogo otdela pozvonochnika; metodicheskie rekomendatsii. Irkutsk: 2013. 32 s.
15. Scheer JK., Tang JA, Smith JS, Acosta Jr FL, Protopsaltis TS, Blondel B et al. Cervical spine alignment, sagittal deformity, and clinical implications: a review. J Neurosurg Spine. 2013; 19 (2): 141–159. https://doi.org/10.3171/2013.4.SPINE12838
16. Ozer AF, Kaner T, Bozdoğan Ç. Sagittal Balance in the Spine. Turkish Neurosurgery. 2014; 24 (1): 13–19.
17. Le Huec JC, Demezon H, Aunoble S. Sagittal parameters of global cervical balance using EOS imaging: normative values from a prospective cohort of asymptomatic volunteers. Eur Spine J. 2015; 24 (1): 63–71. https://doi.org/10.1007/s00586-014-3632-0
18. Liu S, Schwab F, Smith JS, Klineberg E, Ames CP, Mundis G et al. Likelihood of reaching minimal clinically important difference in adult spinal deformity: a comparison of operative and nonoperative treatment. Ochsner J. 2014; 14 (1): 67–77.
19. Vialle R, Levassor N, Rillardon L, Templier A, Skalli W, Guigui P. Radiographic analysis of the sagittal alignment and balance of the spine in asymptomatic subjects. J Bone Joint Surg Am. 2005; 87 (2): 260–7.
20. Lafage V, Schwab F, Skalli W, Hawkinson N, Gagey PM, Ondra S et al. Standing balance and sagittal plane spinal deformity: analysis of spinopelvic and gravity line parameters. Spine. 2008; 33 (14): 1572–78. https://doi: 10.1097/BRS.0b013e31817886a2
21. Pfirrmann CW, Metzdorf A, Zanetti M, Hodler J, Boos N. Magnetic resonance classification of lumbar intervertebral disc degeneration. Spine (Phila Pa 1976). 2001 Sep 1; 26 (17): 1873–8.
22. Avoyan TK. Konservativnoe lechenie bol'nih s sindromom mezhpozvonkovih sustavov pri poyasnichnom osteohondroze [dissertacija). M.: 1998.
23. Zhandarov KA. Stenoz mezhpozvonochnix kanalov sheinogo otdela pozvonochnika. [dissertacija]. M.: 2016.

Литература

1. Капанджи А. И. Позвоночник. Физиология суставов. 6 изд. М.: Изд-во «Эксмо»; 2009. 327 с.
2. Dubousset J, Challier V, Farcy JP, Schwab FJ, Lafage V. Spinal alignment versus spinal balance. In: Haid RW, Schwab FJ, Shaffrey CI, Youssef JA (ed.)/. Global Spinal Alignment: Principles, Pathologies, and Procedures St. Louis, MO: Quality Medical Publishing, 2014. p. 3–9.
3. Dubousset J. Three-dimensional analysis of the scoliotic deformity. In: The pediatric spine: principles and practice. New York: Raven Press; 1994: 479–496.
4. Hasegawa K, Okamoto M, Hatsushikano S, Shimoda H, Ono M, Watanabe K. Normative values of spino-pelvic sagittal alignment, balance, age, and health-related quality of life in a cohort of healthy adult subjects. Eur Spine J. 2016; 25 (11): 3675–86. https://doi.

org/10.1007/s00586-016-4702-2
5. Mac-Thiong JM, Roussouly P, Berthonnaud E, Guigui P. Sagittal parameters of global spinal balance: normative values from a prospective cohort of seven hundred nine Caucasian asymptomatic adults. Spine. 2010; 35 (22): E1193–E1198. https://doi.org/10.1097/brs.0b013e3181e50808
6. Ames CP, Smith JS, Scheer JK, Bess S, Bederman SS, Deviren V et al. Shaffrey Impact of spinopelvic alignment on decision making in deformity surgery in adults: A review. J Neurosurg Spine. 2012; 16 (6): 547–64. https://doi: 10.3171/2012.2.SPINE11320
7. Бурцев А. В., Рябых С. О., Котельников А. О., Губин А. В. Клинические аспекты сагиттального баланса у взрослых. Гений ортопедии. 2017; 23 (2): 228–35. https://doi.org/10.18019/1028-4427-2017-23-2-228-235
8. Калинский Е. Б., Калинский Б. М., Гончарук Ю. Р., Усманова Н. Х. Подходы к лечению повреждений акромиально-ключичного сустава III типа (по Rockwood). Мануальная терапия. 2017; 66 (2): 65–68.
9. Котельников Г. П., Миронов С. П., редакторы. Травматология. Национальное руководство. М.: ГЭОТАР-Медиа; 2008: 808 с.
10. Scott J, Huskisson EC. Vertical or horizontal visual analogue scales. Ann Rheum Dis. 1979; 38: 560.
11. Gould D. et al. Visual Analogue Scale (VAS). Journal of Clinical Nursing 2001; 10: 697–706.
12. Vernon H, Mior, S. (1991). The Neck Disability Index: A study of reliability and validity. Journal of Manipulative and Physiological Therapeutics. 14 (7): 409–15.
13. Bakhtadze MA, Vernon H, Zakharova OB, Kuzminov KO, Bolotov DA. The Neck Disability Index-Russian Language Version (NDI-RU): A Study of Validity and Reliability. Spine (Phila Pa 1976). 2015 Jul 15; 40 (14): 1115–1. DOI: 10.1097/BRS.0000000000000880.
14. Бывальцев В. А., Белых Е. Г., Алексеева Н. В., Сороковиков В. А. Применение шкал и анкет в обследовании пациентов с дегенеративным поражением поясничного отдела позвоночника: методические рекомендации. Иркутск: ФГБУ "НЦРВХ" СО РАМН, 2013. 32 с.
15. Scheer JK., Tang JA, Smith JS, Acosta Jr FL, Protopsaltis TS, Blondel B et al. Cervical spine alignment, sagittal deformity, and clinical implications: a review. J Neurosurg Spine. 2013; 19 (2): 141–159. https://doi.org/10.3171/2013.4.SPINE12838
16. Ozer AF, Kaner T, Bozdoğan Ç. Sagittal Balance in the Spine. Turkish Neurosurgery. 2014; 24 (1): 13–19.
17. Le Huec JC, Demezon H, Aunoble S. Sagittal parameters of global cervical balance using EOS imaging: normative values from a prospective cohort of asymptomatic volunteers. Eur Spine J. 2015; 24 (1): 63–71. https://doi.org/10.1007/s00586-014-3632-0
18. Liu S, Schwab F, Smith JS, Klineberg E, Ames CP, Mundis G et al. Likelihood of reaching minimal clinically important difference in adult spinal deformity: a comparison of operative and nonoperative treatment. Ochsner J. 2014; 14 (1): 67–77.
19. Vialle R, Levassor N, Rillardon L, Templier A, Skalli W, Guigui P. Radiographic analysis of the sagittal alignment and balance of the spine in asymptomatic subjects. J Bone Joint Surg Am. 2005; 87 (2): 260–7.
20. Lafage V, Schwab F, Skalli W, Hawkinson N, Gagey PM, Ondra S et al. Standing balance and sagittal plane spinal deformity: analysis of spinopelvic and gravity line parameters. Spine. 2008; 33 (14): 1572–78. https://doi: 10.1097/BRS.0b013e31817886a2
21. Pfirrmann CW, Metzdorf A, Zanetti M, Hodler J, Boos N. Magnetic resonance classification of lumbar intervertebral disc degeneration. Spine (Phila Pa 1976). 2001 Sep 1; 26 (17): 1873–8.
22. Авоян Т. К. Консервативное лечение больных с синдромом межпозвонковых суставов при поясничном остеохондрозе [диссертация]. М.: 1998.
23. Жандаров К. А. Стеноз межпозвоночных каналов шейного отдела позвоночника [диссертация]. М.: 2016.

KNEE OSTEOCHONDRITIS DESICCANS: SURGERY ALGORITHM

Egiazaryan KA, Lazishvili GD✉, Hramenkova IV, Shpak MA, Badriev DA

Department of Traumatology, Orthopedics and Military Field Surgery,
Pirogov Russian National Research Medical University, Moscow

Knee osteochondritis desiccans, or Koenig's disease, is commonly found in active young people engaged in manual labor, sports etc., i.e. socially active population. Today, we have a good number of surgical method to treatment of this disorder; however, there is still much controversy about their application, and no single approach is considered to be the optimal one. Plus, high-quality biomaterials required for the intervention are sometimes unavailable. The analysis of the results of treatment of patients (spanning several years) proved urgency of the problem and highlighted the necessity to solve a number of related issues. This paper presents the algorithm of surgical treatment of knee osteochondritis desiccans. We have provided surgery validation criteria, suggested optimal methods of correction of local cartilage defects (depending on the degree of damage and patient's age) and outlined some recommendations based on our practical experience.

Keywords: local cartilage defects, knee joint, osteochondritis dissecans, Koenig's disease, osteochondral defect, collagen scaffold, mosaic plastic

✉ **Correspondence should be addressed:** Guram Davidovich Lazishvili
Ostrovityanova 1, Moscow, 117997; guramlaz@gmail.com

Received: 16.05.18 **Accepted:** 23.05.18

DOI: 10.24075/brsmu.2018.020

АЛГОРИТМ ХИРУРГИЧЕСКОГО ЛЕЧЕНИЯ БОЛЬНЫХ С РАССЕКАЮЩИМ ОСТЕОХОНДРИТОМ КОЛЕННОГО СУСТАВА

К. А. Егиазарян, Г. Д. Лазишвили✉, И. В. Храменкова, М. А. Шпак, Д. А. Бадриев

Кафедра травматологии, ортопедии и военно-полевой хирургии,
Российский национальный исследовательский медицинский университет имени Н. И. Пирогова

Наиболее часто рассекающий остеохондрит коленного сустава, или болезнь Кёнига, встречается у активных молодых людей, занятых физическим трудом, спортом, т. е. представителей социально активной прослойки населения. Несмотря на разнообразие современных методик хирургического лечения болезни, остается много спорных вопросов по их применению, отсутствует оптимальный подход и ограничена доступность качественных биоматериалов, требующихся при вмешательстве. Проведенный анализ результатов лечения пациентов за несколько лет показал высокую актуальность и необходимость решения многих вопросов этой проблемы. В работе представлен алгоритм хирургического лечения рассекающего остеохондрита коленного сустава. Обоснованы показания к оперативному вмешательству, предложены оптимальные способы коррекции локальных дефектов хряща в зависимости от стадии его поражения и возраста пациента, даны рекомендации, основанные на практическом опыте авторов.

Ключевые слова: локальные дефекты хряща, коленный сустав, рассекающий остеохондрит, болезнь Кёнига, костно-хрящевой дефект, коллагеновая матрица, «мозаичная» костно-хрящевая аутотрансплантация

✉ **Для корреспонденции:** Гурам Давидович Лазишвили
ул. Островитянова, д. 1, г. Москва, 117997; guramlaz@gmail.com

Статья получена: 16.05.18 **Статья принята к печати:** 23.05.18

DOI: 10.24075/vrgmu.2018.020

Treatment of the hyaline cartilage pathology is a problem regarded by current orthopedics as urgent. Surgery aimed at local cartilage defects correction is one of the most difficult tasks a surgeon can have today.

Osteochondritis desiccans (Koenig's disease) in femoral condyle makes up 2% of all knee joint disorders. The pathology mainly affects people 11 to 13 and 20 to 40 years old.

Every year, surgeons in Europe perform over 300,000 operations aimed at correction of local intraarticular cartilage defects of the knee joint [1]. Many of the previously popular surgery methods applied to remedy the disorder, like cartilaginous plate anchoring, subchondral bone tunneling etc, have proved ineffective and are quite outdated.

In 80-85% of cases, osteochondritis desiccans manifests around the medial femoral condyle; in 10–20% of cases — around lateral femoral condyle; in 4% — on the articular surface of patella and in 0.5–0.7% of cases — around the femoral intercondylar groove. In 14–24% of cases, Koenig's disease is bilateral [2].

The reasons behind damage to cartilage accompanying osteochondritis desiccans are not quite clear. The list of these reasons may include constitutional and genetic factors, ischemia, traumas, bone overload disorders, ossification disorders etc [3]. Probably, Koenig's disease is the result of ischemia and local necrosis of the subchondral bone that spreads onto cartilage. Development of osteochondritis desiccans leads to separation of the subchondral bone's necrotic fragment and its transfer to the joint's cavity.

There are many diverse surgery approaches to the Koenig's disease, and some of them imply making use of advanced biotechnology; however, numerous related questions remain unanswered [4–8]. Simultaneous osteochondral reconstruction (and the necessity thereof) is one of the subjects of discussion. Lack of a common opinion and related standards complicates validation of methods chosen to treat a case of Koenig's disease, especially in juvenile patients with open physes.

Unfortunately, the choice our surgeons have today when treating osteochondritis desiccans is very limited. The reason

behind such a state of affairs is unavailability of a wide range of techniques and tools offered by current biological and cellular technologies. National R&D centers have not yet offered viable alternatives to the imported biomaterials, the cost of which makes them inexpedient in the context of routine treatments in Russian hospitals.

Analysis of the long-term outcomes of bone-cartilage autotransplantation ("mosaic" chondroplasty, commonly used by Russian practitioners) has revealed the drawbacks of this approach: 1) frequently observed non-restoration of the joint surfaces' congruence, as well as that of the defect itself; 2) problematic consequences seen around the patello-femoral articulation. One of the main causes of complications arising during surgery on extensive osteochondral defects of femoral condyles is the deficit of osteoplastic material.

This paper presents the optimal algorithm of surgical treatment of femoral condyle osteochondritis desiccans (depending on the cartilage damage severity) and validation thereof.

Study Design

To develop the optimal treatment algorithm addressing the disorder in question, as well as validation points thereof, we have analyzed the results observed in 184 patients with various chronic knee injuries (full-thickness local cartilage and osteochondral) treated from 1995 to 2017 in Hospital #1 named after N.I. Pirogov.

The patients were divided into two groups, treatment (1st) and control (2nd). The first group included 86 patients; they were treated following current local cartilage defects surgical correction protocols (mono or "mosaic" bone/cartilage auto- or allotransplantation, autologous matrix-induced chondrogenesis - AMIC - implantation of collagen matrix with or without bone grafting) [12].

The second group consisted of 98 patients; their treatment followed older local cartilage defects correction practices (abrasive chondroplasty, subchondral bone micro-fractures, tunneling) [2–5, 6].

Duration of the condition was estimated from case records, i.e. from the day a patient first noticed the disorder to the day that patient was diagnosed with Koenig's disease.

Examination and treatment results assessment methods employed: clinical and functional checkup, MRI and multispiral computed tomography (MSCT); scales used to assess condition in pre- and postoperative periods: ICRS physical activity scale (ICRS — International Cartilage Repair Society), VAS (visual analogue scale), WOMAC knee score [2].

Hounsfield scale was used to analyze and assess treatment results as shown by the CT scans of the patients' knee joints. MOCART scale was employed to assess the MRI scans [9–11].

Inclusion criteria: male and female patients aged 15 to 60 years (mean age 40 ± 1.6 years); chronic full-thickness knee cartilage defects, 3rd and 4th stage (ICRS classification).

Exclusion criteria: age under 15 or over 60; 1st or 2nd stage of the knee cartilage defects (not full-thickness, fresh injury).

We have analyzed the long-term (up to 8 years) treatment results observed in 70 patients (81.4%) of the treatment group and 78 patients (79.6%) of the control group. This is not the entire sample; the reasons behind the discrepancy are unavailability of a number of patients and recency of surgery in some cases.

Below, we outline the knee osteochondritis desiccans surgery algorithm we have developed and employ in our hospital; it is based on the aforementioned research effort.

Knee Osteochondritis Desiccans: Surgical Correction

1. Patients with open physes

Today, Russian hospitals have a number of options when it comes to surgical correction of local osteochondral defects of femoral condyles, intercondyle groove, kneecap.

We believe that osteochondral transplantation is an inappropriate choice for juvenile patients with open physes. Anchoring the detached necrotic osteochondral plate is also a prospectless option. AMIC, collagen matrix implantation onto necrotic subchondral bone, will not result in regeneration of the latter. We have verified that subchondral bone continues to decay when AMIC does not imply using a bone plate. See more on this technology below.

Thus, the method of choice for patients of this age group is tunneling, i.e. drilling holes in the subchondral bone to stimulate repairs done by mesenchymal stem cells that enter through those holes [12]. Lately, we have been doing that arthroscopically, using a 3.5 mm triangular bit drill with a stopper limiting depth to 15 mm (Fig. 1).

2. Patients with closed physes

"Mosaic" osteochondral autotransplantation

If the patient's physes are closed and the osteochondral defect measures less then 10 cm^2, we recommend "mosaic" bone and cartilage autotransplantation.

Planning the operation, it is important to determine if the full-scale osteochondral autotransplantation can be done arthroscopically, since it is not always possible practice this approach to collect donor transplant columns, do "mosaic" osteoplasty and articular surface congruence restoration [13, 14]. As a rule, the arthroscopic access itself imposes such limitations through restricting the use of instruments. Such cases call for "mosaic" chondroplasty (open or minimally invasive variations) [15].

There is an important aspect of surgery to consider, namely location of the transplants. Full-scale chondrogenesis and affected cartilage regeneration require transplants placed as close to each other as possible, almost sticking together or even slightly overlapping.

CT scans made 12 months after surgery prove that osteochondral regeneration in the "mosaic" zone went well (Fig. 2).

Up to early 2017, we resorted to "mosaic" osteochondral allotransplantation when the defect's area was greater than 10 cm^2. We used lyophilized canned femoral condyles as donor allomaterial, which was sterilized with gamma rays. The surgery's technique and the arrangement of transplants were same to osteochondral autotransplantation (Fig. 3).

We believe that this method offers a number of advantages. First off, there is no need to collect autologous donor transplant posts from the sides of the knee joint, which makes the surgery shorter and less traumatic. Secondly, if the defect's area is small, the operation can be done arthroscopically. Thirdly, there is always a good supply of grafting materials, which allows using allotransplants of different diameters for full-scale osteochondral osteoplasty. Fourthly, there is no need to use biomaterials, which makes the surgery considerably less costly. Fifthly, localization of the osteochondral defect does not matter, the method is a viable solution for knee and other joints.

Today, we often resort to the combined (auto- and allo-) "mosaic" osteochondral transplantation (Fig. 4). Typically,

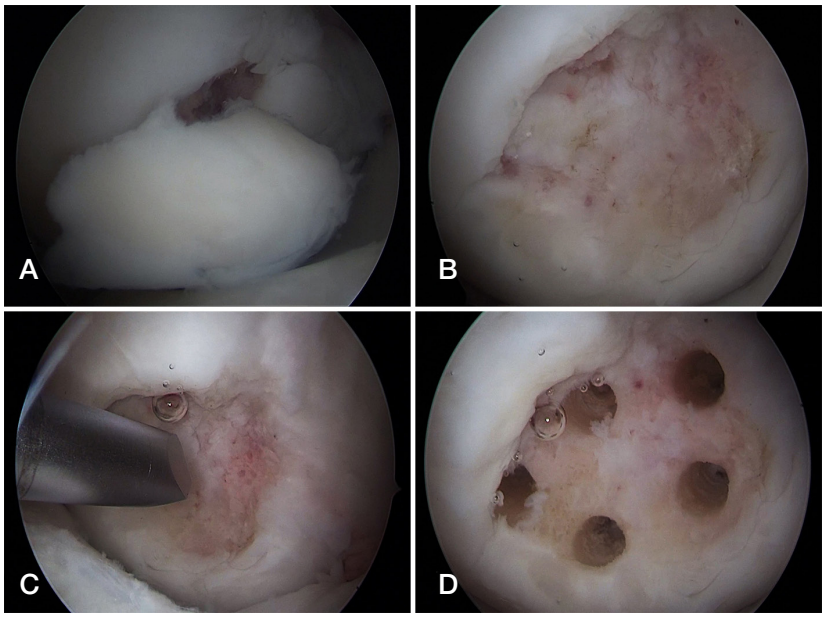

Fig. 1. A. Separated necrotic cartilage plate, arthroscopic view. **B**. Osteochondral defect after removal of the necrotic plate, arthroscopic view. **C**. Drilling holes (tunnels) in the subchondral bone. **D**. Subchondral bone after tunneling

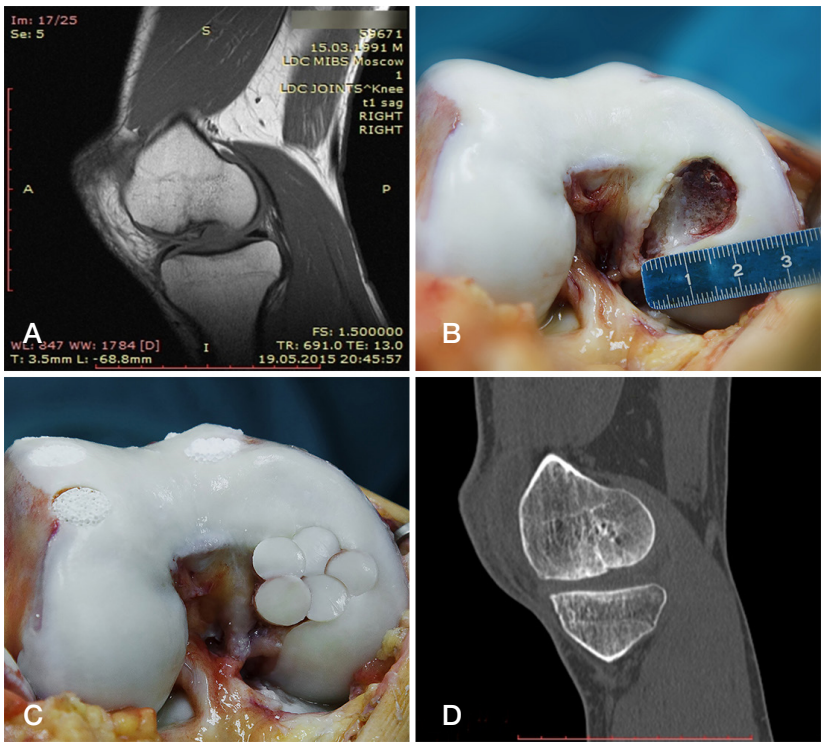

Fig. 2. A. Osteochondritis desiccans affecting medial femoral condyle, MRI scan. **B**. Condyle defect shape and size after sanation. **C**. Result of "mosaic" osteochondral autotransplantation. Donor sites filled with biocomposite bone. **D**. 12 months after operation, MSCT scan. Osteochondral regeneration in the "mosaic" zone went well

it ensures better regeneration of the subchondral bone and cartilaginous surface of the femoral condyle.

Here is the list of our recommendations pertaining to the osteochondral transplantation technique:

– full-scale osteoplasty of a osteochondral defect requires transplants with the diameter of 5–6 mm or greater;

– complete regeneration requires transplants placed as close to each other as possible, sticking together or even slightly overlapping;

– if the defect's area exceeds 10 cm^2, adequate (pre-surgery) assessment of very possibility of complete elimination of that defect is crucial for success; combined auto- and alloplastic approach is a viable solution when there is a risk of shortage of autoplastic material.

Subchondral bone microfracturing (Steadman technique)

From 2002 to 2005, when faced with a 3rd stage local femoral condyles cartilage defect (contacts, 5 cm^2 maximum), we often resorted to subchondral bone microfracturing, or the Steadman technique [2, 4, 5]. This method implies stimulation of chondrogenesis by stem cells obtained through the openings formed. Analysis of the outcomes of such operations showed that they are prospectless: the Steadman's technique does not

deliver the results expected, i.e. cartilage does not regenerate in the affected area. These outcomes are a yet another prove of this fact: normal chondrogenesis requires anchoring stem cells in the cartilage defect area as a super-clot.

Autologous matrix-induced chondrogenesis (AMIC)

Lately, practitioners have been choosing the autologous matrix-induced chondrogenesis technique (AMIC) more often when faced with full-thickness cartilage defects (Fig. 5). AMIC makes use of the above-described reparative ability of mesenchymal stem cells that enter the joint cavity through holes drilled in the subchondral bone [17–22].

Tunneling allows formation of a super-clot of cytokines and red bone marrow stem cells, which stabilizes through implantation onto the matrix defect and stimulates bone and cartilage-like tissue repairs [23, 24].

AMIC offers a number of distinct advantages: it is minimally invasive; it can remedy larger cartilage defects; it is a simple surgery; its effectiveness has been proved — patients suffer

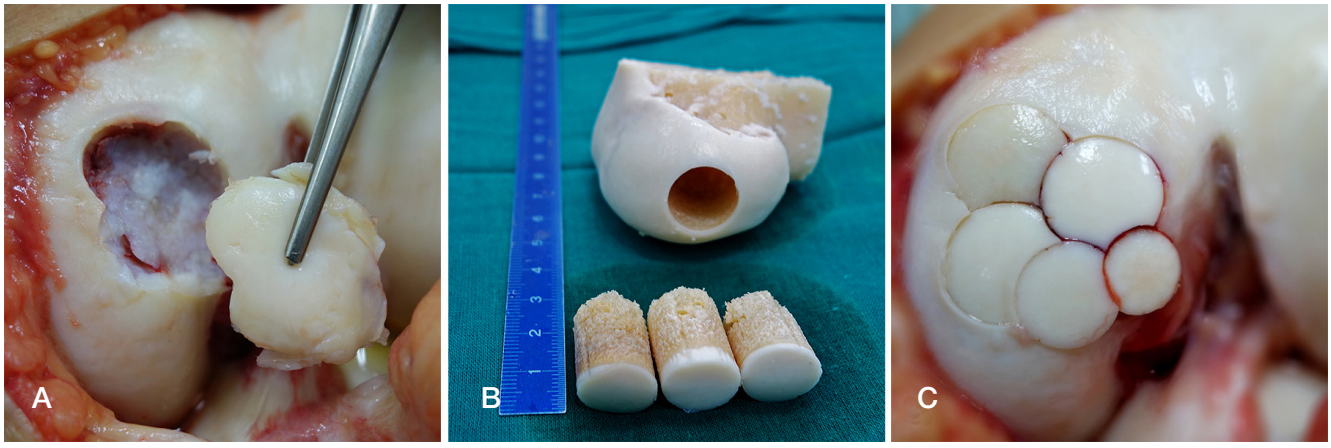

Fig. 3. A. Osteochondral defect of the medial femoral condyle (Koenig's disease). **B**. Allogeneic lyophilized femoral condyle and cylindrical donor transplants (columns, posts). **C**. Result of "mosaic" osteochondral allotransplantation

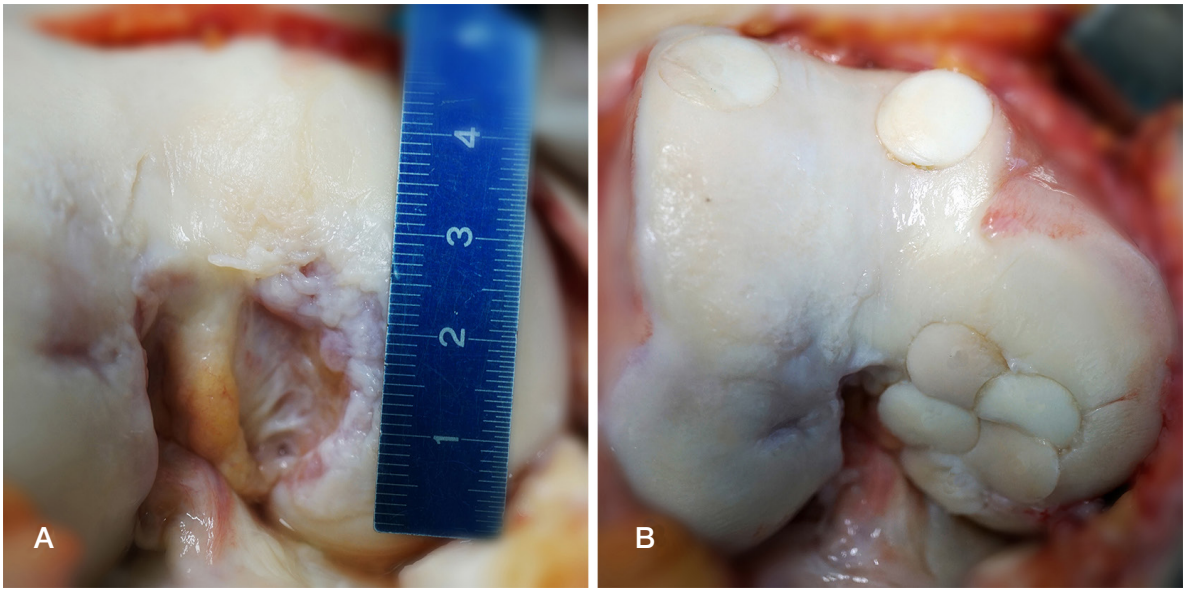

Fig. 4. A. Osteochondral defect of the medial femoral condyle (Koenig's disease), shape and size. **B**. Result of combined osteochondral autotransplantation. A — auto, E — allo

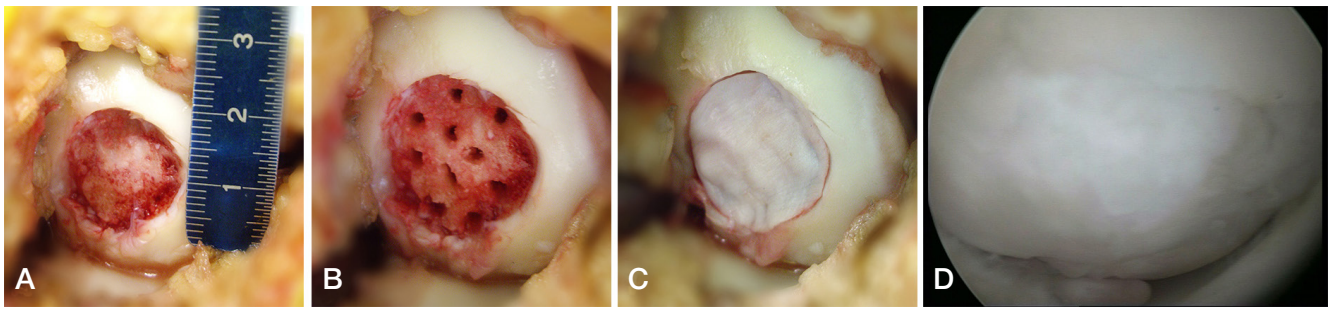

Fig. 5. A. Osteochondral defect of the medial femoral condyle shape and size after sanation. **B**. Subchondral bone after tunneling. **C**. Collagen matrix implantation. **D**. 1.4 years after surgery: condyle defect is completely covered by stable cartilaginous tissue (arthroscopic view)

lesser pain, in some cases the pain was gone completely and knee functions returned in full, which had positive effect on patient satisfaction.

Today, collagen matrix is the most advanced widely available biological material used to repair cartilage tissue, a material that positively affects stem cell differentiation and chondrogenesis.

We believe this operation is the proper choice for patients with 3rd stage of Koenig's disease (full-thickness defects of hyaline cartilage, no damage to subchondral bone). Prerequisites: healthy hyaline cartilage surrounding the defect, viable subchondral bone and unchanged mechanical axis of the lower limb.

Contraindications: multiple cartilage defects, including "kissing lesions"; widespread knee osteoarthritis; systemic autoimmune diseases; knee joint instability caused by ligament and meniscus injury; valgus or varus leg deformations that call for corrective surgery; allergic reactions to collagen.

Special attention should be paid to the state of the subchondral bone: expressed sclerosis there indicates its non-viability. We believe the non-viable part of the bone should be sanitated up to the healthy, bleeding layers, and the defect remedied through osteoplasty. Lack of pinpoint bleeding after subchondral bone tunneling signals of its non-viability, which should alert the surgeon. In such cases, implantation of a collagen matrix without osteoplasty is fruitless.

The list below presents our recommendations based on the analysis of long-term outcomes of AMIC technique application to our patients.

– A mandatory prerequisite for collagen matrix implantation is healthy and stable subchondral bone.

– Deep (over 5 mm) local damage to subchondral bone calls for osteoplasty on the osteochondral defect.

– Simultaneous osteoplasty (on the osteochondral defect, using a biocomposite bone) and matrix implantation is unpromising.

– Physical activity level of the patient should be factored in when planning the surgery. Unfortunately, AMIC and sport of records are incompatible.

CONCLUSION

Having analyzed the outcomes of treatment done in our hospital, as well as available literature and technical capabilities, we optimized the algorithm for surgical treatment of patients suffering from knee osteochondritis desiccans and arrived at a number of conclusions: 1) patients with open physes should undergo removal of the non-viable cartilaginous plate, sanation of the osteochondral defect and subchondral bone tunneling; 2) AMIC technique is the optimal choice for cases where there is a full-thickness local cartilage damage and undamaged subchondral bone; 3) local osteochondral defects measuring less than 10 cm^2 may best be treated with "mosaic" osteochondral autotransplantation; 4) local osteochondral defects measuring 10–15 cm^2 call for combined "mosaic" osteochondral transplantation.

In conclusion, we would like to note that through the objective analysis of errors and complications we have managed to change the stereotypes around local cartilage and osteochondral femoral condyle defects treatment tactics, sort out a number of unpromising technologies and improve the surgery procedures. Nevertheless, surgery on knee osteochondritis desiccans is still is subject containing many controversial issues.

References

1. Anders S, Wiech O, Schaumburger J, et al. Autologus Matrix induced chondrogenesis (AMIC) for focal chondal defects of the knee — first results. J Bone Joint Surg Br. 2009; 91 (Suppl.1): 83–7.
2. Malanin DA, Pisarev VB, Novochadov VV. Vosstanovlenie povregdeniy chryasha v kolennom sustave. Eksperimental'nye i klinicheskie aspekty. Volgograd: Volgogradskoe nauchnoe izdatel'stvo; 2010. 455 c.
3. Alford JW, Cole BJ. Cartilage restoration, part 1: basic science, historical perspective, patient evaluation and treatment options. Am J Sports Med. 2005; 33 (2): 295–306.
4. Solheim E, Hegna J, Inderhaug E, Oyen J, Harlem T, Strand T. Results at 10–14 years after microfracture treatment of articular cartilage defects in the knee. Knee Surg Sports Traumatol Arthroscop. 2016; 24 (5): 1587–93.
5. Xing L, Jiang Y, Gui J, Lu Y, et al. Microfracture combined with osteochondral paste implantation was more effective than microfracture alone for full-thickness cartilage repair. Knee Surg Sports Traumatol Arthroscop. 2013; 21 (8): 1770–76.
6. Laupattarakasem W, Laopaiboon M, Laupattarakasem P, Sumananont C. Arthroscopic debridement for knee osteoarthritis (Review). Cochrane Database Syst Rev. 2008; Issue 1. Art. No.: CD005118. DOI: 10.1002/14651858.CD005118.pub2.
7. Stadnikov AA, Kavalerskiy GM, Arhipov SV, Pavlov VP, Makarov SA, Makarov MA, i dr. Novye metody hirurgicheskogo lecheniya defectov gialinovogo chryasha kolennogo sustava u bol'nyh s gonartrozom. Nauchno-practicheskaya revmatologiya. 2009; 3: 90–3.
8. Tratting S, Ba-Ssalamah A, Pinker K, Plank C, Vescei V, Marlovits S. Magnetic Resonance Imaging. 2005; 23 (7): 779–87.
9. Koval'chul VN. Klassifikaciya povregdeniy chryasha kolennogo sustava. Luchevaya diagnostica, luchevaya terapiya. 2012; 1: 99–106.
10. Golovaha ML, Loskutov AE, Egorov VF. Korrelyacia dannyh magnitno-rezonansnoy tomografii i artroscopii pri travmaticheskih povregdeniyah kolennogo sustava. Praktikyushemu vrachu. 2011; 12 (2): 99–105.
11. Lazishvili GD, Zatikyan VR, Shukyur-Zadeh ER, Kornaev AS, Akmataliev KI, Danilov MA. Actual direction of chondroplasty. Bulletin of Russian State Medical University. 2013; 3: 13–17.
12. Malyshev EE, Korolyov SB, Pavlov DV, Kuvshinov SG. Osteochondral autoplasty of the extensive post-traumatic defect of the proximal tibia. Modern technologies in medicine. 2014; 6 (2): 142–7.
13. Kotel'nikov GP, Larcev YV, Kudashev DS, Zuev-Ratnikov SD, Shorin IS. Mosaicplasty in the treatment of patients with destructive-dystrophic and post-traumatic lesions hyaline cartilage in the knee joint — experimental and clinical aspects. Fundamental research. 2013; 9: 252–5.
14. Zakirova AR. Artroskopicheskoe lechenie hrjashevyh defectov kolennogo sustava. M.: 2010.
15. Caldwell PE, Shelton WR. Indications for allografts. Orthop Clin North Am. 2005; 36 (4): 459–67.
16. Sadlik B, Wiewiorski M. Implantation of a collagen matrix for an AMIC repair during dry arthroscopy. Knee Surg Sports Traumatol Arthrosc. 2015; 23: 2349–52.
17. Gille J, Schuseil E, Wimmer J, et al. Mid-term results of autologus matrix-indused chondrogenesis for treatment of focal cartilage defects in the knee. Knee Surg Sports Traumatol Arthrosc. 2010; 18: 1456. https://doi.org/10.1007/s00167-010-1042-3.
18. Pascarella A, Ciatti R, Pascarella F, et al. Treatment of articular cartilage lesions of the knee joint using a modified AMIC technique.

Knee Surg Sports Traumatol. Arthrosc. 2010; 18: 509–13.
19. Anders S, Wiech O, Schaumburger J, et al. Autologus Matrix induced chondrogenesis (AMIC) for focal chondal defects of the knee – first results. J Bone Jt Surg (Brit.). 2009; 91 (suppl.1): 83–4.
20. Hangody L, Vasarhelyi G, Hangody LR, et al. Autologus osteochondral grafting technique and long-term results. Injury. 2008; 39 (suppl.1): 32–9.
21. Steinwachs M, Kreuz PC. Autologus chondrocyte implantation in chondral defects of the knee with a type I/III collagen membrane: A prospective study with a 3-year follow-up. Arthroscopy. 2007; 23: 381–7.
22. Garkavi AV, Blokov MY. Artroscopicheskaya chondroplastika lokal'nych chryashevyh defectov kolennogo sustava s ispol'zovaniem kollagenovoy membrany CHONDRO–GIDE. Kafedra travmatologii i ortopedii. 2015; 3 (15): 4–7.
23. Jacob RP. AMIC technique for cartilage repair, a single-step surgical intervention as compared to other methods. Eur Cell Mater. 2006; 12 (suppl.1): 26–32.
24. Kramer J, Bohrnsen F, Lindner U, et al. In vivo matrix-guided human mesenchymal stem cells. Cell Mol Life Sci. 2006; 63 (5): 616–26.

Литература

1. Anders S, Wiech O, Schaumburger J, et al. Autologus Matrix induced chondrogenesis (AMIC) for focal chondal defects of the knee — first results. J Bone Joint Surg Br. 2009; 91 (Suppl.1): 83–7.
2. Маланин Д. А., Писарев В. Б., Новочадов В. В. Восстановление повреждений хряща в коленном суставе. Экспериментальные и клинические аспекты. Волгоград: Волгоградское научное издательство; 2010. 455 с.
3. Alford JW, Cole BJ. Cartilage restoration, part 1: basic science, historical perspective, patient evaluation and treatment options. Am J Sports Med. 2005; 33 (2): 295–306.
4. Solheim E, Hegna J, Inderhaug E, Oyen J, Harlem T, Strand T. Results at 10–14 years after microfracture treatment of articular cartilage defects in the knee. Knee Surg Sports Traumatol Arthroscop. 2016; 24 (5): 1587–93.
5. Xing L, Jiang Y, Gui J, Lu Y, et al. Microfracture combined with osteochondral paste implantation was more effective than microfracture alone for full-thickness cartilage repair. Knee Surg Sports Traumatol Arthroscop. 2013; 21 (8): 1770–76.
6. Laupattarakasem W, Laopaiboon M, Laupattarakasem P, Sumananont C. Arthroscopic debridement for knee osteoarthritis (Review). Cochrane Database Syst Rev. 2008; Issue 1. Art. No.: CD005118. DOI: 10.1002/14651858.CD005118.pub2.
7. Стадников А. А., Кавалерский Г. М., Архипов С. В., Павлов В. П., Макаров С. А., Макаров М.А. и др. Новые методы хирургического лечения дефектов гиалинового хряща коленного сустава у больных с гонартрозом. Научно – практическая ревматология. 2009; 3: 90–3.
8. Tratting S, Ba-Ssalamah A, Pinker K, Plank C, Vescei V, Marlovits S. Magnetic Resonance Imaging. 2005; 23 (7): 779–87.
9. Ковальчук В. Н. Классификация поврежденного хряща коленного сустава. Лучевая диагностика, лучевая терапия. 2012; 1: 99–106.
10. Головаха М. Л., Лоскутов А. Е., Егоров В.Ф. Корреляция данных магнитно- резонансной томографии и артроскопии при травматических повреждениях коленного сустава. Практикующему врачу. 2011; 12 (2): 99–105.
11. Лазишвили Г. Д., Затикян В. Р., Шукюр-Заде Э. Р., Корнаев А. С., Акматалиев К. И., Данилов М. А. Актуальные вопросы хондропластики. Вестник РГМУ. 2013; 3: 13–17.
12. Малышев Е. Е., Королев С. Б., Павлов Д. В., Кувшинов С. Г. Костно-хрящевая аутотранплантация обширного посттравматического дефекта проксимального отдела большеберцовой кости. Современные технологии в медицине. 2014; 6 (2): 142–7.
13. Котельников Г. П., Ларцев Ю. В., Кудашев Д. С., Зуев-Ратников С. Д., Шорин И. С. Мозаичная хондропластика в лечении больных с деструктивно-дистрофическими и посттравматическими поражениями гиалинового хряща в коленном суставе – экспериментальные и клинические аспекты. Фундаментальные исследования. Медицинские науки. 2013; 9: 252–5.
14. Закирова А. Р. Артроскопическое лечение хрящевых дефектов коленного сустава. М.: 2010.
15. Caldwell PE, Shelton WR. Indications for allografts. Orthop Clin North Am. 2005; 36 (4): 459–67.
16. Sadlik B, Wiewiorski M. Implantation of a collagen matrix for an AMIC repair during dry arthroscopy. Knee Surg Sports Traumatol Arthrosc. 2015; 23: 2349–52.
17. Gille J, Schuseil E, Wimmer J, et al. Mid-term results of autologus matrix-indused chondrogenesis for treatment of focal cartilage defects in the knee. Knee Surg Sports Traumatol Arthrosc. 2010; 18: 1456. https://doi.org/10.1007/s00167-010-1042-3.
18. Pascarella A, Ciatti R, Pascarella F, et al. Treatment of articular cartilage lesions of the knee joint using a modified AMIC technique. Knee Surg Sports Traumatol. Arthrosc. 2010; 18: 509–13.
19. Anders S, Wiech O, Schaumburger J, et al. Autologus Matrix induced chondrogenesis (AMIC) for focal chondal defects of the knee – first results. J Bone Jt Surg (Brit.). 2009; 91 (suppl.1): 83–4.
20. Hangody L, Vasarhelyi G, Hangody LR, et al. Autologus osteochondral grafting technique and long-term results. Injury. 2008; 39 (suppl.1): 32–9.
21. Steinwachs M, Kreuz PC. Autologus chondrocyte implantation in chondral defects of the knee with a type I/III collagen membrane: A prospective study with a 3-year follow-up. Arthroscopy. 2007; 23: 381–7.
22. Гаркави А. В., Блоков М. Ю. Артроскопическая хондропластика локальных хрящевых дефектов коленного сустава с использованием коллагеновой мембраны CHONDRO–GIDE. Кафедра травматологии и ортопедии. 2015; 3 (15): 4–7.
23. Jacob RP. AMIC technique for cartilage repair, a single-step surgical intervention as compared to other methods. Eur Cell Mater. 2006; 12 (suppl.1): 26–32.
24. Kramer J, Bohrnsen F, Lindner U, et al. In vivo matrix-guided human mesenchymal stem cells. Cell Mol Life Sci. 2006; 63 (5): 616–26.